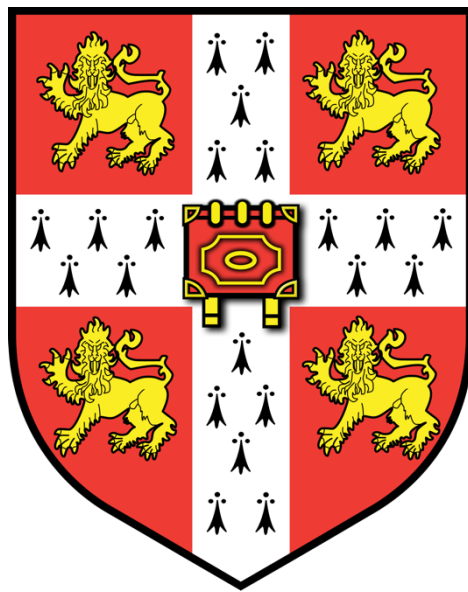


Ancient origins of the chordate forebrain:

Conserved patterning of the anterior  
neuroectoderm in amphioxus



Giacomo Gattoni

Churchill College  
University of Cambridge

This thesis is submitted for the degree of  
Doctor of Philosophy

December 2022



# Declaration

This thesis is the result of my own work and includes nothing which is the outcome of work done in collaboration except as declared in the preface and specified in the text. It is not substantially the same as any work that has already been submitted before for any degree or other qualification except as declared in the preface and specified in the text. It does not exceed the prescribed word limit for the Biology Degree Committee.

Giacomo Gattoni

December 2022



# Summary

## Ancient origins of the chordate forebrain: conserved patterning of the anterior neuroectoderm in amphioxus

Giacomo Gattoni

While the general organization of the chordate central nervous system (CNS) is highly conserved and consists of a dorsal neural tube with an anterior brain, the evolutionary origin of this key aspect of the chordate body plan remains obscure. In recent years, a conserved anterior gene regulatory network (aGRN) has been shown to pattern the larval anterior nervous system of several invertebrates, including the two non-chordate deuterostome phyla (echinoderms and hemichordates), in which the aGRN controls the development of the apical organ. Although clear homologs of the apical organ are not present in chordates, most aGRN genes are expressed in the vertebrate forebrain. In this PhD thesis I trace the evolution of the aGRN across deuterostomes using the cephalochordate amphioxus as the main model organism.

I first show that during amphioxus development aGRN genes are expressed in a similar pattern to the one found in echinoderms and hemichordates, are regulated by Wnt/ $\beta$ -catenin signalling and are active in the anterior neuroectoderm that forms the larval brain. As a comparative system, I also characterize the development of the apical organ in an understudied group of echinoderms, the crinoids. To follow the fate of the amphioxus anterior neuroectoderm, I next investigate neurogenesis, proliferation and cell type differentiation in larval and adult brains. I demonstrate the presence of a hypothalamic-like region in the anterior cerebral vesicle, which derives from the region where the aGRN is active during development. Finally, I explore how changes in the specification of the body axes and in the expression of one of the upstream aGRN genes, FoxQ2, might have underlined the evolution of the complex vertebrate brain.

Taken together, the results presented in this thesis support the conservation across deuterostome evolution of an aGRN that controls the development of the anterior neuroectoderm. In the chordate lineage, the network was integrated to the neurulation program to specify retinal and hypothalamic

areas of the forebrain. Furthermore, this work provides a comprehensive characterization of neuroarchitecture and cell type composition across the amphioxus life cycle, facilitating the comparison with other chordate taxa to reconstruct the evolution of the chordate nervous system.

# Declaration of collaborative work

This work benefited from collaborations with a variety of people, including other students in the Benito-Gutiérrez Lab and other PhD students and faculty from the University of Cambridge and University of Milan. All collaborators are reported here, and additionally highlighted in each chapter where applicable. All data presented in this thesis was analysed by the author.

- ◆ Chapter II, Section 2.3.1: Optimization of *in situ* Hybridization Chain Reaction protocols in amphioxus was done in collaboration with Dr Toby Andrews (Francis Crick Institute), Lara Busby (Department of Genetics, University of Cambridge) and Michael Schwimmer (Department of Zoology, University of Cambridge).
- ◆ Chapter II, Section 2.4.2: EdU treatments were carried out together with Dr Toby Andrews (Francis Crick Institute).
- ◆ Chapter III, Section 3.2.1: Daniel Keitley (Department of Zoology, University of Cambridge) carried out the analysis of the sea urchin and zebrafish scRNAseq datasets
- ◆ Chapter III, Section 3.3: From the RNA sample collected by the author, Ashley Sawle (CRUK, Cambridge Institute) generated the bulk RNAseq dataset for control and Azakenpaullone-treated embryos and advised on the data analysis performed by the author.
- ◆ Chapter IV: The project on crinoid apical organ was carried out in collaboration with Dr Silvia Mercurio and Prof. Roberta Pennati (Department of Environmental Science and Policy, University of Milan). Dr Silvia Mercurio also collected and fixed samples of *Antedon mediterranea* and performed the immunohistochemical experiments in doliolaria larvae for serotonin and GABA.
- ◆ Chapter V, Section 5.4.3: the work on the amphioxus hindbrain stems from the undergraduate degree project of Simon Kershenbaum (now Department of Biology, University of Oxford). Some of the *in situ* Hybridization Chain Reactions analysed by the author in this section were performed by undergraduate students Mark Comer (Imperial College London), Maria Izmirlieva and Madeline Foster-Smith (University of Cambridge). All the data presented here was generated and analysed by the author.
- ◆ Chapter V, Section 5.6.2: Part of the sectioning and *in situ* Hybridization Chain Reaction experiments on the amphioxus adult brain was carried out together with Michael Schwimmer (Department of Zoology, University of Cambridge).

- ◆ Chapter VI, Section 6.2.2: Dr Ben Steventon and Dillan Saunders (Department of Genetics, University of Cambridge) provided advice and training for the use of zebrafish. Dr Andrew Gillis (Marine Biological Laboratory, University of Chicago) provided sections of 8dpf and adult zebrafish heads.
- ◆ Chapter VI, Section 6.2.3: The script for detection of conserved transcription factors binding sites was developed together with Daniel Keitley (Department of Zoology, University of Cambridge).
- ◆ Chapter VI, Section 6.3.2: Claudia Pérez-Calles (now EMBL-European Bioinformatics Institute) performed the phylogenetic analysis and *in situ* Hybridization Chain Reaction experiments on TGF $\beta$  receptors.
- ◆ Appendix III: Dr Andrew Gillis (Marine Biological Laboratory, University of Chicago) provided paraffin-embedded sections of skate embryos and fish larvae and adults.

# Publications

The work in this thesis has contributed to three publications and two manuscripts in preparation for submission:

- ◆ Andrews TGR, **Gattoni G**, Busby L, Schwimmer MA, Benito-Gutiérrez E (2020). Hybridization Chain Reaction for quantitative and multiplex imaging of gene expression in amphioxus embryos and adult tissues. *In situ hybridization protocols*, 179-194, Ed. Humana (NY)
- ◆ Benito-Gutiérrez E, **Gattoni G**, Stemmer M, Rohr S, Schuhmacher LN, Tang J, Marconi A, Jekely G, Arendt D (2021). The dorsoanterior brain of adult amphioxus shares similarities in expression profile and neuronal composition with the vertebrate telencephalon. *BMC Biology*, 19:1-19
- ◆ **Gattoni G\***, Andrews TGR\*, Benito-Gutiérrez E (2021). Restricted proliferation during neurogenesis contributes to regionalization of the amphioxus nervous system. *Frontiers in Neuroscience*, 16:812223
- ◆ (in preparation) Mercurio S, **Gattoni G**, Scari G, Barzaghi B, Benito-Gutiérrez E, Pennati R. Insights into crinoid embryogenesis: from fertilized egg to swimming larva.
- ◆ (in preparation) **Gattoni G**, Keitley D, Sawle A, Benito-Gutiérrez E. An ancient gene regulatory network sets the position of the forebrain in chordates.



# Table of Contents

Declaration	ii
Declaration of collaborative work	v
Publications	vii
Abstract	ix
Table of Contents	xi
<b>Chapter I – Introduction</b>	<b>1</b>
1.1 A brief history of nervous system evolution	1
1.2 EvoDevo and the revolution of comparative biology	3
1.3 Homology: a tricky definition	5
1.4 The vertebrate brain: development and organization	6
1.5 Amphioxus and the evolutionary origin of the chordate brain	9
1.6 Aim of this thesis: a phylogenetic story	13
<b>Chapter II – Materials &amp; Methods</b>	<b>17</b>
2.1 Animal source, rearing and fixation	17
2.1.1 Amphioxus	17
2.1.2 Crinoids	18
2.1.3 Zebrafish	18
2.1.4 Frogs	19
2.1.5 Skates	19
2.2 Immunohistochemistry	19
2.2.1 Amphioxus	19
2.2.2 Crinoids	21
2.2.3 Frogs	21
2.3 <i>In situ</i> hybridization chain reaction: HCR	21
2.3.1 Amphioxus	22
2.3.2 Crinoids	24
2.3.3 Vertebrates	24
2.3.4 Probe synthesis and phylogenetic analysis	25
2.4 Pharmacological treatments of amphioxus embryos	25
	xi

2.4.1 Perturbations of signalling molecules	25
2.4.2 EdU labelling of proliferating cells	26
2.4.3 Inhibition of proliferation through Hydroxyurea treatment	26
2.5 Injection of $\beta$ -catenin morpholinos and Bmp inhibition in frog embryos	28
2.6 Microscopy and image analysis	28
2.6.1 Manual image segmentation with Imaris	28
2.6.2 Automated nuclear segmentation with Ilastik – ADAGE	29
2.7 Sequencing	29
2.7.1 RNAseq	29
2.7.2 scRNAseq	30
<b>Chapter III – Conservation of an ancient anterior gene regulatory network</b>	
<b>patterning the chordate brain</b>	33
3.1 Introduction	33
3.1.1 Larval apical organs and their significance in the evolution of the CNS	33
3.1.2 Development of the apical organ in Ambulacraria: a conserved anterior network	34
3.1.3 Beyond deuterostomes and primary larvae: a short review on apical organs and aGRN across invertebrates	37
3.1.4 Aims of the chapter: a chordate aGRN	39
3.2 Characterization of a conserved deuterostome aGRN	40
3.2.1 Analysis of deuterostome scRNAseq datasets defines a conserved aGRN signature	40
3.2.2 Early genes are expressed in amphioxus	42
3.2.3 Late genes are expressed during gastrulation	47
3.3 Wnt signalling and the amphioxus aGRN	50
3.3.1 Early AZA treatment	50
3.3.2 Late AZA treatment	52
3.4 Discussion	55
3.4.1 Conservation of the aGRN in deuterostomes	55
3.4.2 Dynamic roles of Wnt signalling in chordate development	59
3.4.3 Conclusions	61
<b>Chapter IV – Nervous system development in the feather star</b>	
<i>Antedon mediterranea</i>	65
4.1 Introduction	65

4.1.1 Echinoderm neurobiology: lessons from eleutherozoans	66
4.1.2 A feather star is born: crinoid development	67
4.1.3 The crinoid nervous system	70
4.1.4 Aims of this chapter	70
4.2 Development of the apical organ in the doliolaria larva	71
4.2.1 Cell composition of the apical nervous system	71
4.2.2 Early specification of the apical plate	75
4.3 Discussion	78
4.3.1 AO development and aGRN conservation in crinoids	78
4.3.2 A map of the crinoid larval nervous system	80
4.3.3 Conclusions	82

## **Chapter V – Characterizing the development of cell type diversity in**

<b>the amphioxus nervous system</b>	<b>83</b>
5.1 Introduction	83
5.1.1 The evolution of cell types	83
5.1.2 What do we know about the amphioxus nervous system	84
5.1.3 Aims of the chapter	87
5.2 Early steps in neural development	88
5.2.1 Neurogenesis	88
5.2.2 Axogenesis	92
5.3 Defining amphioxus cell types with single cell RNA sequencing	93
5.4 Characterization of the amphioxus larval brain	97
5.4.1 The anterior cerebral vesicle – a homolog of the secondary prosencephalon	97
5.4.2 The posterior cerebral vesicle	103
5.4.3 The amphioxus hindbrain	103
5.5 Proliferation during amphioxus neurogenesis	106
5.5.1 Following the fate of proliferating cells	107
5.5.2 Inhibition of proliferation causes loss of brain cell types	111
5.6 Amphioxus neuroarchitecture across the life cycle	114
5.6.1 The amphioxus nervous system at metamorphosis	114
5.6.2 Cell populations in the adult brain	115
5.6.3 Distribution of neuropeptides across the amphioxus life cycle	121

5.7 Discussion	123
5.7.1 Differences in neurogenesis and proliferation underlie the regionalization of the amphioxus neural tube	123
5.7.2 Retino-hypothalamic fate of the amphioxus ANE	127
5.7.3 The adult brain	129
5.7.4 Conclusions	131
<b>Chapter VI – The aGRN in vertebrates and the evolution of the vertebrate brain</b>	<b>133</b>
6.1 Introduction	133
6.1.1 Aims of the chapter	133
6.2 What does the <i>FoxQ2</i> say? Conservation of a highly dynamic and poorly known gene	134
6.2.1 Phylogenetic analysis of <i>FoxQ2</i> genes	134
6.2.2 Expression of vertebrate <i>FoxQ2</i>	137
6.2.3 Analysis of <i>FoxQ2</i> cis-regulatory sequences in amphioxus	141
6.3 Apical, animal and anterior: relationship between CNS evolution and body axis formation	142
6.3.1 The organizer is not required for AP patterning	144
6.3.2 The evolution of BMP patterning in chordates	149
6.4 Discussion	154
6.4.1 Patterning and evolution of the vertebrate CNS	154
6.4.2 Conclusions	158
<b>Chapter VII – Discussion</b>	<b>161</b>
7.1 The evolution of the chordate nervous system	161
7.1.1 Tracing the origin of the chordate brain	161
7.1.2 The complex simplicity of the amphioxus nervous system	167
7.1.3 The evolution of the vertebrate forebrain	169
7.2 Conclusions and future directions	170
<b>Bibliography</b>	<b>173</b>
Appendix I – List of abbreviations	193
Appendix II – The mysteries of crinoid metamorphosis	195
Appendix III – Evolution of the endodermal expression of calcitonin	207
Appendix IV – Amphioxus digitalized atlas of gene expression	215

Appendix V – Dataset of gene expression with <i>in situ</i> HCR	221
Appendix VI – Additional material related to Chapter III	227
Appendix VII – Additional material related to Chapter V	231
Appendix VIII: Additional material related to Chapter VI	237
Acknowledgments	245



*It is such a privilege to be alive in the 21st century and to look at the stars and reflect on [the origin and laws of the universe], to look down a microscope into a single cell and see it's prodigious, stupefying complexity.*

*And then realize that there are trillions of those cells in your body, all conspiring together to produce a working machine that can walk, and run, and eat, and have sex, and think, reflect, understand! Understand why we exist, understand where we came from, understand where the universe came from. (...) What a privilege it is for each one of us to have in our heads an organ which is capable of comprehending that, of constructing a model of the universe inside our heads.*

R. Dawkins, Excerpt from "Something from Nothing"

*Never trust anything that can think for itself if you can't see where it keeps its brain.*

J.K. Rowling, "Harry Potter and the Chamber of Secrets"



# Chapter I – Introduction

## 1.1 A brief history of nervous system evolution

Every organism lives in an environment from which it needs to acquire resources and whose biotic and abiotic conditions are constantly changing. This simple principle provides one of the main foundations of the theory of evolution. The phenotypic characteristics that make organisms different from one another are encoded by genes in the DNA, which has three key features: it replicates, it mutates, and it is inherited from one generation to the next. Because the resources needed by organisms are limited, the genes that confer an advantage in obtaining these resources in a specific environment are more likely to be passed on to the next generation, and over time they will spread in the population at the expense of less successful gene variants and combinations (1). Considering this key relationship between the single organism and the environment, it is not surprising that mechanisms that allow cells to interpret and interact with the environment (including other cells) appeared early during the evolution of life (2–4). These early interactions relied on the diffusion of signalling molecules and on their specific binding to receptor proteins on the cell membrane that could trigger an intracellular reaction (5). However, with the evolution of multicellularity in different branches of the tree of life a significant advantage was given by increasing the speed and coordination of signal transmission through chemical transport and electrical conduction (5, 6). Among multicellular eukaryotes, animals (metazoans) are characterized by fast reactions to the environment, extensive motile capabilities and complex behaviour. These features are largely directed and controlled by the nervous system, a tissue that combines chemical and electrical signalling to maximize the speed at which information from the environment is collected and analysed to produce a motor output.

Most of the ~32 living animal phyla – groups of species that share a common body plan - possess neurons, the fundamental unit of the nervous system, suggesting that these cells appeared very early during metazoan evolution (7–9) (Figure 1.1). The reconstruction of nervous system origins is nevertheless hindered by the uncertainties at the base of the animal phylogenetic tree: poriferans (sponges) do not possess a nervous system and have traditionally been considered the sister group of the other metazoans. However, recent genome-wide comparisons have raised the alternative

hypothesis that ctenophores (comb jellies) occupy that position (10, 11) (Figure 1.1). This has profound implications on the origin of the nervous system. In the first scenario, the common ancestor of metazoans did not have a nervous system, which then evolved once in the ancestor of Eumetazoa (all animals except sponges). In the second scenario, the nervous system was either present in the common ancestor of all animals and was lost in the sponge lineage, or it independently evolved twice in comb jellies and Parahoxozoa (group that includes Cnidaria, Placozoa and Bilateria) (12–14). Interestingly, recent studies have also shown that the majority of the neural molecular machinery predates the origin of the nervous system and can even be found in sponges (15). It is still debated whether the first nervous system relied on synaptic transmission or on other forms of cell communication, such as chemical signalling through the paracrine release of small molecules like neuropeptides (8, 16). In any case, a nerve net composed of synaptically communicating neurons was present in the common ancestor of cnidarians and bilaterians (16, 17). While the precise appearance of this ancestor is still unclear, as no traces have been found in the fossil record, the prevailing hypotheses depict them as small marine animals composed, at least in some part of their life cycle, of two layers of ciliated cells, resembling a ciliated gastrula (hence the

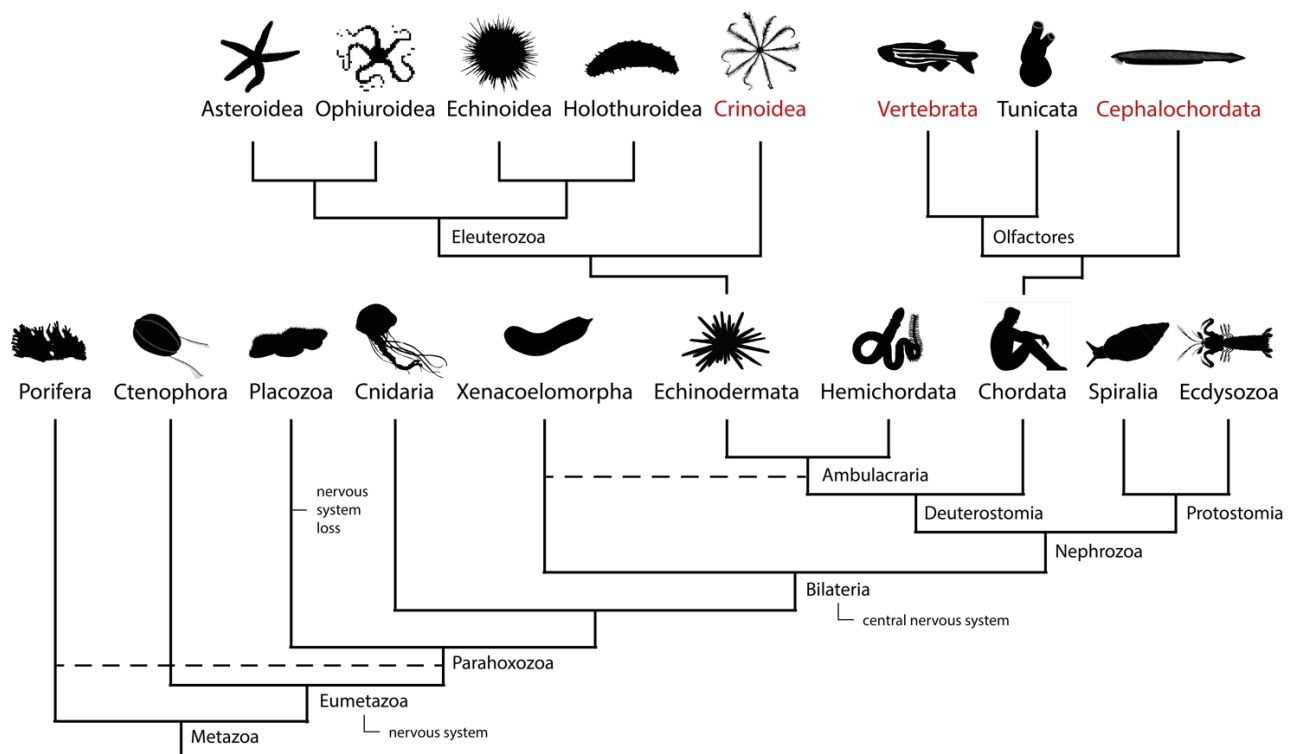


**Figure 1.1.** Phylogenetic relationships among extant animal phyla. Dotted lines indicate alternative phylogenies due to the existing uncertainties in the placement Ctenophora and Xenacoelomorpha. The tree represents one of the proposed scenarios for the evolutionary origin of the nervous system, while alternative hypotheses are described in the text. The groups of animals used in this thesis are highlighted in red. Silhouettes from Phylopic.org.

name *Gastrea* given to this hypothetical ancestor) (17, 18). These early ancestors likely possessed nerve nets distributed along the external, ectodermal layer of the animal, without any signs of centralization. The central nervous system (CNS) is loosely defined as the part of the nervous system where neurons are more concentrated and interconnected, and where sensory information is gathered to produce outputs that can be sent to target tissues (9). CNSs in various forms and degrees of complexity are found throughout the rest of metazoans, the bilaterians. However, the details of the origin of the CNS are still obscure (9, 19–22). The lack of a precise definition of CNS makes it difficult to compare different organisms (see below): it is easy to recognize the CNS when it is large and anatomically well-defined as in vertebrate or insect brains (another term that has qualitative and imprecise definitions), but the distinctions can become blurry in animals with either simple morphology or complex life cycles (9, 23). Furthermore, conflicting hypotheses are difficult to resolve due to the unclear phylogenetic position of another animal phylum, the Xenacoelomorpha. Many xenacoelomorphs possess an anterior CNS connected to a nerve plexus that runs through the body (24, 25). Some phylogenetic analyses indicate that this group branches at the base of Bilateria, before the split between protostomes and deuterostomes (which then form a separate taxon called Nephrozoa). In this scenario the CNS was already present in the ancestor of bilaterians, the Urbilaterian (26). Other studies have alternatively placed xenacoelomorphs within deuterostomes, forming the taxon Xenoambulacraria with echinoderms and hemichordates (27). If this hypothesis is correct, it opens the possibility that nervous systems became centralized independently in the two main bilaterian lineages. The comparison of protostome and deuterostome nervous systems also does not give a clear answer on the ancestral urbilaterian condition. While many of the genes involved in the regionalization of the nervous system are conserved between the two taxa, recent studies on dorsoventral (DV) patterning across phyla have revealed a more dynamic evolution of nerve cords, giving support to the idea of independent evolution followed by occasional convergence (20, 28, 29). The results presented in this thesis contribute to this ongoing debate, and I will propose that at least some aspects of CNS specification are ancestral to Bilateria.

## 1.2 EvoDevo and the revolution of comparative biology

The previous section pointed at some of the remaining uncertainties and controversies in the reconstruction of the history of life, focusing on the difficult placing of enigmatic phyla at key junctions in the tree of life. However, over the years a wealth of information has been acquired on

the evolution of the nervous system, which is all the more remarkable given the startling diversity of neural architectures in modern animals reflecting the variety of their body plans (30, 31). While they are all composed of neurons, the cnidarian nerve nets, the vertebrate brains and spinal cords, the ladder-like nerve cords of flatworms and the pentaradial nerve cords and circumoral nerve rings of echinoderms are difficult to compare to reconstruct which features are ancestral to different phyla.

A way to overcome the problem of the extensive variation in animal forms is to study and compare how nervous systems form during embryonic development. The comparative embryology approach has been popular in the evolutionary field from Darwin onwards for two main theoretical reasons: first, von Baer's laws had long clarified that although ontogeny does not strictly recapitulate phylogeny, general features in the embryo appear earlier in development than specific ones and are more broadly shared among different organisms (32). Second, it soon became clear that evolution works by changing the way traits are built during development: most of the changes in phenotypic characteristics (and therefore most mutations) that are subjected to the scrutiny of natural selection are actually changes in the way they develop in the embryo. After the formulation of the "Modern Synthesis" that united Darwin's work with Mendel's laws, population genetics and paleontology (33), in the second half of the XX century the new field of molecular biology joined forces with evolution, genetics and embryology to look at the genetic control of development in different animals. It was generally thought that different body plans relied on different genes evolving independently in each animal lineage, but early studies completely overturned this hypothesis: many of the genes that control development and body patterning are extremely well conserved and therefore have an ancient origin. The extraordinary discovery led to the establishment of a new field, evolutionary developmental biology (EvoDevo) that started to look with renewed enthusiasm at the similarities and differences between embryos of distantly related organisms (34, 35). It soon became clear that not only are many of these "toolkit genes" extremely conserved, but they are functionally similar and can work from one species to the other. However, if there is such extensive conservation, how can we explain the variety of forms that we see in the natural world? The second revolution of EvoDevo was the discovery that changing when (heterochrony), where (heterotopy) or how much (heterometry) a gene is expressed are some of the predominant ways through which animals evolve. The finding shifted attention from the coding portion of the genome to the regulatory sequences that control gene expression through the binding of transcription factors (36, 37). This came in parallel with the analysis of the complexity of gene regulatory networks (GRNs), models of the set of

transcriptional regulators (including transcription factors) and their interactions that control the specification, differentiation and identity of cells (38). By changing the composition of regulatory sequences or the availability of transcription factors during development, drastic morphological changes can be achieved without modifying the coding sequence of genes (35).

### 1.3 Homology: a tricky definition

Through the EvoDevo approach, we can not only understand the relationships between different structures and animals, but we can uncover *how* these structures evolved: what molecular and developmental changes were favoured during the evolution of specific traits that we see in animals today. As such, EvoDevo has greatly enhanced our ability to reconstruct the features of ancestors to particular groups. This reconstruction is generally based on the principle that if a trait (from genes to organs and systems) is present in all the descendants of an ancestor, the most parsimonious explanation is that the ancestor also possessed the same trait, which was then conserved during the evolution of the descendants. Traits that are shared between organisms due to their descent from a common ancestor are called homologous. The term homology was first introduced by Richard Owen to describe “the same organ in different animals under every variety of form and function” (39), and has since generated a continuous discussion on its precise meaning and application. In recent years, the advancements in our understanding of the complexity of GRNs driving cell type specification (36, 40, 41) and the potential to explore the transcriptome and regulatory landscape in each cell through single cell sequencing technologies (42) have reinvigorated the debate on what should be considered homologous (43, 44). For example, structures that have evolved independently, such as the complex camera eyes of vertebrates and cephalopods or the segmented bodies of annelids, insects and vertebrates, often use orthologous genes wired with a similar regulatory logic during development (35, 45). This is usually explained through the concept of deep homology, which refers to the conservation of ancient GRNs that have been deployed in a similar way in different lineages to form “morphologically disparate animal features” (46). However, a problem with the concept of deep homology is the difficulty in setting an objective threshold on the level of similarity between GRNs. How many genes or interactions must be in common between two species for the structure to be considered deeply homologous? And how is the notion that GRNs can modify extensively during evolution integrated into this concept? If few common genes are enough to define deep homology, then the definition loses power and can lead to erroneous conclusions on the

evolutionary history of characters. If the definition is too stringent, then it fails to account for the broad evolutionary changes that happened in the hundreds of millions of years since the origin of modern animal phyla during the Cambrian (47). In response to these problems, the discussion recently moved to the consideration that homology can be found at all levels of biological organization, from genes/molecules to GRNs, cell types, tissues and whole anatomical structures (48–50). These levels are not necessarily associated from an evolutionary point of view: gene phylogenetic trees, for instance, can be quite distinct from species trees (16, 51). Therefore, homology should reflect the historical continuity of a specific character but should be defined specifically for the *level* of organization that is under investigation. This definition solves some of the problems with deep homology: it takes into account that regulatory networks are often more conserved in the phylogenetic tree than anatomical structures, but also considers that two structures can be homologous at the anatomical level (the brains of vertebrates) even if in each lineage some unique features have evolved that do not have a clear relationship of homology (the different neuronal types that evolved in each vertebrate lineage) (49, 50). Moreover, this approach can take into account those instances of repeated trait loss and reacquisition, a particular version of the (rather old) concept of atavism (52, 53). For example, stick insects (Phasmatodea) likely lost their wings ancestrally but then regained them several times independently (54–56), though this view has been contested (56). At the level of the anatomical structure, stick insects' wings are not homologous to the ones of other flying insects, because they were not continuously present in the ancestors that led to them, and were secondarily reacquired. However, future molecular studies may reveal that many of the genes and the regulatory networks that control their development are in fact homologous (54). Similar examples have been shown for limpet shell coiling and skink digit number (57, 58).

## 1.4 The vertebrate brain: development and organization

While the anatomy and development of the nervous system in many phyla have been described, little is known about how nervous systems changed from one form to the other and how modern taxa evolved their neural organization from common ancestral forms. As mentioned above, this is mainly due to the diversity of neural architectures that does not allow the simple testing of homology based on similarity at different levels of organization. These gaps of knowledge include the origin and evolution of the nervous system in our own phylum, the Chordata. Chordates are divided into three main taxa - vertebrates, tunicates and cephalochordates - that share a common

body plan: a notochord (giving the name to the phylum), pharyngeal slits, a post-anal tail, an endostyle/thyroid and a hollow neural tube (59, 60). The neural tube develops dorsally from an epithelial sheet of neuroectoderm, the neural plate, through the process of neurulation. In all vertebrates, the rostral (i.e. cephalic/anterior) portion of the neuroectoderm develops into a large brain that receives and interprets most of the sensory information and produces outputs that are sent to the body through the rest of the neural tube, the spinal cord (61). Because of its complexity and its role in complex vertebrate behaviour the origin of the brain has long been of great interest for evolutionary biology (17, 23, 31, 62, 63). The vertebrate brain first develops as a three-vesicle expansion of the anterior neural tube: the prosencephalon (forebrain), mesencephalon (midbrain) and rhombencephalon (hindbrain). Prosencephalon and rhombencephalon undergo further subdivision: the forebrain forms the telencephalon and the hypothalamus - together known as the secondary prosencephalon - as well as the diencephalon; the hindbrain forms the metencephalon and myelencephalon, continuous with the spinal cord (Figure 1.2A). Each portion of the brain can be distinguished anatomically as well as molecularly by gene co-expression patterns that give rise to conserved molecular signatures for each region. For example, *Six3*, *Fezf*, *Pax6* and *Otx* genes mark rostral brain areas, while *Irx*, *Gbx* and *Hox* genes are expressed caudally (64–67) (Figure 1.2B).

Early in development, these regions can be subdivided in transient antero-posterior (AP) segments called neuromeres (68). The forebrain is divided into prosomeres, the midbrain into mesomeres and the hindbrain into rhombomeres. These segments can be defined molecularly by gene expression (and anatomically in the case of rhombomeres) and provide a framework for the formation of adult brain regions later in development (Figure 1.2B). The molecular specification of neuromeres precedes the morphological development of brain vesicles, such that they can be detected in the neural plate (68, 69). Furthermore, the neural tube is divided along the DV axis into roof plate, alar plate, basal plate and floor plate. The roof and floor plate are important signalling centres that produce bone morphogenetic proteins (Bmps) and *sonic hedgehog* (*Shh*) respectively (68, 70). According to the prosomeric model, the forebrain is divided into five prosomeres: hp1 and hp2 form the secondary prosencephalon, while p1-p3 form the diencephalon. The hypothalamus is separated from the diencephalon and is the most rostral portion of the neural tube. The telencephalon is therefore a dorsal structure that develops completely from the alar portion of the anterior prosomeres. The eye fields from which the retina develops are located within the alar portion of the hypothalamus before they evaginate (68, 71) (Figure 1.2B).

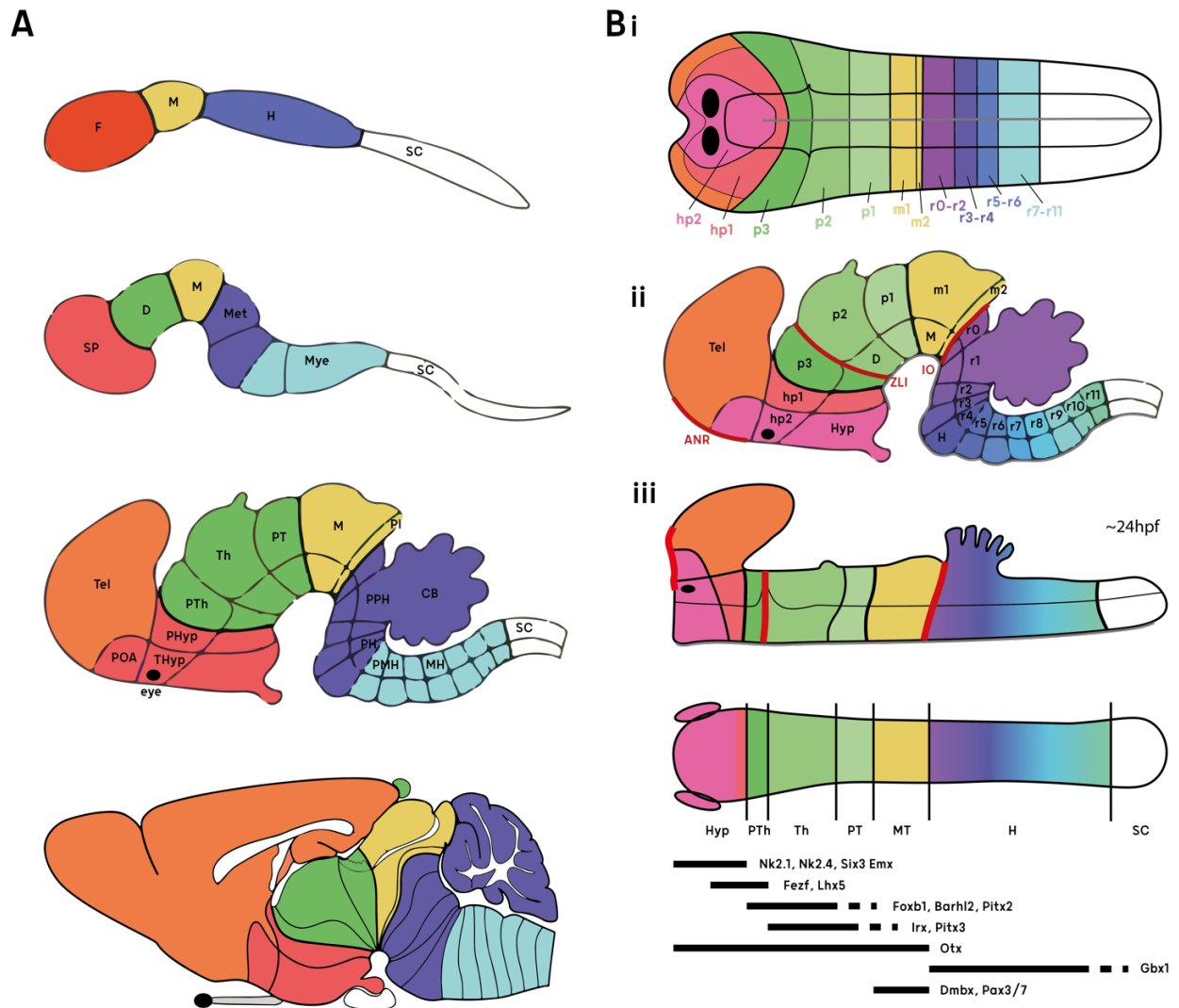


**Figure 1.2.** Developmental organization of the vertebrate brain according to the prosomeric model. **A.** Progressive stages of mouse brain development showing the AP regionalization of the neural tube. The secondary prosencephalon (SP) forms the telencephalon (Tel), optic vesicles and hypothalamus (Hyp), divided in preoptic area (POA) tuberal (THyp) and peduncular (PHyp) hypothalamus. The diencephalon (D) forms the prethalamus (PTh), thalamus (Th) and pretectum (PT). The midbrain forms the midbrain proper (M) and the pre-isthmus (PI). From the hindbrain (H), the metencephalon (Met) forms the prepontine (PPH) (including the cerebellum (CB)) and pontine (PH) areas, while the myelencephalon (Mye) forms the premedullary (PMH) and medullary (MH) areas. **B.** These regions develop from transient rostro-caudal divisions of the neuroectoderm, the neuromeres, which are already visible at the neural plate stage (i, dorsal view). The SP is composed of two prosomeres, hp1-2. While they both contribute to the Hyp, the Tel forms from hp1 and the eyes from hp2. The D forms three prosomeres, p1-p3, which correspond to the three subdivisions later in development. The M forms two mesomeres, m1 and m2, while the H is composed of 11 rhombomeres (r1-r11) plus the isthmus (r0). The three secondary brain organizers form in the neural tube and are indicated in red (ii, mouse brain, lateral view). The neuromeric subdivisions are controlled by the expression of combinations of transcription factors which together specify and maintain their identity (iii shows a linearized schematic of the mouse neural tube shown in ii from lateral (top) and dorsal (bottom) views). Images modified from (69, 423).

Moreover, the entire secondary prosencephalon is not influenced by signalling from the notochord, which in vertebrates is located more posteriorly, but rather from the prechordal mesoderm and anterior endoderm (72). Finally, the specification of different cell types in each region requires three additional signalling centres that form within the brain, called secondary organizers. The anterior neural ridge (ANR) is located in the rostro-dorsal area of the neural tube and secretes fibroblast growth factors (FGFs) that pattern the telencephalon. The zona limitans intrathalamica (ZLI) expresses *Shh* within the diencephalon, separates the prethalamus and thalamus, and forms at the boundary of anterior *Fezf* and posterior *Irx* expression. The isthmic organizer (IO) is located at the midbrain-hindbrain boundary (MHB), separating the expression of anterior *Otx* and posterior *Gbx*, and secretes *Wnt1* and *Fgf8* (64, 72) (Figure 1.2B).

The early development of the brain can therefore be understood in terms of a progressive regionalization and refinement of these regions along the AP and DV axes. The regionalization is influenced by signalling molecules produced within the brain or by surrounding tissues; these signals restrict and maintain molecular signatures and GRNs to specific areas, where the developing neurons will acquire specific characteristics, including the type of neurotransmitters and neuropeptides used and the patterns of connectivity.

## 1.5 Amphioxus and the evolutionary origin of the chordate brain

While the brain regions described above vary from species to species in size and shape, they are clearly shared by all vertebrates and thus date back to their ancestor (62, 73). Therefore, if the ancestor already possessed a complex, regionalized brain, a key question remains: how and when did this structure appeared in evolution? To answer this question, a large number of studies have analysed the nervous system in the two groups of invertebrate chordates, tunicates and cephalochordates (60, 74–76). Both groups have a swimming larval stage with a dorsal neural tube and lack the two rounds of whole genome duplications that occurred during early vertebrate evolution (77). However, tunicates have a fast-evolving genome and a highly derived adult body that forms after a drastic rearrangement and degeneration of larval organs during metamorphosis. This drastic rearrangement includes the CNS, which undergoes extensive degeneration and remains only as a ganglion in the sessile adult (78). On the other hand, cephalochordates are the sister group

of the other chordates, branching at the base of the phylum (Figure 1.1) and maintain all the key chordate features throughout their life cycle (Figure 1.3C). Moreover, they are characterized by a slow rate of amino acid substitution and genome architecture evolution (79, 80) (although more recent studies are revealing a more complex scenario with a high level of gene duplication (81)). Cephalochordates are divided into three genera of filter-feeding animals (*Branchiostoma*, *Asymmetron* and *Epigonychtys*) called amphioxus or lancelet. Initially classified as gastropod molluscs, they were placed as the sister group to vertebrates in the 19<sup>th</sup> century and then moved as the sister group to all other chordates by molecular phylogenetics (82). The key phylogenetic position of amphioxus as well as its genomic and morphological features make it an ideal model to compare with the other chordates to reconstruct the features of the chordate ancestor. It is perhaps unsurprising therefore that with the advent of molecular biology amphioxus has been rediscovered as an important organism for EvoDevo, and a wealth of new studies complemented developmental descriptions from the 19<sup>th</sup> and early 20<sup>th</sup> century with new data on gene expression (75, 83).

Interestingly, the early development of amphioxus resembles that of many ambulacrarians (echinoderms + hemichordates) such as sea urchin. The egg has little yolk and develops through holoblastic cleavage to form a spherical hollow blastula with a single cell layer (Figure 1.3A). This is followed by invagination and then involution of the prospective endomesoderm to form a cup-shaped ciliated gastrula with a posterior blastopore (84). The gastrula then flattens dorso-ventrally and a dorsal neural plate elongates through convergent-extension following the elongation of the rest of the body (Figure 1.3B). As the neural plate starts to fold during neurulation, it is covered by the dorsal epidermal ectoderm that spreads from each side, a process that is different from vertebrate neurulation in which the epidermis covers the neural tube after it has closed. In amphioxus instead the neural tube closes after being internalized, starting from the anterior and posterior tips and continuing towards the centre (84). At the 10 somites (ss) stage neurulation is completed, but the anterior neuropore remains open throughout the animal's life. Towards the end of neurulation, the anterior portion of the neural tube expands to form a cerebral vesicle (CV) visible at the larval stage (Figure 1.3B). While in ascidians metamorphosis causes a complete change of the body plan, the adult amphioxus maintains its chordate features and look even more similar to vertebrates due to the loss of larval asymmetries (Figure 1.3C).

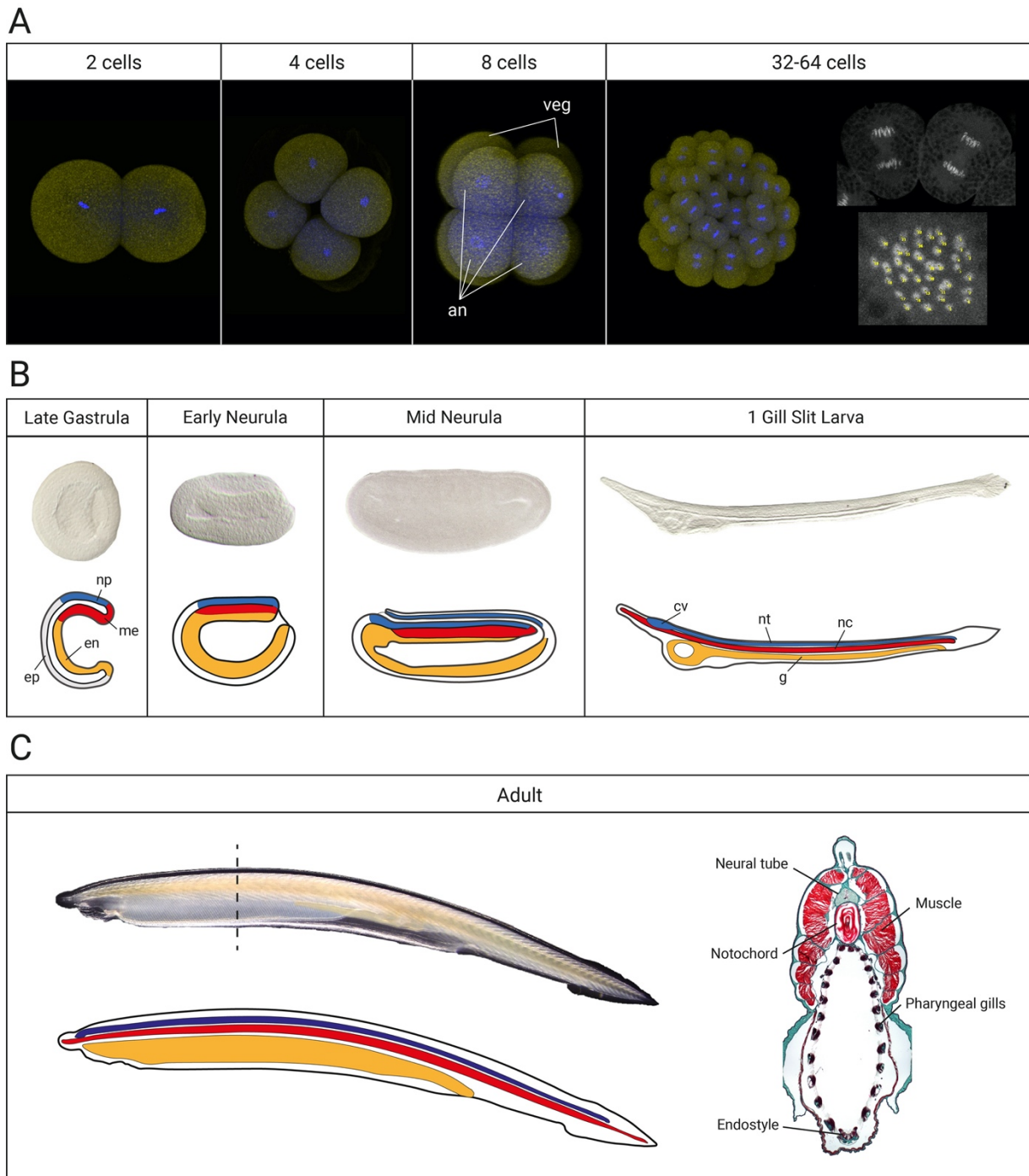


**Figure 1.3.** Cephalochordate development and body plan. **A.** Early embryogenesis shows the first two equal divisions followed by a third equatorial division forming smaller animal cells and bigger vegetal cells. At high magnification it is possible to count 38 chromosomes in mitotic cells, confirming bioinformatic predictions. **B.** Gastrulation and neurulation highlighting the schematic organization of embryonic tissues. **C.** Post-metamorphic amphioxus maintains a similar organization of the larval body. Trichromatic staining of cross sections highlight the presence of typical chordate characters. Abbreviations: an: animal blastomeres, cv: cerebral vesicle, en: endoderm, ep: epidermis, g: gut, me: mesoderm, nc: notochord, np: neural plate, nt: neural tube, veg: vegetal blastomeres.

The amphioxus CV is not regionalized morphologically, but molecular and ultrastructural studies have shown that it is composed of a high number of cell types (85, 86). Furthermore, from early development it displays AP patterns of transcription factor expression that resemble those involved in vertebrate brain regionalization. In particular, the anterior portion of the amphioxus neural plate expresses anterior markers like *Fezf* and *Otx*, which form posterior boundaries with *IrxA* and *Gbx* respectively, similarly to vertebrates (87). Moreover, at the anterior tip of the CV at the larval stage a single eyespot develops, composed of photoreceptors and associated cells that have similar gene expression to retinal neurons (88). Based on these data, a scenario has been proposed in which the molecular regionalization of the neural tube and in particular the presence of an anterior brain precedes the appearance of vertebrates and dates back to the ancestor of all chordates (21, 87, 89). However, in amphioxus no homologs of the secondary brain organizers have been found despite the presence of stark expression boundaries.

But if a brain was present in the chordate ancestor, the question posed about its origin is just pushed back in time: when did the chordate brain evolve? And from what type of nervous system did it evolve? If we broaden the comparative framework to include the other two deuterostome phyla, echinoderms and hemichordates (which together form the taxon Ambulacraria, Figure 1.1), the comparison becomes much more difficult due to the vast differences in body plan among the three phyla. Chordates have a highly centralized CNS, a dorsal tube divided into brain and a spinal cord. Hemichordates have a de-centralized nerve plexus running at the base of the epidermis, characterized by a varying degree of neuron concentrations in the form of cords running dorsally and ventrally in enteropneusts or aggregates associated with the tentacles in pterobranchs (90–92). Echinoderms have a bipartite (eleutherozoans) or tripartite (crinoids) nervous system that follows the derived pentaradial organization of the body plan, generally with a central nerve ring and radial nerves stretching along the arms, where a basiepithelial plexus is also present (93). This diversity means that it is very difficult to understand the ancestral condition in ambulacrarians as well as in deuterostomes. The lack of brain-like structures in adult ambulacrarians is particularly problematic for the reconstruction of brain origins: either a brain-like structure was present in the deuterostome ancestor and lost in the Ambulacraria lineage or the chordate brain evolved independently, which would be in contrast with some of the evidence on the similarities between vertebrate and protostome nervous systems (21, 46, 94).

Turning to development, most groups of echinoderms and hemichordates develop indirectly through a swimming ciliated larval stage. A planktotrophic “dipleurula” larval stage has long been considered ancestral to ambulacrarians (95). Dipleurula-type larvae vary in shape across ambulacrarians and some taxa evolved lecithotrophic larvae (that obtain nutrients from the yolk) or direct development secondarily, but they all possess some shared features: they are bilaterally symmetrical, they swim using cilia arranged in ciliary bands, and they show an apical/anterior concentration of neurons called *apical organ* (AO) (95, 96). The widespread presence of AOs suggests that the ancestor of ambulacrarians had, at least in some stage of its life cycle, an anterior neural structure that was conserved during the evolution of echinoderms’ and hemichordates’ body plans. This is further supported by more recent molecular studies showing deep conservation in the genetic control of AO development (97). The significance of AOs in the evolution of deuterostome nervous systems will be further explored in Chapter III. Moreover, studies in hemichordate embryos have shown that the ectoderm, which is broadly neurogenic, is molecularly regionalized similarly to chordate CNS, with anterior expression of *Six3* and *Otx*, and posterior expression of *Gbx* and *Hox* genes (92). But while stark *Fezf-Irx* and *Otx-Gbx* boundaries are not present in hemichordates, putative homologs to vertebrate brain secondary organizers have been identified (98). This quick overview reveals a seemingly complex evolutionary pattern in which some aspects of nervous system specification and development appear conserved in different deuterostome phyla, while others, including the final adult neural architecture, are widely diverse.

## 1.6 Aims of the thesis: a phylogenetic story

The primary aim of this work is to gain insights into the evolution of chordate CNS patterning, focusing specifically on the anterior portion of the neuroectoderm that gives rise to the brain. To break this vast question into testable hypotheses, I will focus on the evolution of GRNs and signalling pathways that shape nervous system development in deuterostomes. Therefore, I will take a phylogenetic approach by using the European amphioxus *Branchiostoma lanceolatum* as the main model organism but also considering the diversity of deuterostome nervous systems (Figure 1.4). Each chapter focuses on a key step during the evolution of chordate nervous systems:

- ◆ Chapter III identifies a conserved anterior gene regulatory network (aGRN) involved in the specification and patterning of anterior neuroectoderm (ANE) identity in deuterostomes.

- ◆ Chapter IV focuses on the development of the nervous system in an understudied group of echinoderms, the crinoids, to test the conservation of the aGRN across ambulacrarians.
- ◆ Chapter V describes the development of the amphioxus nervous system taking into account the progression of neurogenesis, the regionalization of the brain through cell proliferation and cell type specification, and the postembryonic development of the metamorphic and adult brain.
- ◆ Chapter VI looks at how the aGRN modified in the vertebrate lineage from the condition reconstructed for the chordate ancestor, and how this might have impacted the evolution of the vertebrate brain.

Overall, this thesis sheds light on CNS evolution and brain origin, arguing for the conservation of ANE patterning in deuterostomes despite the wide anatomical differences between phyla. Moreover, my work broadens our knowledge on the development and regionalization of the amphioxus nervous system at single cell resolution, providing a new basis for future functional studies. Finally, I begin to address how the vertebrate nervous system changed from the chordate ancestor, formulating new hypotheses that can be tested in future works.

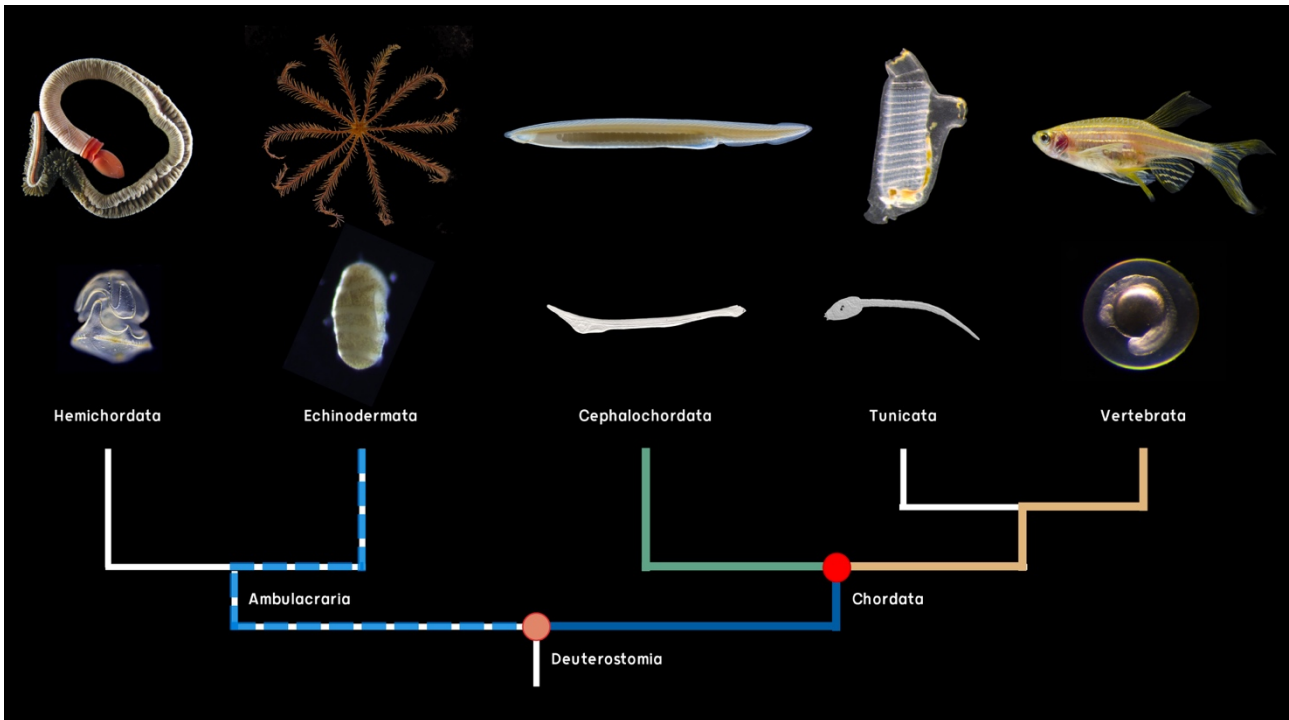


**Figure 1.4.** Conceptual framework and phylogenetic approach of the thesis. The aims can be divided into three themes, addressed in specific results chapters. The first theme (blue) is the origin of the chordate brain from the common ancestor of deuterostomes. This question is divided into two chapters: chapter III focuses on the conservation of an anterior gene regulatory network in the lineage leading to chordates (dark blue), while chapter IV describes the development of the nervous system in crinoid echinoderms in the Ambulacraria lineage (light blue). The second theme (green) is the characterization of development, cell type composition and morphogenesis of the amphioxus nervous system and is discussed in chapter V. The third theme (yellow) is the evolution of vertebrate brain features from the chordate ancestor and is the topic of chapter VI. Representative adult and developmental stages for each group are shown. Hemichordate pictures taken from (165).



## Chapter II – Materials & Methods

As the results described in each chapter use similar methodologies, the materials and methods are presented together and reference to specific sections is provided in the following chapters. A list of abbreviations used in this thesis can be found in Appendix I.

### 2.1 Animal source, rearing and fixation

#### 2.1.1 Amphioxus

##### *Collection and husbandry*

Adult individuals of European amphioxus *Branchiostoma lanceolatum* were collected from three locations: Banyuls-sur-Mer (France), Barcelona (Spain) and Helgoland (Germany). The animals were transported to a custom-made facility in the University of Cambridge (UK), where they were maintained and bred as described in (99). The water was obtained by mixing natural and artificial sea water (ASW, made from sea salt (pro-reef sea salt, Tropic Marin<sup>®</sup>, Germany) diluted in reverse osmosis filtered water). The following water parameters were checked: temperature (between 10°C and 13°C), pH (~8.1) salinity (~52mS), carbonate hardness (KH), level of oxygen (O<sub>2</sub>), ammonia (NH<sub>4</sub>), nitrites (NO<sub>2</sub>), nitrates (NO<sub>3</sub>) and phosphates (PO<sub>4</sub>). Animals were fed with five algae species grown in the facility: *Tetraselmis suecica*, *Nannochloropsis oculata*, *Dunaliella polymorpha*, *Tisochrysis lutea* and *Isochrysis galbana*. Metamorphic stages were collected from the plankton in Kristineberg (Sweden) by Dr Elia Benito-Gutiérrez (Department of Zoology, University of Cambridge).

##### *Spawning and staging*

Spawning was induced between May and July through heat-shock as described in (99). After in vitro fertilization, all embryos were raised in Petri dishes in filtered ASW at 21°C. For early embryos up to the early neurula stage, the nomenclature for staging was taken from (100), while during neurulation the number of somites (ss) was used to unbiasedly identify embryonic stage.

##### *Fixation*

Fixation was performed as described in (101). At the desired stages, embryos were fixed overnight in 3.7% paraformaldehyde (PFA) + 50% MOPS buffer (3-(N-morpholino)propanesulfonic acid; Sigma, M1254) at 4°C, washed in sodium phosphate buffered saline (PBS) and stored in 100%

methanol (MeOH) at -20°C. Adult specimens were anesthetized in 0.016% tricaine in distilled water for 30mins, cut into four sections and then fixed in 3.7% PFA + MOPS for 24 hours at 4°C. Fixed specimens were either stored in MeOH at -20°C or embedded in low-melting agarose and sectioned using a Leica VT100S vibratome as described in (101). Vibratome sectioning was performed by Michael Schwimmer (Department of Zoology, University of Cambridge), and sections were stored in 100% MeOH at -20°C. For brain whole-mount immunohistochemistry (see section 2.2.1) anesthetized animals were pinned to a petri dish coated with hard gelatine and manually dissected using forceps to remove the skin, gut and most of the muscles. The brain and anterior portion of the notochord were then fixed in 3.7% PFA + MOPS overnight at 4°C and stored in MeOH at -20°C.

### 2.1.2 Crinoids

Adults of the feather star *Antedon mediterranea* were collected during winter at Le Grazie, Golfo della Spezia (Italy) by Prof Roberta Pennati and Dr Silvia Mercurio (Department of Environmental Science and Policy, University of Milan, Italy). After collection they were kept in aquaria in ASW (Instant Ocean®, Aquarium System in deionized water). The animals naturally spawned in the aquarium and embryos at selected stages were collected directly from the female arms, where they remain attached until the doliolaria larva stage. The doliolaria stage hatches and swims briefly before attaching to the substrate to metamorphose. Metamorphic stages and post-metamorphic pentacrinoids were therefore collected from plastic grids placed inside each aquarium. All stages were fixed in 4% PFA + MOPS, but before fixation pentacrinoids were relaxed by incubating them in 3.5% MgCl<sub>2</sub> in ASW for 10 minutes. Fixed specimens were stored in 100% MeOH at -20°C.

### 2.1.3 Zebrafish

Embryos of *Danio rerio* were obtained from wild-type lines (Tüpfel Long Fin (TL), AB or AB/TL) from the facility in the Department of Physiology, Development and Neuroscience, University of Cambridge in collaboration with Dr Benjamin Steventon and Dillan Saunders (Department of Genetics, University of Cambridge). Embryos were obtained and raised in standard E3 medium at 28°C. The research on these embryos was done following ethical review by the University of Cambridge Animal Welfare and Ethical Review Body (AWERB). Embryos were staged as in (102), fixed overnight in 4% PFA at 4°C and stored in MeOH 100% at -20°C. Paraffin-embedded microtome

sections of 4% PFA fixed zebrafish adults and larvae at 8 days post fertilization (dpf) were obtained by Dr Andrew Gillis (Marine Biological Laboratory, University of Chicago).

#### 2.1.4 Frogs

Embryos of the African clawed frog *Xenopus laevis* were acquired during the “Embryology: concepts and techniques in modern developmental biology” course at the Marine Biological Laboratory, University of Chicago (Woods Hole, MA, USA). Embryos were reared at 15°C in 1/3 ML medium, staged according to (103), fixed in 4% PFA overnight at 4°C and stored in 100% MeOH at -20°C. The research on frog embryos was done following ethical review by the University of Cambridge Animal Welfare and Ethical Review Body (AWERB).

#### 2.1.5 Skates

Embryos of the little skate *Leucoraja erinacea* were collected at the Marine Biological Laboratory, University of Chicago (Woods Hole, MA, USA) by Dr Andrew Gillis and staged according to (104). After fixation in 4% PFA overnight at 4°C specimens were embedded in paraffin and sectioned by Dr Andrew Gillis as described in (105).

## 2.2 Immunohistochemistry

### 2.2.1 Amphioxus

#### *Embryos and larvae*

Samples were rehydrated through a MeOH/H<sub>2</sub>O series in 4-well plates and bleached by incubating them in bleaching solution (5% hydrogen peroxide, 3% formamide in 0.2X SSC) under bright light on a sheet of aluminium foil for 30 minutes. Embryos were incubated in permeabilization solution (PBS + 1% Triton X-100) overnight at 4°C and then placed in blocking solution (PBT + 0.1% BSA + 5% NGS) for 3 hours at room temperature. Primary antibodies were diluted in block solution and incubated with the samples overnight at 4°C (Table 1). The next day, after excess of antibody was removed through washes in PBT, samples were left for two hours in blocking solution before replacing it with secondary antibodies (Table 1) and DAPI (1 µg/ml) diluted in blocking solution

and incubating overnight in the dark at 4°C. Finally, embryos and larvae were washed thoroughly with PBT and mounted in 80% glycerol in glass-bottomed dishes for imaging.

### *Metamorphosis*

Metamorphic animals are considerably bigger than embryos and larvae, therefore the protocol was modified to include further permeabilization. During the first day, rehydrated and bleached specimens were left overnight in permeabilization solution at 4°C. The following day specimens were treated with Proteinase K (PK) 8 µg/ml in PBT for 10 minutes at 37°C and then post-fixed for 20 minutes in 4% PFA + MOPS.

### *Adults*

Adult sections were processed as described in (106). Sections were permeabilized through overnight incubation in permeabilization solution at 4°C and in PK 1 µg/ml in PBT for 10 minutes at 37°C, followed by fixation for 20 minutes in 4% PFA + MOPS. Brain whole-mounts were bleached for 45 minutes, then treated with permeabilization solution overnight at 4°C and with PK 4 µg/ml for 15 minutes at 37°C and post-fixed in 4% PFA + MOPS for 20 minutes. A longer incubation of 2 days in primary antibody was also used to improve penetration. Both samples were mounted in glass-bottomed dishes in Aqua Polymount, which solidifies preventing bending and movement.

<b>Antigen</b>	<b>Raised in</b>	<b>Supplier</b>	<b>Concentration</b>
Acetylated tubulin	Mouse	Sigma (T6793)	1:250
Glutamate	Rabbit	Sigma (G6642)	1:500
Serotonin	Rabbit	Sigma (S5545)	1:200
Phosphorylated Histone H3	Mouse	Abcam (ab5176)	1:600
Phosphorylated Smad1/5/8	Rabbit	Cell Signaling (9511S)	1:100
Phosphorylated Smad2/3	Rabbit	Abcam (ab118334)	1:10000
XlSox3	Mouse	DSHB (DA5H6)	1:200
Rabbit IgG - 546	Goat	Abcam (150083)	1:250
Mouse IgG - 488	Goat	Invitrogen (84540)	1:250
<i>A. rubens</i> calcitonin (ArCT)	Rabbit	Antiserum (107)	1:3000

**Table 1.** List of antibodies used in this work

### 2.2.2 Crinoids

A new protocol for whole-mount immunohistochemistry on *A. mediterranea* developmental and post-metamorphic stages was optimized as an extension of the one previously designed for sections (108). Samples were rehydrated through a MeOH/H<sub>2</sub>O series in Eppendorf tubes and washed in PBT. Pentacrinoids were decalcified overnight in a solution of 5% EDTA in nuclease free water (nfH<sub>2</sub>O). All samples were bleached in bleaching solution under light on aluminium foil. Doliolaria larvae were bleached for 45 minutes, while embryonic and pentacrinoid stages were bleached for 20 minutes. For permeabilization, doliolaria larvae were then incubated in a stronger version of permeabilization solution (PBS + 1.5% Triton X-100) overnight at 4°C; while embryonic and pentacrinoid stages were incubated in permeabilization solution for 15 and 30 minutes respectively and then left in PBT overnight at 4°C. The following day, doliolaria larvae were further permeabilized with PK treatment at a concentration of 4 µg/ml at 37°C for 10 minutes followed by post-fixation in 4% PFA. Samples were then blocked for 2 hours in a solution of 50%NGS /50%PBT and incubated for two days at 4°C in blocking solution (PBT + 0.1% BSA + 5% NGS) with primary antibody. After several washes in PBT, samples were again incubated in blocking solution which was then replaced with the secondary antibody and DAPI (1 µg/ml) in blocking solution and left overnight in the dark at 4°C. On the last day samples were thoroughly washed in PBT and mounted in 100% glycerol in glass-bottomed dishes.

### 2.2.3 Frogs

Immunofluorescence in *X. laevis* followed the same protocol as for amphioxus, except with no permeabilization solution applied after bleaching.

## 2.3 *In situ* hybridization chain reaction: HCR

Third generation HCR is a fluorescence hybridization technique that allows multiplex detection of up to 5 genes in a single specimen with high signal-to-background ratio (109). The technique is based on the use of two technologies: first, a set of 25 nucleotide long probe pairs (the individual probes of the pair are separated by 2 nucleotides) each containing half of an additional sequence called initiator. Second, two sets of fluorophore-tagged hairpins (H1 and H2), of which H2 can bind to H1 and H1 can bind to both H2 and the full initiator. The use of a split initiator reduces noise as H1 will

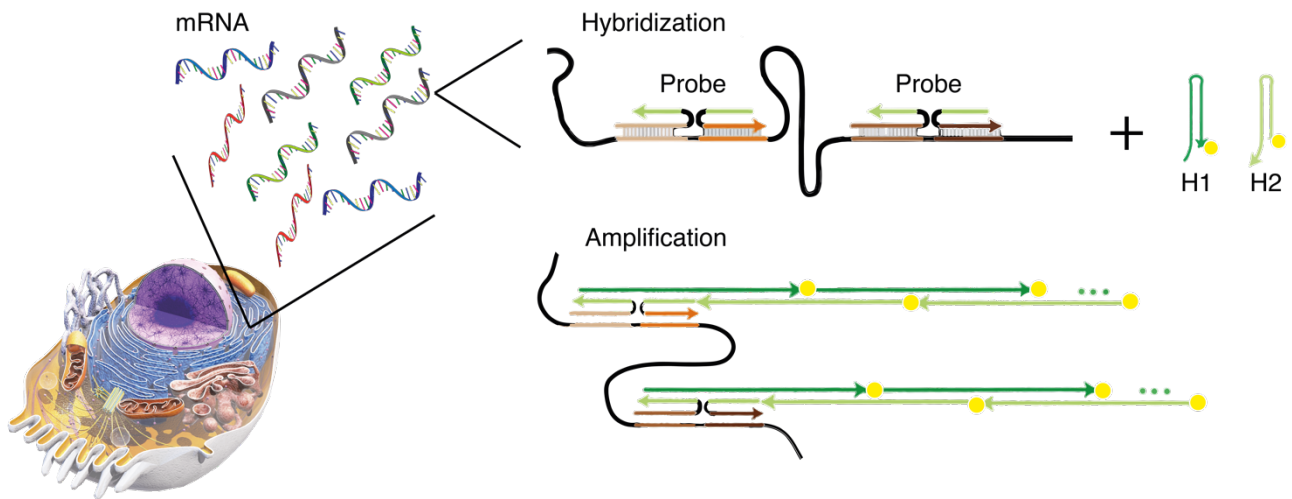


**Figure 2.1** Schematic representation of the HCR protocol modified from (109).

only bind to it when the probe pair is in the correct position, therefore triggering the start of signal amplification with the chain binding of more H2 and H1 hairpins (Figure 2.1). The features of HCR and its adaptability to multiple organisms make this technique ideal to characterize cell types during development. In the course of my PhD I have optimized HCR protocols for amphioxus embryonic, larval and adult stages (together with Dr Toby Andrews (Francis Crick Institute), Lara Busby (Department of Genetics, University of Cambridge) and Michael Schwimmer (Department of Zoology, University of Cambridge)) as described in (101), as well as for embryonic, larval and post-metamorphic stages of *A. mediterranea*.

### 2.3.1 Amphioxus

#### *Embryos and larvae*

Fixed amphioxus embryos and larvae were rehydrated through a MeOH/H<sub>2</sub>O series in 4-well plates and bleached in bleaching solution (5% hydrogen peroxide, 3% formamide in 0.2X SSC) under bright light on a sheet of aluminium foil. Early embryos up to the G3 stage were incubated for 20 minutes, while later stages were incubated for 35 minutes. The bleaching solution was removed with washes in PBT followed by incubation in permeabilization solution (PBS + 1% Triton X-100) for 2h at room temperature (this time was reduced to 15 minutes for B stage embryos). Specimens were then transferred in hybridization buffer (30% formamide, 9 mM citric acid pH 6, 50 µg/ml heparin, 1x Denhardt's solution, 10% dextran sulfate in 5X SSC + 0.1% Tween 20) for 2h at 37°C and then incubated overnight in hybridization buffer + probes (see section 2.2.4) overnight at 37°C (hybridization step). The following day embryos were washed six times in wash buffer (30%

formamide, 9 mM citric acid pH 6, 50 µg/ml heparin in 5X SSC + 0.1% Tween 20) for 15 minutes each, then washed in 5X SSC + 0.1% Triton X-100 (SSCT) and left in amplification buffer (10% dextran sulfate in 5X SSC + 0.1% Tween 20) for 30 minutes. During this time the hairpins were snap-cooled and diluted in amplification buffer to a concentration of 0.03 µM. The samples were then added to 100 µl of amplification mix in an Eppendorf tube and left overnight at room temperature in the dark (amplification step). On the third day embryos were thoroughly washed in SSCT several times in the dark and then transferred in PBT and incubated overnight in PBT + 1 µg/ml DAPI at 4°C in the dark. Finally, samples were mounted in 80% glycerol in glass-bottomed dishes for imaging.

Images of all HCR experiments performed on five amphioxus developmental stages (late gastrula/G5, early neurula/N0, mid neurula/7ss, early larva/12-14ss, four days old larva/1gs) are shown in Appendix V. Throughout the rest of the thesis several figures will analyse gene co-expression at specific stages, but the appendix serves as a reference for the entire developmental expression.

#### *Metamorphic and adult stages*

Metamorphic animals were further permeabilized as described for immunohistochemistry in section 2.2.1. Adult vibratome sections were also processed through a modified version of the protocol as described in (101). Sections were permeabilized through overnight incubation in permeabilization solution at 4°C and in PK 1 µg/ml in PBT for 10 minutes at 37°C, followed by fixation for 20 minutes in 4% PFA + MOPS. For large sections, hybridization was carried out for at least 18 hours. Metamorphic and adult samples were mounted in glass-bottomed dishes in Aqua Polymount (Polysciences, cat. 18606) to avoid bending and movement.

#### *Combination with immunofluorescence*

A key advantage of HCR is that it can easily be combined with other fluorescent techniques such as immunofluorescence. After the amplification step, embryos were washed thoroughly in SSCT, then washed in PBT and transferred in block solution for 1 hour. Samples were then incubated in primary and secondary antibody as described in section 2.2.1.

### 2.3.2 Crinoids

A whole mount HCR protocol was optimized in embryonic, larval and post-metamorphic stages of *A. mediterranea* by combining aspects of the amphioxus HCR protocol with the chromogenic *in situ* hybridization protocol previously designed for this crinoid species (108). All samples were rehydrated through a MeOH/H<sub>2</sub>O series in Eppendorf tubes and washed in PBT. As early embryonic stages are extremely fragile, all the solutions were introduced gently in the tube to avoid breaking the embryos. Pentacrinoids were decalcified overnight in a solution of 5% EDTA in nuclease free water (nfH<sub>2</sub>O). All samples were bleached in bleaching solution on aluminium foil. Doliolaria larvae were bleached for 45 minutes, while embryonic and pentacrinoid stages were bleached for 20 minutes. Doliolaria larvae were incubated in permeabilization solution overnight at 4°C; while embryonic and pentacrinoid stages were incubated for 15 and 30 minutes respectively and then left in PBT overnight at 4°C. The following day, doliolaria larvae were further permeabilized with PK treatment at a concentration of 4 µg/ml at 37°C for 8 minutes followed by post-fixation in 4% PFA. All stages were pre-hybridized in hybridization buffer for 2 hours at 37°C and then incubated with probes in hybridization buffer for 5 days at 37°C. After 6 washed in wash buffer and several in SSCT, samples were left in amplification buffer for 30 minutes and then incubated for at least 20 hours at room temperature in the dark with the hairpins. All samples were washed in SSCT the following day and incubated overnight with PBT + 1µg/ml DAPI at 4°C in the dark. Finally, samples were mounted in 100% glycerol in glass-bottomed dishes for imaging.

### 2.3.3 Vertebrates

#### *Zebrafish and frogs whole mount*

HCRs on *D. rerio* and *X. laevis* embryos were carried out following (109, 110) and a modified version of the protocol from the LaBonne Lab (Northwestern University) respectively. Rehydrated frog embryos were bleached for ~1 hour at room temperature until the pigment disappeared. Fish and frog embryos were then incubated in permeabilization solution for 1 hour at room temperature, then prehybridized and left overnight at 37°C in hybridization buffer + probes. On the second day they were washed in wash buffer, SSCT and amplification buffer, and left overnight in the dark in amplification buffer + hairpins. The following day excess hairpins were washed away with SSCT and nuclei are stained with DAPI 1µg/ml in PBT, either for 2 hours or overnight, then samples were mounted in 100% glycerol in glass-bottomed dishes for imaging.

### *Zebrafish and skate sections*

A version of the HCR protocol modified by the Gillis Lab (Marine Biological Laboratory, University of Chicago) was used for paraffin sections of *D. rerio* and *L. erinacea*. Sections were dewaxed in HistoSol and rehydrated through a EtOH/H<sub>2</sub>O series, then treated with PK (10 µg/ml in PBS) for 10 minutes at 37°C. The slides were rinsed, pre-hybridized in hybridization buffer for 30 minutes at 37°C and then left overnight in hybridization buffer + probes at 37°C in a humidified chamber, covered by a glass coverslip. On the second day sections were washed in a wash buffer/SSCT series at 37°C, then rinsed in SSCT and incubated for 30 minutes in amplification buffer. Samples were then left overnight at room temperature in a dark humidified chamber with amplification buffer + hairpins, covered by a parafilm coverslip. Slides were washed in SSCT the following day and mounted with a glass coverslip in fluoromount G (ThermoFisher, cat. 00-4958-02) + DAPI (1 µg/ml).

### 2.3.4 Probe synthesis and phylogenetic analysis

HCR probes were generated from mRNA sequences of genes of interest retrieved from transcriptomes of each species studied, and corresponding probes were ordered from Molecular Instruments®: (110) for *B. lanceolatum*; (111) for *A. mediterranea*; the GRCz11 version of *D. rerio*'s genome; the v10.1 assembly of *X. laevis*' genome; the little skate transcriptome from Dr Andrew Gillis Lab (Marine Biological Laboratory, University of Chicago) for *L. erinacea*. All probes used in this work are listed in Table 2. For *B. lanceolatum*, *A. mediterranea* and *L. erinacea* sequences were searched in the transcriptomes using the Reciprocal Best Hits BLAST approach using orthologous sequences from other deuterostome species. For unpublished genes, the orthology was then tested with phylogenetic analysis using SeaView (112). Protein sequences were aligned using Muscle and phylogenetic tree was constructed using the Neighbour Joining method with 1000 bootstrap repetitions.

## 2.4 Pharmacological treatments of amphioxus embryos

### 2.4.1 Perturbations of signalling molecules

#### *Wnt signalling*

To evaluate the effects of Wnt signalling on amphioxus development I overactivated and inhibited Wnt signalling through pharmacological treatment with two drugs: 1-azakenpaullone (AZA, Sigma-

Aldrich, cat. A3734) is a strong GSK-3 inhibitor that overactivates Wnt signalling (113); iCRT14 (iCRT, Tocris Bioscience, cat. 4299) is an inhibitor of  $\beta$ -catenin-responsive transcription that can be used to inhibit Wnt/ $\beta$ -catenin signalling (114).

Live embryos were raised at 21°C and treated at two different time points:

- ◆ Early treatment: B stage (4.5hpf) to N0 stage (12hpf)
- ◆ Late treatment: G5 stage (8hpf) to 7ss stage (18hpf)

At the desired stage embryos were transferred into small beakers with either the two drugs diluted in 10ml of ASW or an equal volume of dimethylsulfoxide (DMSO; Sigma, 276855). AZA was used at a concentration of 10 $\mu$ M for all time points, while iCRT was used at 50 $\mu$ M except for the late treatment, where it was used at a concentration of 100 $\mu$ M. At the end of each treatment samples were fixed in 3.7% PFA + MOPS.

#### 2.4.2 EdU labelling of proliferating cells

Labelling and tracking of proliferating cells during amphioxus development was carried out using 5-Ethynyl-2'-deoxyuridine (EdU, Invitrogen, A10044), a thymidine analogue that can be incorporated during DNA replication and can then be fluorescently detected using a fluorescent azide (115). During embryonic development, EdU was applied in filtered ASW at a concentration of 20 $\mu$ M for 2 hours at the desired stage. For EdU pulse analysis, embryos were fixed after 2 hours incubation, while for EdU pulse-chase experiments embryos were transferred into clean ASW after 2 hours incubation and left to develop until the 12ss stage before fixation. Fluorescent detection of EdU was performed using a Click-it EdU Alexa Fluor 647 Imaging Kit (Invitrogen, Waltham, MA, USA). As advised for enhanced signal, the copper reagent was replenished halfway through the protocol. When EdU detection was combined with immunohistochemistry or HCR, it was performed as a final step after DAPI (1  $\mu$ g/ml) incubation.

#### 2.4.3 Inhibition of proliferation through Hydroxyurea treatment

Live embryos were treated with 2  $\mu$ M hydroxyurea (HU, Sigma, cat. H8627), which inhibits cell proliferation by decreasing production of deoxyribonucleotides, or an equal volume of DMSO, diluted in filtered ASW. This was performed either between the G5 stage (gastrula) and 14ss stages (8 hpf to 34 hpf at 21°C), or the 6ss and the 12ss and 14ss stages (18 hpf to either 30 or 34 hpf at 21°C).

Gene	Reference	Initiator	Pair n°	Gene	Reference	Initiator	Pair n°
<i>ACVR1</i>	BL21996	B5	14	<i>Nodal</i>	BL07701	B3	20
<i>ACVR2</i>	BL23367	B2	20	<i>Notch</i>	BL19990	B3	20
<i>ankAT</i>	BL21259	B2	17	<i>Otp</i>	BL13404	B3 – B5	15
<i>Axin</i>	BL22437	B1	20	<i>Otx</i>	BL18685	B5	17
<i>Bmal</i>	BL01005	B2	19	<i>Pax2/5/8</i>	Reconstructed	B2	15
<i>Bmp2/4</i>	BL12966	B5	16	<i>Prox</i>	BL13719	B3	20
<i>BMPR1</i>	BL03672	B3	20	<i>Rx</i>	BL10535	B2	15
<i>BMPR2</i>	BL18556	B1	18	<i>SerT</i>	BL96109	B1	16
<i>Brn2</i>	BL16866	B5	19	<i>sFRP1/2/5a</i>	BL13243	B1	20
<i>Bsx</i>	BL06267	B5	10	<i>sFRP1/2/5b</i>	Reconstructed	B5	20
<i>ChAT</i>	BL13872	B2	20	<i>Six3/6</i>	BL96109	B1 - B2	9
<i>Chrd</i>	BL24510	B2	20	<i>SoxB1c</i>	BL03503	B3 – B5	12
<i>CTFP1</i>	BL17224	B5	7	<i>Tcf3</i>	BL18640	B2	20
<i>CTFP2</i>	BL17227	B1	12	<i>VGAT</i>	BL19817	B3	20
<i>CTFP3</i>	BL07853	B3	17	<i>VGlut</i>	BL22589	B3	14
<i>Dkk1</i>	BL11331	B2	12	<i>VMAT</i>	BL11246	B5	20
<i>Dkk3</i>	BL23931	B2	12	<i>Vt</i>	BL24431	B2	9
<i>Elav</i>	BL11117	B5	20	<i>Wnt8</i>	BL09252	B3	16
<i>Fezf</i>	Reconstructed	B3	10	<i>Zic</i>	BL15923	B1	10
<i>FoxD</i>	BL05120	B2	19	<i>FoxQ2</i>	/	B5	4
<i>FoxG</i>	BL11067	B3	16	<i>Lhx2/9</i>	/	B3	11
<i>FoxJ</i>	BL13340	B1	20	<i>Six3/6</i>	/	B2	12
<i>FoxQ2a</i>	BL22763	B5	12	<i>Wnt8</i>	/	B3	5
<i>FoxQ2b</i>	BL05937	B3	18	<i>Fezf2</i>	NM_131636	B1	18
<i>FoxQ2c</i>	BL02175	B2	13	<i>FoxQ2</i>	NM_001104941	B5	12
<i>Frz5/8</i>	BL13381	B3	20	<i>Rx3</i>	NM_131227	B3	12
<i>Gad67</i>	BL12286	B2	13	<i>Six3</i>	NM_131363	B2	17
<i>Gbx</i>	BL21529	B1	15	<i>Irx7</i>	NM_131881	B5	11
<i>Hmx</i>	BL00743	B1	16	<i>FoxQ2</i>	/	B2	9
<i>Lhx2/9b</i>	BL18410	B5	8	<i>Gbx2a</i>	NM_001090431	B2	10
<i>Ngn</i>	BL06125	B1	14	<i>Six3b</i>	AF183571	B5	12
<i>Nk2.1</i>	BL15126	B1	20				

**Table 2.** List of HCR probes used in this thesis. Colours represent animal species: blue: *B. lanceolatum*; orange: *A. mediterranea*; green: *D. rerio*; grey: *L. erinacea*; yellow: *X. laevis*. Some sequences were not found in the amphioxus transcriptome and therefore were reconstructed from the genome.

## 2.5 Injection of $\beta$ -catenin morpholinos and Bmp inhibition in frog embryos

Experiments on live *X. laevis* embryos were carried out during the “Embryology: concepts and techniques in modern developmental biology” course at the Marine Biological Laboratory, University of Chicago (Woods Hole, MA, USA). Fertilized eggs were injected with either a morpholino antisense oligo specific for *X. laevis*  $\beta$ -catenin ( $\beta$ -catMO) (116) at a concentration of 40 $\mu$ M, or a standard control morpholino (COMO, sequence 5'-CCTCTTACCTCAGTTACAATTTATA-3') (GeneTools, LLC). Injections were performed using a Leica M125C stereomicroscope using a Narishige micromanipulator on two stages: at the 2 cells stage, both cells were injected with the morpholinos, while at 4 cells stage, only the two lighter cells were injected, which correspond to the dorsal side of the animal. After injection embryos were grown in 1/3 ML medium up to stage 8, and then were treated with 10  $\mu$ M K02288 (Sigma-Aldrich, cat. SML1307), a Bmp signalling inhibitor that inhibits BMP type I receptor kinases, up to stage 17, when they were fixed in 4% PFA.

## 2.6 Microscopy and image analysis

Two confocal microscopes were used to acquire images for this work: an Olympus V3000 inverted confocal microscope, using 10X air and 30X oil objectives, 405, 488, 561, 594 and 647 lasers; and a Leica SP8 inverted confocal microscope with tunable laser, using a 40x oil objective. All images were captured at 1024x1024 size.

Most images are presented as maximum or standard deviation projections produced in Fiji (117). In specific cases, nuclear signal was isolated by using an inverted binary mask of the DAPI channel and subtracting it to the other channels.

### 2.6.1 Manual image segmentation with Imaris

For manual segmentation, Z-stacks of stained amphioxus embryos were imported in IMARIS (IMARIS 9.7.2, Bitplane, Oxford Instruments). The different tissues were manually segmented using the “surface” function, drawing splines around the cell nuclei visible through the DAPI signal every 4 slices in transverse section.

For the comparison of the neural plate in control and AZA-treated embryos at the 7ss stage, the neural plate was segmented in 16 embryos (8 AZA treated, 8 controls), using *Elav* expression to validate the precision of the segmentation. In the segmented neural plate cells were counted manually using the DAPI signal, while volumes were calculated automatically by IMARIS.

### 2.6.2 Automated nuclear segmentation with Ilastik

To create composite pseudo-embryos with expression of multiple genes with the ADAGE (Amphioxus Digitalized Atlas of Gene Expression) method (explained in Appendix IV), nuclear segmentation was carried out on z-stacks of embryos at the N0 and 7ss stage in collaboration with Dr Toby Andrews (Francis Crick Institute). First, an auto-context pipeline in Ilastik was used (118): I generated a training sample for each of the two stages using a posterior section of the z-stack containing an even representation of different embryonic tissues. In order to resolve adjacent objects to generate a label image, hysteresis thresholding was used setting a high threshold of 0.9 and a low threshold of 0.6. The training for each stage was then applied in batch to all the images, and the resulting map is then overlaid into each image as a separate channel. Using the 3D ROI manager plugin, the mean intensity of HCR signal in each nucleus and the position of each nucleus along the XYZ axes were calculated and stored in a .csv file, which was then imported in R for the ADAGE pipeline.

## 2.7 Sequencing

### 2.7.1 RNAseq

#### *RNA extraction*

Embryos destined to bulk RNA sequencing were transferred to Eppendorf tubes and fast-frozen in liquid nitrogen after removal of excess ASW. Control and treated embryos stored frozen at -80°C were ground with an electric pestle in a 1.5ml tube while thawing and then total RNA was extracted using Norgen Total RNA Purification Plus Kit (Catalog n° #48300). Purified RNA was stored at -80°C. RNA quantity and quality were checked using a BioAnalyzer (Appendix VI, Figure A6.3).

### *Sequencing and analysis*

All samples were sequenced at the CRUK Cambridge Institute using Illumina sequencing. The raw data was analysed and normalized by Ashley Sawle (CRUK Cambridge Institute). Briefly, raw read quality was assessed using FastQC (version 0.11.9) and transcript expression was quantified with Salmon (version 1.3.0) (119) using the transcriptome generated in (110). Transcript level expression values were imported into R and summarised to gene level using the Bioconductor package tximport and counts were then normalized for library size and composition bias using DESeq2 (120). For the analysis and interpretation of gene expression changes, the identity of ~450 genes was individually checked by reconstructing orthology relationships using the Reciprocal Best Hits BLAST approach.

### 2.7.2 scRNAseq

#### *Tissue dissociation and isolation of single cells*

Amphioxus embryos were raised to two stages of development: N0 (10hpf) and 7ss (18hpf). At the desired stage, they were collected in low-binding 1.5 ml tubes for dissociation, which was performed by a combination of mechanical and enzymatic methods. Embryos were successively treated with two enzyme cocktails (enzymes from Worthington Biochemical Corporation, USA) diluted in Ca<sup>2+</sup>-Mg<sup>2+</sup>-free artificial sea water (CMFSW) at pH 9:

#### Enzyme cocktail 1:

Collagenase 1 0.2%: degrades collagen and dissociate desmosomes, used to dissociate connective and epithelial tissues; it is inactivated by EDTA.

Elastase 0.5%: works on connective tissue and basal lamina of epithelia; it is specifically able to degrade elastin.

Dispase 2X (from 100X stock): general and mild protease that help dissociate tissues without destroying cell membranes; it is inactivated by EDTA.

Hyaluronidase ~1000u/ml: degrades hyaluronic acid and chondroitin sulfate, useful for connective tissues and epithelial junctions.

#### Enzyme cocktail 2:

Trypsin 0.5%: a serine protease that breaks down proteins.

EDTA: Ethylenediaminetetraacetic acid sequesters Ca<sup>2+</sup> ions which helps to dissociate desmosomes.

The live cell stain calcein (2 $\mu$ g/ml) was added to each cocktail to label living cells. The cocktails were pre-warmed at 37°C before use. 200 $\mu$ l of cocktail 1 was added to the tubes containing embryos and left for 10 minutes at 37°C. During this time, embryos generally fall to the bottom of the tube, so it was possible to remove most of cocktail 1 and add 250 $\mu$ l of cocktail 2. Embryos were left in cocktail 2 for ~2 minutes, during which they were continuously agitated using a 200 $\mu$ l Pasteur pipette. After this treatment the tubes were centrifuged at 5 g for 10 seconds; the cells pelleted at the bottom of the tube, the liquid was removed and CMFSW + 1% BSA was added gently to avoid resuspension of the pellet. The solution was then removed and more CMFSW + 1% BSA was added. The solution containing cells was gently pipetted with a 200 $\mu$ l Pasteur pipette for 30 second to avoid reaggregation of the cells. The cell suspension was then filtered into a different 1.5ml tube using a 40 $\mu$ l mesh to remove aggregates and was then kept on ice. Live cells were concentrated using cellenONE x1 cell sorter (Cellenion, France) (cellenONE machine was operated by Wing-Kit Leung at CRUK Cambridge Institute), collected in CMFSW and processed using the 10X Chromium method. Quality control and normalization of sequenced data was performed by Daniel Keitley (Department of Zoology, University of Cambridge) to produce a normalized count matrix that was analysed as a SingleCellExperiment object in R using the *scran* package (121). Uniform Manifold Approximation and Projection (UMAP) dimensionality reduction was used for plotting gene expression across cells in the dataset, and k-mer clustering was used to define clusters of cells (the scripts used for this analysis can be obtained at <https://github.com/giacomogattoni/Thesis>).



# Chapter III – Conservation of an ancient anterior gene regulatory network patterning the chordate brain

## 3.1 Introduction

### 3.1.1 Larval apical organs and their significance in the evolution of the CNS

Animal development can be broadly divided into two categories: direct development, when the embryo develops into a miniature version of the adult, and indirect development, in which the embryo forms a transient and sexually immature larva that metamorphoses into the final adult form. Larvae usually have distinct morphologies from adult forms and occupy different ecological niches (122, 123) but, aside from these general attributes, the precise definitions of larva and metamorphosis remain ambiguous. In this work, a “soft” concept of larva will be preferred: the term will include both maximally indirect development, in which the larva goes through a dramatic morphological rearrangement of the body plan at metamorphosis, and minimally indirect development, in which metamorphosis occurs more gradually and larval structures can be integrated into the adult (122, 124).

Larvae have long occupied a central stage in the scenarios on animal evolution, starting from Ernst Haeckel’s recapitulation theory, which stated that larvae of modern animals correspond to the adult forms of their ancestors, a concept summarised in his famous phrase “ontogeny recapitulates phylogeny” (125). Almost 150 years later, the evolution of animal life cycles is still a highly debated topic, to understand whether indirect or direct development is ancestral to specific taxa such as bilaterians or deuterostomes (97, 122, 126–128). The interest in larval stages is mainly justified by the fact that indirect development is found across the metazoan phylogenetic tree (123). In particular, many marine invertebrates are characterized by small, swimming ciliated larvae that facilitate the dispersal of the population, especially in animals with sessile or not very motile adult forms (95, 123) (Appendix VI, Figure A6.1). These larvae can rely on two nutrition strategies: planktotrophic larvae possess a digestive system and feed on plankton; lecithotrophic larvae have a large reserve of yolk in the form of droplets or in specialized organs and therefore do not need to feed until the yolk reserve is depleted. To some authors, the widespread presence of marine larvae indicates that a

biphasic life cycle is ancestral to bilaterians or even eumetazoans (17, 97, 128). For example, Jägersten introduced the genealogical term “primary larva” to indicate a hypothetical “*type of larva that has persisted in ontogeny without interruption since its first appearance*” (129). In this view, modern marine larvae are derived from an ancestral larval type and are, at least in terms of developmental stage, homologous. While some recent genomic data argues for an ancestral biphasic life cycle (130), this hypothesis still remains highly contentious (126, 127). As will be clarified through the thesis, this work focuses on the evolution of the nervous system and is not directly related to the evolution of life cycles. However, I thought it was necessary to highlight the key position of larval forms in the evolutionary debate, as larval nervous systems will be considered and have a key role throughout the thesis.

In fact, most marine ciliated larvae possess common traits including the presence of apical organs (AOs), sensory-neurosecretory structures that form the anterior part of the larval nervous system (96, 128, 131). AOs have been described in cnidarians, spiralian and deuterostomes and are composed of serotonergic and often neuropeptidergic neurons generally found in association with an apical tuft of sensory cilia (Appendix VI, Figure A6.1) (96, 128, 132). These neurons are thought to be involved in the control of larval swimming and in settlement and metamorphosis, although experimental validation remains scarce (133, 134). AOs are often the most conspicuous part of the larval nervous system and have sometimes been considered the “larval CNS” (17, 135). The pseudo-centralized nature of AOs, their widespread distribution and the similarity in cell types have made them attractive models to study nervous system evolution and have even been used to test the evolution of animal life cycles and the concept of primary larva (97, 128, 136–138).

### 3.1.2 Development of the apical organ in Ambulacraria: a conserved anterior network

While the homology of indirect development in eumetazoans and bilaterians is still debated, it has long been recognized that a larval stage is an ancestral trait of ambulacrarians. In fact, all major groups of echinoderms and hemichordates possess a planktotrophic or lecithotrophic larva, although direct development evolved independently in both phyla (139, 140). These larval forms (See Table 3.1) are defined as “dipleurula-type” as they derive from a hypothetical planktotrophic larva, the dipleurula, characterized by bilateral symmetry, a complete gut, motile cilia arranged in bands and an anterior AO (96, 128). AOs form from the ectoderm at the animal pole of dipleurula-

type larvae but their structure differs markedly in different taxa: in hemichordates, echinoids and holothuroids they remain concentrated in a single structure while in asteroids and ophiuroids they form bilateral clusters associated with epidermal ciliary bands (96, 141).

The cell type composition, developmental origin and molecular specification of the AO have been elucidated in exquisite detail in sea urchin (Figure 3.1). The echinopluteus larva possess an AO located dorsal to the mouth and the ciliary band, and consisting of at least four neuronal types, of which three are serotonergic (141, 142). The AO develops early, as serotonergic markers are already detectable during gastrulation (96, 143), and is specified by a gene regulatory network established by complex signalling interactions active throughout the embryo and involved in the formation of the animal-vegetal (AV) axis (141, 144–147). In this work, I call this the *anterior gene regulatory network* (aGRN) following the definition given in previous works (145, 148). In early embryos at the maternal to zygotic transition, the transcription factors *Six3/6* and *FoxQ2* are expressed on the animal side of the embryo, while vegetally they are repressed by maternal Wnt/ $\beta$ -catenin signalling (149–151). The early blastula is therefore characterized by a broad *Six3/6-FoxQ2*-positive domain; this expression domain progressively restricts apically due to non-canonical Wnt signalling that acts through interactions of Wnt1 and Wnt8 with the Frz5/8 receptor (147, 151, 152). At the animal pole, *Six3/6*, *FoxQ2* and curiously Wnt-Frz5/8 signalling itself activate the expression of secreted Wnt inhibitors of the sFRP and Dkk families that prevent the complete downregulation of *Six3/6* and *FoxQ2* (151–154). sFRP1/2/5 binds to Frz receptors reducing their availability for Wnt ligands, while Dkk1 and Dkk3 act by blocking the interaction of Wnts with their co-receptor LRP5/6. The area where *Six3/6* and *FoxQ2* remain active at the animal pole is called apical plate (97, 141, 147, 154). Here, these genes directly or indirectly control the expression of downstream factors that overall

Taxon	Echinoderms					Hemichordates
	Crinoidea	Asteroidea	Ophiuroidea	Echinoidea	Holothuroidea	Enteropneusts
Species name	Sea lilies Feather stars	Sea stars	Brittlestars	Sea urchins Sand dollars	Sea cucumbers	Acorn worms
Larval type	Doliolaria	Bipinnaria Brachiolaria	Ophiopluteus	Echinopluteus	Auricularia Doliolaria	Tornaria

**Table 3.1.** Dipleurula-type larval stages of indirectly-developing ambulacrarians

confer the identity to AO cells, including *Fezf*, *Nk2.1*, *Hbn*, *Rx*, *Lhx2/9*, *Ac-Sc*, *Delta*, *Zic* and *Zfhx1* (145, 146, 155).

The interactions between members of the aGRN have been mainly tested through pharmacological treatments and knock-down experiments with morpholinos. By inhibiting maternal  $\beta$ -catenin accumulation the *Six3/6* domain is expanded and the entire embryo is specified as neural (151, 154–156), while overactivation of Wnt/ $\beta$ -catenin signalling inhibits *Six3/6* and *FoxQ2* expression and consequently causes the loss of the AO (151, 156). Knock-down of *Six3/6* and *FoxQ2* also leads to larvae without AOs and was shown to inhibit *Fezf*, *Hbn* and *Nk2.1* (145, 149, 155, 157, 158). Conversely, over-expression of *Six3/6* causes an expansion of the apical neurogenic territory (150). The expression pattern and functional analysis of orthologous genes in asteroids and indirectly-developing hemichordates have further highlighted the conservation of the aGRN in Ambulacraria (159–164). In both cases *Six3/6* and *FoxQ2* are expressed early in the animal side of the embryo while Wnt/ $\beta$ -catenin signalling is active at the vegetal pole. *sFRP* and *Dkk* transcripts also appear at the animal tip, blocking the restriction of *Six3/6* and *FoxQ2* expression controlled by *Wnt1*, *Wnt8* and *Frz5/8*. The formation of a *Six3/6-FoxQ2*-positive apical plate is necessary for the activation of downstream genes like *Fezf*, *Hbn*, *Rx* and *Lhx2/9* which in turn control the formation of AO neurons (96, 165, 166).

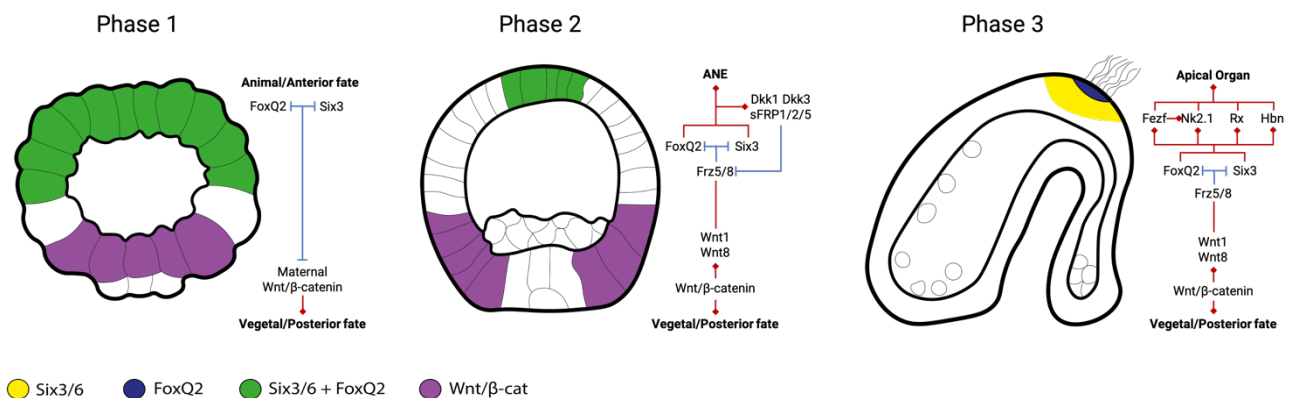


**Figure 3.1.** Phases of AO specification in sea urchin embryos. The schematic represents known interaction between aGRN genes and show a three-step system of AO development. First,  $\beta$ -catenin represses the early expression of *Six3/6* and *FoxQ2* and activates Wnt at the vegetal pole. Second, Wnt1 and Wnt8 restrict *Six3/6* and *FoxQ2* towards the animal tip of the embryo. There, they activate *sFRP* and *Dkk* Wnt inhibitors that prevent the complete downregulation of the aGRN, defining the apical plate. Third, downstream genes in the apical plate control differentiation of AO neurons.

### 3.1.3 Beyond deuterostomes and primary larvae: a short review on apical organs and aGRN across invertebrates

The neurogenic tissue specified by the aGRN within the apical plate in the anterior portion of the body in ambulacrarians is called *anterior neuroectoderm* (ANE) (146). The thorough investigations on the molecular details of ANE development described above have revealed an ancient patterning system that controls the formation of the main body axis and the AO in ambulacrarians, but also represent the basis for broader testing of ANE conservation in metazoans. The information on the expression and function of aGRN genes in a variety of phyla is scattered across the literature and have been considered together only recently (97, 128, 145). Here, I briefly summarise the data available for protostomes and cnidarians to highlight the extreme conservation of the aGRN across metazoans (Figure 3.2; Appendix VI, Figure A6.1).

#### *Protostomia, Spiralia*

The taxon Spiralia includes a large number of phyla whose internal relationships are still highly debated. Despite the incredible diversity of spiralian body plans, many phyla possess trochophore-type larvae characterized by a swimming ciliary ring, the prototroch (128). Many of these larvae have been shown to develop AOs consisting of flask-shaped serotonergic and peptidergic cells often associated with other neurons (128, 167). Although the number of cells and the degree of complexity of these AOs can vary significantly, they have been described in annelids (168–171), molluscs (172–176), brachiopods (177, 178), nemerteans (179, 180), phoronids (181, 182), entoprocts (183), bryozoans (184) and possibly platyhelminthes (185). In annelids, molluscs, brachiopods and nemerteans gene expression studies have revealed a high degree of similarity with ambulacrarians in the specification of the apical plate on the anterior portion of the body and the formation of the AO (97, 178, 186–189). In these four groups *Six3/6* and *FoxQ2* are expressed in the animal side of the embryo and in cells that will form the AO. Moreover, in annelids and brachiopods *Fezf*, *Nk2.1* and *Hbn* are also expressed in AO precursors, and experiments on the polychaete *Platynereis dumerilii* showed that these genes are similarly controlled by Wnt signalling acting through *Frz5/8* (97, 178).

#### *Protostomia, Ecdysozoa*

While many ecdysozoans have indirect development, their larvae look very different from the marine ciliated forms seen in other metazoans, and do not possess AOs. However, several aGRN

genes described in sea urchin are expressed in the head and anterior brain in members of the “Panarthropoda” taxon (Arthropoda, Onychophora, Tardigrada). *Six3/6* is expressed in the anterior head region from early development in insects, chelicerates, myriapods, onychophorans and tardigrades (190–194). In the insect *Tribolium castaneum* and the spider *Parasteatoda tepidariorum*, *Six3/6* and *FoxQ2* interact with each other, are negatively regulated by Wnt signalling and control the formation of the labrum and parts of the protocerebrum, including the central complex (148, 193, 195). *FoxQ2* and *Fezf* are also known to pattern part of the protocerebrum in *Drosophila* (196, 197). Finally, a detailed expression analysis in the centipede *Strigamia maritima* showed that *Six3/6*, *FoxQ2*, *Rx* and *Hbn* are expressed within the “anterior medial region” of the head (194). These cells provide an axonal scaffold for the subsequent development of internalized neuroblasts and differentiate into neurosecretory cell types.

### Cnidaria

Cnidarians display a variety of life cycle strategies, but many different groups possess planula larvae. In the planulae of the anthozoan *Nematostella vectensis*, the hydrozoan *Clava multicornis* and the scyphozoan *Aurelia* there is a concentration of larval-specific neurons on the aboral side of the body (198–200). In *Nematostella*, these neurons are arranged as a ring around an apical tuft of cilia, while in *Clava* they are distributed on the entire aboral surface. These neurons do not appear to use

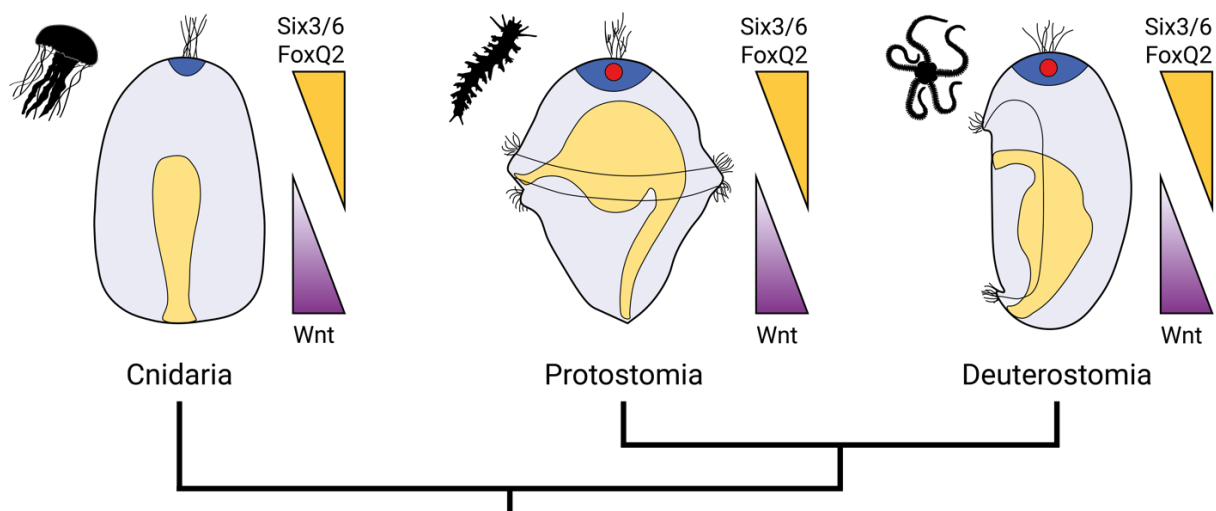


**Figure 3.2.** Conservation of aGRN across Eumetazoa. Schematic representation of larval stages of cnidarians (planula), spiralian protostomes (trochophore) and ambulacrarian deuterostomes (dipleurula), showing Wnt activity on the oral/vegetal side and *Six3/6-FoxQ2* expression on the aboral/animal side, where the ANE will form (blue). In bilaterian larvae, the ANE contains serotonergic neurons (red).

serotonin as a neurotransmitter, but they express a variety of neuropeptides such as RFamide, RPamide and GLWamide (199–201). Moreover, studies on *Nematostella* have revealed that the aboral domain is characterized by similar genes to ambulacrarian apical plate, including *Six3/6*, *FoxQ2*, *Frz5/8*, *sFRP1/2/5*, *Dkk1* and *Rx* (202, 203). The expression of *Six3/6* and *FoxQ2* is negatively regulated by oral Wnt/ $\beta$ -catenin signalling and restricts through *Frz5/8* activity to the aboral tip where the sensory cells form (203–205). These similarities have led many authors to regard the aboral sensory organ of the cnidarian nervous system as homologous to the AO, suggesting that the aGRN might have first evolved in the eumetazoan ancestor. The recent discovery of a similar control of vegetal fate in bilaterians and oral fate in cnidarians have further supported the homology between the AP axis of bilaterians with the aboral-oral axis in cnidarians, supporting the inclusion of cnidarian apical organs in the list of ANE tissues (206). However, it must be noted that while *Hbn*, *Nk2.1* and *Otp* are generally associated with the ANE in bilaterians, they are expressed orally in cnidarians, suggesting that the network was modified during the evolution of bilaterians (207).

#### 3.1.4 Aims of the chapter: a chordate aGRN?

The widespread presence of AOs in ambulacrarians, spiralian and cnidarians and their similarity to the anterior CNS of panarthropods supports the hypothesis that the ANE might be a conserved feature of eumetazoan development and was present in the common ancestor of deuterostomes (145) (Figure 3.2). However, the relationship between the AO of ambulacrarians and the chordate brain remains obscure. Similar to arthropods, despite the absence of AOs in vertebrates many of the aGRN genes are expressed in the brain (208, 209). *Six3/6* is one of the key players in the specification of the secondary prosencephalon and has reciprocally inhibitory interactions with Wnt ligands produced by the posterior forebrain (210, 211). Wnt inhibitors of the sFRP family are also expressed in the secondary prosencephalon and block the activity of Wnt ligands (65, 208). Additionally, *Fezf*, *Nk2.1* and *Rx* are known to contribute to regionalize the secondary prosencephalon into hypothalamic, telencephalic and retinal territories (64, 67, 68, 71, 208, 209, 212). While these factors suggest the conservation of the aGRN in vertebrates, there are also significant differences. The aGRN is active from early development in the animal ectoderm of many invertebrate embryos, but in vertebrates these genes are expressed only later in development and restricted to the nervous system. Furthermore, *FoxQ2* is a key upstream member of the aGRN in eumetazoans but is not expressed during vertebrate development at all and was lost in multiple vertebrate groups (213).

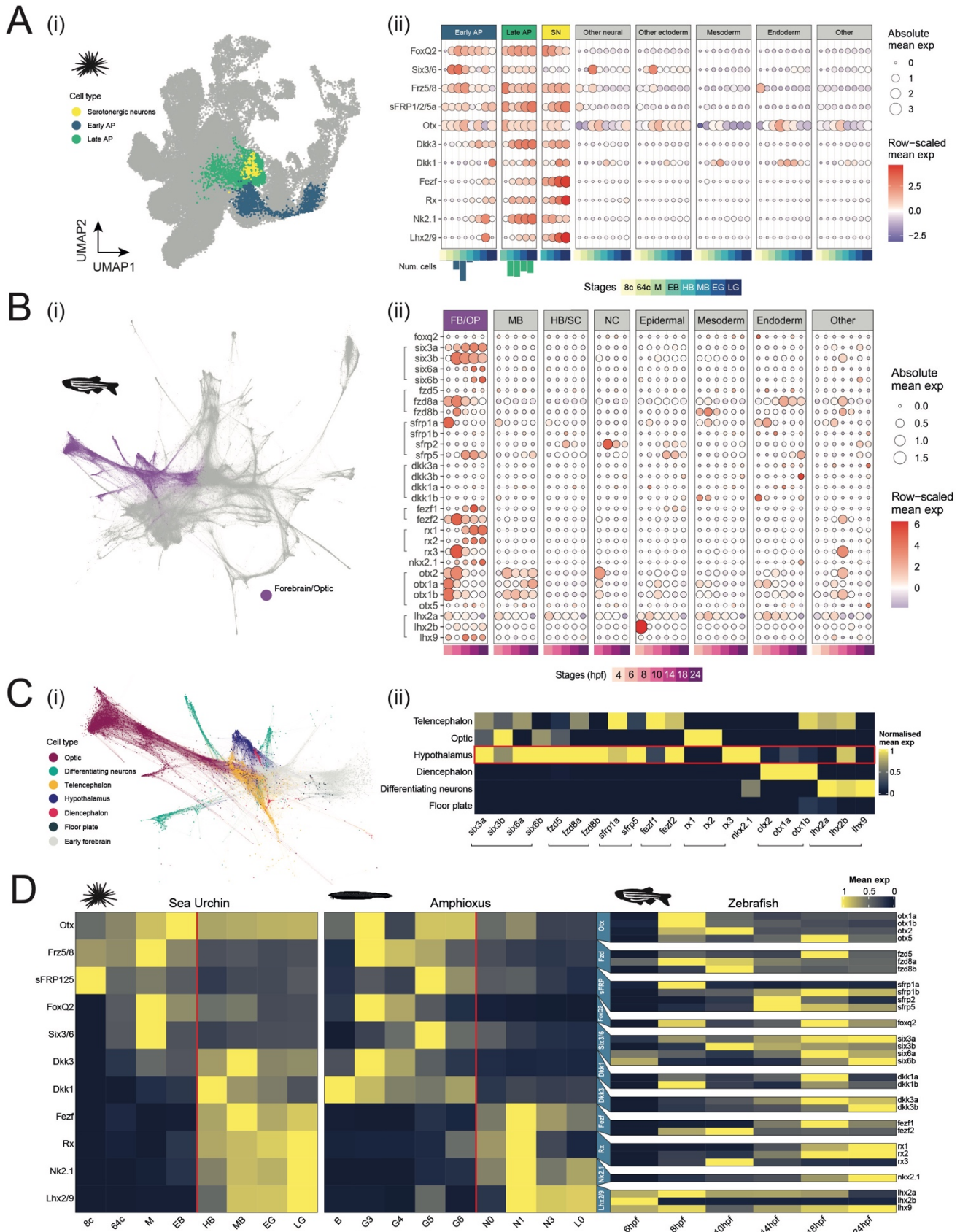
Amphioxus development is characterized by early broad expression of *Six3/6* and *FoxQ2* at the animal pole, resembling the condition of ambulacrarians (214, 215). The embryo forms a swimming ciliated larva, but the nervous system is already typically chordate, with a dorsal neural tube and anterior brain. In this chapter, I investigate the conservation of the aGRN in chordates using amphioxus. I first compare deuterostome scRNAseq datasets to define a conserved ANE molecular signature. I then test the presence of this signature in amphioxus development and the control of aGRN genes by Wnt signalling.

## 3.2 Characterization of a conserved deuterostome aGRN

### 3.2.1 Analysis of deuterostome scRNAseq datasets defines conserved aGRN signature

My first objective was to obtain a conserved list of aGRN candidates in deuterostomes and gain a complete view of their expression across development, taking into account the differentiation of ectodermal cell types that is happening alongside the formation of the body axes. To this end, together with Daniel Keitley (Department of Zoology, University of Cambridge) I analysed and compared recently published single cell RNA sequencing (scRNAseq) developmental datasets of two deuterostome species: the sea urchin *Strongylocentrotus purpuratus* (Echinodermata) (216), in which the aGRN has been well characterized, and zebrafish (Chordata) (217). The code for this analysis is available at <https://github.com/eBGLab/AmphiApicalOrgan>.

In the sea urchin, by plotting the ectodermal expression of 11 aGRN genes (*FoxQ2*, *Six3/6*, *Frz5/8*, *sFRP1/2/5a*, *Dkk3*, *Dkk1*, *Fezf*, *Rx*, *Nk2.1*, *Otx*, *Lhx2/9*) across developmental time, a clear developmental sequence is visible: in an early phase the upstream genes *Six3/6* and *FoxQ2* start to be expressed zygotically at the 64-cells stage, together with the broad maternally expressed *Otx*, *Frz5/8* and *sFRP1/2/5* and followed by the other Wnt inhibitors *Dkk1* and *Dkk3*. After hatching of the blastula, a late phase begins with the activation of downstream genes *Fezf*, *Rx*, *Nk2.1* and *Lhx2/9*. Based on these results, we re-annotated the dataset to include these two populations named “early apical plate” and “late apical plate” (Figure 3.3A) and showed that the complete combination of these transcription factors is unique to these cell types. By quantifying the number of cells in these two clusters at each developmental stage, we showed that most “early apical plate” cells are found at morula and early blastula stages, while “late apical plate” cells appear from the hatching blastula.



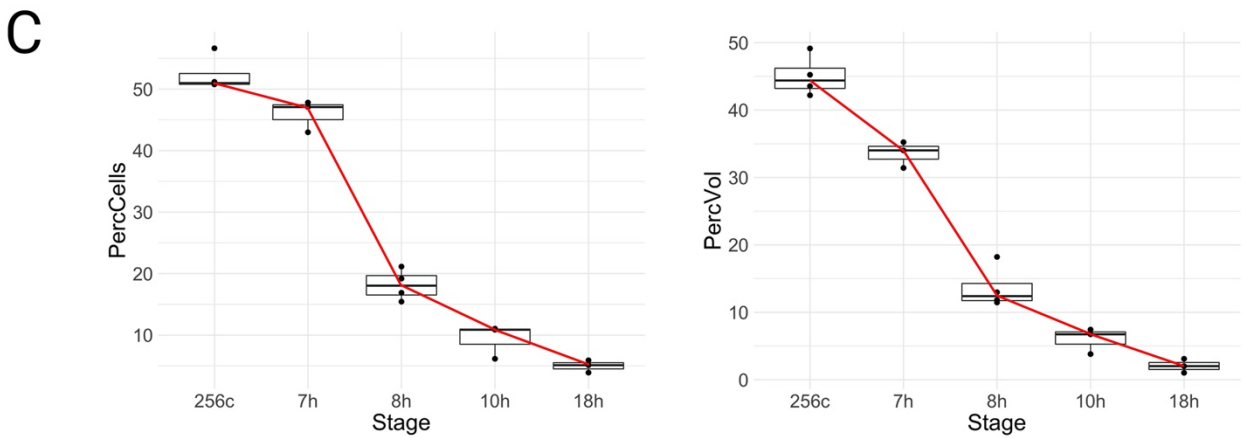
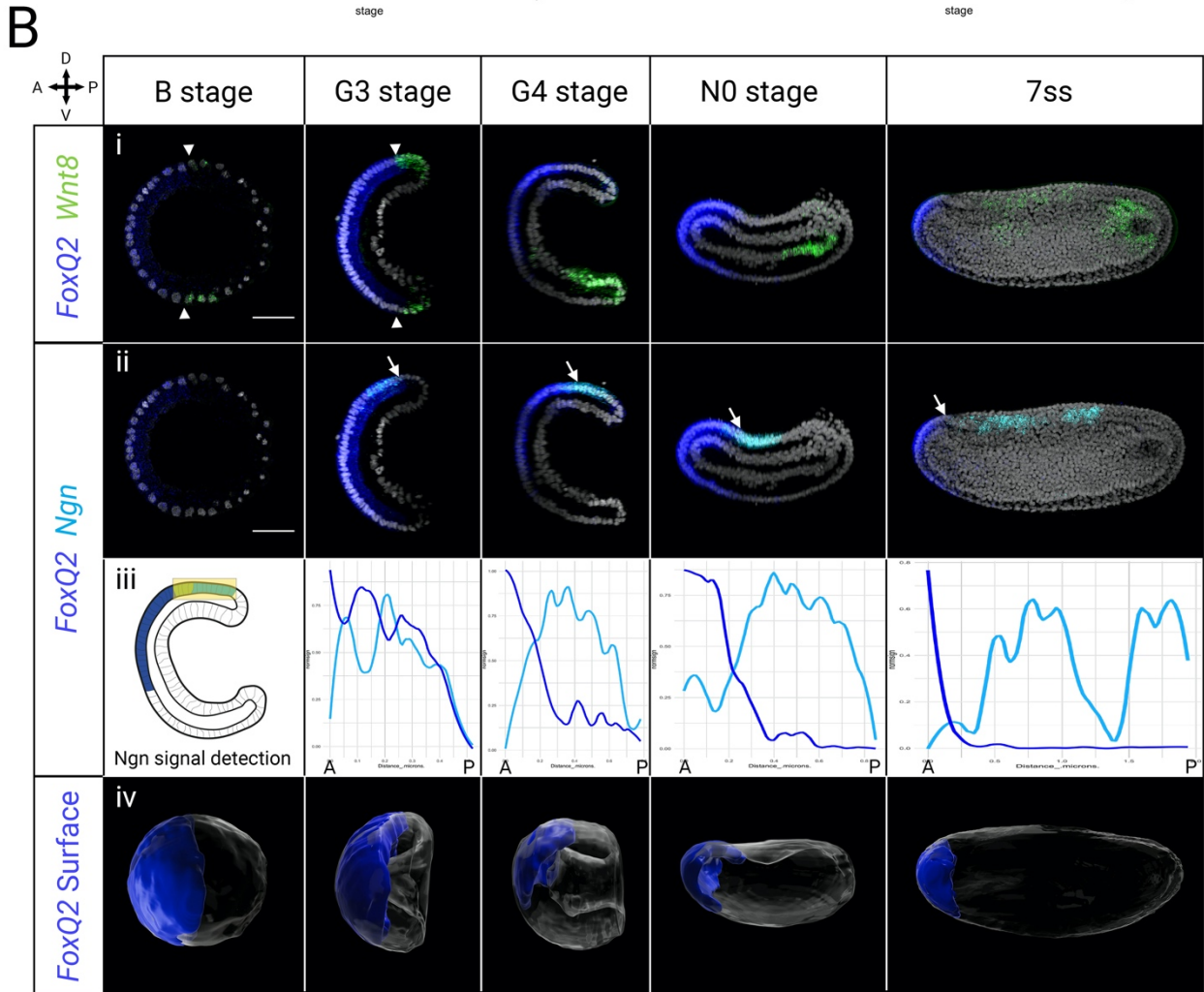
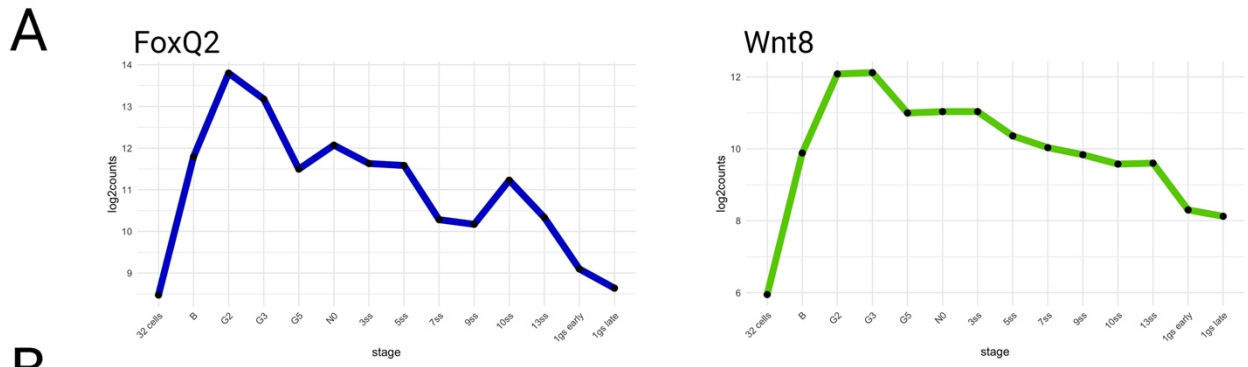
< **Figure 3.3.** Identification of a conserved deuterostome aGRN signature in developmental scRNAseq datasets. **A.** i) UMAP plot of sea urchin single-cell transcriptomics data based on (216) highlighting early and late apical plate (AP) cell types. Within the late AP cluster, serotonergic neurons (SN) can be identified. ii) Dotplot showing the mean expression of previously reported aGRN genes across sea urchin cell types, including the early and late AP. Within each cell type, the multiple dots for each gene correspond to the developmental stages in which the expression is detected, color-coded at the bottom of the plot (8c, 8-cells; 64c, 64-cells; M, morula; EB, early blastula; HB, hatched blastula; MB, mesenchyme blastula; EG, early gastrula; LG, late gastrula). Normalized values across each gene are represented by the dot colour, allowing for comparisons between genes with different absolute mean levels of expression (represented by dot size). For early and late AP cell types, the bar plots positioned below the dotplot show the relative proportion of cells across developmental stages, highlighting that early AP cells are concentrated at the M and EB stages while late AP cells are primarily detected from the HB stage onwards. **B.** i) Force-directed graph layout of zebrafish single-cell data from (217) highlighting forebrain cells. ii) Mean expression of aGRN orthologs across zebrafish cell types and developmental stages highlights a broad signature in the zebrafish forebrain. The organization of the dotplot matches the one described for sea urchin in (A), but in this dataset different stages are represented by hours post fertilization (hpf). Brackets highlight paralog groups. **C.** i) Subclusters representing re-annotated forebrain populations visualized through a force-directed graph layout. ii) Distribution of aGRN genes in forebrain cell types. The red square indicates the hypothalamus where the strongest aGRN signature is detected. **D.** Comparison of aGRN gene expression across developmental stages in ectodermal tissues of sea urchin, amphioxus (218) and zebrafish. In both sea urchin and amphioxus a biphasic pattern of expression is highlighted by a red line, while in zebrafish the distinction between early and late phases is not visible.

This subdivision recapitulates previous experimental data on the phases of AO development: early restriction of *Six3/6* and *FoxQ2* by Wnt signalling modulated by Wnt inhibitors, and late downstream activation of genes that specify cell types in the apical plate. Only from the late gastrula serotonergic neurons of the AO can be identified within this domain by the expression of *Tph* and are marked by strong *Fezf* expression (Figure 3.3A-D).

By plotting the orthologs of the same genes in the zebrafish developmental dataset, we found that a similar combination of transcription factors, solely excluding *FoxQ2*, demarcates the forebrain (Figure 3.3B). Although not all paralogs for each gene are expressed there, at least one of the orthologs of *Six3/6*, *Frz5/8*, *sFRP1/2/5*, *Fezf*, *Rx*, *Nkx2.1*, *Otx* and *Lhx2/9* localize within the cluster. In zebrafish however the genes appear at later stages when the forebrain is already specified as neuroectoderm, while in echinoderms the aGRN signature is visible already at the blastula stage and will specify both neural- and non-neural cell types (145). To identify which forebrain cells possess the identified signature, we reannotated the forebrain cluster defined by Wagner and collaborators to further characterize its cell types according the prosomeric model, using markers that are known to define different forebrain areas (Figure 3.3C). Plotting the combination of aGRN transcription factors in forebrain cell types revealed that the signature is present within the hypothalamus, and to a lesser extent in the retina and the telencephalon, while it is absent from the diencephalon and the floor plate (Figure 3.3C).

Overall, the analysis of deuterostome scRNAseq datasets supports the notion that the AO is specified sequentially, revealing the clear sequence of aGRN activation that ties with the progress of cell differentiation and neurogenesis. Furthermore, it allowed the identification of a conserved set of 11 genes that sequentially activate during the formation of the apical organ in sea urchin and the specification of the hypothalamic region in zebrafish.

**Figure 3.4.** Early expression of *FoxQ2* in amphioxus (overleaf). **A.** Analysis of RNAseq data across amphioxus development (79) shows that *FoxQ2* and *Wnt8* are active from the blastula stage, while there is no maternal expression. Their expression peaks during gastrulation and then decreases in late stages. **B.** Co-detection of *FoxQ2* (blue), *Wnt8* (green) and *Ngn* (cyan) from blastula to 7ss stage. Early *FoxQ2* on the animal side forms a boundary with an equatorial *Wnt8* ring that persists in early stages of gastrulation (arrowheads) (i). The *FoxQ2* domain initially includes the early neural plate, but with *FoxQ2* restriction during gastrulation it progressively disappears. Arrow points to posterior limit of *FoxQ2* expression (ii, iii). The *FoxQ2* restriction is highlighted by segmenting *FoxQ2*-positive tissue with Imaris (iv). Scale bars are 50 $\mu$ m. **C.** Calculation of the relative number of *FoxQ2*-positive cells and the percentage of embryo volume occupied by *FoxQ2* demonstrates the restriction of *FoxQ2* domain across gastrulation.



### 3.2.2 Early genes are expressed in amphioxus

I next set out to characterise the expression dynamics of orthologs of the identified conserved set of genes during the development of amphioxus. The expression of aGRN markers in echinoderm and zebrafish scRNAseq datasets was first compared with a recent single nuclei RNAseq dataset from *B. floridae* (218), to understand whether a similar signature could be identified (Figure 3.3D).

By plotting aGRN genes across developmental time I detected a biphasic activation of gene expression similar to the one in sea urchin. Early phase genes (*FoxQ2a*, *Six3/6*, *Frz5/8*, *sFRP1/2/5a*) appeared from the blastula (B) to the late gastrula (G6) stage, followed by late phase genes (*Fezf*, *Rx*, *Nk2.1* and *Lhx2/9b*) turning on during neurulation. At the beginning of the larval phase (L0), the serotonergic marker *Tph* also appeared (Figure 3.3D). I further analysed the bulk RNAseq dataset for *B. lanceolatum* development published by Marlétaz and collaborators (79), to show that *FoxQ2a* (for simplicity called *FoxQ2* in the rest of the chapter, but the distinction between different *FoxQ2* paralogs is discussed in Chapter VI) is first activated at the blastula stage together with *Wnt8*, which is known to control the restriction of *Six3/6* and *FoxQ2* in sea urchin (151) (Figure 3.4A). The sequence of activation and the expression dynamics of aGRN genes in amphioxus resembles the one seen in the sea urchin scRNAseq dataset.

I then investigated the spatial co-expression patterns of these candidate genes using HCR. I first applied it to define the expression of *FoxQ2* and *Wnt8* from the blastula to the mid-neurula stage. These two genes were co-detected with the early neural marker Neurogenin (*Ngn*) to relate their expression to the development of the CNS (Figure 3.4B). At the B stage (blastula, 4.5hpf) *FoxQ2* transcripts were detected in the entire animal territory and *Wnt8* was expressed in a band around the equator of the embryo, abutting the *FoxQ2*-positive domain (Figure 3.4Bi). During gastrulation at the G3 stage (6hpf) *FoxQ2* remained expressed throughout the animal pole, while *Wnt8* was localized around the external surface of the blastopore. *Ngn* started to be visible in a dorsal band of positive cells that was entirely located within the *FoxQ2* domain (Figure 3.4Bii-iii). At the G5 stage (8hpf), *FoxQ2* started to restrict towards the anterior side of the embryo and became dorsalized, disappearing from the ventral side. At the same time, *Wnt8* was detected in the lateral and ventral mesendoderm. The dorsal band of *Ngn*-positive neural progenitors expanded, and as a consequence of *FoxQ2* restriction only the anteriormost cells showed co-expression of the two genes (Figure

3.4Biii). During neurulation, the neural tube progressively extends along the AP axis and *FoxQ2* restricts to the animal-dorsal pole, such that by the 7ss stage it is only expressed in the anteriormost tip of the ectoderm, outside of the nervous system (Figure 3.4Bii-iii). *Wnt8* continued to mark ventral endoderm, presomitic mesoderm, all the somites except the first pair and appeared in clusters of neurons in the trunk region of the neural tube (Figure 3.4Bi). To quantify the extent of *FoxQ2* restriction, I segmented the *FoxQ2* domain in embryos from different stages using Imaris and calculated the relative volume and relative number of *FoxQ2*-positive cells (Figure 3.4Biv). Both parameters markedly decreased during development, most prominently during gastrulation between G3 and G5 stage (Figure 3.4C). This demonstrates that the initial radial expression of *FoxQ2* and its restriction during gastrulation resembled the establishment of animal and vegetal fields and the early phases of ANE specification in ambulacrarian larvae.

I then focused on the combination of four genes that act in the early phase of restriction of the aGRN territory towards the animal pole in sea urchin (*FoxQ2*, *Six3/6*, *Frz5/8* and *sFRP1/2/5a*) in three developmental stages encompassing amphioxus late gastrulation and neurulation: G5 (late gastrula), N0 (early neurula) and 7ss (Figure 3.5A). All genes were expressed in the anterior-dorsal ectoderm at the G5 stage. While *FoxQ2*, *Six3/6* and *Frz5/8* were co-expressed in a broad ectodermal area, *sFRP1/2/5a* appears dorsally restricted within this co-expression domain. In the early and mid-neurula *Six3/6* and *Frz5/8* followed the same restriction seen for *FoxQ2*, but at 7ss they were still expressed in the anterior tip of the nervous system (Figure 3.5A). *Frz5/8* marked the anteriormost part of the neural tube while *Six3/6* split into two populations: an anterior cluster of cells at the tip of the neural plate and posterior, post-infundibular population, separated by a small region devoid of *Six3/6* that I termed “intercalated *Six3/6*-negative region” (219). During this restriction *sFRP1/2/5a* remains expressed at the anterior-dorsal tip of the animal, corresponding to the anterior limit between the neural tube and the non-neural ectoderm. The expression of the Wnt inhibitor *Dkk3* was also consistent with a conserved role in blocking anterior restriction of *Six3/6* and *FoxQ2* (220), while *Dkk1* only appears at the border of the future cerebral vesicle (CV) at the 7ss stage (Appendix V).

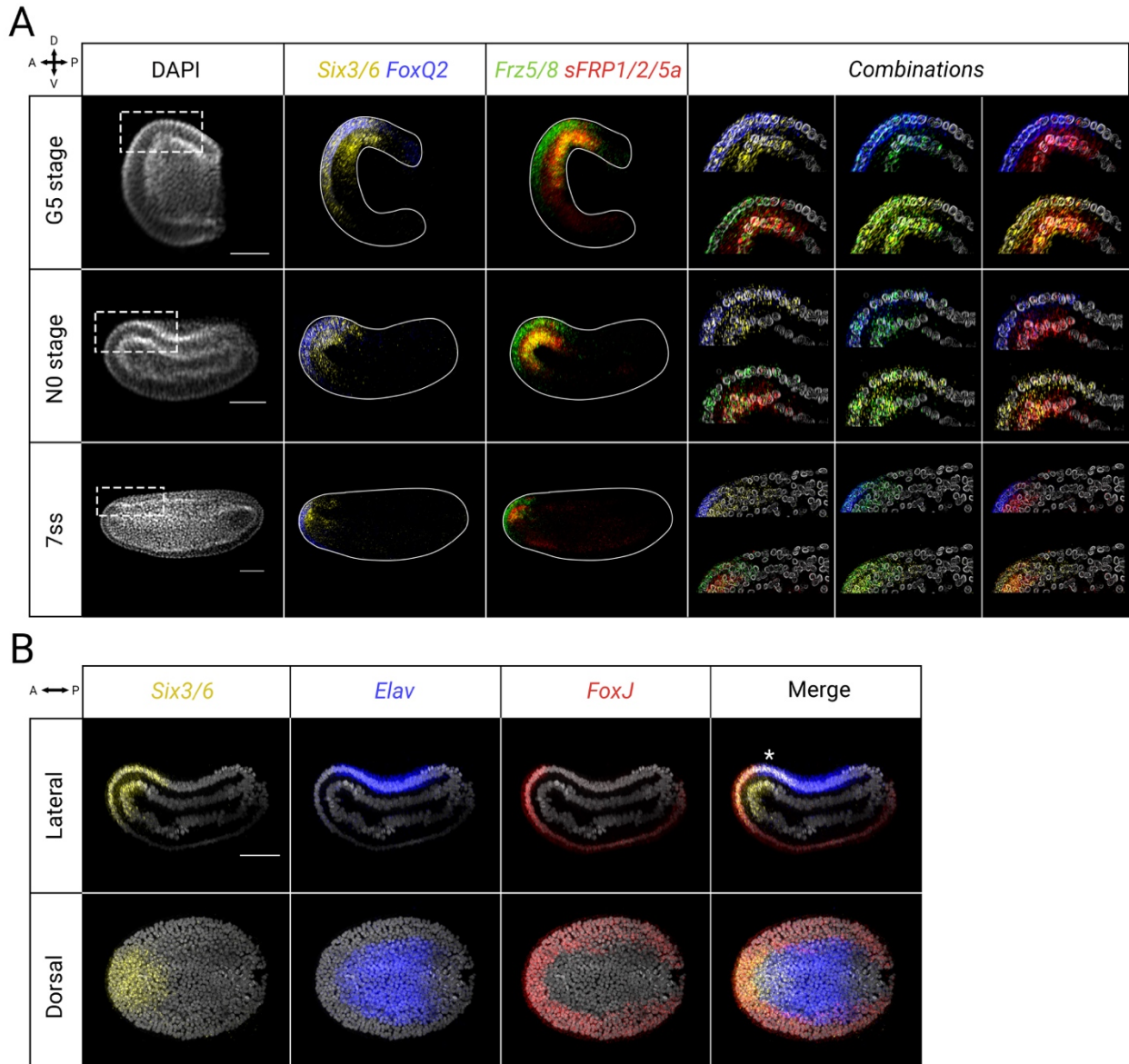


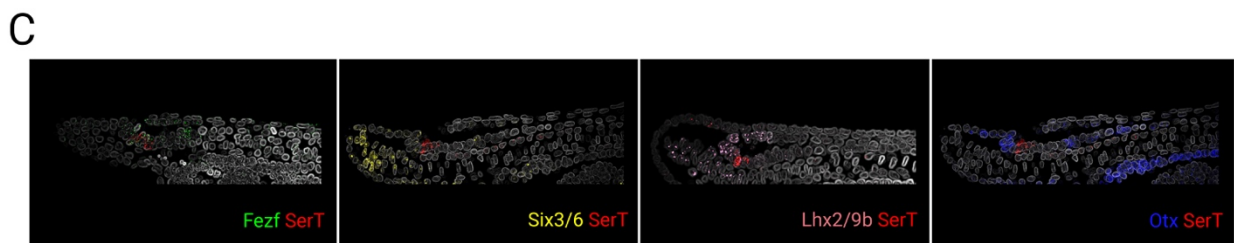
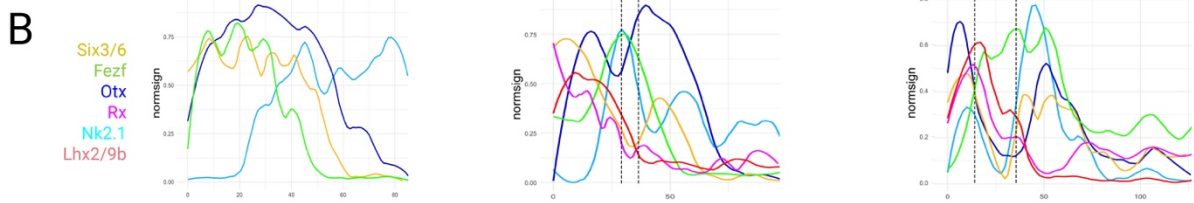
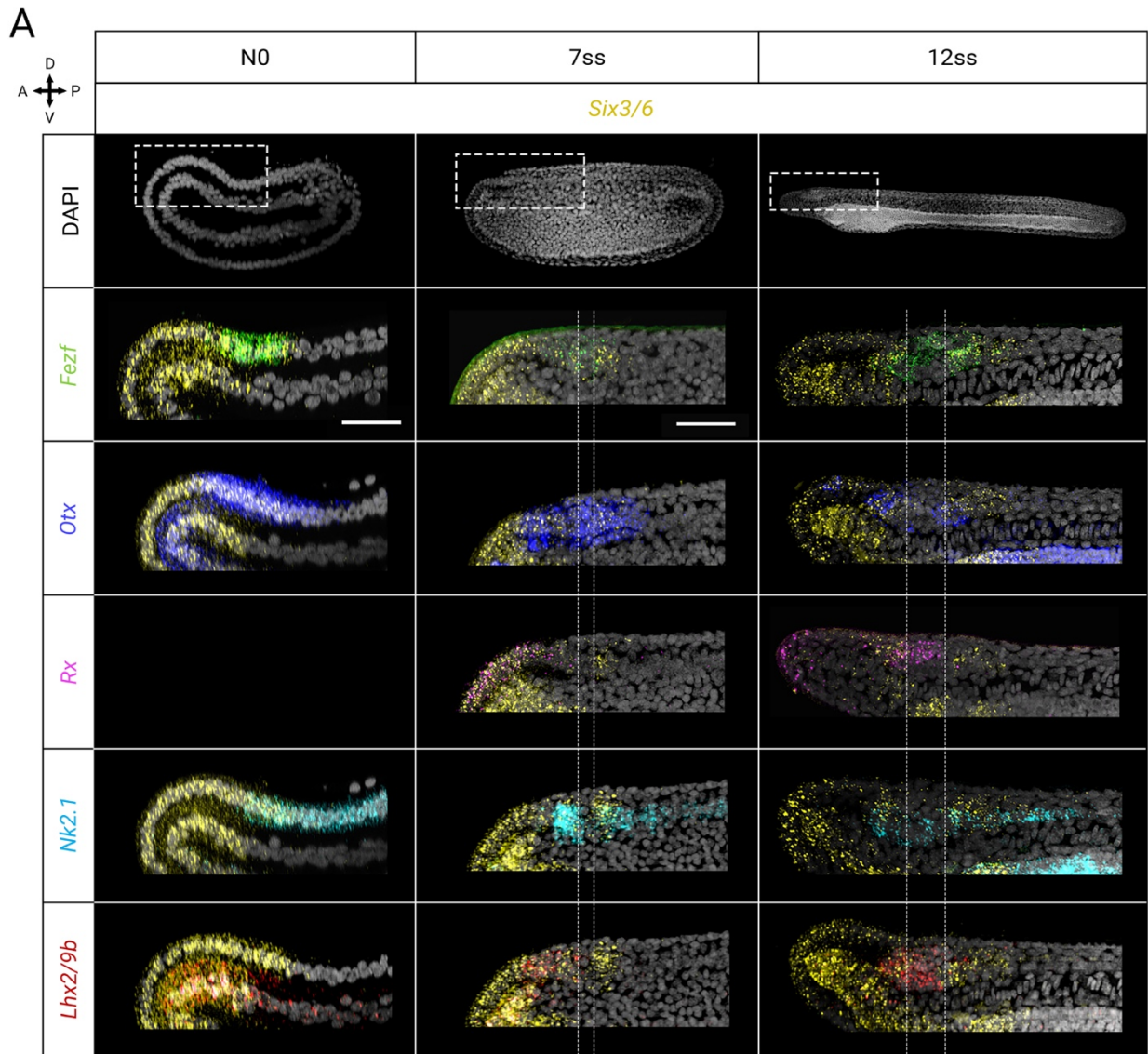
**Figure 3.5.** Co-expression and anterior restriction of early aGRN genes during neurulation. **A.** Combination of *Six3/6* (yellow), *FoxQ2* (blue), *Frz5/8* (green) and *sFRP1/2/5a* (red) expression in late gastrula (G5), early neurula (N0) and mid neurula (7ss) stages. Dashed boxes in the DAPI channel indicate the anterior-dorsal ectoderm in which all combinations are presented. In these magnifications nuclear edges are shown to improve visualization of co-expression. **B.** Co-localization of *Six3/6* (yellow), *Elav* (blue, neural) and *FoxJ* (red, non-neural) in N0 stage embryos demonstrate that *Six3/6* is expressed in both neural and non neural ectoderm. Scale bars are 50 $\mu$ m.

A notable feature of ANE development in planktonic larvae is that the broad animal expression of early members of the network (such as *Six3/6* and *FoxQ2*) precedes the appearance of neural progenitors and comprises both future neural and non-neural ectodermal cells (141, 145). After showing that *FoxQ2* is expressed before the appearance of the neural plate (Figure 3.4B), I detected the expression of *Six3/6* together with the pan-neural marker *Elav* and the ciliated cell marker *FoxJ* in N0 embryos (Figure 3.5B). At this stage, *FoxJ* is found exclusively in non-neural ectodermal cells and is mutually exclusive with *Elav*, forming a boundary that clearly defines the two ectodermal tissues (Figure 3.5B). Here I show that *Six3/6* is expressed in both anterior-dorsal *Elav*-positive cells and the anteriormost *FoxJ*-positive cells. As development progresses and the ectodermal derivatives become distinguishable morphologically, *Six3/6* restricted towards the anterior pole but continued to be expressed in both neural and non-neural anterior tissues (Figure 3.5A). The expression patterns described here closely resemble those of ambulacrarian larvae, suggesting that the early aGRN was maintained at the origin of the chordate phylum.

### 3.2.3 Late genes are expressed during gastrulation

Next, I considered downstream “late phase” genes to determine whether they are expressed in the region where the early aGRN is active in amphioxus. I investigated the developmental expression of *Six3/6* with *Fezf*, *Otx*, *Rx*, *Nk2.1* and *Lhx2/9b* in four different stages spanning amphioxus neurulation: G5, N0, 7ss and 12ss (early larva) (Figure 3.6). To better visualize the co-expression of each gene with *Six3/6*, I also used Fiji to invert the colours and use a red-cyan palette which highlights areas of signal overlap in black (Appendix VI, Figure A6.2).

**Figure 3.6.** Late aGRN genes are expressed in the anterior brain during amphioxus neurulation (overleaf). **A.** Analysis of *Six3/6* (yellow) co-expression in the anterior ectoderm with late aGRN genes *Fezf* (green), *Otx* (blue), *Rx* (magenta), *Nk2.1* (cyan) and *Lhx2/9* (pink) from early neurula (N0) to early larva (12ss). Dashed lines delimit the intercalated *Six3/6*-negative region. **B.** Expression plots showing relative position of each gene along the AP axis within the amphioxus neuroectoderm. **C.** Profiling of serotonergic neurons in the amphioxus early larva (14ss). Co-detection of serotonergic marker *SerT* (red) with *Fezf*, *Six3/6*, *Lhx2/9* and *Otx*. Nuclear signal was masked using the DAPI channel. Scale bars are 50µm.



All the 5 genes progressively appeared in the anterior-dorsal ectoderm during neurulation, so that by the 7ss stage they were all expressed in the amphioxus CV (Figure 3.6A). At the beginning of neurulation *Fezf* transcripts were localized in the anterior tip of the neural plate. The expression also restricted to individual cells at the end of neurulation, marking the region posterior to the frontal eye, the dorsal roof of the CV and cells posterior to the infundibular organ (composed of secretory cells that produce the Reissner's fiber). *Otx* is already expressed on the dorsal side of the late gastrula stage, and at N0 it reaches more posteriorly than *Six3/6* and *Fezf*. It remained localized in a similar position marking all cells of the anterior neural tube during neurulation, while at 12ss it disappeared from the intercalated *Six3/6*-negative region and started to break up into individual cells within the brain, including the frontal eye, the roof of the CV and cells posterior to the infundibular organ.

At the 7ss stage the first sign of *Rx* appeared in the anterior ectoderm and the tip of the neural tube in the anterior *Six3/6*-positive population, where it continued to be expressed after the formation of the CV. *Nk2.1* was expressed in floor plate progenitors from the late gastrula stage, but by 7ss a new population appeared in the intercalated *Six3/6*-negative region of the brain which persisted at 12ss. Moreover, at the end of neurulation a few cells of the frontal eye complex also started to express *Nk2.1*. Finally, *Lhx2/9b* was expressed in the anterior tip of the endoderm during neurulation, but a new domain appeared in the anterior CV in 7ss embryos and persisted to the larval stage.

A hallmark of AOs that develop through the aGRN in marine larvae is the presence of serotonergic neurons (96). Previous investigations had highlighted the presence of the serotonergic marker *SerT* at the anterior tip of the CV, corresponding to Row2 cells of the frontal eye complex (221). By co-detecting selected aGRN genes and *SerT* at 14ss, I found that serotonergic co-express *Fezf*, while only in few larvae the anteriormost cells of the *SerT* cluster were also positive for *Six3/6* (Figure 3.6C). On the other hand, *SerT* signal does not co-localize with *Otx*, which marks Row1 and pigment cells directly anterior to the serotonergic cluster, or with *Lhx2/9*.

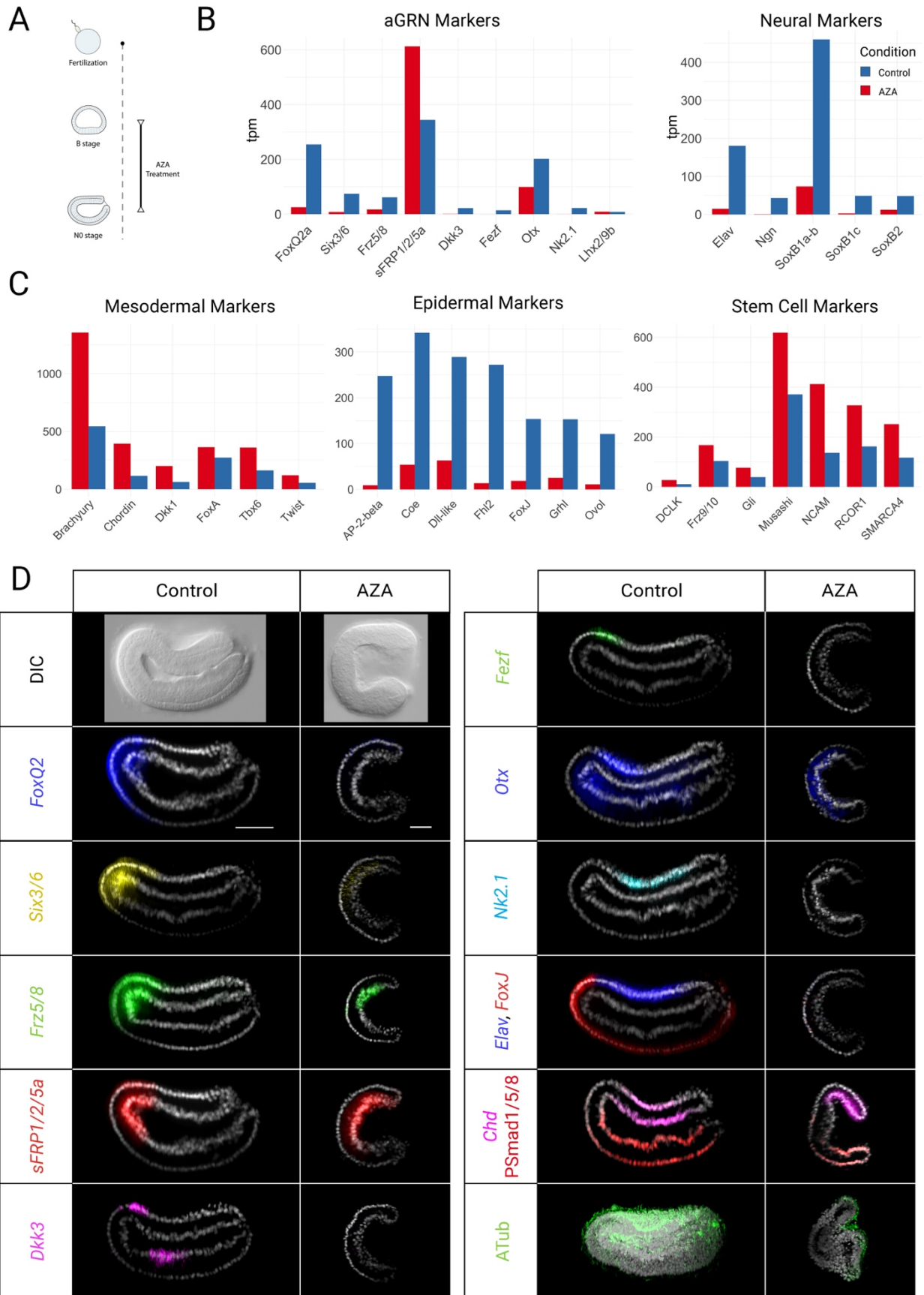
Overall, gene expression data from amphioxus neurulation shows that aGRN genes are activated in similar domains and in a similar temporal sequence as in Ambulacraria ANE patterning, defining an increasingly diverse number of cell populations in the anterior part of the nervous system that include serotonergic neurons.

### 3.3 Wnt signalling and the amphioxus aGRN

In eumetazoan larvae the expression of *Six3/6* and *FoxQ2* is negatively regulated by members of the Wnt family, in particular *Wnt1* and *Wnt8* (97, 151, 161, 204). Previous experiments have shown that ectopic activation of Wnt/ $\beta$ -catenin signalling results in the loss of the aGRN (97, 156, 205). In amphioxus the expression pattern of *Wnt8* suggests a similar role that however remains untested. To understand whether the structure of the amphioxus aGRN is also influenced by Wnt/ $\beta$ -catenin, I interfered with Wnt signalling through pharmacological treatments with Azakenpaullone (AZA) that overactivates Wnt signalling. Developing embryos were treated at different developmental timepoints: from B stage, when *FoxQ2* first starts to be expressed, to the N0 stage; and from the G5 stage, when the neural plate is already specified (Figure 3.7) until the 7ss stage, when late phase genes are detected in the anterior part of the neural plate (see Figure 3.8). Changes in gene expression between control and treated embryos were analysed through bulk RNAseq and HCR.

#### 3.3.1 Early AZA treatment

When Wnt signalling is overactivated from the beginning of zygotic transcription (Figure 3.7A), embryos at the N0 stage showed an incomplete gastrulation: the vegetal pole invaginated to form an outer epiblast and an inner hypoblast, but the blastopore remained wide open posteriorly and the embryo did not flatten dorsoventrally as in normal development (Figure 3.7D). Early apical markers *FoxQ2*, *Six3/6*, *Frz5/8*, *sFRP1/2/5a* and *Dkk3* decreased or disappeared following AZA treatment, together with the few late phase members that are expressed anteriorly at the early neurula stage, such as *Otx* and *Fezf* (Figure 3.7B). Interestingly, changes in the spatial distribution of these transcripts observed by HCR showed that the loss of expression was specific to the ectoderm. *Six3/6*, *Frz5/8*, *sFRP1/2/5a* and *Otx* continued to be expressed in the mesendoderm, meaning they were specifically downregulated in the anterior/dorsal ectoderm (Figure 3.7D). This result explains why in the bulk RNAseq dataset *sFRP1/2/5a* actually increased in counts and shows that results from whole-organism methods like RNAseq should always be interpreted carefully. Similarly, *Lhx2/9* does not show a significant change in AZA treated embryos as at the N0 stage it marks anterior mesodermal cells (Appendix V).



< **Figure 3.7.** Wnt overactivation during early stages causes loss of aGRN genes and blocks neural specification. **A.** Experimental design of early Azakenpaullone treatment. **B.** Differential expression between control and treated embryos shows a decrease in both aGRN and neural genes. **C.** Changes in the expression of mesodermal, epidermal and stem cell markers following AZA treatment indicate mesoderm expansion and loss of epidermal differentiation. **D.** Spatial distribution of selected genes in control and treated N0 embryos show ectoderm-specific loss of aGRN markers and of neural and non-neural genes without evidence for changes in dorsoventral patterning. Scale bars are 50 $\mu$ m.

Next, I investigated the context in which these changes were happening by looking at the expression of neural, ectodermal and mesodermal genes. Early pan-neural markers including *Elav* disappeared following Wnt overactivation, in accordance with previous investigations (220, 222), while mesodermal markers were upregulated (Figure 3.7C). To test whether the loss of neural ectoderm was due to a disruption of DV axis formation, I tested the expression of *Chordin* (*Chd*), a dorsal marker in chordates, and the localization of phosphorylated Smad1/5/8 (PSmad1/5/8), an effector of ventral Bmp signalling (223, 224). The two markers were correctly localized at opposite sides of both control and treated embryos, although the neural expression of *Chd* was reduced in AZA treated embryos (Figure 3.7D). This indicates that the treatment at the stages considered does not disrupt DV patterning. Curiously however, markers of the non-neural ectoderm were also downregulated at this stage (Figure 3.7C). The increased expression of stem cell markers, such as *Musashi*, *Ncam*, *Rcor1* and *Smarca4* suggests that ectodermal cells may have retained an uncommitted signature following early Wnt overactivation (Figure 3.7C). In support of this hypothesis, immunolocalization of acetylated tubulin shows that while control embryos are completely ciliated at this stage, treated embryos only have cilia on the inner mesendodermal layer (Figure 3.7D).

### 3.3.2 Late AZA treatment

The early treatment showed that Wnt signalling regulates the aGRN and inhibits the specification of the amphioxus nervous system during gastrulation. Therefore, I next treated embryos from the late gastrula stage, when neural progenitors can be detected in the dorsal side of the embryo (Figure 3.8A). Treated embryos were ciliated and completed gastrulation forming the main tissues characteristic of this stage: the ectoderm was divided into neural plate and non-neural ectoderm; endoderm and mesoderm were distinguishable and the latter was clearly divided into axial (notochord) and paraxial (somites) mesoderm (Figure 3.8B).

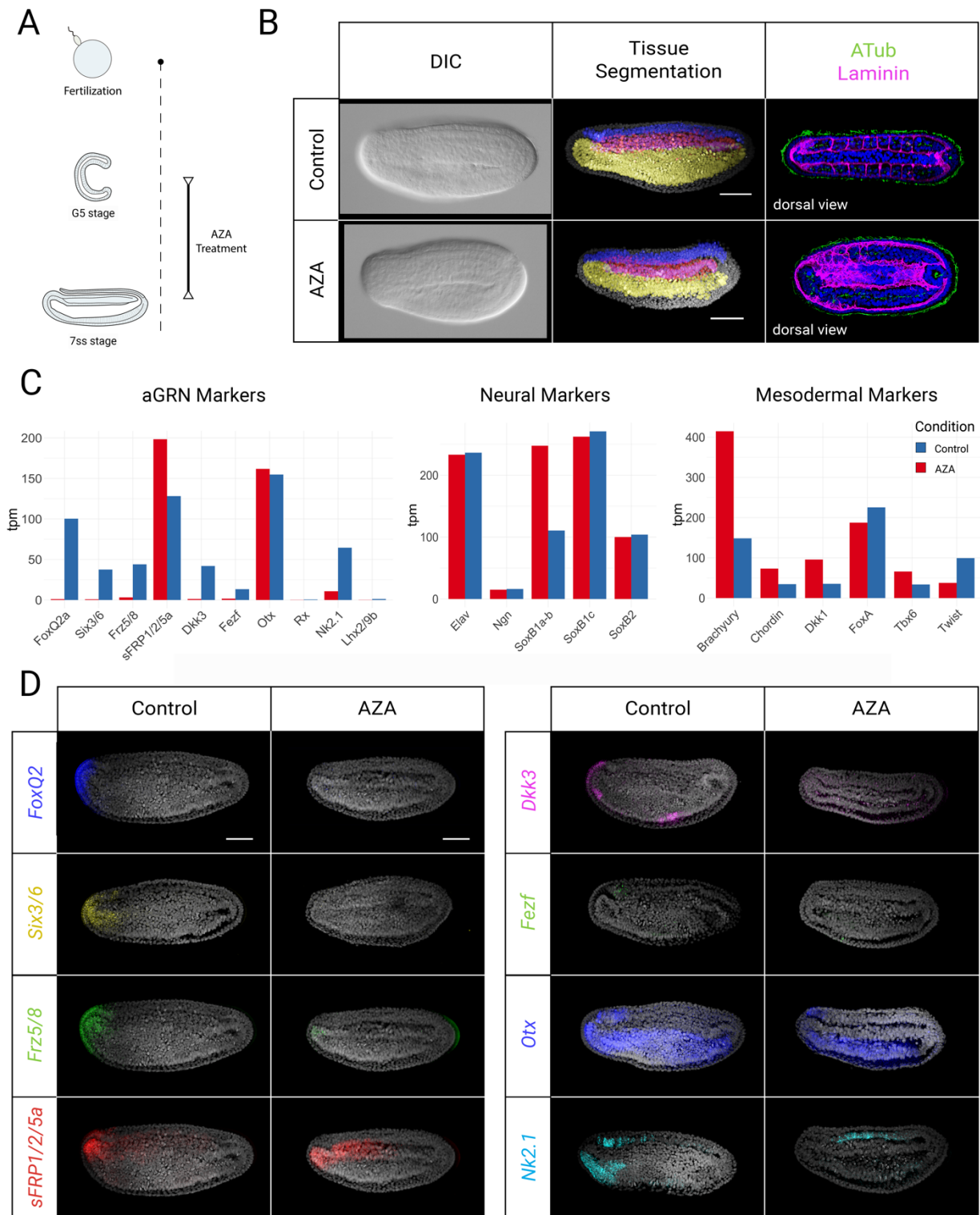


**Figure 3.8.** Late Wnt overactivation causes aGRN inhibition without affecting neural specification. **A.** Experimental setup of late Azakenpaullone treatment. **B.** Morphological changes following late Wnt overactivation. **C.** Differential expression of aGRN, neural and mesodermal markers demonstrate that while the aGRN is still controlled by Wnt at this stage the neural plate forms normally. **D.** Spatial detection of aGRN markers indicates that the effect of Wnt overactivation is specific to the anterior ectoderm. Scale bars are 50 $\mu$ m.

However, there were visible phenotypic alterations: the anteriormost part of the epidermis was flattened, so that the neural plate reached the anteriormost tip of the embryo, and the somite boundaries did not form correctly, either maintaining a continuous presomitic mesoderm at each side of the notochord or showing incomplete inter-somitic membranes (Figure 3.8B). Following AZA treatment, the expression of both early and late aGRN genes was severely downregulated in the ectoderm: *FoxQ2*, *Six3/6*, *Frz5/8*, *sFRP1/2/5a* and *Dkk3* disappeared from both neural and non-neural ectoderm, neural expression of *Fezf* was lost and *Otx* was restricted to the anterior tip of the neural plate (Figure 3.8C-D). Curiously, *Nk2.1* disappeared in the brain of treated embryos but persisted in floor plate cells along the neural plate, suggesting that the two populations are specified through different and independent mechanisms (Figure 3.8D).

These results indicate that Wnt signalling can still control the aGRN even after gastrulation. However, at this stage no significant decrease of neural markers was detected in treated embryos (Figure 3.8C), and *Elav* was still expressed in the dorsal neural plate and the peripheral nervous system (Figure 3.9A). Moreover, *FoxJ* transcripts could be detected throughout the non-neural ectoderm and in the trunk region of the neural tube following treatment, but were absent anteriorly in both control and treated embryos (Figure 3.9A). These results suggested that the formation of the neural plate is not affected by the treatment at this stage. To confirm this, I segmented the neural plate using Imaris and found no significant difference in cell number (n=12, Student t-test, p=0.607) or volume (n=16, Student t-test, p=0.591) between treatment and control (Figure 3.9B). It is important to note however that while *Elav* expression in the neural plate normally becomes segmented at the 7ss stage, in treated embryos it remained broad, hinting at a role of Wnt signalling in the regionalization and maturation of the trunk neural plate (Figure 3.9A). This idea is further reinforced by the increased expression of *SoxB1a* in treated embryos compared to control (Figure 3.8C), as this gene is active in the early neural plate but is replaced by its paralog *SoxB1c* during neurulation (225).

The evidence that Wnt does not disrupt the development of the neural plate at the stage considered meant that I could examine the effects on gene expression in the nervous system due to the loss of the aGRN, and specifically understand the impact this has on the identity of anterior cells. I compared the expression of the anterior markers *Otx* and *Pax4/6* and the posterior markers *Gbx* and *Hox1* (Figure 3.9C). Wnt overactivation causes the reduction of anterior gene expression and the expansion and shift of posterior genes. *Otx* and *Gbx* normally form a boundary behind CV, which is

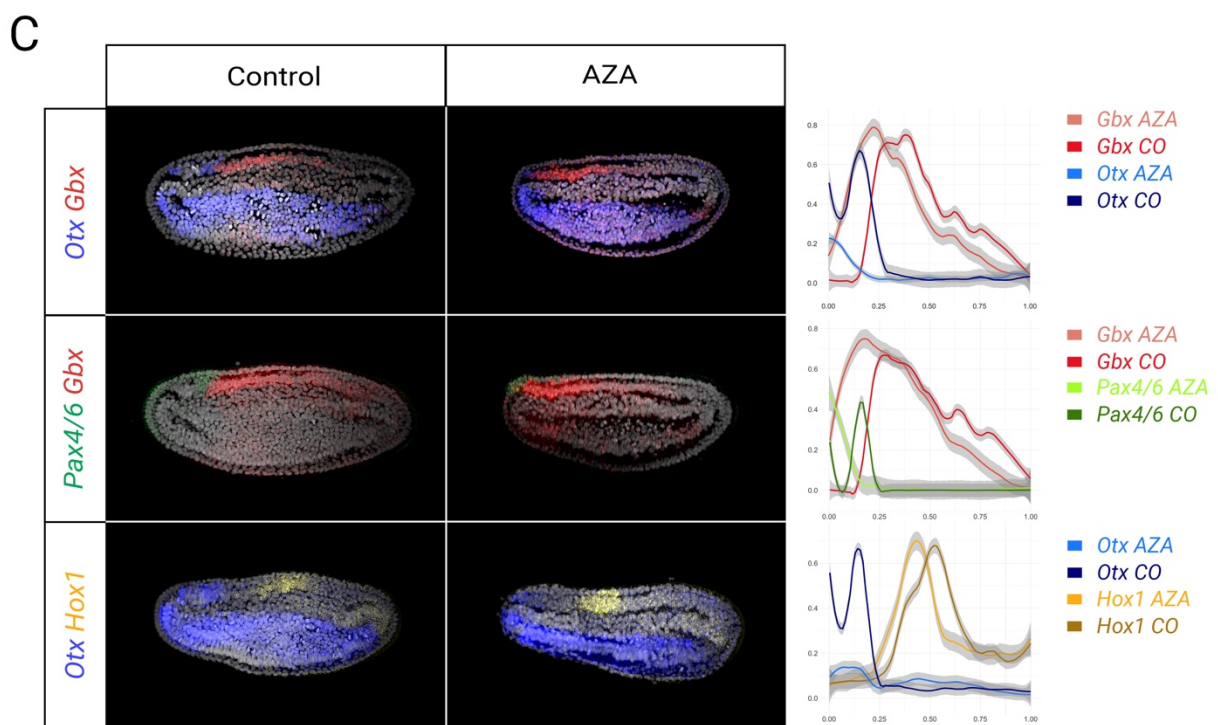
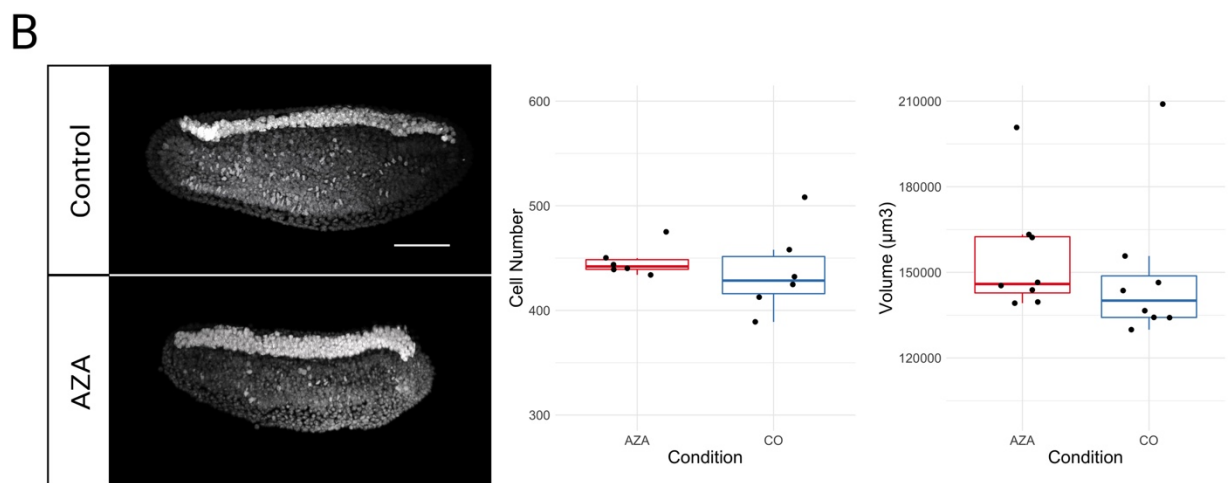
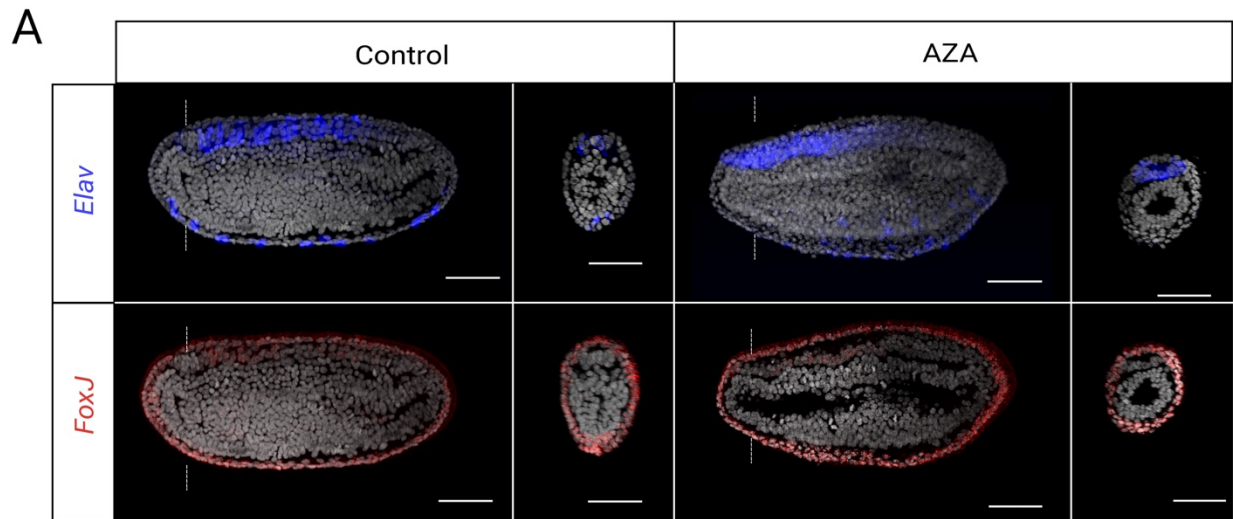
thought to correspond to the anterior limit of a hindbrain-like region (see Chapter V), but in treated embryos strong *Gbx* expression marked anterior cells in the neural plate and *Otx* and *Pax4/6* remained only in the anteriormost cells of the neural plate (and in some anterior-dorsal epidermal cells for *Pax4/6*). Similarly, the trunk expression of *Hox1* is anteriorized following AZA treatment.

Taken together, the experiments I performed on Wnt overactivation indicate that an aGRN is present in amphioxus, divided into early and late phases that are negatively regulated by Wnt signalling similarly to ambulacrarian larvae. The aGRN is necessary to confer anterior neuroectoderm identity, but not to specify cells as neurons: overactivation of Wnt does not reduce the number of cells in the neural tube, but anterior neurons lose the expression of anterior markers and acquire posterior fate.

## 3.4 Discussion

### 3.4.1 Conservation of the aGRN in deuterostomes

The comparison of modern chordates has revealed that their common ancestor possessed a dorsal hollow neural tube with an anterior brain, but the origin of this central aspect of the chordate bauplan remains unknown. Most of the scenarios proposed since Garstang's now discarded "auricularia hypothesis" have focused on the comparison of chordates with their sister group, the Ambulacraria (these hypotheses will be further discussed in Chapter VII) (63, 226, 227). However, the adult nervous systems of ambulacrarians have been notoriously difficult to interpret and have been studied in an evolutionary framework only recently (136, 228). Conversely, the swimming larval stages of echinoderms and hemichordates possess several morphological similarities, including neurons associated with ciliary bands and a sensory-neurosecretory AO specified from an ANE territory. A series of studies from the Range and Yaguchi groups have reconstructed a large part of the regulatory interactions that overall specify the AO in sea urchin while others have highlighted the conservation of this network in other ambulacrarians (146, 149, 150, 161, 162). As many of the genes that are involved in the formation of the AO in ambulacrarians are also found in the vertebrate brain, some authors hypothesised that the anterior neural territory (ANE) is homologous in deuterostomes (and possibly in all bilaterians), and that it is specified by a conserved aGRN (145, 146).



< **Figure 3.9.** Loss of aGRN by late Wnt overactivation leads to posteriorization of the anterior neural plate. **A.** Expression pattern of neural marker *Elav* (blue) and ciliated cell marker *FoxJ* (red) does not change significantly between control and Azakenpaullone treatment during neurulation. **B.** Late Wnt overactivation does not change cell number and volume of the neural plate at the 7ss stage. Neural plate nuclei are false-colored in white. **C.** HCR detection of anterior and posterior markers in the neural plate at 7ss. The anterior markers *Otx* (blue) and *Pax4/6* (green) are strongly downregulated in treated embryos and remain only at the anterior tip of the neural tube, while posterior markers *Gbx* (red) and *Hox1* (yellow) extend and shift anteriorly. Scale bars are 50 $\mu$ m.

Here, surveying a sea urchin developmental scRNAseq dataset highlighted 11 genes that are involved in the formation of the AO. Orthologs of 10 of these genes were also expressed in the zebrafish forebrain, with the exception of *FoxQ2*. Many of these genes are also expressed in other cell populations, both in sea urchin and zebrafish, but the combination was unique to these specific cell types. These results are in accordance with a recent study that hypothesized the conservation of the bilaterian neurogenic programme based on the conserved expression of a similar set of genes (the study also highlights *Hbn* as a main marker of the ANE: this gene appeared in our analysis too but was not considered because it has been lost in the chordate lineage) (145). Previous hypotheses on the conservation of the ANE however were not able to account for the differences in the expression of these genes: in sea urchin the early aGRN we identified starts at the morula stage throughout the animal half of the embryo. In vertebrates the orthologous genes are expressed within the neural plate, and more specifically the most complete combination is found in the hypothalamus. If the two networks are homologous, how are these differences explained, and how did they arise during deuterostome evolution? Analysis of the aGRN in amphioxus allowed me to address these questions: the early portion of the network, including *FoxQ2*, is active on the entire animal half of amphioxus embryos, supporting a conserved expression between ambulacrarians and chordates. The anterior restriction of early aGRN genes in amphioxus, their expression in both neural and non-neural tissues and the temporal activation of late aGRN genes are all more similar to ambulacrarians than vertebrates. And yet, in the nervous system aGRN genes are expressed in the most anterior region which is thought to be homologous to the vertebrate secondary prosencephalon (87) (see Chapter V). This suggests a “continuous”, stepwise scenario in which the aGRN was maintained on the anterior side of the embryo during chordate evolution, and then the early expression was lost in the vertebrate lineage, where the aGRN become restricted to the nervous system only.

Functional tests on aGRN genes further support this scenario: in echinoderms the inhibition of the aGRN at different levels leads to the loss of the AO: knocking down *Six3/6*, *FoxQ2*, *Fezf*, *Nk2.1* or *Lhx2/9* causes the absence of serotonergic neurons in echinoderm larvae (149, 150, 154, 157). Similarly, in vertebrates many of the aGRN genes are required for the correct development of the forebrain: the absence of *sFRP* or *Six3/6* paralogs causes loss of anterior structures, and *Fezf/Nk2.1* and *Rx* are required for the correct development of the hypothalamus and retina respectively (229–232). In both taxa, these effects can be replicated by the ectopic activation of Wnt signalling (in particular *Wnt8*), though the source of Wnt is different in ambulacrarians and vertebrates (156, 161, 233, 234). In echinoderms, Wnt signalling that can inhibit the aGRN is active at the vegetal pole of the embryo by the maternal accumulation of  $\beta$ -catenin, while in vertebrates the forebrain is affected by Wnt ligands produced by the diencephalon (211, 235, 236). Based on these results, if the aGRN was conserved during chordate evolution, I would expect Wnt signalling to continue to control the expression of aGRN genes in both neural and non-neural ectoderm. In amphioxus, early Wnt ligands are concentrated at the vegetal pole, similar to echinoderms (237). The results of my Wnt overactivation experiments show that Wnt signalling inhibits the entire ectodermal expression of aGRN genes throughout gastrulation and neurulation, again indicating a conserved control of aGRN localization in deuterostome embryos. However, the late AZA treatment, in which the neural plate was not reduced but lost expression of anterior genes, demonstrated that the network is not required to specify or maintain neuronal fate, but to instruct neural progenitors to a particular (anterior) identity. This mechanism is in accordance with data from both starfish and sea urchin. In starfish, inhibition of *Six3/6* leads to the loss of serotonergic neurons, but the rest of the neurons, which are scattered across the early ectoderm and are marked by *SoxC* are still present (162). In sea urchin, the neurogenesis pattern is already restricted to precise domains (238), so it is more difficult to test the effect of aGRN inhibition on neurogenesis. Even so, a previous experiment by Range combined *Six3/6* knock-down and Wnt inhibition and revealed that the other aGRN genes still expanded throughout the entire embryo, as they did when only Wnt signalling was inhibited (152). Range concludes that sea urchin *Six3/6* is mainly involved in the inhibition of Wnt signalling on the animal side, and not in the direct control of downstream genes. Overall, these results suggest that the main function of the early aGRN is likely the instruction of “anterior” positional information, by producing a Wnt-free environment that guides the expression of downstream genes that specify anterior neural fate.

As a final note, it is important to consider that there are some interesting differences between the aGRN in amphioxus and ambulacrarians. The early aGRN in amphioxus appears to become dorsal already during gastrulation, while the early expression of *Six3/6*, *FoxQ2* and *Frz5/8* is radial in ambulacrarians. The treatments carried out in this thesis did not allow me to investigate how this dorsalization is controlled, but it would be interesting in the future to understand if and how the mechanisms of DV patterning might be involved in the dorsalization of the aGRN (see Chapter VI). In sea urchin, *FoxQ2* is known to inhibit Nodal signalling restricting it to the ventral side (149, 155). As Nodal is one of the regulators of DV regionalization in chordates (and particularly crucial for the specification of the neuroectoderm in amphioxus), it would be a primary candidate for testing its interactions with the aGRN.

### 3.4.2 Dynamic roles of Wnt signalling in chordate development

As described above, Wnt signalling is the main regulator of the ambulacrarian aGRN. The role of Wnt/ $\beta$ -catenin signalling has been thoroughly elucidated in both echinoderms and hemichordates and has revealed its evolutionary conservation:  $\beta$ -catenin localizes at the vegetal pole where it controls mesendodermal fate, while at the same time Wnt/ $\beta$ -catenin signalling limits ectodermal fate to the animal side of the embryo (141, 146, 147, 239). Numerous studies have now shown that the prospective ectoderm is initially neurogenic, but Wnt signalling restricts the expression of *Six3/6* and *FoxQ2* and the ANE fate to the animal tip of the ectoderm (146). These roles have been validated by experimentally manipulating the expression or activity of Wnt proteins and early apical patterning members, including *Six3/6*, *FoxQ2*, *Frz5/8*, *sFRP1/2/5*, *Dkk1* and *Dkk3*, mainly through drug and morpholino treatments (151–153, 156, 161, 239).

Similar experiments have been previously carried out in amphioxus embryos. Overactivation of Wnt signalling with Lithium Chloride (LiCl) at the onset of gastrulation and with BIO from the 16-cell and early gastrula stages revealed that Wnt controls mesodermal specification and posterior fate, decreasing the expression of the anterior markers *FoxQ2* and *Otx* (222, 240). In a recent study, treatment with CHIR99021 (which inhibits  $\beta$ -catenin phosphorylation) at the 1-cell stage dorsalized amphioxus embryos at the gastrula stage, while the same treatment at the blastula stage had no effect on the expression pattern of dorsal genes (241). Additionally, inhibition of *Dkk3* translation with Morpholino was shown to cause loss of amphioxus head and anterior markers (220). These

results suggested that in amphioxus Wnt/ $\beta$ -catenin signalling is involved in both AV axis specification, similarly to ambulacrarians, and early specification of dorsal fate, a process that was previously considered a vertebrate innovation. In vertebrates, in fact,  $\beta$ -catenin accumulates dorsally after fertilization and is essential for the formation of the organizer, while during gastrulation Wnt signalling changes function and starts to contribute to ventral/posterior fate (234, 241–243).

Here I provide new insights on Wnt function by treating amphioxus embryos at two successive stages with the GSK3 inhibitor Azakenpaullone. Treatment from the blastula stage, when zygotic expression of *FoxQ2* is starting, resulted in the repression of neural induction and expansion of mesodermal tissue, corroborating previous results. These effects are not due to repression of dorsal fate, as *Chd/PSmad1/5/8* localization is unaltered in treated embryos. At the same time, ectopic activation of Wnt caused the downregulation of all apical patterning genes in both neural and non-neural ectoderm, indicating a conserved role of Wnt signalling in the control of apical patterning genes and specification of ANE in deuterostomes. Importantly, the mesendodermal expression of *Six3/6*, *Frz5/8*, *sFRP1/2/5a* and *Otx* was not depleted following treatment, indicating that Wnt signalling is specifically acting on ectodermal apical patterning at this stage. I also performed AZA treatment at the late neurula stage, when the neural plate has been specified. As expected, the treatment at this stage did not result in neural inhibition, as the position and morphology of the neural plate was preserved. Yet, all aGRN markers analysed were still downregulated in the ectoderm and the anterior portion of the embryo's head was truncated, so that the neural tube reached the anterior tip of the animal. Like in early neurulas, the inhibition is specifically restricted to the anterior ectoderm and nervous system, which will form the larval CV: *Nk2.1* remained expressed in the floor plate, while the anterior brain population disappeared in treated embryos. The anterior nervous system is posteriorized following Wnt overactivation; *Gbx* expression is expanded anteriorly and, at the same time, the anterior marker *Otx* is reduced to only few cells at the tip of the neural plate.

According to these results and previous work on amphioxus Wnt signalling, I propose three stages of Wnt activity during amphioxus embryogenesis:

1. During cleavage, dorsal accumulation of  $\beta$ -catenin on the vegetal/dorsal side, possibly of maternal origin, is necessary to specify dorsal fate and for the development of the dorsal organizer, as recently elucidated (241).

2. Starting from the blastula stage, Wnt/ $\beta$ -catenin signalling controls posterior fate and can repress neural induction if activated ectopically. At this stage, apical marker *FoxQ2* starts to be expressed in the animal pole while *Wnt8* forms an abutting ring in the vegetal half of the embryo. During gastrulation, neural progenitors appear within the *FoxQ2* domain; we hypothesize that this might be a necessary condition and that ectopic Wnt expression might repress neural domains by eliminating *FoxQ2* expression. To test this, experimental inhibition of *FoxQ2* is required. Apical markers begin to restrict towards the anterior side of the embryo and at the same time their expression becomes dorsalized, indicating that regulators of DV axis are acting on apical patterning in amphioxus, although the mechanism remains to be investigated.

3. By the late gastrula stage, the neural plate is specified and Wnt overactivation no longer inhibit its formation. However, Wnt continues to specify posterior and mesodermal fates and to control the restriction of apical patterning genes in the ectoderm, eventually restricting them to the amphioxus brain, where they contribute to its differentiation and acquisition of ANE fate.

### 3.4.3 Conclusions

The key question posed in this chapter was whether an aGRN, which is thought to be ancestral to bilaterians, was conserved during chordate evolution and was still involved in the development of the anterior portion of the neuroectoderm, the ANE. My results on amphioxus development show for the first time that the aGRN network is present in a chordate:

- ◆ I identified a conserved set of genes expressed during ANE formation in deuterostomes: *FoxQ2*, *Six3/6*, *Frz5/8*, *sFRP1/2/5*, *Dkk3*, *Fezf*, *Otx*, *Rx*, *Nk2.1* and *Lhx2/9*. These genes represent the core of the aGRN in deuterostomes. With the exception of *FoxQ2*, this molecular signature is also present in the vertebrate forebrain, and specifically within the hypothalamus.
- ◆ In amphioxus, aGRN genes are expressed in a clear temporal sequence, divided in an early phase with *FoxQ2*, *Six3/6* and the Wnt inhibitors *sFRP1/2/5* and *Dkk3* during the early stages of gastrulation, and a late phase with downstream genes *Fezf*, *Rx*, *Nk2.1* and *Lhx2/9* that appear during neurulation. The expression dynamic is similar to the one found in ambulacrarians and is in stark contrast with vertebrates, in which the genes are expressed only within the neural plate.

- ◆ The network of ANE genes is controlled by early vegetal Wnt in both ambulacrarians and amphioxus, as overactivation of Wnt signalling leads to the downregulation of all aGRN markers considered.
- ◆ The aGRN has a role in the specification of anterior neural identity in amphioxus: downregulating the aGRN when the neural plate is specified leads to posteriorization of the neural tube.

In the rest of the thesis, I will further investigate the conservation of the aGRN in deuterostomes and explore the questions that spring from the discoveries made in this chapter: what is the fate of the anterior region of the neural tube in which the aGRN is active in amphioxus? And how did the complex vertebrate brain evolve from the chordate ancestor?



# Chapter IV – Nervous system development in the feather star *Antedon mediterranea*

## 4.1 Introduction

In the preface to the echinoderm volume of her monumental series on invertebrate biology, the distinguished zoologist Libbie Henrietta Hyman wrote: “*I also here salute the echinoderms as a noble group especially designed to puzzle the zoologist*” (244). This provocative statement refers to the curious features of the body plan in this phylum: echinoderms are bilaterians, but the adult body is organized in five rays – the radia or arms - around a central axis, a derived condition called pentaradial symmetry. Consequently, adult echinoderms do not show clear AP, DV and LR axes and their body is instead divided in an oral and aboral surface. Other echinoderm features include: a calcitic mesodermal endoskeleton organized in a characteristic porous structure - the stereom; a coelom-derived water vascular system used for feeding, locomotion and respiration; a connective tissue whose mechanical properties can be quickly and intentionally changed by the animal, called mutable collagenous tissue; and high regenerative abilities (93, 245). The phylum is divided into five extant taxa of marine animals. Echinoids (sea urchin, sand dollars), holothuroids (sea cucumbers), asteroids (sea stars) and ophiuroids (brittle stars) form a conspicuous group called Eleutherozoa, while crinoids (sea lilies, feather stars) belong to the taxon *Pelmatozoa* and are the sister group to the rest of the phylum (See Figure 1.1) (246, 247). Most echinoderms develop indirectly through a bilaterally symmetric larval stage, suggesting that a *dipleurula*-type larva is ancestral to the phylum. The larva then undergoes a dramatic - and poorly understood - metamorphosis in which the pentaradial organization of the adult is established. Embryological and larval development have been comprehensively studied in eleutherozoans, especially due to the historical importance of sea urchin as a model organism in developmental biology (248–250). Conversely, crinoids are a critically understudied group, and knowledge on their biology and development remains scarce. However, crinoids occupy a key phylogenetic position to reconstruct the early events in echinoderm evolution, and to correctly compare them with other phyla. In this chapter, I characterize nervous system development in the feather star *Antedon mediterranea*, focusing on the specification of the AO to provide a more complete comparison of aGRN evolution across deuterostomes.

#### 4.1.1 Echinoderm neurobiology: lessons from eleutherozoans

The development of the nervous system has been described extensively in echinoids and asteroids. Broadly speaking, the larval nervous system is associated with four structures: the AO, the ciliary band, the mouth and the gut (141, 238) (Figure 4.1). The AO constitutes the “central”, ganglionic-like structure of the larva, it includes serotonergic and peptidergic neurons and forms in the apical plate as described in Chapter III (96). Depending on the species, the AO can be more or less integrated with the ciliary bands, where other cholinergic neurons form the ciliary band nervous system (135). Serotonergic, dopaminergic and GABAergic populations appear in planktotrophic species in association with the mouth and gut (135, 142). Sea urchins have an additional group of dopaminergic and cholinergic cells, the postoral neurons, that develop early and are positioned ventrally between the mouth and the ciliary band (141, 142). Larval neurons also express a variety of neuropeptides, and the recent analysis of sea urchin scRNAseq datasets have revealed up to 12 neuronal types (Figure 4.1A) (142, 251). Moreover, while the structure of the larval nervous systems appears similar in eleutherozoans, there are important differences in the specification of the neuroectoderm during embryogenesis. In sea urchin, neurogenesis is initiated in only three domains in the embryo, where neural progenitors can be identified: the ANE, the ciliary band and the gut (141, 238, 252). On the other hand, in starfish the ectoderm has a broad neurogenic potential and differentiating progenitors migrate to the ciliary bands after specification (Figure 4.1B) (162, 253).

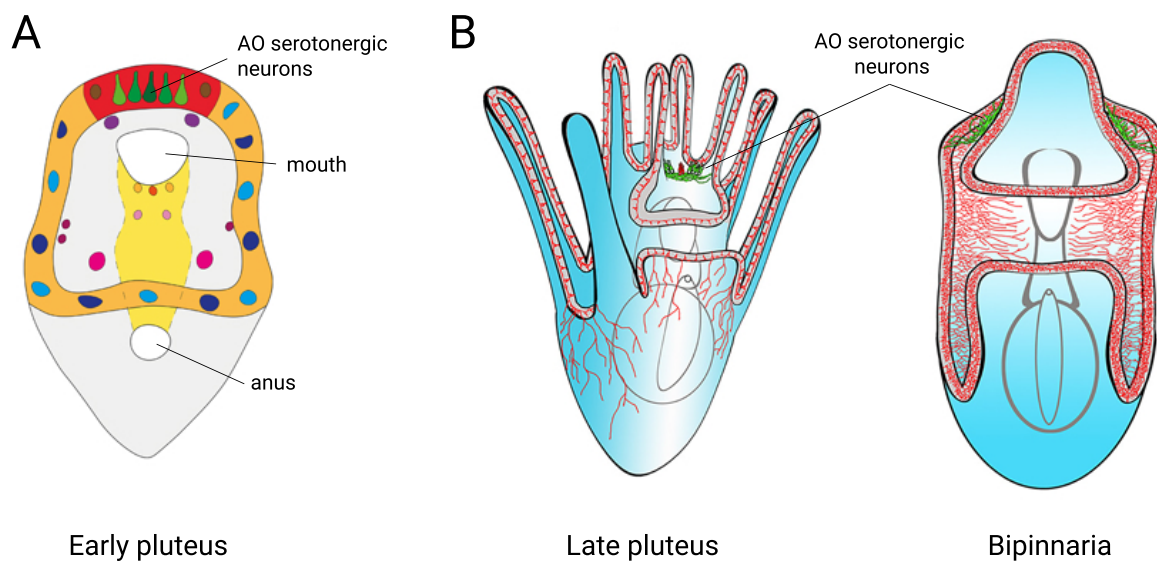


**Figure 4.1.** Larval nervous system of eleutherozoans echinoderms. **A.** Diversity of neural cell types in the sea urchin pluteus nervous system. **B.** Organization of the larval nervous system in sea urchin and sea star larvae. Images modified from (135, 142).

At metamorphosis the larval nervous system degenerates, and a new nervous system develops in the adult. While echinoids are the model for echinoderm development, their adult form is less accessible due to the hard skeleton; information on adult neuroanatomy and physiology therefore mainly comes from stellate echinoderms (sea stars and brittle stars) and sea cucumbers (228, 254). The adult nervous system of echinoderms is poorly centralized and generally follows the pentaradial symmetry scheme. A circumoral nerve ring runs around the mouth, from which radial nerve cords enter and run through each radius. The CNS in eleutherozoans is divided in two interconnected components: the ectoneural system is the most superficial on the oral side of the body and is the largest part of their nervous systems; the hyponeural system is found aborally from the ectoneural and is thought to have a primarily motor function. These components are in contact with an extensive and diffuse neural plexus that innervates several structures in the body (93, 254, 255). Neurons within the CNS have been shown to express a variety of neurotransmitters, such as acetylcholine, GABA and dopamine (but curiously not serotonin), and to use a wide array of neuropeptides, which have fundamental roles in echinoderm activities such as feeding, movement and reproduction (93, 256). The formation of the adult nervous system after metamorphosis is poorly understood, but recently the optimization of culturing techniques for several eleutherozoans have allowed the investigation of echinoderm juveniles, revealing that they already possess a circumoral nerve ring and radial nerve cords, separated in ectoneural and hyponeural components, and a broad basiepidermal plexus (228, 257).

#### 4.1.2 A feather star is born: crinoid development

While crinoids have been largely ignored after the dawn of molecular biology, thorough descriptions of their anatomy and development were produced during the first half of the 19<sup>th</sup> century (244, 258, 259) and adult crinoids have been used as models for regeneration (260). There are two types of crinoids: sea lilies are sessile and remain attached to the substrate throughout their life by a stalk; feather stars have sessile juveniles but then detach from the stalk as free-living adults. The ancestral form is stalked, but feather stars are not monophyletic, as stalked forms re-evolved at least twice from stalkless crinoids (261). Information on crinoid development comes from few feather star genera (*Antedon*, *Florometra* and *Anneissia*) and one sea lily (*Metacrinus*). These groups develop indirectly through a yolk-rich lecithotrophic doliolaria larva, but curiously sea lilies also

possess an early and transient auricularia-type larva (262, 263). During holoblastic cleavage, the yolk is divided into the blastomeres and the spherical blastula undergoes invagination from the vegetal pole at the beginning of gastrulation (258, 264, 265). The blastopore closes after gastrulation and the archenteron becomes a closed sac surrounded by numerous mesenchymal cells that delaminate into the blastocoel during gastrulation. After blastopore closure, the archenteron divides into two cavities, the somatocoel and enterohydrocoel; the latter will further divide into hydrocoel (ventral), axocoel (anterior) and enteric sac (dorsal), but the gut remains closed until after metamorphosis, when both mouth and anus will form. The ectoderm is initially fully ciliated but then cilia arrange into circumferential bands and an apical tuft at the level of the anterior apical pit (in sea lilies there is a previous transient phase with longitudinal ciliary bands similar to the auricularia larvae of sea cucumbers). Moreover, the ectoderm develops two ventral ciliated grooves: the adhesive pit secretes adhesive molecules for settlement, and the vestibule which will form the mouth after metamorphosis. The doliolaria larva is then ready to hatch (Figure 4.2A) (108, 244, 258, 263, 266).

After a short swimming period, the larvae settle and undergo metamorphosis forming the transient post-metamorphic cystidean stage. This metamorphosis causes a drastic change of the body plan, but contrary to eleutherozoans most larval tissues are rearranged and integrated into the adult (244, 267, 268). The cystidean stage is sessile and is divided in two parts: the calyx contains most of the organs and has ten skeletal plates, while the stalk secures the animal to the substratum and is supported by columnar ossicles. The doliolaria settles on its anterior surface, which will become the stalk, while the oral surface of the calyx forms from the posterior side of the larva (108, 263, 269). After completing the development of the gut and forming the first tube feet - part of the water vascular system used by crinoids for feeding – cystideans become juvenile pentacrinoids, which will detach from the stalk after several weeks in feather stars, becoming free-living (Figure 4.2B). In adult crinoids the oral surface faces upwards towards the water column and has both an oral and anal opening, so that the gut is U-shaped. Adults have a variable number (usually a multiple of 5) of arms that form from an initial five-arm pentacrinoid stage. Each arm is supported by a series of brachial ossicles and has an oral ambulacral groove lined with tube feet that are used for capturing food (Figure 4.2C) (270).

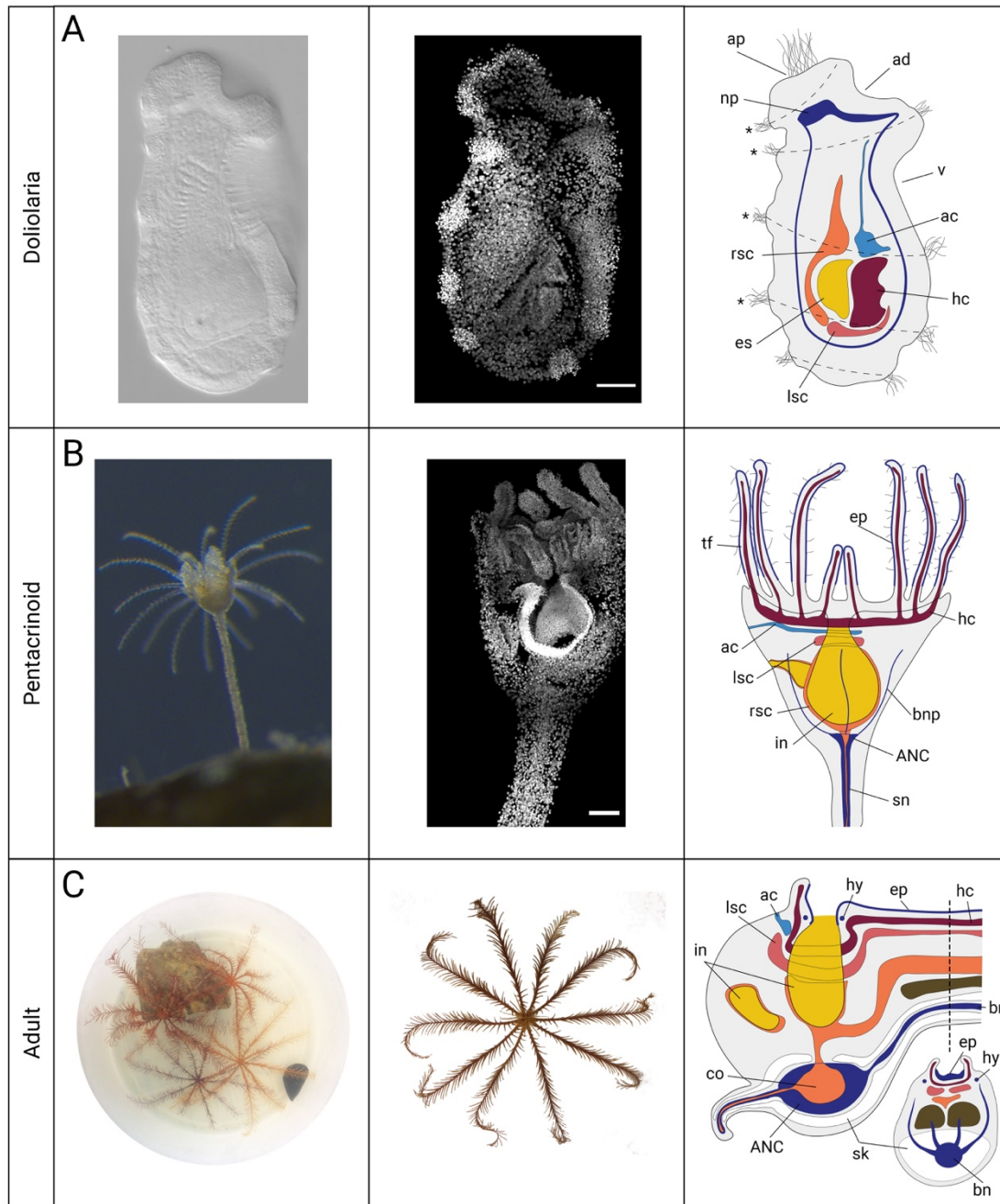


**Figure 4.2.** Anatomy of larval, post-metamorphic and adult stages of the crinoid *Antedon mediterranea*. **A.** DIC image, DAPI staining and schematic organization of the doliolaria larva. **B.** Stereomicroscope picture, DAPI staining and schematic organization of the post-metamorphic pentacrinoid juvenile. **C.** Appearance and morphology of the *A. mediterranea* adults. The schematic focuses on a longitudinal section of the calyx and a cross-section of the arm. Scale bars are 50µm. ac: axocoel (light blue), ad: adhesive pit, ANC: aboral nerve centre, ap: apical pit, ep: ectoneural plexus, bn: brachial nerve, bnp: brachial nerve primordia, co: chambered organ, es: enteric sac (yellow), hc: hydrocoel (purple), hy: hyponeural cords, in: intestine, lsc: left somatocoel (pink), np: neural plexus, rsc: right somatocoel (orange), sk: skeleton, sn: stalk nerve, tf: tube feet, v: vestibulum.

### 4.1.3 The crinoid nervous system

It is unclear when and where neurogenesis is first initiated during crinoid development, but in the sea lily *Metacrinus rotundus* serotonergic cells start to be visible on the apical surface already in the uniformly ciliated embryo after gastrulation (262). In the doliolaria larva, the nervous system is composed of two parts: a neural plexus running at the base of the epidermis throughout the embryo and an anterior serotonergic AO located below the apical pit (Figure 4.2A). Curiously, in *A. mediterranea* the plexus does not seem to be concentrated at the level of the ciliary bands but is thicker on the anterior side under the AO, forming a dense neuropil of nerve fibers with several cell bodies embedded within the plexus (108, 262).

The scant data on crinoid metamorphosis suggests that the larval nervous system degenerates during settlement and the adult nervous system develops secondarily. While eleutherozoans have two components of the adult CNS, crinoids have a tripartite CNS composed of an ectoneural, hyponeural and entoneural system (Figure 4.2B-C). Ectoneural and hyponeural nerve cords form a circumoral ring and radial nerve cords on the oral side of the animal. The ectoneural system is integrated in the ambulacral groove and faces the external environment, while the hyponeural system runs in thin cords embedded in the connective tissue below the oral epidermis (93, 270). The most conspicuous component of the crinoid CNS is however the entoneural system positioned on the aboral side. The entoneural system is composed of an aboral nerve centre (ANC) at the base of the calyx from which brachial nerves enter each arm and run within the ossicles, branching into the pinnules. From the brachial nerve, projections contact the muscles and ligaments of the arm (260, 270). The adult nervous system forms during the cystidean and pentacrinoid stages: at the base of the calyx, the ANC is first visible, from which projections run into the stalk while five thin branches project orally (108). The ectoneural system forms a dense net on the tube feet, and scattered neurons are also found throughout the epidermis of the calyx (Figure 4.2B) (108, 262). Overall, the general organization of the nervous system in crinoids has been described, but little is known about the cell type composition and the way larval and adult nervous systems develop (Appendix II).

### 4.1.4 Aims of this chapter

During my Master's Degree at the University of Milan, I started to describe the development of the nervous system in the feather star *Antedon mediterranea* (108). During my PhD I have continued to

collaborate with the laboratory of Prof. Roberta Pennati to optimize new protocols aimed at investigating the specification of the AO in crinoids. These advancements are useful in the context of this project to understand the conservation and diversity of aGRN patterning across deuterostomes, and more broadly to establish crinoids as a new model in EvoDevo to understand body plan evolution in echinoderms and deuterostomes.

## 4.2 Development of the apical organ in the doliolaria larva

### 4.2.1 Cell composition of the apical nervous system

My first aim was to characterize the neural populations in the doliolaria larva by detecting the distribution of different neurotransmitters. The cells of the doliolaria are very rich in yolk, which hinders the penetration of antibodies and probes for immunohistochemistry and *in situ* hybridization as well as the imaging, since the embryos are not transparent. For this reason, during my Master's thesis project I developed protocols for immunohistochemistry on paraffin sections, which allowed to describe the distribution of serotonergic and GABAergic neurons (108). However, the small size of these embryos meant that it was not trivial to embed them correctly for longitudinal or sagittal sectioning, and the results were often difficult to interpret in the three-dimensional context of the larva. Therefore, I have optimized a protocol for whole-mount immunohistochemistry that relies on harsher permeabilization steps using TritonX and Proteinase K, and a long bleaching step using formaldehyde and hydrogen peroxide to clarify the larval tissues (see Chapter II). I first tested the new protocol by detecting the localization of acetylated tubulin that specifically labelled cilia (Figure 4.3A). Externally, the antibody marked the five ciliary bands, the vestibule and apical tuft (Figure 4.3Ai-ii). A high magnification of the bands showed that the cilia run among the tightly packed nuclei (Figure 4.3v). Within the larval body, the antibody showed that the coelomic cavities (and to a lesser extent the enteric sac) are ciliated, though the cilia were shorter than those of the bands (Figure 4.3Aiii). The staining allowed me to reconstruct the shape of the coeloms: the right somatocoel projects anteriorly within the mesenchyme (right somatocoel projection), while the axocoel forms the hydropore and a second, much thinner projection located ventro-laterally from the somatocoel and almost reaching the anteriormost tip of the mesenchyme (axocoel projection) (Figure 4.3Aiv). Under the apical pit, at the level of the prospective AO, short immunoreactive filaments were seen in association with several cells (Figure 4.3Avi).

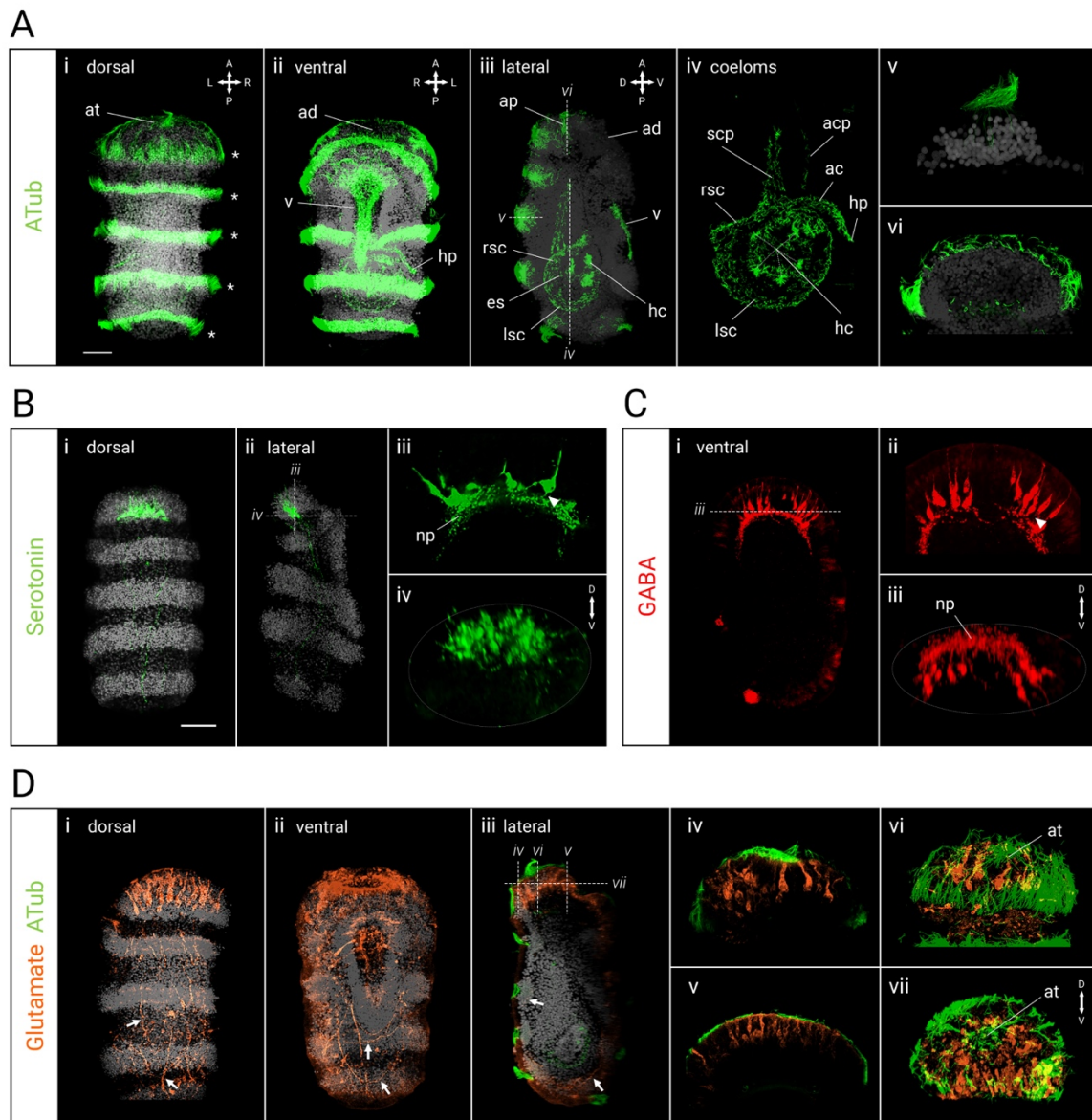
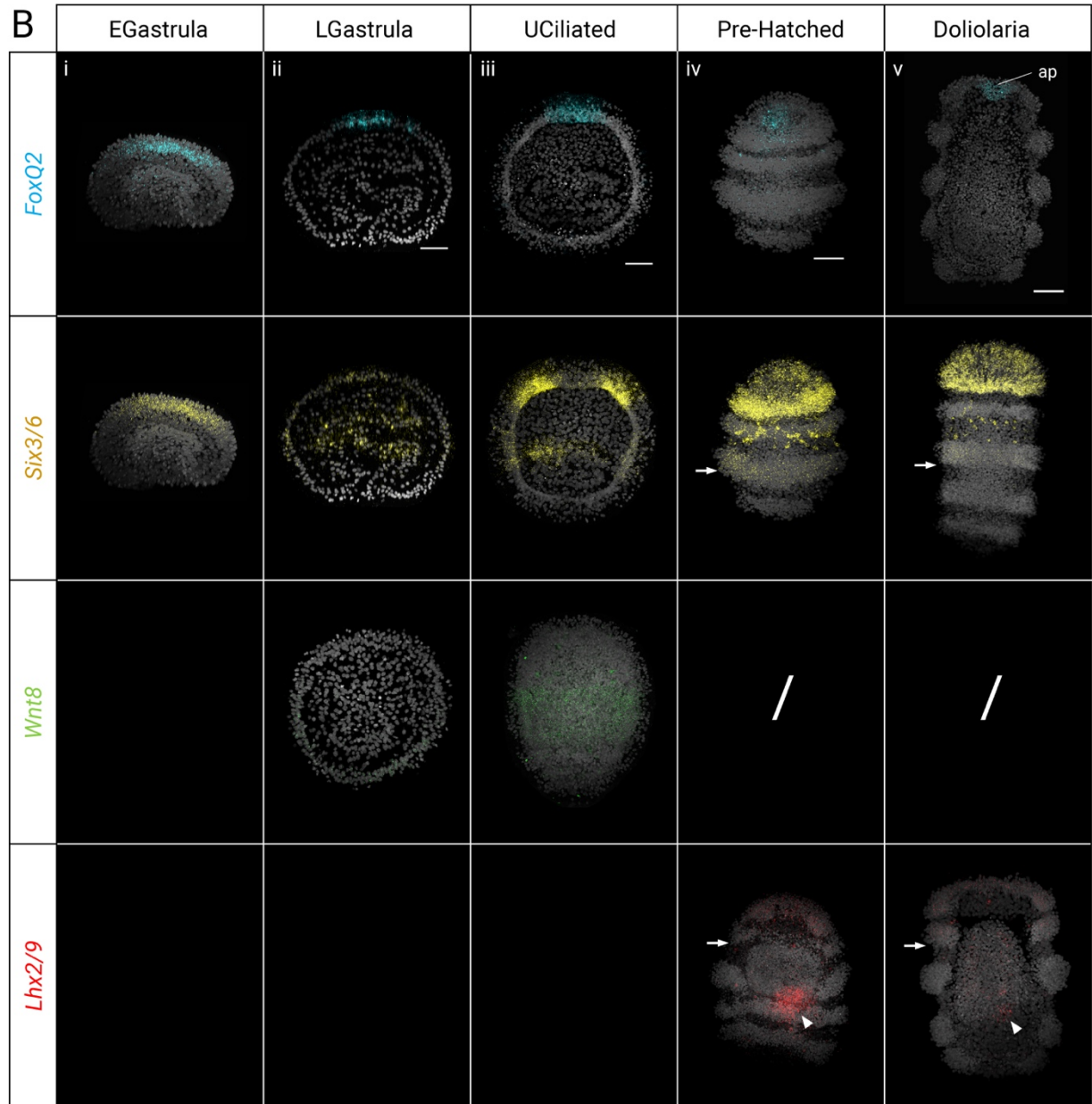
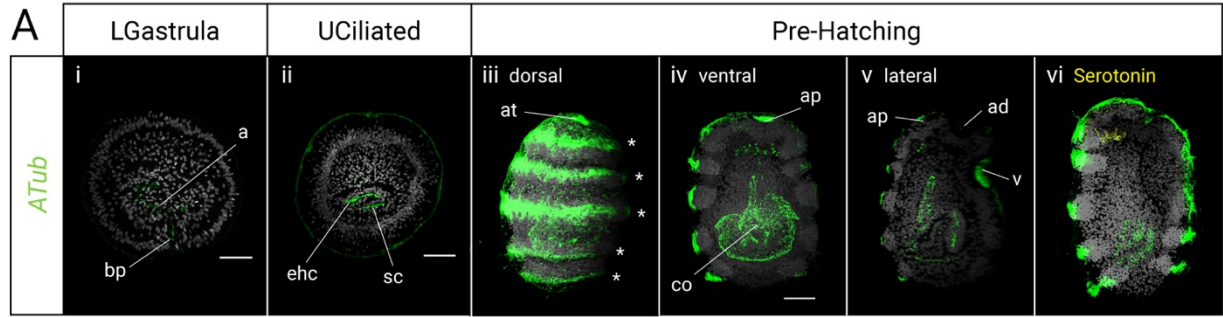


**Figure 4.3.** Characterization of neural populations in the doliolaria larva by whole mount immunofluorescence. **A.** Anti-acetylated tubulin antibody (green) marks external (i-iii, v) and internal (iii-iv, vi) cilia, including the five ciliary bands (asterisks) (i-iii, v), the apical tuft (i), the vestibular cilia (ii), cilia associated with the coelomic cavities (iv) and with the anterior neural plexus (vi). **B.** Distribution of serotonin immunoreactivity (green) in the apical organ (i-ii). These cells are bottle shaped, project into the anterior plexus (iii, arrowhead) and are concentrated dorsally (iv). **C.** GABAergic neurons (red) are found anteriorly (i), project in the anterior plexus (ii, arrowhead) and are concentrated ventrally (iii). **D.** Anti-glutamate antibody (orange) label cells and fibers anteriorly and along the body (arrows) (i-iii). Dorsally, large cells are arranged around the apical tuft (iv, vi-vii). Ventrally cells are organized around the adhesive pit (v). Scalebar is 50 $\mu$ m. ac: axocoel, acp: axocoel projection, ad: adhesive pit, ap: apical pit, at: apical tuft, es: enteric sac, hc: hydrocoel, hp: hydropore, lsc: left somatocoel, np: neural plexus, rsc: right somatocoel, scp: somatocoel projection, v: vestibule.

The distribution of acetylated tubulin immunoreactivity demonstrated that the new protocol allows the full penetration of antibodies in the larva. Together with the Pennati Lab in Milan, we therefore applied it to test the distribution of three neurotransmitters: serotonin, GABA and glutamate. Immunofluorescence against serotonin (reaction performed by Silvia Mercurio, University of Milan) labelled a large cluster of approximately 30 cells located on the anterior-dorsal side of the animal, just above the position where the neuropil of the nerve plexus is thicker (Figure 4.3Bi-ii). These cells appeared flask-shaped: they reached the anterior-dorsal surface of the embryo, where the apical pit is located, and then projected to the thickened anterior plexus (Figure 4.3Biii-iv). From there, axonal projections ran along the dorsal and lateral sides of the plexus up to the posterior region of the animal. GABA-immunoreactive neurons were also found on the anterior portion of the larva (reaction performed by Silvia Mercurio, University of Milan), but were localized ventrally around the adhesive pit (Figure 4.3Ci). We found two bilateral clusters of ~8 flask-shaped neurons each, from which thin projections reached the surface between apical and adhesive pit while the axons projected dorsally to enter the dense neuropil of the plexus (Figure 4.3Cii-iii). Moreover, these projections did not run along the body of the animal but remained anterior. The antibody against glutamate labelled a large number of cells and processes throughout the larva (Figure 4.3Di-iii). The majority of glutamatergic cells were still located anteriorly. Here, different glutamatergic cell types seem to be present: on the dorsal surface large flask-shaped cells surrounded the apical pit but did not have extensive axonal projections (Figure 4.3Div,vi-vii); on the ventral side numerous small bipolar cells were distributed along the edge of the adhesive pit (Figure 4.3Dv). Moreover, several glutamatergic neurons were labelled both dorsally and ventrally along the larval body. These cells send projections along the AP axis, and ventrally the axons appear to loop around the posterior end of the doliolaria (Figure 4.3Dii). In summary, this analysis revealed the presence of multiple neural cell types and highlighted the complexity of the crinoid doliolaria. I defined an anterior-dorsal AO composed of a large number of serotonergic neurons. The crinoid AO is located at the level of the first ciliary band, but the somata of serotonergic neurons are located deep within the epithelium and are not directly associated with the thickened band.



< **Figure 4.4.** Morphological characterization and expression of aGRN markers during *A. mediterranea* embryogenesis. **A.** Localization of acetylated tubulin (green) in late gastrula, uniformly ciliated and pre-hatching stages showing cilia in the archenteron, in the ciliary bands (asterisks) and within the neural plexus, closely associated with serotonergic neurons (yellow). **B.** Localization of *FoxQ2* (blue) *Six3/6* (yellow) *Wnt8* (green) and *Lhx2/9* (magenta) visualized through *in situ* HCR in early gastrula (i), late gastrula (ii), uniformly ciliated (iii), pre hatching (iv) and doliolaria (v) stages. Arrows indicate the posterior limit of *Six3/6* and *Lhx2/9* at the third and second ciliary band respectively. Arrowheads point at the expression of *Lhx2/9* in the hydrocoel. White slashes imply that transcripts were not detected while blank fields indicate that the expression has not been investigated at the corresponding stage. a: archenteron, ad: adhesive pit, ap: apical plate, at: apical tuft, bp: blastopore, ehc: enterohydrocoel, sc: somatocoel, v: vestibulum. Scale bars are 50µm.

#### 4.2.2 Early specification of the apical plate

Having described the AO in doliolaria larvae, I was interested in understanding how this structure developed. However, aside from early morphological descriptions, little is known on the early embryogenesis in feather stars (265). One of the reasons for this lack of data is that in many feather stars (including *Antedon*) fertilized eggs grow attached to specialized genital pinnules in the female's arms until they hatch as mature swimming larvae (108, 271). The difficulties in collecting and rearing embryos hinder the use of crinoids in developmental and evodevo studies. Therefore, the Pennati Lab at the University of Milan has optimized *in vitro* development of *A. mediterranea* embryos, which made it possible to access early developmental stages. I adapted the immunofluorescence protocol on early embryos and developed *in situ* HCR on both embryos and larvae to characterize the development of AO cell types and test the presence of the aGRN in crinoids. I analysed four stage of development in addition to the doliolaria larva: early gastrula (20hpf), late gastrula (26hpf), uniformly ciliated larva (48hpf) and pre-hatching doliolaria (72hpf). Immunofluorescence for acetylated tubulin during embryogenesis showed that invaginated mesendodermal cells are the first to become ciliated at 26hpf (Figure 4.4Ai-ii), while in the pre-hatching doliolaria the major structures of the larva were already present: the ciliary bands, the apical tuft, the vestibule and the coelomic cavities, including the somatocoel and axocoel anterior projections (Figure 4.4Aiii-v). Moreover, the ciliary rings characteristic of the anterior plexus were visible. Serotonin immunoreactivity in this stage showed a small number of positive cells in the AO (Figure 4.4Avi), which were not present in the uniformly ciliated stage (data not shown).

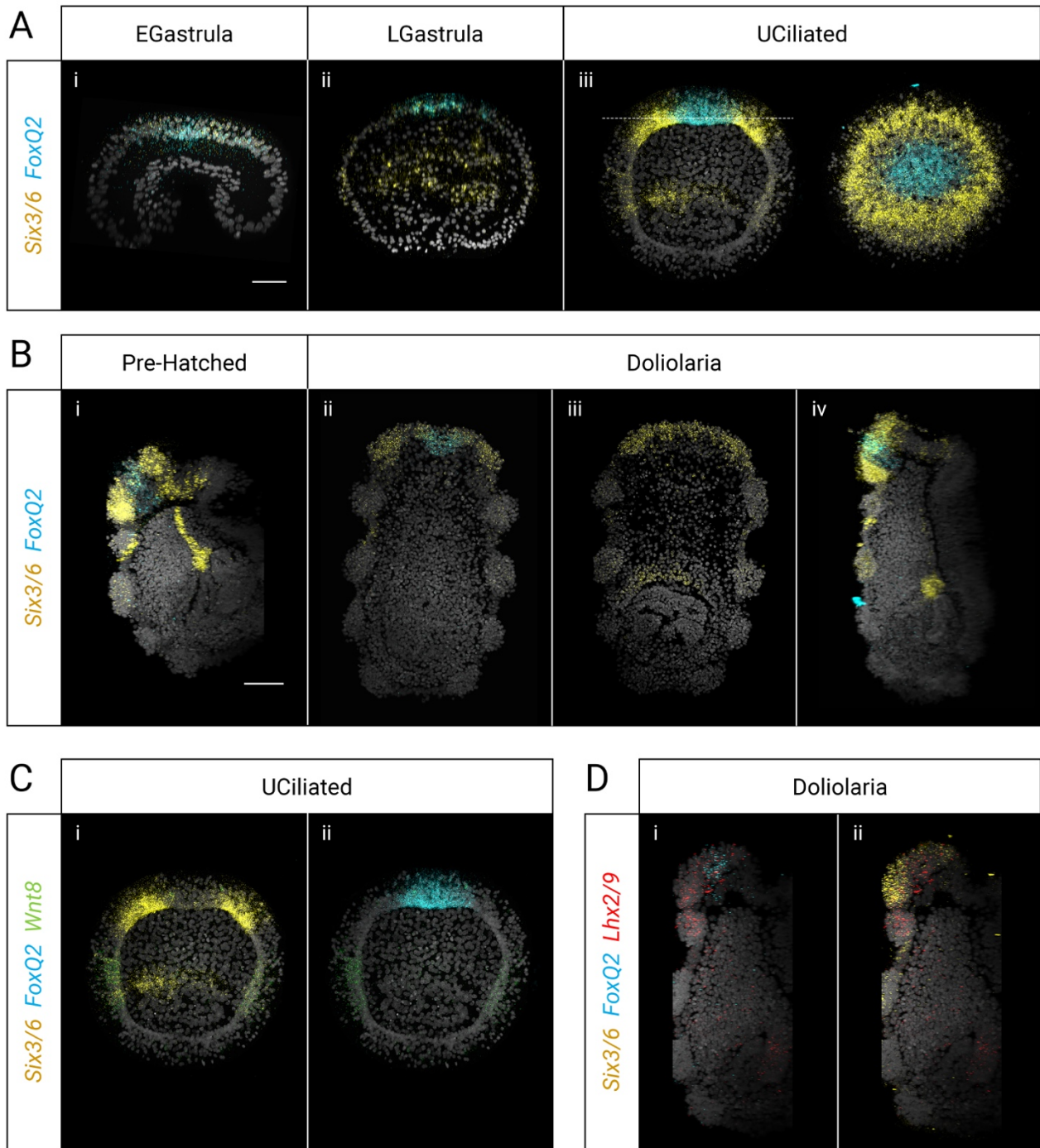


**Figure 4.5.** Co-expression of aGRN markers define the crinoid ANE. **A.** Co-localization of *Six3/6* (yellow) and *FoxQ2* (cyan) during embryogenesis, showing early broad co-expression followed by restriction of *FoxQ2* and loss of *Six3/6* expression in the *FoxQ2* domain. **B.** Co-detection of *Six3/6* and *FoxQ2* in the larva, showing *FoxQ2* expression in the apical pit surrounded by *Six3/6*. **C.** Expression of *Wnt8* in the posterior side of the embryo detected together with *Six3/6* and *FoxQ2*. **D.** Co-localization of *Lhx2/9* (red) with *FoxQ2* in the apical pit and with *Six3/6* in the apical domain. Scale bars are 50 $\mu$ m.

I next wanted to understand whether these serotonergic neurons develop within the context of an aGRN similar to other echinoderms. I searched for aGRN genes in the *A. mediterranea* transcriptome generated by the Elphick Lab (272) and found convincing orthologs of *FoxQ2* and *Six3/6*, (early apical plate markers in sea urchin), *Lhx2/9* (late apical plate) and *Wnt8* (involved in aGRN restriction). In the early gastrula, *FoxQ2* and *Six3/6* were expressed broadly on the anterior side of the ectoderm (Figure 4.4Bi, Figure 4.5Ai). At the late gastrula stage *FoxQ2* had already restricted to the animal pole, while *Six3/6* was still broad and co-expressed with *FoxQ2* on the anterior tip (Figure 4.4Bii, Figure 4.5Aii). Furthermore, *Six3/6* also started to be expressed in mesendodermal cells on the tip of the archenteron cavity, while cells closer to the blastopore did not show any expression. On the vegetal side of the ectoderm, weak *Wnt8* signal could be observed at this stage. In the uniformly ciliated stage *FoxQ2* transcripts were found at the apical tip of the embryo, in a region devoid of *Six3/6* which instead formed a ring around *FoxQ2* (Figure 4.4Biii, Figure 4.5Aiii). A second population of *Six3/6*-positive cells was located more vegetally, and surprisingly co-expressed *Wnt8* (Figure 4.5C). Finally, *Six3/6* was expressed in the anterior wall of the enterohydrocoel.

In the pre-hatching doliolaria, the concentric expression of *FoxQ2* and *Six3/6* was still evident: *FoxQ2* labelled cells of the apical pit, while *Six3/6* was localized in the first ciliary band and in the developing adhesive pit (Figure 4.4Biv, Figure 4.5Bi). Weaker *Six3/6* expression was detected in the second and third ciliary band, and a new cell population with strong *Six3/6* expression appeared just under the second ciliary band. Inside the larva, *Six3/6* now labels the axocoel, including the anterior projection of the coelom that reaches the anterior tip of the mesenchyme. At this stage, *Wnt8* seemingly disappeared from the ectoderm, while *Lhx2/9* was expressed in ectodermal and mesodermal derivatives (Figure 4.4Biv). In the ectoderm, *Lhx2/9* transcripts were localized on the dorsal side in the first two ciliary bands, while in the mesoderm they were found in the hydrocoel. The expression of these markers remained similar in the swimming doliolaria: *FoxQ2* clearly marked the apical pit, in cells that co-expressed *Lhx2/9* (Figure 4.5D), *Six3/6* labelled the rest of the anterior portion of the larva up to the third ciliary band, and *Lhx2/9* was expressed only dorsally (not in the adhesive pit) (Figure 4.4Bv, Figure 4.5Bii-iv). The other cluster of ectodermal *Six3/6*-positive cells positioned dorsally between the second and third ciliary bands, while in the mesoderm *Six3/6* continued to label the axocoel and *Lhx2/9* marked the hydrocoel (Figure 4.4Bv). Overall, the expression dynamic of *Six3/6*, *FoxQ2*, *Wnt8* and *Lhx2/9* and the localization of serotonergic neurons supports the conservation of the aGRN specifying the AO in crinoids.

## 4.3 Discussion

As described in Chapter III, an EvoDevo approach to the problem of the origin of the chordate nervous system consists in the comparison between chordates and their closest relatives, echinoderms and hemichordates. In order to reconstruct ancestral features within Ambulacraria, it is important to obtain data from the different taxa that belong to these two phyla. In fact, the necessity of broad taxonomic sampling for the correct reconstruction of homologies is one of the themes of modern evolutionary biology (28, 273). With this in mind, in this chapter I have described the development of the nervous system in *A. mediterranea*, a member of the understudied echinoderm taxon Crinoidea.

### 4.3.1 AO development and aGRN conservation in crinoids

My analysis focused on the characterization of the AO in the doliolaria larva. Previous studies highlighted the presence of serotonergic neurons on the anterior ectoderm of crinoid larvae (108, 262), but the technical issues of existing protocols and the scant data on embryogenesis had limited the description of the three-dimensional organization and early development of the larval nervous system. Using the newly optimized protocols for whole mount immunohistochemistry and *in situ* HCR, combined with the availability of early embryonic stages thanks to the effort of the Pennati Lab at the University of Milan, I was able to provide a more comprehensive characterization of the doliolaria nervous system and its molecular specification (Figure 4.6A).

The hatched doliolaria possess about 30 flask-shaped serotonergic cells located on the anterior-dorsal end of the larva under the ciliated apical pit. These neurons are located near the first ciliary band but are not embedded in the ciliary epithelium. These cells send projections to the apical neuropil within the nerve plexus and from there run along the body of the larva. While the connectivity of serotonergic cells in echinoderms is still unclear, these results suggest that AO neurons connect with other parts of the neural plexus to direct larval activities. The number of serotonergic cells varies across echinoderms: in sea urchins there are initially only 4-6 serotonergic cells, but they multiply during development (141, 274); the starfish bipinnaria and the holothuroid auricularia already have 30-50 and 20-22 serotonergic neurons respectively (96, 135, 275, 276). Moreover, the position of the AO with respect to the ciliary band is also variable: in starfish

serotonergic neurons are born throughout the apical surface of the larva and then migrate to form a dorsal bilateral structure within the ciliary band; in sea urchins the AO is positioned dorsal to the ciliary band (96, 141). The dorsal position of both AOs is particularly interesting as the crinoid AO and apical pit are also located dorsally, while the ventral-anterior side is occupied by the adhesive pit. In other echinoderms, the aGRN is involved in the positioning and specification of the ANE, and in echinoids interactions between ventral nodal, dorsal Bmp and apical FoxQ2 overall contribute to position serotonergic neurons on the dorsal side of the ANE (141, 149, 155, 162).

To explore whether an aGRN patterned the AO in crinoids, I characterized the co-expression of two early phase aGRN genes, *FoxQ2* and *Six3/6*, the late phase gene *Lhx2/9* and one of the mediators of the aGRN *Wnt8* across larval development. Previous chromogenic *in situ* analysis in sea lily and feather star larvae showed that *Six3/6* is expressed in the anterior portion of the ectoderm (277, 278). Here, I provide the first instance of multiplex fluorescent *in situ* hybridization in crinoids, showing that the expression of *FoxQ2* and *Six3/6* is already visible during gastrulation in a broad ectodermal domain and then restricts anteriorly. *FoxQ2* restricts more than *Six3/6*, and after gastrulation, *Six3/6* disappears from the *FoxQ2* domain and forms a ring around the anterior tip of the animal. The area included within the strong *Six3/6* expression and the *FoxQ2* domain corresponds to the apical plate where the ANE will form, similar to other marine ciliated larvae (97). *Wnt8* is instead localized in the ectoderm around the blastopore, but curiously after gastrulation this expression overlaps with a posterior band of *Six3/6*. I speculate that these cells will form the third ciliary band, the most posterior limit of *Six3/6* expression in the doliolaria. The co-localization of Wnt signalling and *Six3/6* is curious, as the two are known to have reciprocal inhibitory effects (150, 151), and could be due to the absence of Wnt receptors on these cells, which should be investigated in future studies. After the formation of the apical plate, *Lhx2/9* starts to be expressed within the first two ciliary band and is shown to co-express with *FoxQ2* anteriorly, similarly to sea urchins (see Chapter III).

Overall, the apical expression dynamic of these genes is similar to sea urchin, particularly regarding the concentric expression domains of *Six3/6* and *FoxQ2* (150). The *FoxQ2*-positive and *Six3/6*-negative region forms the apical pit, where the majority of the AO serotonergic neurons are located (Figure 4.6B). The presence of a *Six3/6*-free region in both echinoids and crinoids seems to suggest that this mode of AO development is ancestral to echinoderms and possibly to Eumetazoa, as a similar pattern has been described in annelids and sea anemone larvae (97). However, this

hypothesis needs to be considered carefully as in other larvae, including starfish and hemichordates, the ringed expression is not present and *Six3/6* and *FoxQ2* often forms domains of nested co-expression (160, 162). It is possible therefore that changes in the regulatory interactions between these early transcription factors underlie these taxon-specific differences (135, 162, 252). Moreover, it would be interesting to further characterize the AP and DV patterning in crinoids to understand whether a mechanism for the dorsalization of the AO similar to the one active in sea urchins is common to all echinoderms.

#### 4.3.2 A map of the crinoid larval nervous system

The localization of different neurotransmitters revealed additional components of the larval nervous system (Figure 4.6A). Around the apical pit, large glutamatergic cells are present, which could represent support cells often associated with AOs (128). The adhesive pit was also shown to contain numerous GABAergic and glutamatergic neurons. The GABAergic neurons project in the anterior neuropil, but do not seem to send axons along the larval body. If serotonergic neurons of the AO

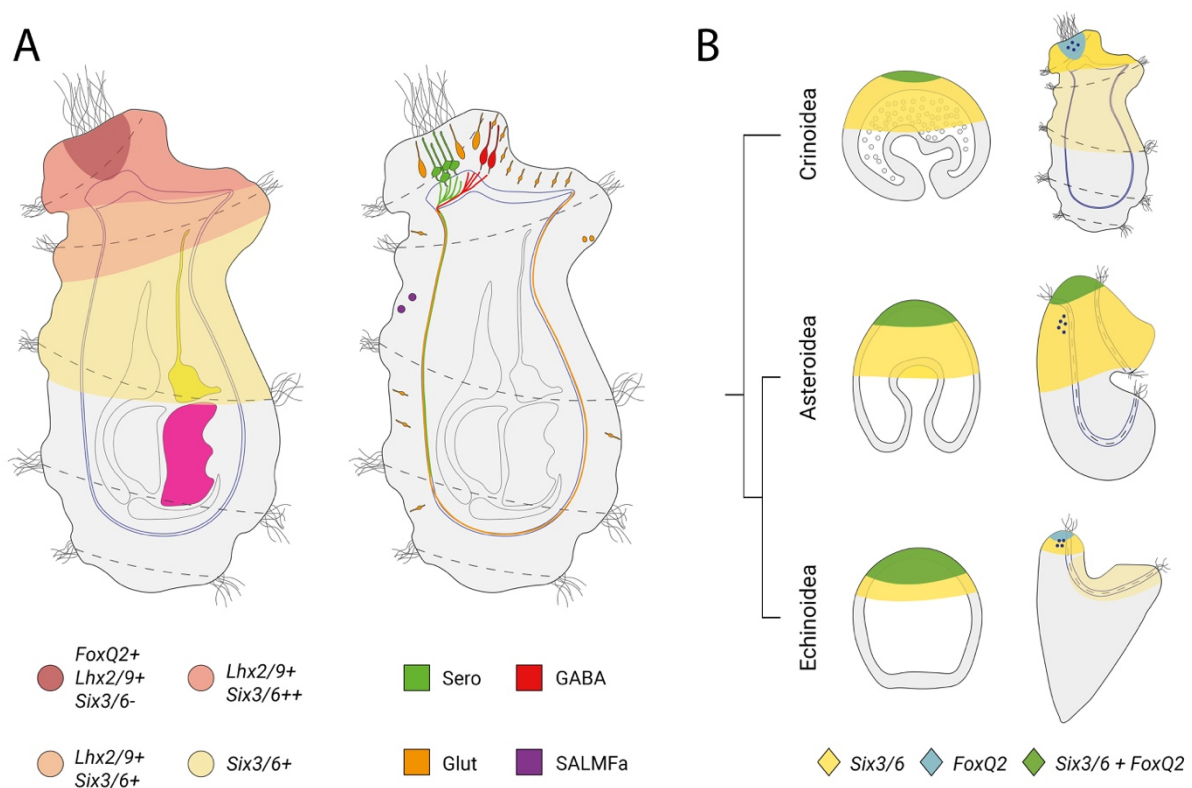


**Figure 4.6.** Summary of the crinoid larval nervous system. **A.** Expression data and neural populations in the doliolaria larva. **B.** comparison of early aGRN expression across echinoderms.

have a sensory function, as described in other larvae, then it is possible that they interact with GABAergic neurons to direct settlement and metamorphosis. In fact, GABA has been previously found to be involved in metamorphosis in sea urchin and gastropod larvae (279–281). Interestingly, these cells are all distributed within the apical plate, marked by strong *Six3/6* expression, and could therefore mean that the majority of the larval nervous system, concentrated on the anterior side, develops under the influence of the aGRN.

Previous microscopy analyses have shown the presence of a diffuse nerve plexus in the doliolaria, but the identity of these cells was still unknown. In addition to the serotonergic projections, I have found several glutamatergic neurons and fibers scattered along the epidermis both ventrally and dorsally, suggesting that the crinoid plexus contains a large glutamatergic component, possibly with an excitatory role. In a recent study we have also characterized the localization of SALMFamides, a class of neuropeptides that has been thoroughly described in echinoderms (282, 283). In the doliolaria larva we found 15-20 cells that express the F-type SALMFamide precursor located dorso-laterally between the second and third ciliary band, suggesting the presence of several neural populations within the plexus (284). Interestingly, in this work I have found *Six3/6* positive cells located in a similar position in the doliolaria. Although co-expression was not tested, it is tempting to speculate that these are the neuropeptidergic cells previously described (284). In asteroid and echinoid larvae, SALMFamides have been detected in neurons located close to the AO and in post oral neurons of the sea urchin pluteus (285, 286). The crinoid SALMFamidergic cells are further away from the AO, but still located within the first three ciliary bands where expression of *Six3/6* is detected. The localization of glutamatergic and peptidergic cells showed that contrary to all eleutherozoans studied to date, the distribution of the neural plexus does not follow the ciliary bands, and a concentration of neuronal cell bodies or neurites is not seen associated to the thickened epithelium of the bands. This could be due to incomplete sampling, particularly of cholinergic cells that constitute a large part of the eleutherozoans ciliary band nervous system (135, 142), but generally suggests that the rest of the echinoderm larval nervous system is less conserved than the ANE.

### 4.3.3 Conclusions

In this chapter I have developed protocols for whole mount immunohistochemistry and *in situ* HCR to investigate the development of the crinoid nervous system. The analysis represents the most comprehensive description of the crinoid larval nervous system to date, revealing a complex organization and the presence of a high number of morphologically and functionally diverse cell types. In particular, I describe an anterior AO characterized by a conspicuous group of serotonergic neurons that develop in an apical plate delimited by *Six3/6* and *FoxQ2* expression. These results support the homology of dipleurula-type larvae in ambulacrarians and the conservation of an aGRN patterning the ANE that forms the AO. They also help establish crinoids as an important model to study the evolution of the echinoderm body plan.

# Chapter V – Characterizing the development of cell type diversity in the amphioxus nervous system

## 5.1 Introduction

In the first part of my thesis, I identified a conserved aGRN that is involved in the specification of the ANE. This network has an ancient origin, likely dating back to the Eumetazoa ancestor, and was conserved through deuterostome evolution. In Chapter III I showed that the network is still present in cephalochordates, meaning that it was conserved in the chordate ancestor. The following question was to define the contributions of the ANE cells to the amphioxus larva, when functional neurons are differentiated. With this overarching aim, in this chapter I analysed neurogenesis, cell type diversity and morphogenesis in the amphioxus brain to understand the fate of ANE derivatives in the context of the developing amphioxus CNS.

### 5.1.1 The evolution of cell types

In amphioxus, the aGRN is required to confer the correct identity to the anterior neural plate, which will form the cerebral vesicle (CV) of the larva. A key follow-up for a thorough comparison of aGRN across deuterostomes is to examine the “anterior” identity in the amphioxus nervous system, i.e. which cell types are present in the amphioxus brain and how they compare with the neuronal populations in other chordates and in ambulacrarians. While in the previous chapters I have investigated nervous system patterning and regionalization, the fate of neural precursors in which the aGRN is active has not been considered in depth. However, comparing cell types is a key step in the definition of homology, as molecular evolution underlies the formation of new cell types (16, 287). In fact, cell types can be defined as “a population of cells expressing the same set of orthologous genes for specification and differentiation, to implement a defined cellular phenotype” – a molecular or developmental definition (44) – as well as “a set of cells that change in evolution together, partially independently from other cells, and are evolutionarily more closely related to each other than to other cells” – an evolutionary definition (40). A cell type expresses a unique combination of genes (generally encoding transcription factors), often called a “core regulatory complex”, that overall specifies its identity (40). New cell types evolve by assembling, modifying or co-opting core

regulatory complexes, creating or modifying GRNs that direct cell differentiation into a particular phenotype. This definition allows the reconstruction of cell type homology similarly to species, by tracing the similarities and differences in cells molecular fingerprint across the phylogenetic tree. By analysing the co-expression pattern of multiple genes in the amphioxus nervous system and integrating information on how neurons are specified during neurogenesis, we can identify cell types that can effectively be compared with other deuterostome species.

### 5.1.2 What do we know about the amphioxus nervous system?

Early microscopy work by Kowalevsky and Hatschek showed that the amphioxus CNS forms through a process similar to vertebrate neurulation (288, 289). A dorsal neural plate is first visible as the cup-shaped gastrula flattens dorsoventrally: a depression forms on the dorsal side of the larva and the non-neural ectoderm at each side extends over it, defining and enclosing the neural plate. The neural plate folds and closes, forming the neural tube composed of a single cell layer arranged around a central ventricular canal. After closure, the CV forms as an enlarged part of the anterior neural tube, which remains open to the environment through the neuropore (Figure 5.1A). With the establishment of amphioxus as a model in EvoDevo, a large number of studies through the early 2000s was dedicated to the analysis of gene expression during amphioxus development (reviewed for example in (83, 89)). Combining old morphological descriptions with new gene expression analyses, the amphioxus nervous system was shown to be divided into different regions with proposed homology to corresponding areas of the vertebrate CNS (85–87, 89).

Following these studies, the larval CV can be divided in two portions: the anterior CV corresponds to the enlarged portion of the neural tube and spans from the anteriormost tip of the neural tube to the infundibular cells (secretory cells that produce the Reissner's fiber that runs along the neural canal); the posterior CV starts from the infundibular region to approximately the boundary between the first and second somite (290–292) (Figure 5.1B). The anterior CV includes the frontal eye complex, characterized by pigmented cells and four rows of photoreceptors and associated cells (including Row2 serotonergic neurons), and the preinfundibular neurons (291) (Figure 5.1B). Ultrastructural studies have shown that many of the anterior CV cells project to a post-infundibular neuropil with few synapses but many varicosities, suggesting a predominantly paracrine and neurosecretory mode of transmission (290, 291). A recent expression analysis during early

neurulation suggested that this region is homologous to the secondary prosencephalon of vertebrates, a hypothesis supported by the absence of the floor plate in the anterior CV (87). In fact, according to the prosomeric model the infundibular cells should represent the rostral-most tip of the amphioxus neural tube, and the anterior CV would correspond to the secondary prosencephalon of vertebrates (68, 87). While other studies have highlighted the similarities between the frontal eye and the vertebrate retina (293–295), the identity of neurons in the rest of the anterior CV remains to be tested. The posterior CV was hypothesised to have a di-mesencephalic identity by gene expression and includes the initial part of the floor plate, which continues posteriorly (85, 87). The molecular regionalization of the early neural plate suggests that the posterior limit of this region is located at the expression boundary between *Otx* and *Gbx* (87). During larval life, two prominent structures form in this region: the dorsal lamellar body and the primary motor centre. The lamellar body is a photoreceptor structure that includes dopaminergic neurons and has been associated with the vertebrate epiphysis (295, 296). The primary motor centre receives contacts from both the anterior CV (through the post-infundibular neuropile) and peripheral neurons and contains motoneurons that are thought to control bursts of larval swimming in response to sensory stimuli (291, 297).

Posterior to the first somite, the neural tube was hypothesised to assume a hindbrain-like signature based on the expression of *Gbx* and *Hox* genes and the presence of two ventro-lateral rows of repeated cholinergic (motor), GABAergic and glycinergic neurons (87, 221, 298). At this level, the cross section of the neural tube is composed of ~8-9 cells arranged in a single layer around the ventricular canal, including a floor plate formed by a single row of ventral cells (Figure 5.1C). On each side of the floor plate there are two rows of ventrolateral neurons expressing neurotransmitters and sending projections in two ventrolateral tracts. On a medial level there are two mediolateral cells, while dorsally there are two-three dorsolateral cells on each side of the single row of roof plate cells (291, 299). The floor plate and mediolateral cells express the glial marker *EAAT2*, suggesting that these are in fact glial cells (299). While the identity of cells in the posterior portion of the neural tube behind the sixth somite remains unclear, the presence of posterior *Hox* genes suggests that it might be homologous to the vertebrate spinal cord (87, 300).

Very little is known about the development and growth of the nervous system during the extended larval period and metamorphosis, but the adult neural tube is larger and more complex than in the

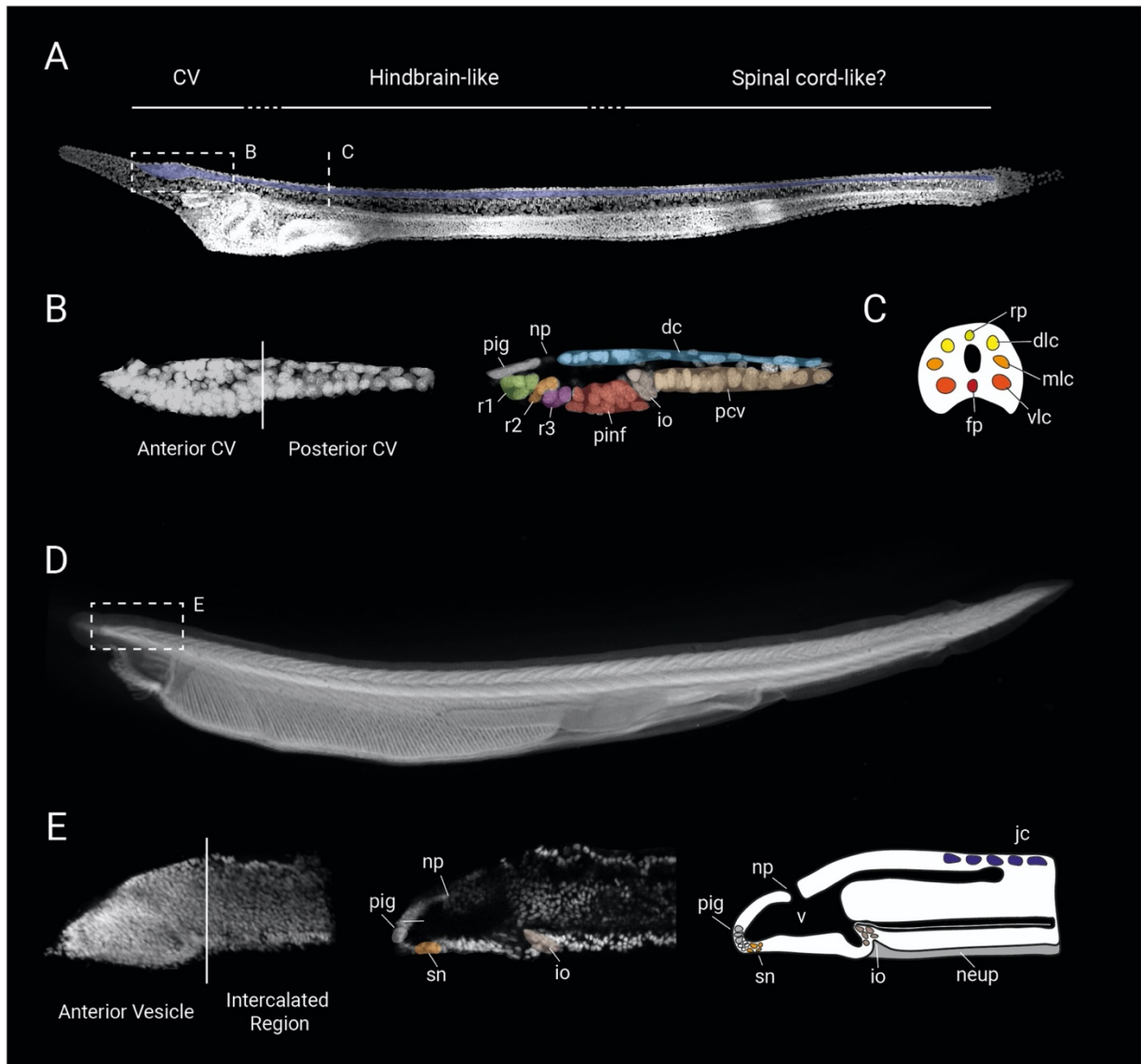


**Figure 5.1.** Larval and adult nervous system in amphioxus. **A.** One gill slit larva stained with DAPI and with CNS false-coloured in blue. **B.** Magnification of the larval brain false-coloured to represent previously described cell types. **C.** Cross section of the trunk nervous system of a larva. Nuclei represent the dorso-ventral arrangement of the CNS. **D.** Adult specimen stained with DAPI. **E.** Magnification and schematic representation of the adult brain with few recognized cell types. CV: cerebral vesicle, dc: dorsal cells, dlc: dorsolateral cells, fp: floor plate, io: infundibular organ, jc: Joseph cells, mlc: mediolateral cells, neup: neuropil, np: neuropore, pcv: posterior cerebral vesicle, pig: pigment cells, pinf: preinfundibular region, r1: row1, r2: row2, r3: row3/4, rp: roof plate, sn: serotonergic neurons, vlc: ventrolateral cells.

larva (291, 301–303) (Figure 5.1D-E). The neurons' somata are concentrated around the apical ventricular canal, which now has a slit shape with a small ventral expansion, while the axons occupy more basal portions in the tube. The anterior neuropore is present but opens sideways following the rotation of the body at metamorphosis. The anterior portion of the tube continues to enlarge, forming the anterior vesicle with a large medial ventricle that terminates at the level of the infundibular organ, now composed of a large number of infundibular cells (106, 302) (Figure 5.1E). The frontal eye also grows, but the cell type composition of this region is poorly understood. Posterior to the vesicle is the intercalated region, which contains specialized cell types such as Joseph cells, large dorsal photoreceptor cells (86, 291) (Figure 5.1E). While the morphology of the anterior vesicle together with the presence of the frontal eye and infundibular organ suggests that it corresponds to the larval anterior CV, the relationship between the intercalated region and the larval Di-Mes and hindbrain-like regions is still unclear.

Overall, a vast amount of information is available on the development of the amphioxus CNS. Gene expression studies have revealed a high degree of molecular regionalisation in the amphioxus CNS, despite the morphological simplicity of the neural tube, and morphologically diverse neuronal populations have been described in late larvae and adults using electron microscopy. However, it is still difficult to piece together this information to understand the dynamic process that drives neurogenesis in amphioxus. (106, 219, 299, 304). Moreover, most molecular studies up until now have focused on one gene at a time using chromogenic *in situ* hybridization, often considering only few stages that do not necessarily recapitulate the entire developmental process. As a consequence, we know still relatively little about the diversity of cell types in the larval and adult brain and the molecular and morphogenetic processes that generate this diversity during development.

### 5.1.3 Aims of the chapter

This chapter has two parallel aims:

- ◆ To describe the development, regionalization and cell type diversity of amphioxus brain, from early neurogenesis to the adult CNS;
- ◆ To investigate the neuronal identity of the ANE of amphioxus, as defined by the presence of the aGRN, and compare it to other deuterostomes, particularly to vertebrates.

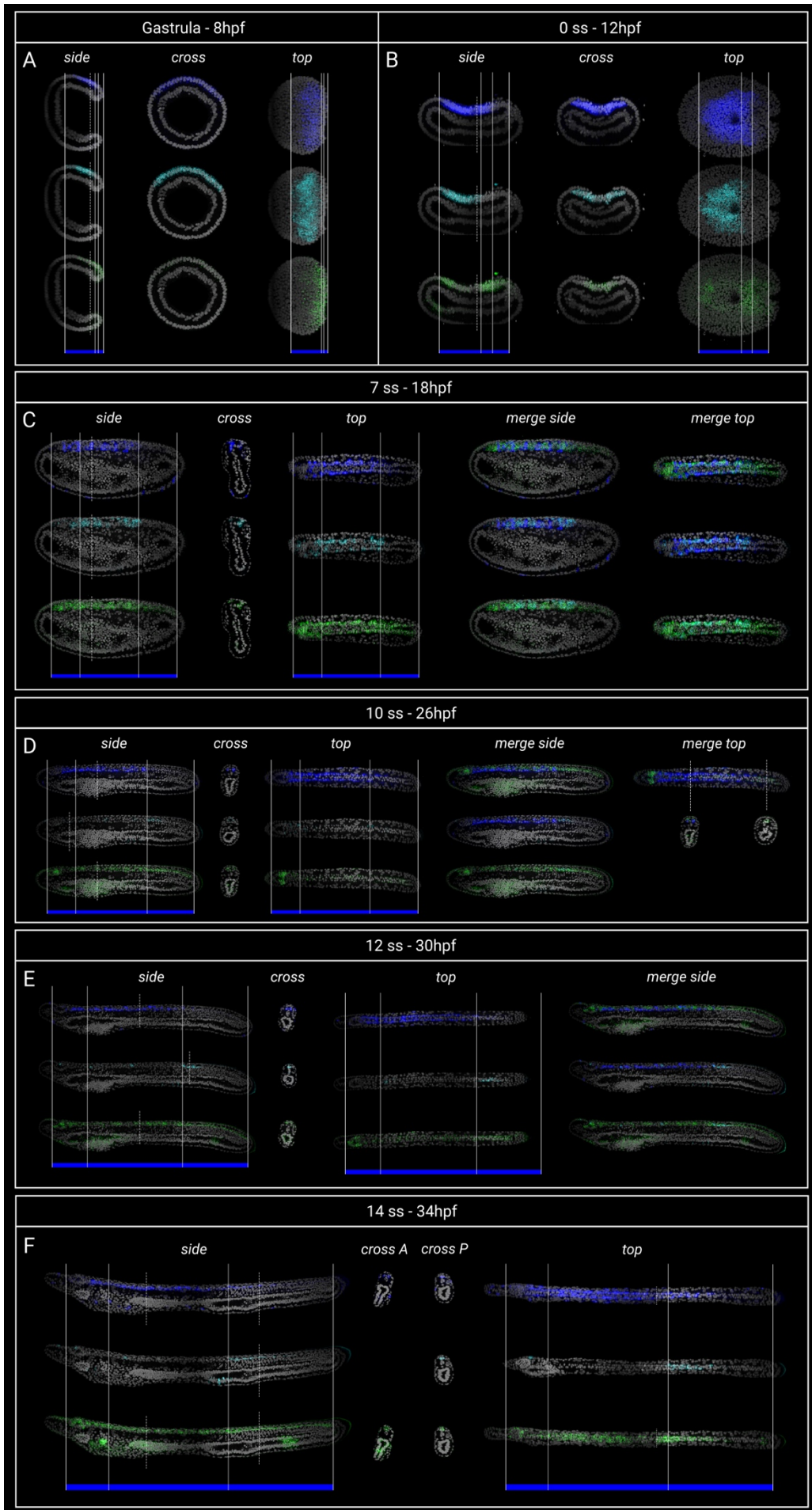
The two objectives are considered together as a detailed comparative analysis of the chordate CNS requires a multi-scale approach that integrates research on the molecular control of neural differentiation with the neurogenetic and morphogenetic processes that shape the neural tube during development. A more complete understanding of CNS development would not only benefit the comparative potential but would be particularly interesting given the simplicity of amphioxus nervous system, with the possibility of visualising the effects of patterning and morphogenetic processes in an environment with low cell number.

In this chapter, I first use a combination of HCR and immunofluorescence to describe neurogenesis and molecular regionalization in the amphioxus brain. I optimize a protocol for scRNAseq to describe cell type diversity during neurulation and analysed the co-expression of a large number of genes to define cell populations in the larval brain. These analyses allowed me to define a hypothalamic-like region within the amphioxus CV. I then showed that this region develops under the influence of the aGRN by fate-mapping proliferating cells across development.

## 5.2 Early steps in neural development

### 5.2.1 Neurogenesis

As described above, previous studies have defined regions of the early embryonic nervous system that are thought to correspond to homologous areas in vertebrates (87). However, these results have not been considered in the context of the pattern of neurogenesis across the neural tube, and therefore little is known about how these regions develop. Understanding the influence of amphioxus neurogenesis on the regionalization of the CNS is key to understand when particular populations are born. Therefore, I started by investigating the co-expression across development of three neurogenesis markers: *SoxB1c*, *Ngn* and *Elav*. In other bilaterians, including vertebrates, members of the SoxB family are expressed in cells that have the potential to produce neurons, at the same time maintaining an undifferentiated phase; *Ngn* acts as a proneuronal gene to trigger neuronal specification; and *Elav* is expressed in committed progenitors and differentiating neurons (305). The individual expression of these genes in amphioxus has been described previously (306, 307), but here I analyse the co-expression of the three markers with the specific aim of characterizing the origin of neural tube regionalization.



< **Figure 5.2.** Progression of amphioxus neurogenesis visualized through detection of neural markers *SoxB1* (green), *Ngn* (cyan) and *Elav* (blue) at G5 (**A**), N0 (**B**), 7ss (**C**), 10ss (**D**), 12ss (**E**) and 14ss (**F**) stages. White lines indicate the regions of the nervous system as defined by the expression of the three markers. Cross sections are taken at the level indicated by dashed (**C-F**). In dorsal views at 14ss the anterior and posterior halves of the embryo are presented as a composite of two projections, separated by dotted lines, due to the bending of the embryo (**F**).

The neural plate is specified very early within the ectoderm: already at the beginning of gastrulation (G3) the neural marker *Ngn* is expressed in a thin line of cells (Appendix VII, Figure A7.1). By the cup-shaped gastrula stage (G5) all three markers labelled a band on the dorsal side of the embryo, corresponding to the neural plate, which did not reach the anterior tip but occupied the posterior 2/3<sup>rd</sup> of the dorsal ectoderm (Figure 5.2A). The early neural plate is very wide, spanning around a third of the ectoderm in cross section. *Ngn* expression reached the anterior tip of the neural plate, while *Elav* started more posteriorly. *SoxB1c* was expressed only in the posterior side of the neuroectoderm up to the dorsal lip of the blastopore, but its paralogs *SoxB1a* and *SoxB1b* are found throughout the neural plate and turn off at later stages (225). Interestingly, both *Ngn* and *Elav* did not reach the blastopore lip, and *Elav* reached more posteriorly (by one additional row of cells) than *Ngn* (Figure 5.2A). In the early neurula (N0), the neural plate starts to be covered by the dorsal epidermis and concomitantly it elongates assuming a somewhat triangular shape (visible in dorsal view), narrow anteriorly and wider posteriorly (Figure 5.2B). Both *Ngn* and *Elav* now reached the tip of the neuroectoderm, where cells started to express *SoxB1c*. Posteriorly, *Elav* was clearly expressed more posteriorly than *Ngn*, but did not reach the posterior end of the neural plate, which continued to be *SoxB1c*-positive. The differences in the expression pattern of these three genes already in the early stages of specification of the neuroectoderm indicate that neurogenesis proceeds at different rates along the AP axis.

At the 7ss stage, the neural plate is covered by the dorsal epidermis but has not yet closed. While the expression domains of the three neurogenic genes were broad and homogeneous in early stages, from the 7ss neurula they start to fragment (Figure 5.2C). *SoxB1c* was expressed throughout the AP axis, but between the second and sixth somite (corresponding to the hindbrain-like region, see section 5.4.3) it was not continuous as some ventral cells, approximately located at the somite boundaries, were devoid of expression. *Ngn* disappeared from the floor plate and the anterior neural

plate during neurulation (Appendix VII, Figure A7.1) and its expression progressively became scattered in the hindbrain-like region, remaining in sparse cell clusters in which it is co-expressed with *SoxB1c*. *Elav* expression restricted to only few cells in the floor plate and few posterior cells in the anterior neural plate, and became segmented in the hindbrain-like region. Here, *Elav* marked cells located medially and medio-laterally at each side of the floor plate (likely corresponding to ventrolateral cells of the neural tube) concentrated at the somite boundaries. The co-expression analysis showed that *Elav*-positive cells correspond to the gaps in *SoxB1c* and *Ngn*, suggesting that ventrolateral cells at the somite boundaries in the hindbrain-like regions are among the first cells that start to differentiate. Moreover, the posterior boundary of both *Elav* and *Ngn* now coincided with the boundary between the sixth and seventh somite, supporting this landmark as the end of the hindbrain-like region. At the 10ss stage, the expansion of the anterior CV is clearly visible and shows strong expression of *SoxB1c* (Figure 5.2D). The neural tube is now closed: in the hindbrain-like region, *SoxB1c* was expressed dorsally and in the floor plate but not in ventrolateral cells, while it remained broadly expressed in the posterior neural plate. *Ngn* transcripts were detected in scattered cells in the CV but they almost disappeared in the hindbrain-like region, remaining in few dorsolateral cells. Surprisingly, a new domain appeared in cells immediately posterior to the sixth somite. Conversely, the expression of *Elav* disappeared from the anterior CV but was present in most ventrolateral cells, in the region where *SoxB1c* was not expressed. In addition, few cells located mediolaterally and within the floor plate were also *Elav*-positive and *SoxB1c*-negative. The posterior limit was still at the boundary of the sixth and seventh somite.

At the beginning of larval stage (12ss), the pattern of the three genes remained similar (Figure 5.2E). *SoxB1c* was found dorsally in the hindbrain-like region and broadly in the posterior neural tube but now a prominent ventral area of the anterior CV was devoid of expression. *Ngn* transcripts were detected in the roof of the anterior CV, in sparse dorsal cells of the hindbrain-like region and in the posterior neural tube. The expression of *Elav* also remained similar, but at this stage almost all positive cells occupied a ventrolateral position. The expression of the three markers in the CV and hindbrain-like region remained unchanged at the 14ss stage, but in the posterior neural tube (from the seventh somite) the number of *Ngn*-positive neurons increased, and some of these posterior cells started expressing *Elav* (Figure 5.2F). Although it was difficult to detect clearly due to the packing of posterior cells, *Elav*-positive cells appeared to be *SoxB1c*-negative.

Taken together, the pattern of neurogenesis along the AP axis supports the division of the neural tube into anterior and posterior CV, hindbrain-like and spinal cord-like regions. These appear to develop at different rates, and particularly the spinal cord-like region begins the process of differentiation only after the onset of larval life.

### 5.2.2 Axogenesis

Alongside the molecular control of neurogenesis, neural differentiation involves the formation of axonal projections, which will determine the morphology and connectivity of the mature neuron. In a previous work immunohistochemistry for acetylated tubulin was used to mark axons in *B. belcheri* (308). Here, I used a similar approach with immunofluorescence to detect neural projections in *B. lanceolatum*. The antibody labels tubulin present in both axons and cilia: this is problematic for visualising axons as the entire embryo starts to be ciliated from the gastrula stage (Figure 5.3A). Therefore, I used Imaris to isolate epidermal, somitic and endodermal cilia and visualise only neural fibers and the cilia of the ventricular canal. At 8ss, ventricular cilia were strongly immunoreactive but only faint positivity could be detected in the anterior half of the embryo (Figure 5.3Bi). Already at 9 somites however, several neurons in the hindbrain-like region and the posterior CV were stained, and thin immunopositive tracts could be detected in the ventral portion of the neural plate (Figure 5.3Bii). At this stage peripheral neurons started to extend axons towards the CNS. Anterior peripheral neurons were already clearly defined, while in the trunk only thin projections were visible. At 10ss, well defined ventral axonal tracts were labelled by the antibody in the neural tube (Figure 5.3Biii). Moreover, peripheral neurons both anteriorly and laterally reached the neural tube. At 11ss, several cells in the neural tube showed strong immunopositivity to the antibody (Figure 5.3Biv). The anterior peripheral neurons could be seen extending their projections within the anterior CV, forming the rostral nerves; laterally, single or paired peripheral neurons projected to the neural tube, entering through the dorsal roots. Finally, at 14ss the ventrolateral axonal tracts thickened considerably and reached the posterior end of the neural tube (Figure 5.3Bv). The anterior peripheral neurons located in the rostrum entered the CV through the rostral nerves but appeared to project to the posterior CV, where strongly immunoreactive fibers marked the neuropil region. Peripheral neurons located at the side of the brain instead entered the posterior CV through the first dorsal root. Overall, the appearance of central and peripheral projections in amphioxus closely follows the progression of neurogenesis.

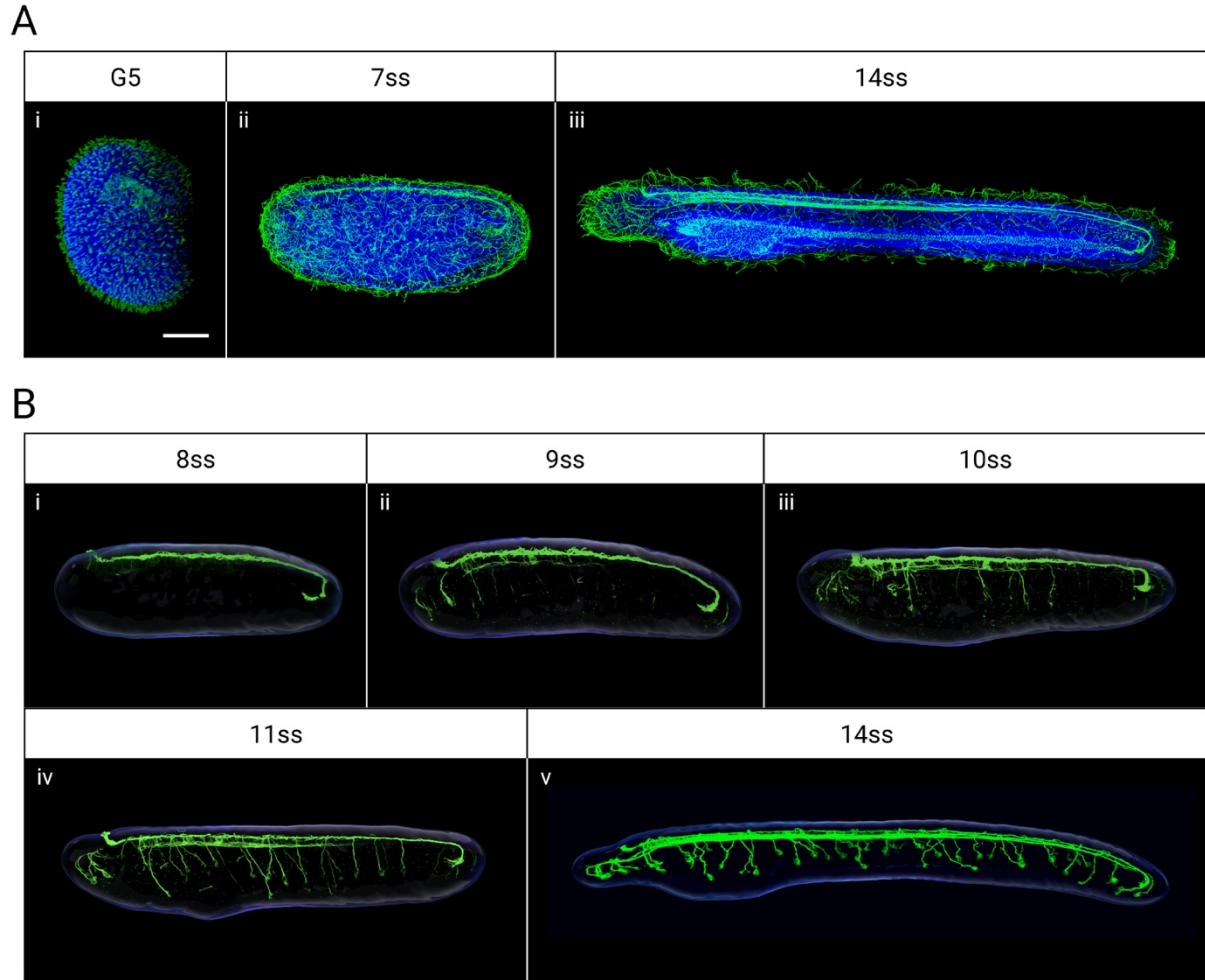


**Figure 5.3.** Following axon maturation by immunohistochemistry for acetylated tubulin. **A.** Ciliogenesis in amphioxus development visualized at G5 (i), 7ss (ii) and 14ss (iii) stages. As all cells are ciliated from gastrulation, it is difficult to discern neural projections. **B.** Segmented images of neurulating embryos in which cilia have been removed with Imaris, revealing the development of axonal projections. Scale bar is 50 $\mu$ m.

### 5.3 Defining amphioxus cell types with single cell RNA sequencing

Having described the progression of neuronal differentiation in the CNS, I next wanted to focus on the diversity of cell types that are found throughout development up to the larval stage, when neurons are differentiated and functional. scRNAseq allows the analysis of the transcriptome of single cells within the organism and has become a standard method to reconstruct cell types (42, 287, 309, 310). Because of its predictive power and the vast amount of data produced with each experiment, numerous scRNAseq methods and pipelines have been developed in the last decade (311). The basic principles behind these pipelines are similar: individual cells (or cell nuclei) are

dissociated from the organism and isolated; the RNA (usually mRNA) is extracted from each cell and reverse transcribed into cDNA, which is amplified and then sequenced (309, 312). A key initial step is the isolation of single cells that are going to be sequenced (313, 314). Several pipelines use live cells to preserve the maximum amount of mRNA and avoid confusing signal from gene expression related to cell death. It is important that single cells are properly isolated through this step as only individual cells must be considered for downstream analysis to avoid misinterpretation of cell types. Ideally, an even representation of cells from the whole embryo should be captured, but the various tissues in the embryo, especially at late stages, can have very different mechanical properties and react differently to dissociation techniques.

To obtain a catalogue of cell types during amphioxus development, during the amphioxus spawning seasons throughout my PhD I designed a protocol for single cell dissociation in amphioxus embryos together with Michael Schwimmer and Dr Elia Benito-Gutiérrez (Department of Zoology, University of Cambridge) (Figure 5.4A). After several rounds of optimization, we used a combination of mechanical and enzymatic dissociation: embryos were treated with two enzyme cocktails and at the same time were mechanically shaken using a Pasteur pipette (details of the protocol in Chapter II). The enzymatic digestion was performed in CMFSW to prevent osmotic shock and avoid reaggregation of cells after dissociation. Embryos were passed through two enzyme cocktails warmed at 37°C: the first one contained enzymes that are inhibited by (collagenase, dispase) or do not require (elastase, hyaluronidase) EDTA, while the second cocktail contained Trypsin and EDTA, with the double aim of stopping collagenase and dispase action and continue enzymatic digestion. In both cocktails, calcein was used to label live cells, which were then isolated using a specialized sorting machine called cellenONE (Cellenion, France) operated by Wing-Kit Leung (CRUK, Cambridge Institute) (Figure 5.4A) (315). The cell suspension was loaded into a thin capillary capable of dispensing droplets of ~500pl. The capillary is placed in front of a camera that can capture optic and fluorescent images. For each droplet, the camera detects whether a single alive cell is present. With this method, it is possible to keep only live cells and have a library of images for each cell to check its quality. We also found that cellenONE can work using CMFSW as a medium, a great advantage for avoiding stress/cell death-related gene expression. This solved a problem I encountered in initial experiments where live cells were isolated using fluorescence activated cell sorting, which instead uses PBS as a medium, resulting in increased cell death.

This dissociation protocol allowed me to obtain in high quality live cells from embryos at N0 and 7ss stages that could be processed for scRNAseq. Library preparation, reverse transcription and sequencing were performed by Katarzyna Kania (CRUK, Cambridge Institute) using 10X Genomics technology (Figure 5.4A). This is a droplet-based pipeline that enables the analysis of a large number of cells with high capture efficiency and resolution. It is based on a microfluidic system that forces cells into a line through a narrow tube and then inserts each cell into a single oil droplet together with enzymes for cell lysis, retrotranscription and PCR amplification and beads for mRNA capture.

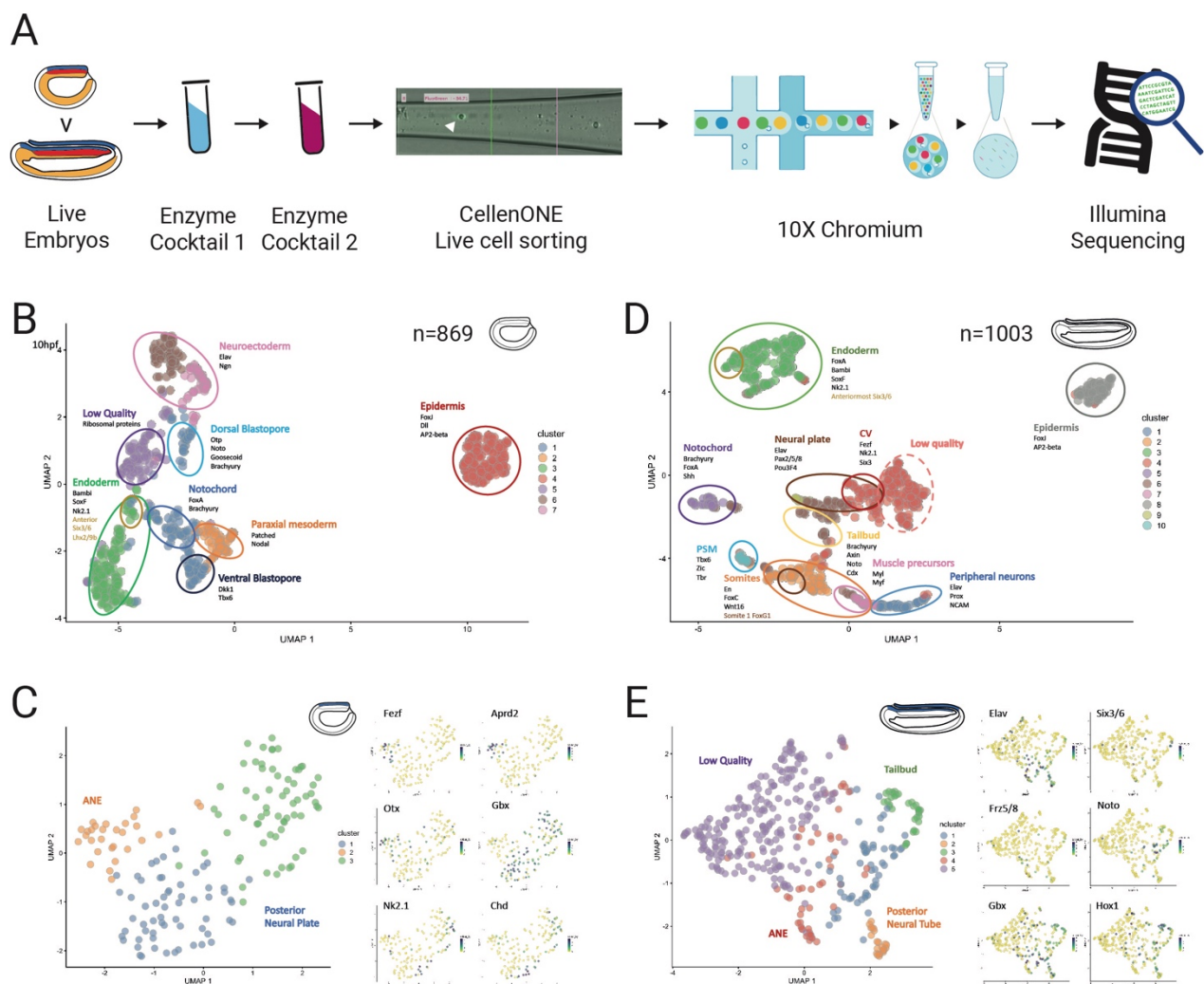


**Figure 5.4.** Single cell RNA sequencing of amphioxus embryos. **A.** Experimental design and pipeline for the dissociation and 10X sequencing of live cells from N0 and 7ss embryos. **B.** UMAP plot of N0 embryos showing 8 main assigned cell types. **C.** Re-clustering of neuroectoderm cells allows the distinction of anterior and posterior neural plate based on expression of known genes. **D.** UMAP plot for 7ss embryos with 11 mapped cell types. **E.** Brain, neural plate neurons and tailbud cells can be re-clustered to further define antero-posterior areas.

Each bead is covered by small nucleotide sequences containing a PCR primer, a barcode, unique molecular identifiers (UMIs) and a poly(T) tail used to specifically capture mRNA molecules, which are then reverse transcribed and amplified for sequencing. Each sequenced molecule therefore contains, in addition to the gene sequence, a barcode that indicates the cell from which the gene was sequenced and a UMI that is used to tell how many times the RNA molecule has been amplified.

Quality control, filtering and normalization of the sequencing data were performed by Daniel Keitley (Department of Zoology, University of Cambridge), who provided a count matrix to use for the analysis of cell types in the embryos. I next set out to annotate cell types in the two developmental datasets. The analysis also constituted a test beyond the standard quality controls to evaluate the level of completeness of the datasets for future uses by the Benito-Gutiérrez laboratory. The cell type annotation was based on the gene expression analysis carried out during my thesis and previous data in the literature (Appendix VII, Figure A7.2). For early neurula (N0) embryos we obtained ~850 cells representing all the major cell types of this stage (Figure 5.4B). Neural and non-neural ectoderm were defined by expression of *Elav-Ngn* and *Foxj-AP2 $\beta$*  respectively (316). The endoderm formed a single large cluster while the mesoderm could be distinguished into notochord and paraxial/presomitic mesoderm. In addition, I could identify cells belonging to the small population at the anterior boundary between mesoderm and endoderm, expressing *Six3/6* and *Lhx2/9a*. Curiously, dorsal and ventral blastoporal populations were clearly distinguishable in the UMAP plot: the dorsal blastopore expressed the organizer gene *Gsc* in addition to *Otp* (Appendix V) and *Brachyury* and *Noto* as previously described (84), while the ventral blastopore continuous with the posterior endoderm had high expression of *Dkk1* and *Tbx6/16*. Further sub-clustering of neural (clusters 6-7) and non-neural (cluster 4) ectoderm showed that different cell types could be defined corresponding to the major AP divisions of the body. In particular, aGRN genes were co-expressed in specific subsets of the neural and non-neural ectoderms, in a complementary pattern with posterior markers such as *Gbx* and *Hox1* (Figure 5.4C). Within the neuroectoderm cluster, the floor plate could also be distinguished by the expression *Nk2.1* and *Chd* (Figure 5.4C). It is interesting that, despite the similar expression of aGRN genes in neural and non-neural ectoderm, the two clusters are clearly separate. The analysis also allowed me to discover novel candidate markers for particular areas. For example, an amphioxus-specific paired-like homeobox gene with high sequence similarity to *Rx*, *Aprd2*, was enriched in the ANE and anterior epidermis, where the rest of the early aGRN is also expressed (Figure 5.4C). At the mid neurula (7ss) stage, the analysis of ~1000 sequenced cells

showed that the number of cell types increased following the development of embryonic tissues (Figure 5.4D). The neural plate and epidermis were still separated clearly by expression of *Elav* and *FoxJ/AP2 $\beta$*  respectively, but now within the neural plate the CV and trunk neuroectoderm could be distinguished. Moreover, at this stage peripheral neurons were grouped in a separate cluster expressing *Elav* and *Prox* (317). Mesodermal cells were divided into several types: the notochord was defined by the expression of *Brachyury*, *FoxA* and *Shh*, while somites expressed *En*, *FoxC* and *Wnt16* (318). Within somites, a group of cells already expressed muscle markers such as myosin (*Myl*) and *Myf*. Another cluster was defined as presomitic mesoderm based on expression of *Tbx6*, *Zic* and *Tbr* (84). Finally, a group of cells that clustered with the neural plate were found to have a tailbud signature, likely deriving from the dorsal blastopore lip of the N0 stage, expressing *Brachyury*, *Axin*, *Noto*, *Cdx* and *Otp* (84). The endoderm also formed a conspicuous cluster marked by *FoxA*, *Bambi* and *SoxF*, within which the anteriormost portion expressing *Six3/6* could still be detected. I isolated and subclustered neural plate cells (clusters 4, 6 and 9, which included the tailbud) to define the level of regionalization of the neuroectoderm (Figure 5.4E). The distinctions between the CV (subcluster 4, expressing *Elav*, *Frz5/8* and *Six3/6*), the trunk neural plate (subcluster 2 and part of subcluster 1, expressing *Elav*, *Hox1* and *Gbx*) and the tailbud (subcluster 3 and part of subcluster 1, expressing *Hox1*, *Gbx* and *Noto* but not *Elav*) could be identified, but subcluster 5 contained cells of low quality.

Taken together, these results show that the two scRNAseq datasets obtained with the newly optimized dissociation protocol contain all the main cell populations of amphioxus neurulas at N0 and 7ss stages. Having completed the cell type annotation, the datasets are now ready to be used for a thorough characterization of cell types during amphioxus neurulation. More generally, this scRNAseq dataset is a useful tool that will facilitate future amphioxus research beyond the scope of this project.

## 5.4 Characterization of the amphioxus larval brain

### 5.4.1 The anterior cerebral vesicle – a homolog of the secondary prosencephalon

In Chapter III I provided evidence of the conservation of ANE patterning in deuterostomes and showed that aGRN genes are expressed in the anterior neural plate of amphioxus embryos.

Furthermore, analysis of zebrafish scRNAseq data highlighted that a similar molecular signature could be detected in the vertebrate secondary prosencephalon, which gives rise to the retina, telencephalon and hypothalamus. With the double aim of characterizing the amphioxus brain and testing the homology of chordate brain cell types, I analysed the expression of 19 genes (*Bsx*, *CTFP1*, *CTFP2*, *CTFP3*, *Fezf*, *FoxD*, *Frz5/8*, *Hmx*, *Lhx2/9b*, *miR-7*, *Nk2.1*, *Otp*, *Otx*, *Pax4/6*, *Rx*, *SerT*, *Six3/6*, *Vglut*, *Zic*) in amphioxus brains at the early larva (14ss) and the more mature 1gs (4dpf) larva. The developmental expression from gastrula to larva for *Bsx*, *CTFP1*, *CTFP2*, *CTFP3*, *Hmx*, *Lhx2/9* and *Otp* is described here for the first time and can be found in Appendix V.

Interestingly, the initial broad distribution of aGRN genes fragmented to label different neural populations scattered across the CV of the larva, suggesting that several cell types differentiate at the start of larval life (see Chapter III). From the 7ss stage, the expression of *Six3/6* resolves the anterior neural plate in three areas: a pre-infundibular *Six3/6*-positive domain at the anterior tip of the neuroectoderm, a post-infundibular *Six3/6*-positive domain and an intercalated pre-infundibular *Six3/6*-negative domain. The terms “pre-“ and “post-infundibular“ refer to the fact that the three domains persist after the closure of the neural tube and are visible in the larval brain, where the infundibular cells separate the anterior and posterior CV. These domains provide a reference to locate the expression of other genes and divide the CV into distinct regions.

In Chapter III I have showed that at 7ss *Nk2.1* and *Fezf*, early markers of vertebrate hypothalamic fate, are expressed in the intercalated *Six3/6*-negative region, suggesting that it might represent a hypothalamic homolog. I therefore looked at the distribution of markers of hypothalamic cell types at the larval stage (Figure 5.5). The markers were chosen by interrogating a scRNAseq dataset of the zebrafish brain at 48 hpf (319) (Appendix VII, Figure A7.3). *Otp* is expressed in the hypothalamus, diencephalon and hindbrain of vertebrates, where it contributes to specify a variety of neuronal cell types (320). In amphioxus, *Otp* has been previously reported in the trunk region of the nervous system at the 7ss stage (87). Extending the analysis to later stages, I found that *Otp* was progressively upregulated in the CV (Appendix VII, Figure A7.3). First, at 10ss, in a pair of ventro-medially located cells in the posterior *Six3/6*-positive region (which become more numerous at 14ss). Second, from 12 ss, in two prominent ventro-lateral clusters located in the intercalated *Six3/6*-negative region (Figure 5.5A-B). *FoxD* is another well-known hypothalamic marker and is expressed in the intercalated *Six3/6*-negative region at 7ss (Appendix V). It remained expressed in the same region at 14ss and

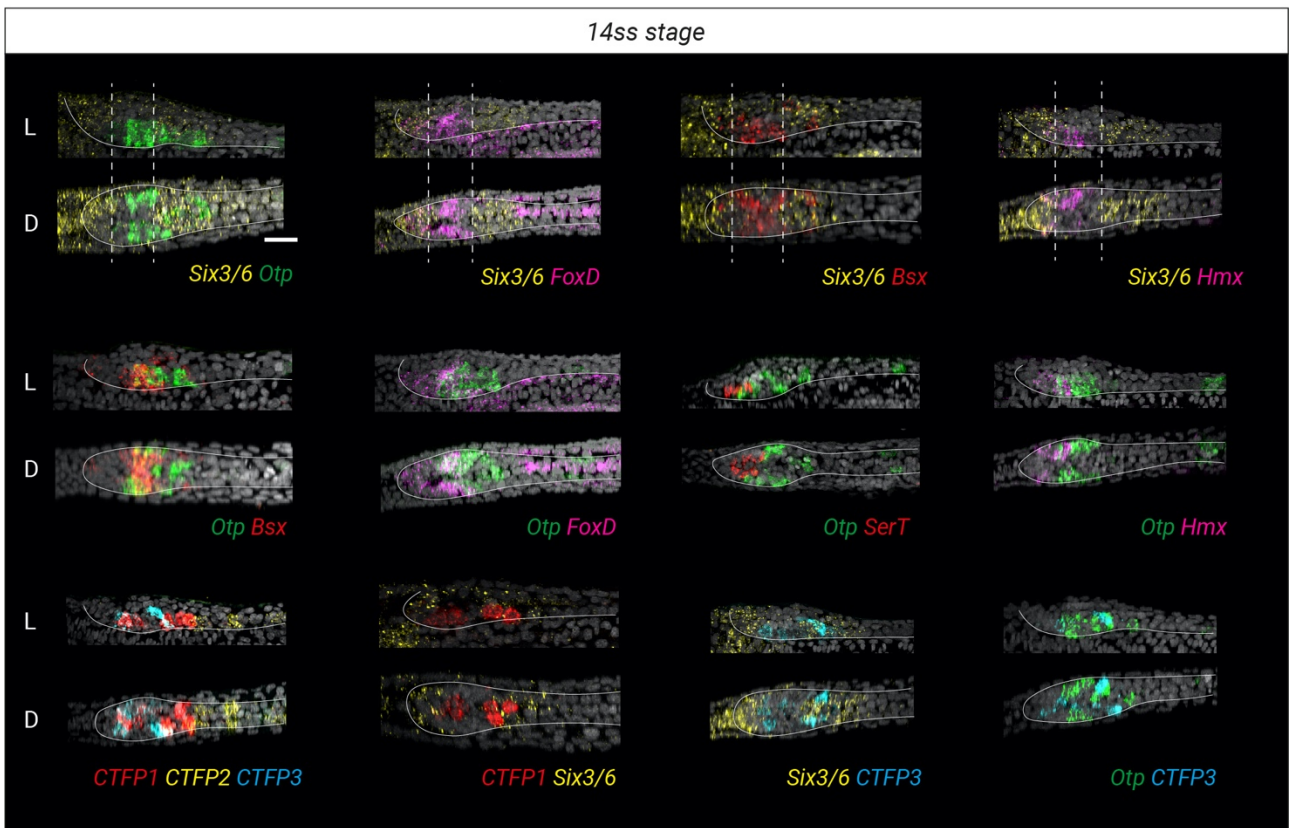
reached more dorsally than *Otp* (Figure 5.5A-B). I next analysed the expression of another hypothalamic marker, *Bsx* (321, 322). At 14ss *Bsx* labels three populations in the CV: a small anterior group in the *Six3/6*-positive region, a domain in the posterior *Six3/6*-positive region (postinfundibular) comprising ventral and dorsal cells, and a large number of ventral cells in the intercalated *Six3/6*-negative area (Figure 5.5A-B). Here, *Bsx* was co-expressed with *Otp* in lateral cells, but additional *Bsx*-positive/*Otp*-negative cells were found medially. *Hmx2* and *Hmx3* are required for correct hypothalamic development in mice (323) and are found in the zebrafish hypothalamus (Appendix VII, Figure A7.3). In amphioxus early larvae *Hmx* signal was visible in the brain, in an anterior pair of lateral cells and a more posterior group of cells interspersed among *Otp* neurons (Figure 5.5A-B).

The vertebrate hypothalamus is also characterized by the expression of miR-7, a microRNA known to be associated with neurosecretory centres in protostomes and deuterostomes (324). In amphioxus miR-7 was previously shown to be expressed in the CV and the pre-oral pit (325). I therefore used HCR to co-detect miR-7 with *Six3/6* and *Otp* at the 1gs stage. miR-7 transcripts were localized ventrally and laterally in the anterior CV but were absent from the brain roof (Figure 5.5C). The expression did not reach the anteriormost tip and it extended to the end of the intercalated *Six3/6*-negative region. The pre-infundibular clusters of *Otp* neurons therefore were entirely located within the miR-7 domain (Figure 5.5C). Given the association of miR-7 with neurosecretory systems, and the neurosecretory nature of AOs, I investigated the expression of the three amphioxus neuropeptides of the calcitonin/CGRP family (calcitonin family proteins, CTFPs) (326, 327). In vertebrates, calcitonin and CGRP are alternatively spliced forms of the same gene (*CALCA*): calcitonin is produced by C-cells and acts as a hormone, while CGRP is expressed in the nervous system, where it acts as a neuropeptide (328). Here we show that the three paralogs have a dynamic expression pattern in amphioxus: *CTFP1* and *CTFP2* were first co-expressed in the anterior nervous system at the 7ss stage (Appendix V). While *CTFP1* continued to be expressed in both the anterior and posterior CV, mostly in medial cells, *CTFP2* abruptly changed its pattern to mark cells in the posterior CV and the trunk nervous system at 14ss (Figure 5.5A-B). At the same stage, *CTFP3* appeared in the CV and the infundibular organ (Figure 5.6A-B). At the larval stage, *CTFP3* remained expressed in the anterior CV within the miR-7 domain, while *CTFP1* restricted to the posterior CV (Figure 5.5C).

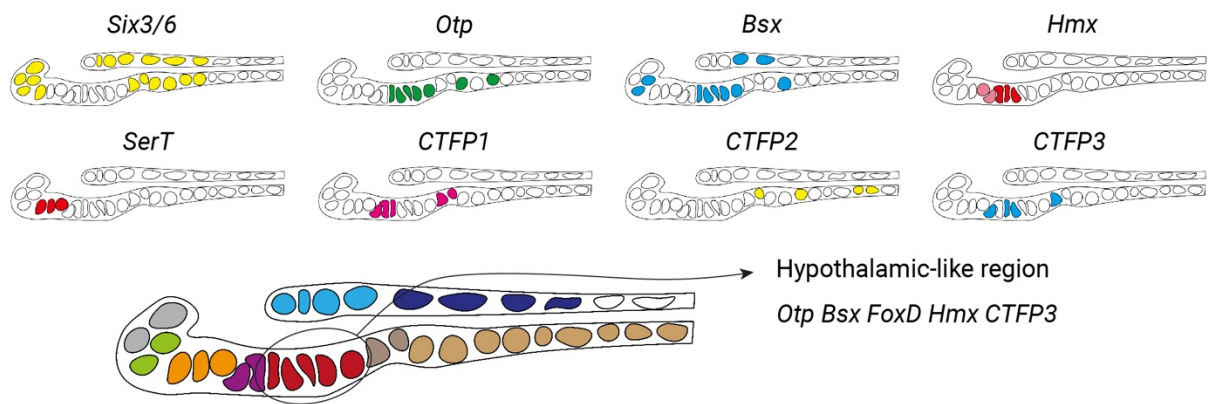
The distribution of the selected markers indicates that the ventral intercalated *Six3/6*-negative region of the CV is homologous to the vertebrate hypothalamus and includes neurosecretory cell types. This region is contiguous with the anterior frontal eye, which is perhaps the most studied portion of the larval nervous system. Previous work in fact showed that the eye is organized into five “rows” of cells at the 1gs stage: adjacent to the neuropore are few pigmented cells expressing *Otx*, followed by row1 photoreceptors also expressing *Otx*, row2 serotonergic neurons and two rows of associated cells expressing *Pax4/6* and *Rx*, forming a structure that resembles a simplified version of the vertebrate retina (290, 293, 294). Using *Otx*, *SerT*, *Pax4/6* I identified these cell types in both 14ss and 1gs larvae (Figure 5.6). At the 14ss stage, frontal eye cells are not yet arranged in precise rows: *Otx* formed an arch (in dorsal view) below the neuropore, corresponding to the anterior *Six3/6*-positive domain marking pigment and row1 cells, while *SerT*-positive neurons were located medially and *Pax4/6*-positive neurons were positioned laterally behind the *Six3/6*-*Otx* domain. Only rare *SerT*-positive cells were co-expressing *Six3/6*. I then expanded the previous characterization of frontal eye cell types (Figure 5.6). *Frz5/8*, *Zic*, *Lhx2/9* and possibly *Rx* were expressed in pigment cells. *Frz5/8*, *Rx*, *Nk2.1*, *Lhx2/9*, *Bsx* labelled row1 photoreceptor cells, which were shown to be glutamatergic based on expression of *Vglut*. Row2 serotonergic neurons were also marked by *Frz5/8*, *Fezf*, and possibly *FoxD*. Row3/4 neurons also expressed *Rx*, *Fezf*, *FoxD*, *CTFP1* and possibly *Lhx2/9* and *Hmx*. Contrary to a previous immunofluorescence analysis (294), these cells did not express *Vglut* and so were not considered glutamatergic. This analysis showed that the ventral side of the anterior CV has a retino-hypothalamic molecular signature, including glutamatergic, serotonergic and peptidergic cell types. On the other hand, the dorsal layer did not show markers of differentiated neurons and continued to express early ANE markers, such as *Six3/6*, *Rx*, *Fezf*, *Otx*, *Lhx2/9* and *Frz5/8*. Finally, the roof of the neural tube was positive for *Zic* throughout its length, suggesting that this gene is involved in the DV patterning of the neural tube.

**Figure 5.5.** Characterization of the hypothalamic region of the amphioxus cerebral vesicle (overleaf). **A.** Expression of *Six3/6* (yellow), *Otp* (green), *FoxD* (magenta), *Bsx* (red), *Hmx* (magenta), *SerT* (red), *CTFP1* (red), *CTFP2* (yellow), *CTFP3* (cyan) in early larvae (14ss). Co-expression pairs are presented in lateral (L) and dorsal (D) views. White lines delineate the neural tube, dashed lines delimit the intercalated *Six3/6*-negative region. **B.** Schematic representation of hypothalamic gene expression in a sagittal section of the larval brain. **C.** Co-detection of *Six3/6*, miR-7 mature transcripts (magenta), *Otp*, *Bsx* (cyan), *CTFP1*, *CTFP2* and *CTFP3* in one gill slit larvae. Scale bar is 20µm.

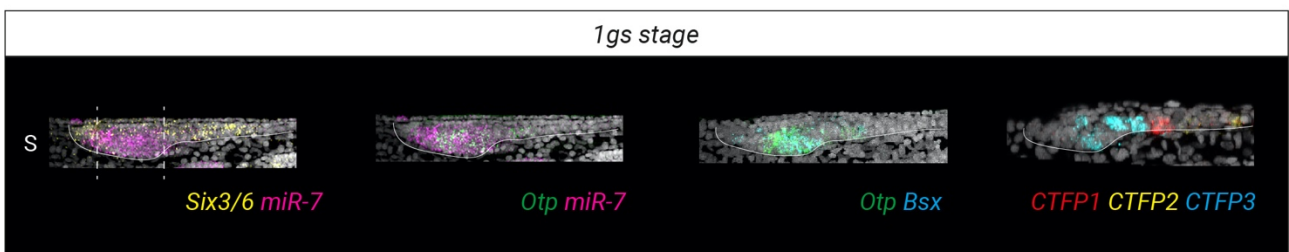
A



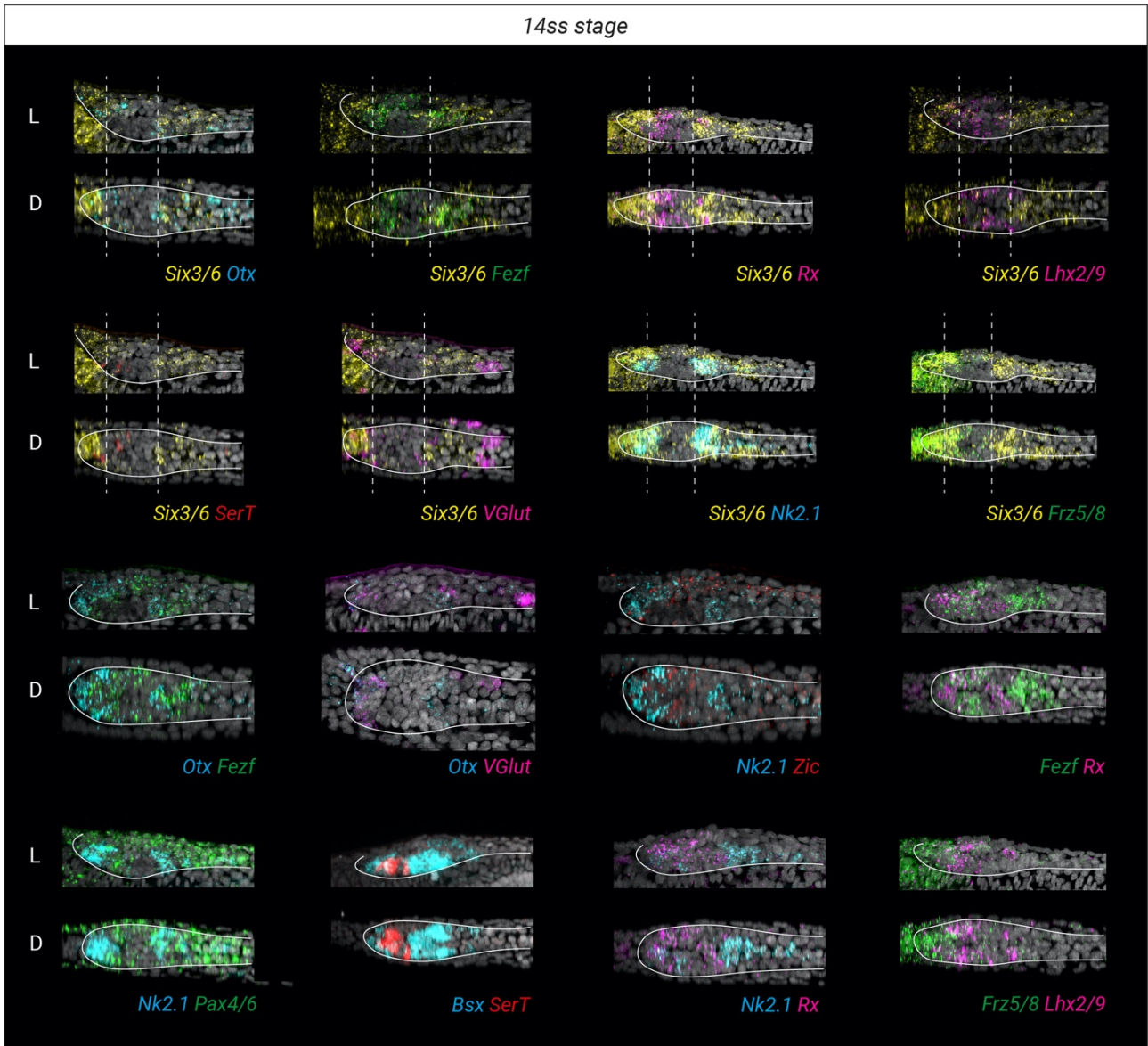
B



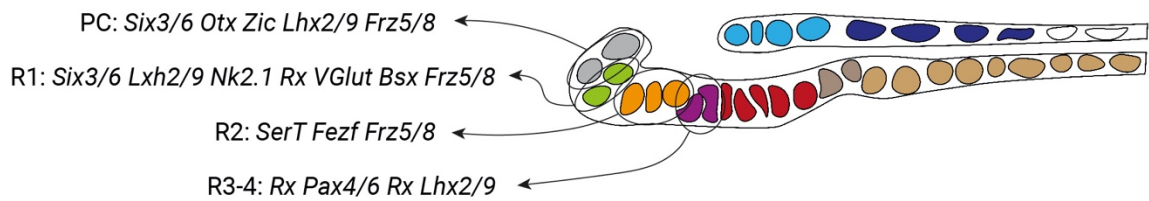
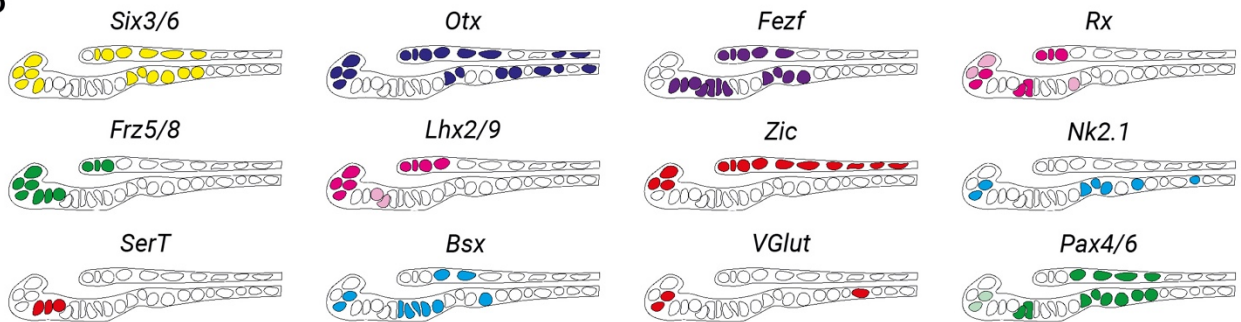
C



A



B



< **Figure 5.6.** Molecular characterization of cell types in the amphioxus frontal eye complex. Combinations of *Six3/6* (yellow), *Otx* (cyan), *Fezf* (green), *Rx* (magenta), *Lhx2/9a* (magenta), *SerT* (red), *Vglut* (magenta), *Nk2.1* (cyan), *Frz5/8* (green) and *Zic* (red) expression in early larvae (14ss). Co-expression pairs are presented in lateral (L) and dorsal (D) views. White lines delineate the neural tube, dashed lines delimit the intercalated *Six3/6*-negative region. **B.** Schematic representation of frontal eye cell types and their gene expression in a sagittal section of the early larval brain.

#### 5.4.2 The posterior cerebral vesicle

The posterior, postinfundibular CV has been hypothesized to have a di-mesencephalic signature based on the expression of genes such as *Pax4/6* and *Otx* (87). However, this area also contains the posterior *Six3/6*-positive domain, which is not found in the vertebrate brain and might be an amphioxus-specific trait. Infundibular cells expressed *Six3/6*, *Fezf*, *Otx*, *Nk2.1*, *Pax4/6* and *CTFP1* (Figure 5.5; Figure 5.6). On each side of infundibular cells was a pair of large neurons expressing *CTFP3*. The posterior *Six3/6*-positive domain expressed *Pax4/6*, *Fezf* and *Otx*, and contained other *CTFP1*-positive cells which were interspersed between the posterior *Otp* cells. Cells expressing *CTFP2* were also found more posteriorly within the CV and along the trunk (see below). The posterior limit of *Six3/6* expression was not coincident with the posterior limit of *Otx*, as previously described (87): *Otx* reached more posteriorly, arriving at the boundary between the first and second somite, while *Six3/6* stopped more anteriorly together with *Pax4/6*, at the level of the posterior glutamatergic neurons that will form the primary motor centre. Dorsally, *Six3/6*, *Pax4/6* and *Bsx* were expressed in the area that forms the lamellar body, a photoreceptor organ possibly homologous to the epiphysis (86, 296).

#### 5.4.3 The amphioxus hindbrain

The region between the second and sixth somite is thought to be a homolog to the vertebrate hindbrain (87, 291). Despite the lack of overtly segmented neuromeres, within this region several genes are expressed in a segmented pattern in ventrolateral cells, which differentiate in cholinergic, GABAergic and glycinergic neurons (221). Accordingly, the expression of *Elav* starts to be segmented at this stage and coincides with cells at the somite boundary (317). The hindbrain-like area is also posterior to the boundary of expression between *Otx* and *Gbx* at the 7ss stage, in a manner

similar to the midbrain-hindbrain boundary of vertebrates (87). I therefore decided to investigate the development and diversity of cell types within this region.

As part of the project of Simon Kershenbaum, an undergraduate student in our lab, we first considered the position and formation of the anterior *Otx-Gbx* boundary by co-detecting the two genes across development (Figure 5.7A). Already at G5, when the neural plate has just been specified, *Otx* labelled the ANE while *Gbx* was expressed in a complementary manner in the posterior neural and non-neural ectoderm, forming a slightly bent ring around the DV axis of the animal (as the ventral lip of the blastopore do not show *Gbx* expression) (Figure 5.7Ai). At N0 and 7ss, the expression remained mutually exclusive in the neural tube, with a boundary located at the border between the first and second somite pair (Figure 5.7Aii-iii). However, at 7ss *Gbx* extended slightly more anteriorly on the ventral side than the dorsal side. Surprisingly, at the larval stage the two genes did not form a stark boundary but were co-expressed in a small cluster of cells anterior to the first somite boundary (Figure 5.7Aiv).

Next, I wanted to investigate the cell type composition of the hindbrain-like region, given the number of different genes that have a segmented expression pattern. I therefore co-detected the three main neurotransmitter markers previously identified in this area – *VGAT* for glycinergic neurons, *VGAT+GAD67* for GABAergic neurons and *Chat* for cholinergic neurons – with four additional markers that have not been considered in previous works: *Otp*, *Hmx*, *Vt* and *CTFP2* (Figure 5.7B). The experiments were carried out in 12ss embryos, a stage in which the neurogenesis analysis showed that most ventrolateral cells were located in a single line and differentiating into mature neurons (Figure 5.2). The simple tissue morphology and the low and stable number of ventro-lateral cells within this region – ~34-35 at 12ss – meant that by using one marker (*VGAT*) in all HCR experiments, embryos labelled with different combinations could be easily compared to construct a comprehensive map of cell types (Figure 5.7C). This part of the project was carried out with the help of three undergraduate students, Mark Comer, Madeline Foster-Smith and Maria Izmirlieva, and revealed an unexpected variety of cell types in the amphioxus hindbrain, with different neurons along the AP axis expressing different combinations of the seven genes.

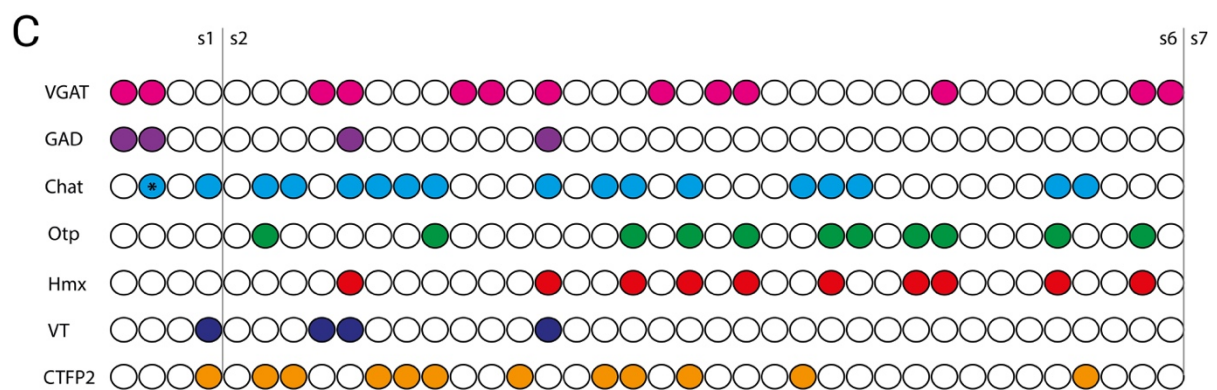
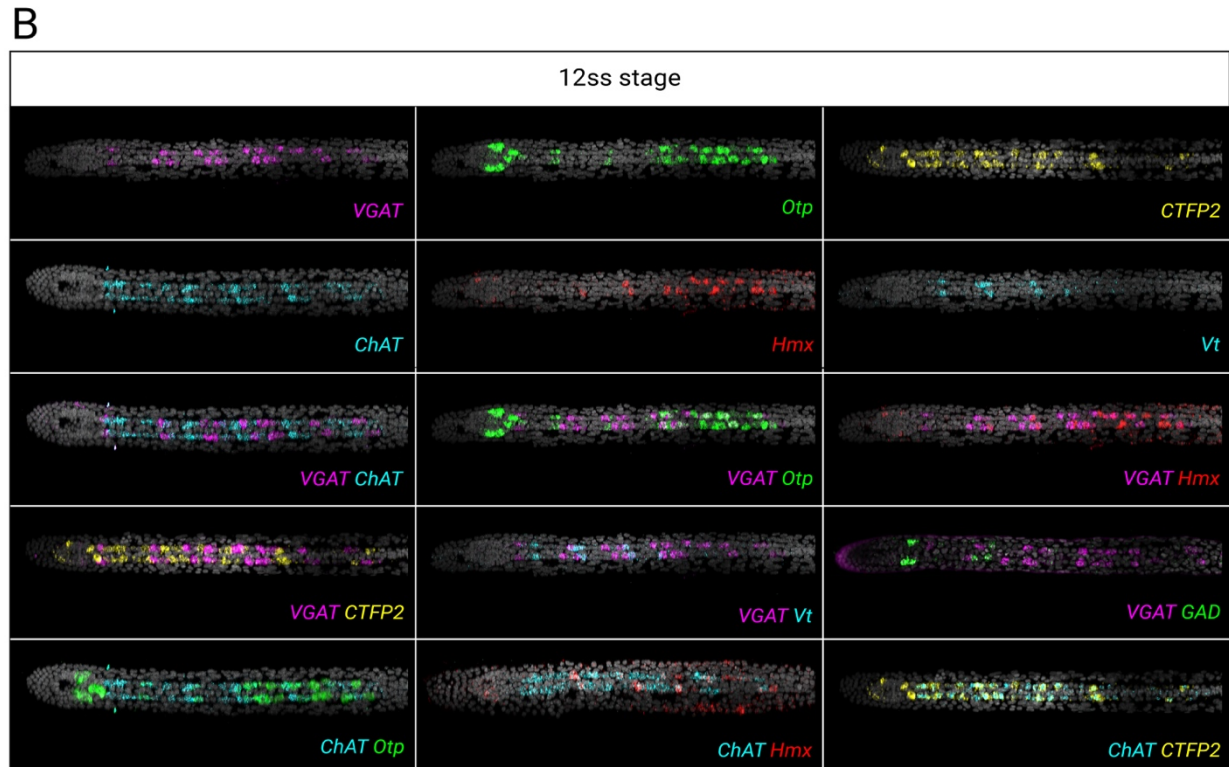
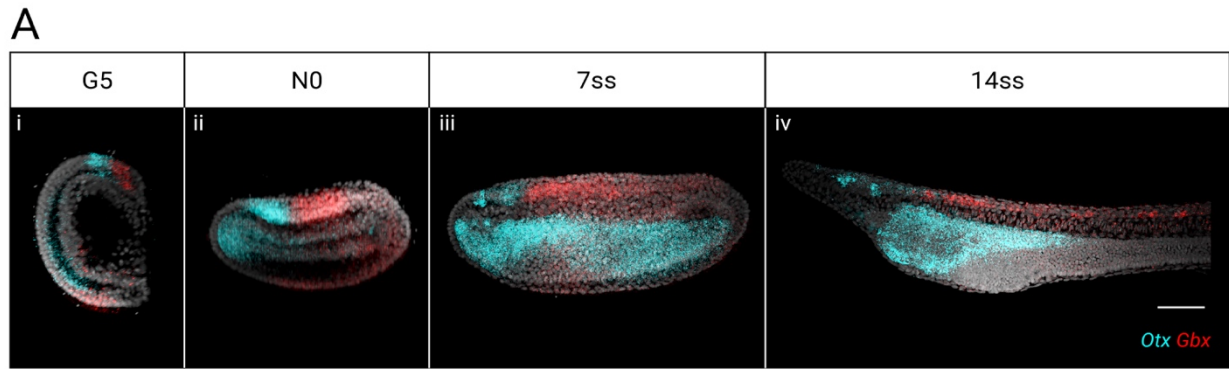


**Figure 5.7.** Characterization of cell type diversity in the amphioxus hindbrain. **A.** Position of the midbrain-hindbrain boundary defined by the expression of *Otx* and *Gbx*. The expression boundary between these two genes found early in development (i-iii) is partially lost at the larval stage (iv). (continued overleaf)

**Figure 5.7. continued B.** Co-expression of six markers in ventrolateral cells of the hindbrain-like region. Genes include neurotransmitter markers *VGAT* (magenta) and *ChAT* (cyan), transcription factors *Otp* (green) and *Hmx* (red) and neuropeptide precursors *CTFP2* (yellow) and *Vt* (cyan). All images are in dorsal view. **C.** Cell type map in the left row of ventrolateral cells in the amphioxus hindbrain, based on the expression shown in B. Scale bar is 50µm.

While *VGAT* and *Chat* mostly labelled separate neuronal populations - as expected by the fact that they mark neurons encoding different neurotransmitters - surprisingly two pairs of cells co-expressed the two markers. These are the two pairs of cells that also expressed *GAD*, indicating that they might be at a junction between GABAergic and cholinergic fate. In addition, these neurons expressed *Hmx* and the vasopressin-oxytocin-type neuropeptide vasotocin (*Vt*). The co-localization of several markers suggests that these four cells represents a complex cell type, possibly with multiple functions. It would be interesting to follow its projections to identify how it is connected with the rest of the nervous system. Next to the first pair of these *GAD*-expressing cells, a pair of glycinergic neurons also expressed *Vt*, while the other *Vt*-positive cells were located at the posterior boundary of the CV and were cholinergic neurons, showing that this neuropeptide can function in a variety of neuronal types. Conversely, *CTFP2* was expressed only in cholinergic neurons of the anterior portion of the hindbrain. *Otp* also had a peculiar pattern: anteriorly within the hindbrain, two pairs of *Otp*-positive cells were cholinergic and expressed *CTFP2*, while posteriorly this gene was found in cholinergic, glycinergic and other unknown neurons. However, in most of these posterior cells *Otp* was co-expressed with *Hmx*. This analysis demonstrates a surprising variety of cell types in the amphioxus hindbrain and opens new questions on how this diversity is generated during the formation of the hindbrain that could be elucidated in future studies.

## 5.5 Proliferation during amphioxus neurogenesis

The increase in cell type diversity observed during development occurs concomitantly with morphogenetic processes that are physically shaping the tissues of the embryo. In fact, cells are specified and differentiate within tissues that are dynamically changing in shape, size and cellular architecture. One of the major morphogenetic processes that has critical functions during development is cell division, which impacts tissue size, final cell number and cell differentiation across the embryo, including in the nervous system. In vertebrate embryos, the initially single-

layered neuroepithelium is progressively patterned by intrinsic and extrinsic cues that drive its cells into specific cellular behaviours and specialised modes of cell division (329, 330). Vertebrate neuroepithelial progenitors proliferate extensively across the AP axis: staining with PCNA in embryos of the little skate *Leucoraja erinacea* for example shows a large number of mitotic cells across the surface of the neural plate and neural tube (Appendix VII, Figure 7.4). Depending on the division mode, progenitors can increase cell numbers in specific populations, augment the progenitor pool or produce neuroblasts that differentiate into different types of neurons (331–333). For example, in the vertebrate telencephalon asymmetric divisions are key to layer the cortex, as well as to influence neuronal migratory routes and to diversify the neuronal type repertoire (334).

In amphioxus, previous studies have reported spatially restricted proliferation in the anterior tip of the neural tube and the posterior floor plate at the mid-neurula stage (335). By labelling cells in S-phase with EdU and mitotic cells with phosphorylated histone H3 immunostaining our group had previously shown that during neurulation – between 5ss and 10ss - proliferation is restricted to two polarized domains at the anterior and posterior tips of the neural tube (219). Between these two proliferative domains, cells in the trunk neural plate do not divide until the 12ss stage, when proliferation is detected at low level across the AP axis. The peculiar pattern of cell division, and in particular the restricted proliferation at the anterior tip of the neural plate that forms the CV, suggests that proliferation could have specific contributions to the development and regionalization of the nervous system. For this reason, I analysed the pattern of neural proliferation in the context of neurogenesis and followed the fate of proliferating cells to determine their contribution to the larval nervous system.

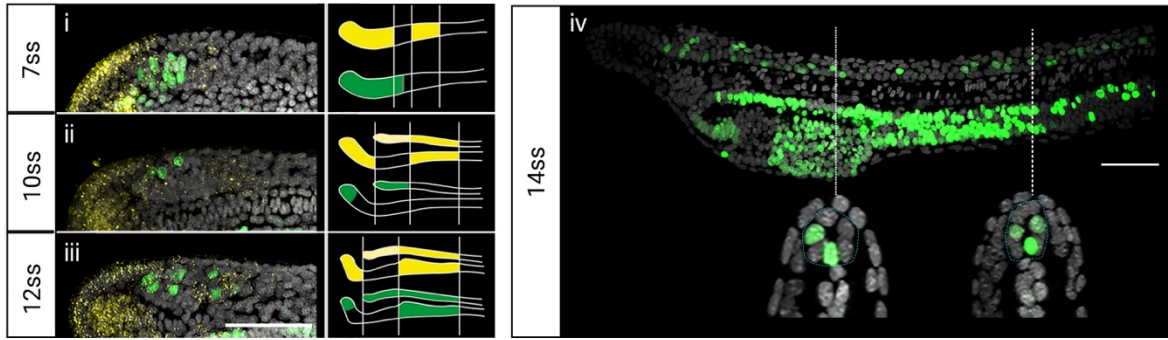
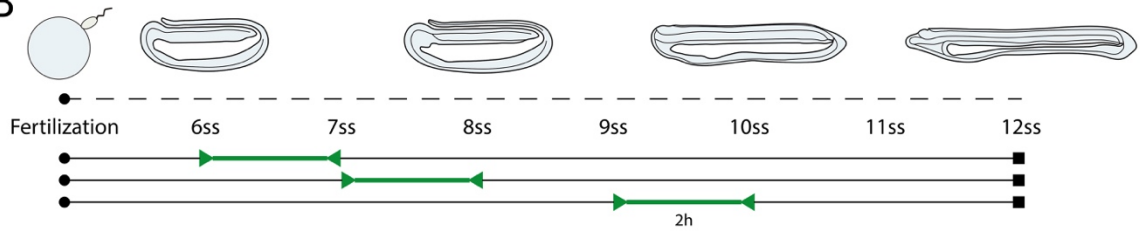
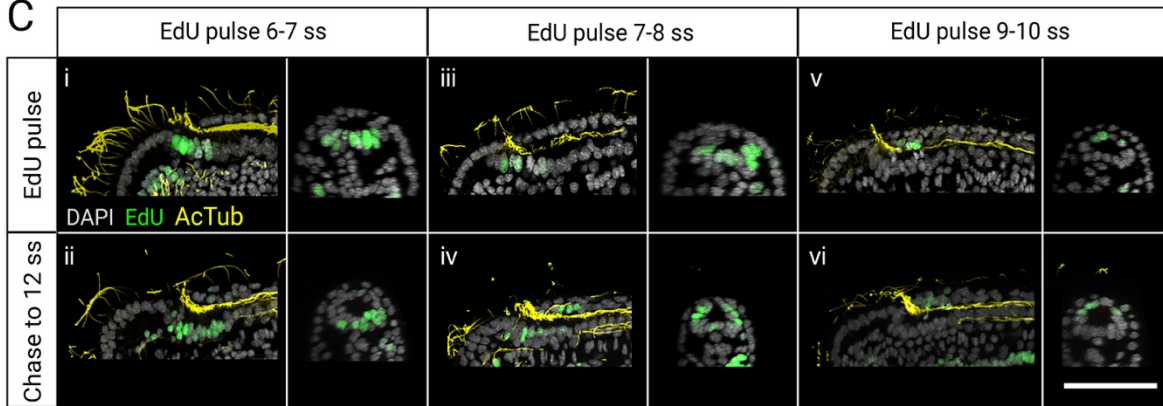
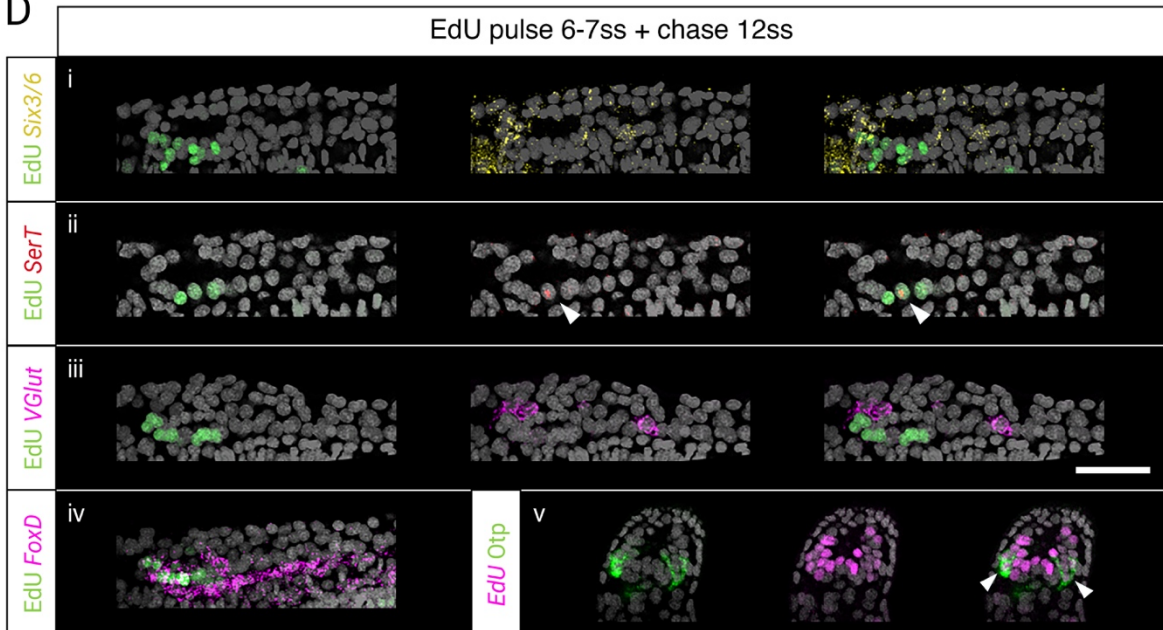
#### 5.5.1 Following the fate of proliferating cells

To better characterize the anterior proliferative domain, I combined EdU detection with *Six3/6* profiling by HCR. At 7ss, EdU labelled a relatively large group of cells in the anterior *Six3/6*-positive and intercalated *Six3/6* negative region, whereas no EdU-positive cells were found in the posterior *Six3/6*-positive cluster (Figure 5.8Ai). At 10ss, cell division declined, such that only 3-5 EdU-positive cells were identified in the anterior tip or dorsal region of the developing CV, within the anterior *Six3/6*-positive cluster (Figure 5.8Aii). At 12ss, the number of EdU-positive cells in the anterior-dorsal CV increased, and proliferating cells appeared also in the posterior *Six3/6*-positive region.

(Figure 5.8Aiii). In the posterior proliferative domain, previous analysis of serial transverse sections stained with EdU at 7ss showed that cell division occurs broadly in the posterior neural plate during axial elongation but restricts to the most medial-ventral cells at more anterior axial positions (219). When proliferation resumes in the trunk domain at the 12-14ss stage, EdU staining shows that proliferating cells are located only in the floor plate and in medio-lateral cells (Figure 5.8Aiv).

Having defined the proliferative domains during amphioxus neurogenesis, I next followed their contribution to the larval CNS using an EdU pulse-chase approach. Proliferating cells were labelled with 2h EdU pulses at three stages of development: between 6-7ss, 7-8ss and 9-10ss (Figure 5.8B-C). After the EdU treatment, embryos were washed and left to develop in fresh sea water until the 12ss stage (Figure 5.8B). EdU is retained by proliferating cells, making it possible to follow their fate across development. Within the anterior proliferative domain, cells divide at different rates in the three successive stages and contribute to different areas of the larval CV. At 6-7ss proliferation was seen in cells located medially in the neural plate, and their daughter cells remained ventral at 12ss, meaning they contribute broadly to the ventral side of the CV along its anteroposterior axis (Figure 5.8Ci-ii).

**Figure 5.8.** Analysis of proliferation in the amphioxus nervous system. (overleaf) **A.** EdU incorporation (green) during neurogenesis. (i-iii) Lateral z-projections of the cerebral vesicle at 7, 10 and 12ss stages showing EdU incorporation and co-localisation with *Six3/6* (yellow), using HCR in situ hybridization. (iv) Sagittal and cross projections of 14ss early larvae with EdU localization (iv). **B.** Experimental design of EdU pulse-chase experiments. **C.** Fate of anterior proliferating cells across neurulation visualized with EdU pulse-chase and acetylated tubulin immunofluorescence (yellow). (i-ii) EdU pulses at 6-7ss marked ventral brain cells that remained ventral in the cerebral vesicle of 12ss embryos. (iii-vi) At later stages lateral and dorsal proliferating cells in the brain, as shown by Edu pulses between 7-8ss (iii-iv) and 9-10ss (v-vi) contributed to progressively dorsal cell populations. **D.** Brain expression of *Six3/6*, neurotransmitter markers *SerT* (red) and *VGlut* (magenta), and hypothalamic markers *FoxD* (magenta) and *Otp* (green) in embryos pulsed with EdU at 6-7 ss and chased to 12 ss. Scale bars are 50µm.

**A****B****C****D**

In contrast, EdU-positive cells labelled in the anterior neural plate between 7ss and 8ss were positioned more laterally, and therefore contributed most significantly to the dorso-lateral walls of the CV after neurulation (Figure 5.8Ciii-iv). Finally, those labelled between 9ss and 10ss contributed exclusively to the dorsal side of the CV (Figure 5.8Cv-vi). Considered together, these data suggest that cell division in the brain is spatially restricted, increasing cell numbers locally in a ventral-to-dorsal temporal sequence. Meanwhile, proliferative cells in the posterior neural tube specifically contributed to elongation of the posterior floor plate and become dispersed across the posterior third of the neural tube, behind the boundary between the 6<sup>th</sup> and 7<sup>th</sup> somite (219).

Following the fate of proliferating cells in the anterior neural plate at the 7ss stage showed that they contribute to the ventral CV of the larva, which has a retino-hypothalamic signature as described in paragraph 5.4.1. In chapter III, I showed that the anterior *Six3/6*-positive and intercalated *Six3/6*-negative regions at 7ss stage correspond to the area where the aGRN is active during early development. The similar position along the AP axis suggests that the retino-hypothalamic cells differentiate from the ANE in which the aGRN is active. By combining the pulse-chase approach with *in situ* HCR I next sought to test the precise contribution of the ANE to the larval brain. I pulsed embryos with EdU between the 6ss and 7ss stage, raised them up to the 12ss stage and then detected the expression of *Six3/6* together with four markers of different cell types of the larva: *Vglut*, which marks row1 cells in the frontal eye; *SerT*, which labels row2 serotonergic neurons; and the transcription factors *Otp* and *FoxD*, which are expressed within the hypothalamic-like region (Figure 5.8D). While the majority of *Six3/6* cells are EdU-negative, a few cells double *Six3/6*-EdU-positive were located at the most anterior end of the CV (Figure 5.8Di). Strikingly, serotonergic, *Otp*-positive and *FoxD*-positive neurons were EdU-positive, indicating that they derive from progenitors proliferating between 6-7ss (Figure 5.8Dii-iii). Conversely, none of the glutamatergic neurons marked by *VGlut* were EdU-positive, suggesting that these cells were born earlier in development, before the 7ss stage (Figure 5.8Div). These results confirm that the retino-hypothalamic cells of the amphioxus CV develop from the area in which the aGRN is active during the formation of the neural plate.

### 5.5.2 Inhibition of proliferation causes loss of brain cell types

Progenitors that give rise to the anterior and posterior CV proliferate at different rates during neurulation. After tracing the distribution and fates of proliferative cells, I sought to assess the functional contributions of cell division to neural tube morphogenesis and brain. To this end, cell division was inhibited using hydroxyurea (HU) to arrest DNA synthesis. I first tested the effect of blocking proliferation throughout neurulation by treating embryos from mid-gastrulation (8 hpf), when cell division is widespread throughout the embryo (335), to the early larva stage (14ss) (Figure 5.9A). Surprisingly, HU-treated embryos remained viable until the 14ss stage and despite widespread cell death (indicated by pyknotic DAPI-stained nuclei) the major patterns of the body plan were intact. Immunostaining for acetylated tubulin in both control and treated embryos showed a central neural canal internalized beneath the surface ectoderm and axonal tracts running on the ventral side of the neural tube (Figure 5.9A). The neural tube of HU-treated embryos had a clearly defined CV that opened anteriorly through the neuropore and had rostral axonal projections similar to DMSO-treated control embryos. Furthermore, peripheral epidermal sensory neurons formed normally along the body axis and projected to the neural tube, although the size of each neuron was visibly larger than in control embryos (Figure 5.9A). These observations demonstrate the developmental robustness of the nervous system anlage in amphioxus, which forms even in the absence of proliferation during early neurogenesis. However, HU-treated embryos failed to elongate, reaching less than half the AP length of DMSO-treated siblings by 14ss, indicating that proliferation may be dispensable at the stages treated to achieve correct tissue composition and topology, but it is key to confer specific body traits with proper geometry.

Having found that cell division is dispensable for the formation of the neural tube, I focused on the brain and investigated the role of proliferation in cell type diversification. Cell division was arrested for a shorter interval of time, starting at the 6ss stage, when proliferation is specifically localised in the brain, and raised these embryos up to the 12ss and 14ss stages (Figure 5.9B). I then examined the effects of proliferation inhibition using several markers expressed in the anterior and posterior CV: the serotonergic marker *SerT*, the glutamatergic marker *VGlut* and the transcription factors *Six3/6*, *Fezf*, *Otp* and *Bsx*. I first looked at two markers, *Six3/6* and *Fezf*, that define broad subdivisions of the CV. The treated embryos did not show any changes in *Six3/6* expression, which had the typical tripartite arrangement as in controls (Figure 5.9Bi). This observation was consistent with these

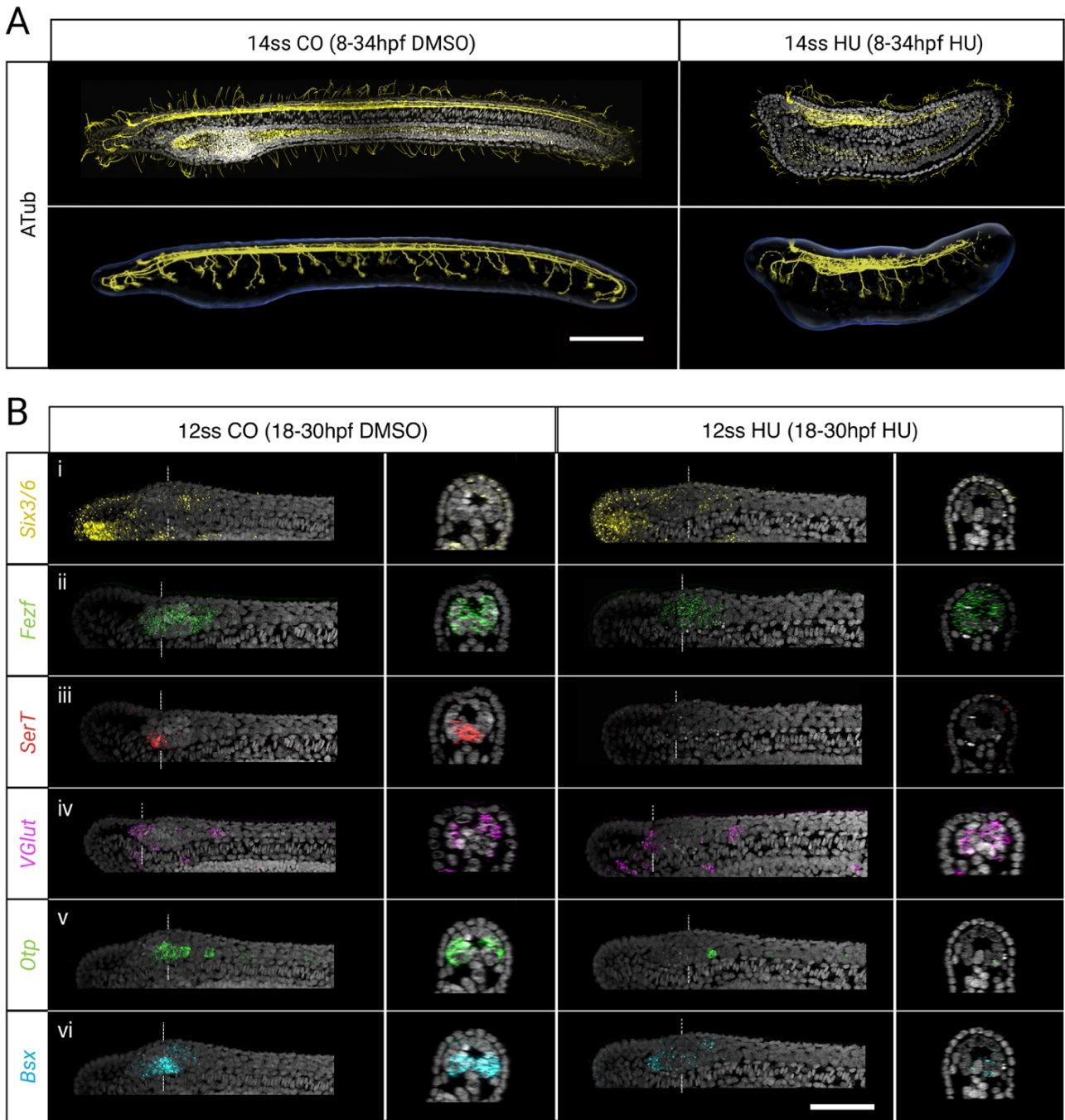


**Figure 5.9.** Inhibition of proliferation by treatment with hydroxyurea (HU) causes loss of brain cell types. **A.** Long HU treatment from gastrulation (G5) to early larval stage (14ss). Acetylated tubulin immunofluorescence highlights the cilia and nervous system in control and treated embryos. **B.** Change in the expression of transcription factors *Six3/6* (yellow), *Fezf* (green), *Otp* (green), *Bsx* (cyan) and neurotransmitter markers *VGlut* (magenta) and *SerT* (red) in embryos treated with HU from the 7ss to the 12ss stage analysed with *in situ* HCR. Scalebars are 50 $\mu$ m.

domains forming prior to axial elongation and before the anterior CV starts proliferating, at stages before HU was administered. In control embryos, the initially broad expression of *Fezf* started to disappear from the ventral intercalated *Six3/6*-negative region of the anterior CV at 12ss. This region corresponds to the hypothalamic-like area where most *Otp*-positive cells are located. When proliferation was inhibited with HU, the *Fezf* domain remained broad at both 12ss and 14ss (Figure 5.9Bii). The change in expression of *Fezf* suggests that while the broad regionalization of the brain remains the same, as shown by *Six3/6*, there might be a change in the maturation of brain cell types when proliferation is inhibited.

I therefore tested the expression of different CV cell type markers using a similar approach to the EdU pulse-chase. HU-treated embryos were devoid of the small cluster of row2 serotonergic neurons that contribute to the frontal eye complex. This suggests that localised proliferation is needed to generate this entire row of serotonergic neurons, as confirmed by the co-localization of EdU and *SerT* (Figure 5.9Biii). On the contrary, I did not see any differences on the expression of the glutamate transporter *VGlut*, which localised in the anterior *Six3/6*-positive domain and caudally to the posterior *Six3/6*-positive cluster in 12ss and 14ss embryos (Figure 5.9iv). I next focused on two hypothalamic markers *Otp* and *Bsx*. As described in paragraph 5.4.1, at 12ss *Otp* is expressed in two regions of the larval CV: in two prominent ventro-lateral clusters located in the intercalated *Six3/6*-negative region of the anterior CV and in a pair of ventro-medially located cells in the posterior *Six3/6*-positive region, at a post-infundibular level. In 12ss embryos treated at the 6ss stage, the ventro-lateral clusters of *Otp*-positive neurons in the intercalated *Six3/6*-negative pre-infundibular region were lost, while the posterior post-infundibular pair of *Otp*-positive cells was not affected (Figure 5.9Bv). As for *SerT*, this experiment, combined with the co-localization of *Otp* signal and EdU, indicates that a burst of proliferation between the 6 and 7ss stage is required for the formation of the full repertoire of hypothalamic cell types. Treated embryos raised to 14ss stage also lost the anterior clusters, but additionally had less cells in the post-infundibular ventro-medial cluster compared to controls, suggesting that proliferating cells in the posterior CV between 12ss and 14ss might be contributing to amplify the post-infundibular *Otp* cluster at these stages of development (Appendix VII, Figure A7.4). In 12ss larvae, *Bsx* is expressed in three domains in control embryos: in cells of the frontal eye located within the anterior *Six3/6*-positive domain; in a large cluster of medial and lateral cells in the hypothalamic intercalated *Six3/6*-negative region; and in dorsal and ventral cells of the posterior CV. Confirming the results obtained with *Otp*, treated embryos

specifically lost the hypothalamic *Bsx* cluster, while they maintained the expression in frontal eye cells and in the posterior CV (Figure 5.9Bvi). In summary, the inhibition of cell division during the formation of the CV demonstrated that precisely timed bursts of proliferation are necessary for the correct specification of brain cell types in amphioxus.

## 5.6 Amphioxus neuroarchitecture across the life cycle

Due to the difficulties in collecting and growing late larval stages, our knowledge on amphioxus metamorphosis and of the adult nervous system is much more fragmentary than for early development. As my description of neurogenesis and neurotransmitter expression showed that a conspicuous medio-dorsal portion of the early larval CNS remains undifferentiated (See section 5.2.1), I analysed the localization of neurotransmitters, neuropeptides and transcription factors in pre-metamorphic and adult specimens to obtain a more comprehensive characterization of the amphioxus nervous system.

### 5.6.1 The amphioxus nervous system at metamorphosis

Amphioxus larvae grow continuously throughout their life, requiring harsher permeabilization steps for the penetration of probes and antibodies, but their size is small enough that whole-mount imaging is still possible. Before metamorphosis, the neural tube and notochord have thickened, and the anterior CV has become more conspicuous (Figure 5.10A). Immunostaining for acetylated tubulin highlighted more than 50 pairs of dorsal nerve roots, and highly ciliated gill slits and gut (Figure 5.10A). To investigate the general architecture of the metamorphic nervous system I detected the expression of *SerT* for serotonergic neurons, *GAD67* for GABAergic neurons, *VGlut* for glutamatergic neurons, *VMAT* for monoaminergic (serotonin, dopamine) neurons and *ChAT* for cholinergic neurons (5.11B). On the ventral side of the CV, numerous serotonergic neurons expressing *SerT* and *VMAT* were found behind the cells of the frontal eye (5.11Bi-ii, vii). Low *VGlut* signal could be detected dorso-laterally and few GABAergic cells were visible on the dorsal roof of the vesicle (5.11Biii). On the posterior end of the anterior CV, above the infundibular organ, *VMAT*-positive cells were also present (5.11Bii). While serotonergic neurons were already present in the 1gs larva and increased in number towards metamorphosis, dorsal cells were not differentiated earlier and therefore represent new cell populations. Behind the infundibular organ the posterior CV

contained lateral GABAergic neurons expressing *GAD* and a prominent cluster of dorsal *VMAT*-positive cells that are likely dopaminergic based on studies on earlier developmental stages (336) (Figure 5.10Bii, iv, viii, ix). Ventrally, just posterior to infundibular cells, two small clusters of neurons with weak expression of *SerT* were also visible (Figure 5.10Bi, ix). More posteriorly, glutamatergic cells were positioned medio-laterally, and at a similar level were also the first ventral *ChAT*-positive neurons (Figure 5.10Biii, v). Along the trunk, the structure of the neural tube became more regular: GABAergic and glutamatergic neurons were concentrated on the dorsal and dorsolateral portions, while cholinergic cells occupied more ventral positions (Figure 5.10Biii, iv, v, x). Interestingly however, the relative proportions of *GAD*-positive and *VGlut*-positive neurons changed along the AP axis: in the anterior third of the larva GABAergic neurons were more abundant, while in the posterior half glutamatergic cells were more concentrated (Figure 5.10Bvi).

To my knowledge, this was the first attempt at a comprehensive characterization of nervous system architecture in pre-metamorphic amphioxus. I discovered that new cell types appear during larval development and that the nervous system acquires a more complex structure already before metamorphosis.

### 5.6.2 Cell populations in the adult brain

Having established the architecture of the nervous system before metamorphosis, I was then interested in understanding what happens to the brain in the adult stage. Due to their large size, the investigation of cell type diversity in the adult brain was carried out on vibratome sections. Part of this analysis was done in collaboration with another PhD student in our group, Michael Schwimmer (Department of Zoology, University of Cambridge). The positional identity of each section was determined by looking at the shape of the ventricular cavity and the presence of particular cell types. Sections were grouped in five types: the anterior vesicle, divided in two regions: one at the level of the neuropore with a circular ventricular shape in sections, and an adjacent one with a triangular ventricular shape in sections; the infundibular region, with a prominent ventral infundibular organ; the intercalated region, with a vertical dumbbell ventricular shape and the presence of dorsal Joseph cells; and the posterior neural tube, with a flattened elliptical ventricle shape (Figure 5.11Ai-v).

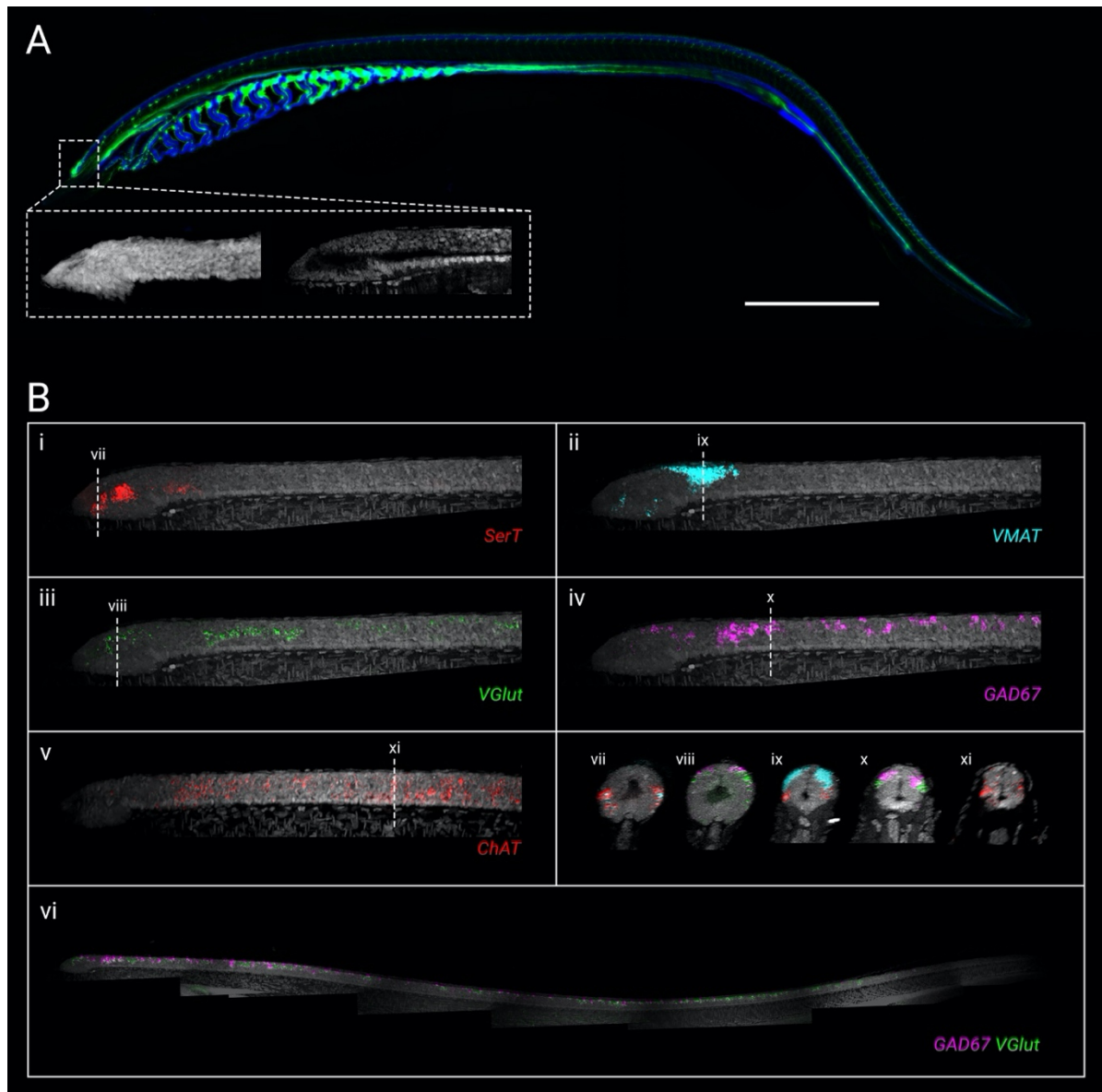


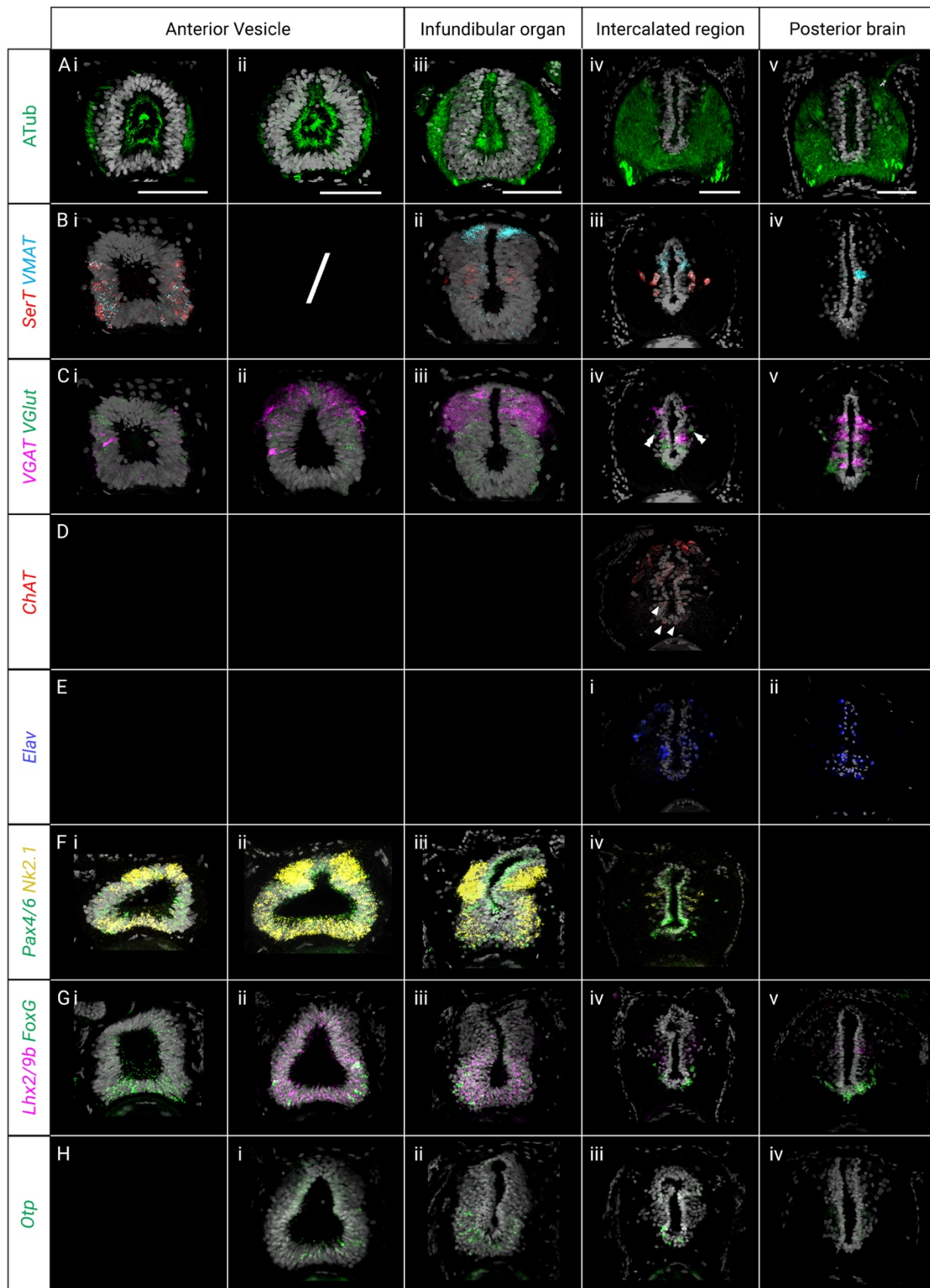
**Figure 5.10.** Characterization of the amphioxus pre-metamorphic nervous system. **A.** Distribution of acetylated tubulin immunoreactivity (green) in whole mount pre-metamorphic stages. The dashed inset shows the brain at pre-metamorphosis stained with DAPI. Scale bar is 150 $\mu$ m. **B.** Expression of neurotransmitter markers *SerT* (i, red), *VMAT* (ii, cyan), *VGlut* (iii, green), *GAD67* (iv, magenta) and *ChAT* (v, red) in the anterior nervous system, and co-expression of *GAD67* and *VGlut* throughout the neural tube (vi). Dashed lines indicate cross sections that are shown in vii-xi.

We first analysed the expression of neurotransmitter markers (*SerT*, *GAD67*, *VGlut*, *ChAT*, *VMAT*), similarly to what was shown above for metamorphic animals, with the help of Jemima Williams, an undergraduate student. A large number of serotonergic neurons could be seen associated with the frontal eye, forming two bilateral clusters that expressed *SerT* and *VMAT* (Figure 5.11Bi). Dorsal to these cells few glutamatergic neurons are also visible (Figure 5.11Ci). Behind this area, in the medial

portion of the anterior vesicle, GABAergic (*GAD*-positive) and glutamatergic (*VGlut*-positive) neurons were observed dorsally (Figure 5.11Cii). Around the infundibular organ, *GAD* transcripts were also concentrated across the dorsal half of the neural tube, while glutamatergic neurons could be found both dorsally, interspersed between GABAergic cells, and ventrally (Figure 5.11Ciii). Few *SerT*-positive cells were located mediolaterally, but these did not express *VMAT*: the latter was instead concentrated in neurons of the dorsal roof (Figure 5.11Bii).

In the intercalated region, the proportion of axonal projections in the CNS increases, and thick ventrolateral tracts are highlighted by acetylated tubulin staining. GABAergic neurons were distributed dorso-laterally while glutamatergic neurons were concentrated ventrally, in contrast with the dorsal accumulation found in the anterior vesicle (Figure 5.11Civ). *VMAT*-positive cells, likely dopaminergic neurons (106), were still concentrated dorsally, but a new population was also found at each side of the ventricular surface (Figure 5.11Biii). These cells strongly expressed both *SerT* and *VMAT* and likely represent the cluster of decussating serotonergic neurons previously identified in our lab (337). Curiously, a few of these cells also expressed *VGlut* (arrows in Figure 5.11Civ). At this level, the cholinergic marker *Chat* was detected in ventral neurons and in dorsal Joseph cells, confirming our previous investigation of *VAcHT* expression (106) (Figure 5.11D). Even more posteriorly, both GABAergic and glutamatergic neurons were found on the lateral walls of the ventricle, with *GAD* positivity neurons generally extending more dorsally than *VGlut* (Figure 5.11Cv). *VMAT* was not expressed dorsally anymore but instead was found in large scattered mediolateral cells (Figure 5.11Biv).

Along the intercalated region and the rest of the neural tube, neurotransmitter distribution indicated that many differentiated cells are not found in direct contact with the ventricular surface but are instead located slightly more basally within the tissue. This distribution seems to support the data on adult proliferation previously obtained by the lab and showing cell nuclei translocating to sub-ventricular positions after cell division (106). To further explore the pattern of neural maturation, I investigated the expression of *Elav* in posterior brain regions (Figure 5.11E). Intriguingly, many ventricular cells were not positive to *Elav*, suggesting that they might still be undifferentiated and proliferating. Conversely, adjacent cells in more basal positions and dorsal Joseph cells were highly expressing *Elav*, supporting the notion that indeed several amphioxus cell types translocate from ventricular to subventricular positions when differentiating, similar to vertebrates.



< **Figure 5.11.** Characterization of cell types in the adult brain. **A.** Vibratome sections at five levels (i-v) along the anteroposterior axis, identified by the shape that the ventricular cavity assumes in sections and by the pattern of acetylated tubulin (green). **B-H.** Cell types are detected with *in situ* HCR for *SerT* (red), *VMAT* (cyan), *VGAT* (magenta), *VGlut* (green), *ChAT* (red), *Elav* (blue), *Pax4/6* (green), *Nk2.1* (yellow), *FoxG* (green), *Lhx2/9b* (magenta) and *Otp* (green). White slashes imply that transcripts were not detected while blank fields indicate that the expression has not been investigated in the corresponding section. Scale bars are 50µm.

To complement the analysis of the amphioxus brain neuroarchitecture, I further described the distribution of selected transcription factors. At the level of the frontal eye, *Pax4/6* and *FoxG1* were expressed across the AP and DV axes, though the latter was more concentrated in ventral positions (Figure 5.11Fi, Gi), while *Nk2.1* formed two clusters located ventrally and dorsally (Figure 5.11Fi). In medial sections the pattern of *Pax4/6* and *Nk2.1* remained similar, though the dorsal *Nk2.1*-positive domains was now clearly split in two dorsolateral populations (Figure 5.11Fii, Gii). At this level, ventral cells also expressed *FoxG1* (only low signal could be detected dorsally) and the hypothalamic marker *Otp* (Figure 5.11Gii, Hi). Moreover, most cells were *Lhx2/9b*-positive (Figure 5.11Gii). In the infundibular region, *Pax4/6* was expressed in the ventricular surface and in ventral cells, in a region where *FoxG1*, *Otp* and *Lhx2/9b* expression was also concentrated (Figure 5.11Fiii, Giii, Hii). Dorsal *Nk2.1* was still separated in two domains at each side of the roof (suggesting that dorsal *VMAT*-positive cells were *Nk2.1*-negative) (Figure 5.11Fiii). In the intercalated region, *Pax4/6* transcripts were found in the ventricular surface, suggesting that at this level it may label progenitor cells, and in scattered subventricular cells (Figure 5.11Fiv). The expression of *FoxG1* and *Otp* remained ventral, while *Nk2.1* and *Lhx2/9b* were detected in mediolateral cells (Figure 5.11Fiv, Giv, Hiii). This expression pattern remained similar in more posterior sections (Figure 5.11Gv, Hiv).

The use of HCRs allowed me to explore cell type distribution in the amphioxus brain but gave limited information on the pattern of connectivity between these neurons. We therefore tried to optimise a protocol for whole brain immunohistochemistry to investigate further adult neural complexity. Anesthetised animals were manually dissected using forceps to remove skin, gut and part of the muscles. The inner layer of muscles and the notochord are tightly attached to the neural tube and so are difficult to remove without damaging the brain. For this reason, we fixed these three

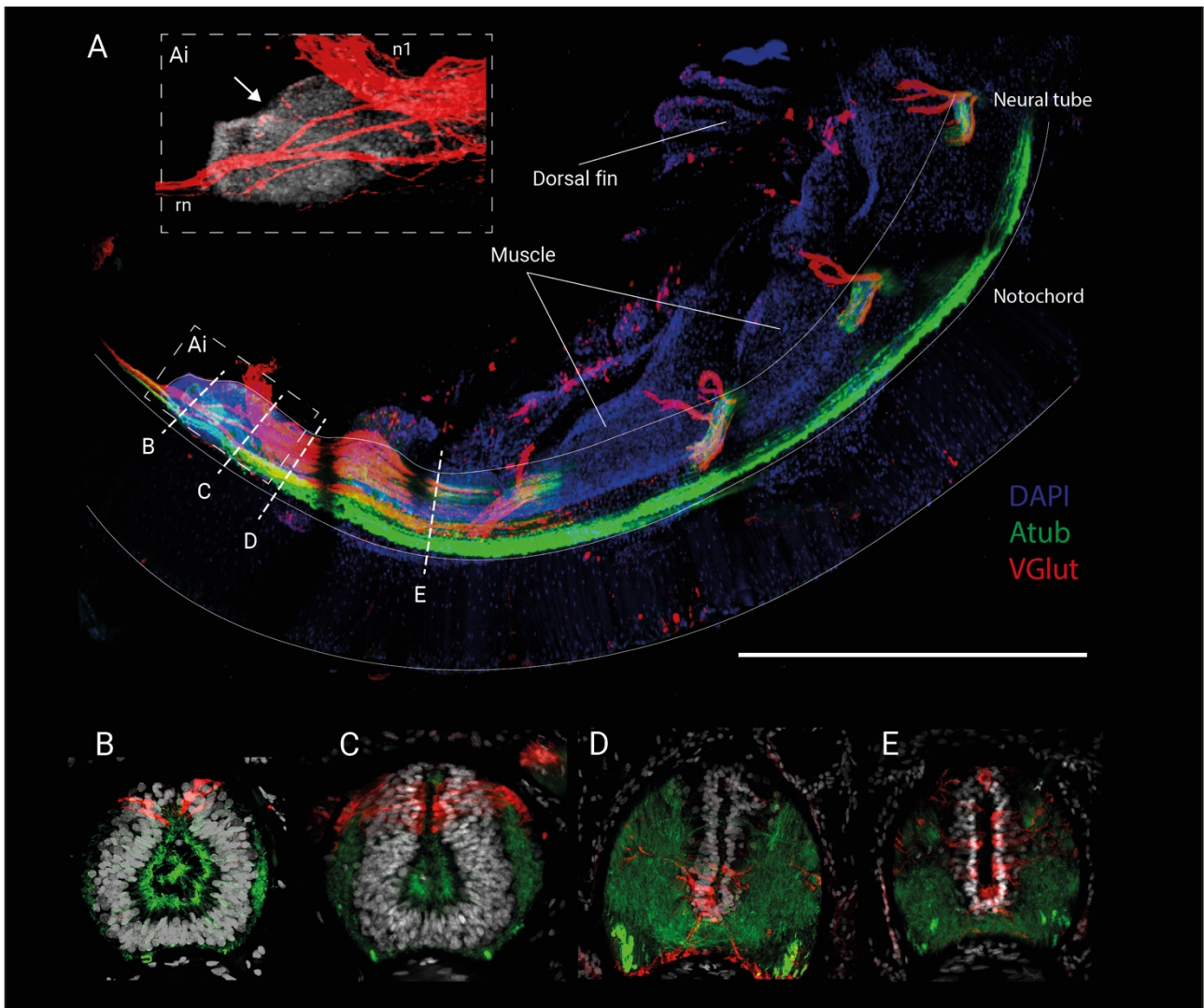


**Figure 5.12.** Distribution of glutamate immunoreactivity in the adult brain. **A.** Whole mount immunohistochemistry for glutamate (red) and acetylated tubulin (green). Inset (Ai) in dashed box shows a magnification of the brain indicating cell bodies of the *pars anterodorsalis* (arrow). Fibers are seen projecting to the radial nerves (rn) and coming into the nervous system from the nerve roots (n1). Scalebar is 0.5mm. DAPI staining is shown in blue in the main panel and in grey in magnification. **B-E.** Vibratome sections at the levels indicated in A showing glutamatergic cell bodies and projections. The neuropil is visualized with acetylated tubulin.

tissues together and started to optimize an immunofluorescence protocol with long PK permeabilization using antibodies against acetylated tubulin and glutamate (Figure 5.12A). The results on whole-mounts were then compared with the same immunofluorescence carried out in vibratome sections (Figure 5.12B-E). In the brain, the antibody strongly labelled anterior neural projections in the brain that extend to the frontal nerves and run mediolaterally towards the

intercalated region (Figure 5.12A-Ai). We also saw the dorsal glutamatergic neurons of the anterior vesicle and infundibular region (Figure 5.12Ai), which could be clearly visualized in sections (Figure 5.12B-C), though the current resolution did not permit following their projections. More posteriorly, strongly labelled axons were seen dorsolaterally in both whole brains and sections (Figure 5.12A, D, E). The sections further show that, consistent with the results of *VGlut* expression, glutamatergic neurons in the anterior intercalated regions are found ventrally (Figure 5.12D) while more posteriorly they are scattered along ventricular and subventricular cells (Figure 5.12E).

### 5.6.3 Distribution of neuropeptides across the amphioxus life cycle

The complex distribution of brain cell types in larvae and adults prompted me to examine neuropeptide signalling by combining RNAseq and expression data. Neuropeptides are a large and ancient family of small signalling molecules that have prominent roles in animal physiology and behaviour. They are excellent candidates to explore cell type diversity as they are often co-expressed in neurons in complex combinations alongside neurotransmitters, acting as neuromodulators or as paracrine signals. Previously, the neuropeptide repertoire of the amphioxus *B. floridae* was recovered from transcriptomic data (338). I used this dataset to recover the sequence of 24 orthologous neuropeptides in *B. lanceolatum*. I first looked at the level of neuropeptide expression across development by querying the dataset generated by our lab on embryos raised at 21°C (Figure 5.13Ai). Most neuropeptides start to be expressed in the early larval stages and are highly active in the pre-metamorphic phase. For adults, I exploited the dataset on expression in different organs produced by Marlétaz and collaborators (79) and showed that the majority of these neuropeptide precursors are concentrated in the nervous system, and to a lesser extent in the gut (Figure 5.13Aii). Finally, our group had previously obtained bulk RNAseq data comparing the amphioxus head with the rest of the body. The dataset was processed by Ashley Sawle, and I used it to test the differences in neuropeptide expression along the body (Figure 5.13Aiii). Many neuropeptides were enriched in the head: of those highly expressed in the nervous system, *CTFP1*, orexigenic-type, *PDTPD*, RFamide types 2 and 5, secretogranin-type, orexin-type, *TPH2*, *Vt* and *CART*-peptide-type precursors were all upregulated anteriorly. On the other hand, the *GFP*amide-type, *PLDPIR*amide and glycoprotein hormone-type precursors, which were enriched in the gut, were upregulated in the posterior half of the body, suggesting a role in the digestive system.

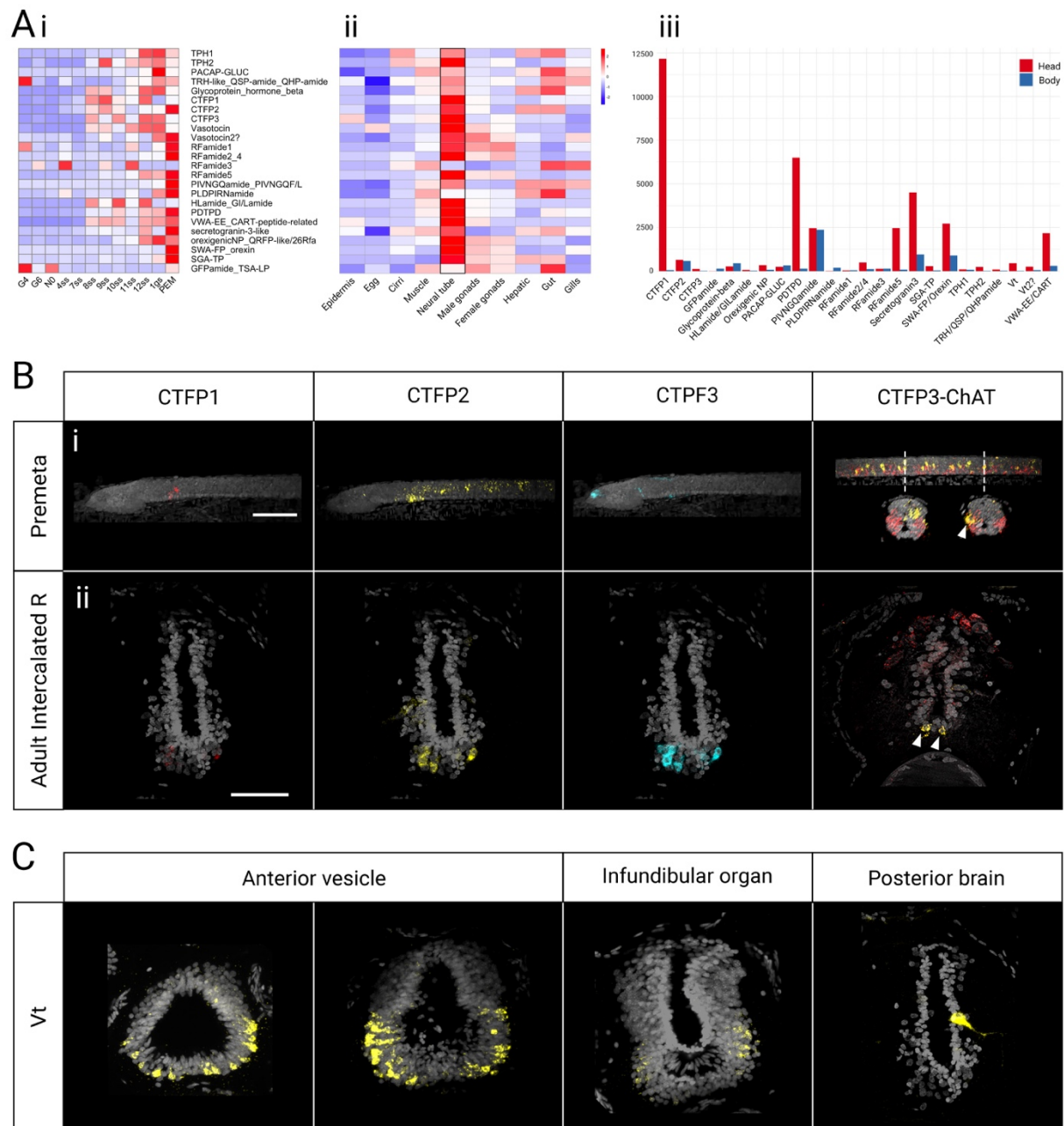


**Figure 5.13.** Distribution of neuropeptides in the amphioxus life cycle. **A.** Analysis of neuropeptide expression with RNAseq. Graphs refer to our datasets across development (i), to a published dataset of adult tissues (79) (ii), and to our dataset comparing the head with the rest of the body (iii). **B.** Expression of calcitonin family neuropeptide (CTFPs) precursors in pre-metamorphic (i) and adult (ii) stages. In both stages a proportion of *CTFP2* cells (yellow) is co-expressed with *ChAT* (red) (arrowheads). **C.** Expression of vasopressin-oxytocin neuropeptide (*Vt*) precursor in the adult nervous system. Scalebar is 50 $\mu$ m.

Having discovered an accumulation of neuropeptides within the nervous system, I next considered the spatial expression in pre-metamorphic and adult animals of four neuropeptide precursors belonging to two classes: the three paralogs of calcitonin-type neuropeptides, *CTFP1*, *CTFP2* and *CTFP3*, and the vasopressin-oxytocin-type neuropeptide *Vt* (Figure 5.13B-C). Before metamorphosis (Figure 5.13Bi), *CTFP2* was broadly expressed in the anterior neural tube: in the posterior CV, *CTFP2* was co-expressed with *ChAT* in the most anterior motoneurons, likely belonging to the primary motor centre. The other two calcitonin paralogs were also expressed in this region, though not in the same cells. More posteriorly in the neural tube, *CTFP2* was expressed in ventrolateral and mediolateral neurons: most of these cells were cholinergic, but some of the more dorsal *CTFP2*-positive neurons had a different identity as they did not express *ChAT*. In the adult, *CTFP2* was still co-expressed with *ChAT* in ventral cells of the intercalated region, together with the other two paralogs *CTFP1* and *CTFP3*, indicating that these ventral cholinergic neurons express a mix of calcitonin-type peptides (Figure 5.13Bii). However, mediolaterally some cells expressed exclusively *CTFP2*. Given its broad expression in cholinergic cells of the hindbrain in early larval stages, and the fact that in adults it seems to be expressed across the AP axis, I speculate that in pre-metamorphic and adult animals *CTFP2* is found across the neural tube in ventral populations. Contrary to pre-metamorphic stages, in adults the anterior vesicle had a large cluster of ventral *Vt*-positive cells, located in the area where *Otp* and *FoxG1* were also highly expressed (Figure 5.13C). Conversely, in the intercalated region only scattered cells expressed *Vt*.

In summary, the reconstruction of cell types revealed an increasingly complex and diverse nervous system forming in late stages of the amphioxus life cycle, including the formation of new populations on the dorsal side of the brain and the increase in neuropeptidergic signalling.

## 5.7 Discussion

### 5.7.1 Differences in neurogenesis and proliferation underlie the regionalization of the amphioxus neural tube

One of the primary aims of this chapter was to characterize the development of cell type diversity in the amphioxus CNS, with a focus on the formation of the brain. The rationale behind this goal is that taking into account developmental origin, patterning, cell type composition and morphogenesis

can help tracing the evolution of particular traits and comparing distantly related species. This in turn is crucial to define common features as well as characters that evolved secondarily in each lineage. Previous studies demonstrated substantial differences in cellular morphology and gene expression along the amphioxus neural tube, despite its morphological simplicity (85, 87). However, the developmental basis of this regionalization is poorly understood. Combining the data on the expression of neurogenic markers and the pattern of proliferation across embryonic development, the general principles that guide this regionalization start to emerge (Figure 5.14).

Based on my results, the neural tube can be divided into four domains: anterior CV, posterior CV, hindbrain region and spinal cord region. The pre-infundibular anterior CV, which includes the anterior *Six3/6*-positive domain and the intercalated *Six3/6*-negative region, has a peculiar pattern of neurogenesis and proliferation that is very different from the rest of the neural tube. All three neurogenic markers considered (*SoxB1*, *Ngn* and *Elav*) are expressed very early at gastrula stages, but *Ngn* and *Elav* are quickly downregulated during neurulation. Moreover, from the 6ss stage progenitors start to proliferate specifically in this area. Cell division occurs in a ventral-to-dorsal direction, thereby contributing to different areas of the brain at distinct time points in development. In particular, the first burst of division in ventral cells give rise to neural populations in the retinal and hypothalamic regions of the larval brain, including serotonergic neurons of the frontal eye and *Otp*-positive neurons of the hypothalamus. In these regions, proliferation is required to contribute with new cells at specific times and sites to be fated to particular types. On the other hand, glutamatergic neurons of the frontal eye are born at gastrulation, independently from the proliferation seen during neurulation, showing that the anterior CV in the larva is composed of a mix of gastrulation- and neurulation-derived cells. The posterior CV starts from the infundibular organ and include the posterior *Six3/6*-positive domain, although it reaches more caudally than previously hypothesized, up to the first somitic boundary (87). The posterior limit corresponds to the *Otx-Gbx* boundary at the 7ss stage, although later in development this boundary is not as clearly defined. Interestingly, the expression of neurogenic markers in this region is indistinguishable from the more caudal hindbrain (see below), further suggesting that the development of the anterior CV is controlled by different mechanisms than the rest of the neural tube. However, cells in the posterior CV starts to proliferate before those of the hindbrain from the 12ss stage, likely to expand the number of cell types as demonstrated by the increase in posterior *Otp* cells.

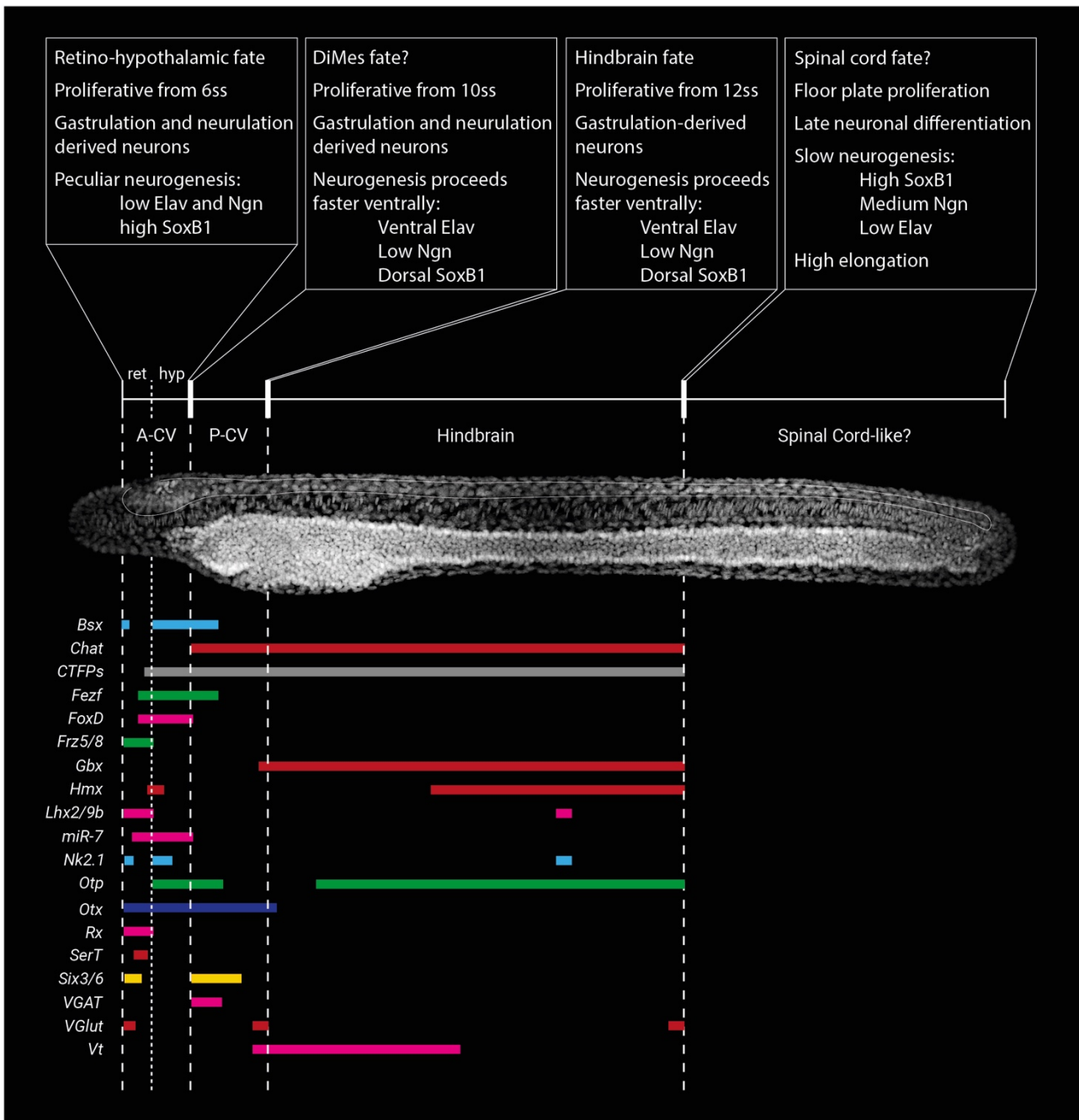


**Figure 5.14.** Comprehensive view of central nervous system regionalization in amphioxus early larvae based on gene expression, cell type identity, neurogenesis progression and proliferation pattern. The neural tube is divided into an anterior cerebral vesicle (A-CV), comprising retinal (ret) and hypothalamic (hyp) derivatives, posterior cerebral vesicle (P-CV), hindbrain-like and spinal cord-like regions.

The hindbrain region spans from the second to the sixth somite pair. Here, the progression of neurogenesis across neurulation is very dynamic. The floor plate is specified quite early, as shown by *Nk2.1* expression and by the loss of *Ngn* expression. Moreover, ventro-lateral cells differentiate early, turning off *SoxB1* and *Ngn* and expressing high levels of *Elav*. *Elav*-positive progenitors are not all positioned ventrally at the 7ss stage, when they are also found dorsolaterally at the level of the somite boundaries. At later stages these cells progressively occupy more ventral positions and differentiate into a surprising variety of cell types. The absence of proliferation in this area during neurulation indicates that, with the elongation of the neural tube, the precursors of ventrolateral neurons, which are initially distributed along the DV axis, reach their final position as they are differentiating. This also means that all larval neurons in the hindbrain are gastrulation-derived. Previous studies have shown that retinoic acid is responsible for the regionalization of the trunk neural tube, controlling the expression of *Hox* genes similarly to vertebrates (240). Given the exceptional variety and low number of neurons in the amphioxus hindbrain, I speculate that the precise specification of such a complex mix of cell types is controlled by paracrine or cell-to-cell interactions. This might be driven by Notch signalling, which is involved in hindbrain regionalization in vertebrates (339, 340). Starting from this characterization, future work could explore how the composition of the hindbrain changes when these signalling pathways are experimentally manipulated. Interestingly, proliferation in the trunk neural tube at 14ss occurs specifically in floor plate and medio-lateral cells. Both cell types have recently been described as having a glial-like molecular signature in the early larva (299). Bozzo and collaborators speculate that proliferation of medio-lateral cells expressing the glial marker EAAT2 results in the formation of ependymal and ependymogial cells in late larva stages (341). My results provide experimental support for this hypothesis: while ventro-lateral cells already express neural markers, such as neurotransmitter synthesis and transport proteins (221) and member of the adenosine deaminase acting on RNA (ADAR) family with functions in RNA-editing (317), medio-lateral cells are still dividing at the beginning of the larval stage and could therefore represent progenitors that maintain a glial signature and have a supporting role in the larval neural tube.

Posterior to the sixth somite is the spinal cord-like region, where the cell type composition of the neural tube changes abruptly and few neurotransmitter genes are expressed. This distinction is reflected by the specific types of neurogenesis and morphogenesis. While the early marker *SoxB1c* transcripts are localized posteriorly from the gastrula stage, *Ngn* and *Elav* only start to be expressed

at larval life, indicating that this region remains undifferentiated during neurulation. However, floor plate cells in this posterior domain are proliferating throughout neurulation and contributing to the elongation of the neural tube. Interestingly, during his PhD project Toby Andrews (Francis Crick Institute) showed that the posterior neural tube is thinner than the hindbrain region due to a more prominent convergent-extension process (84). Overall, the behaviour of cells in the spinal cord region is consistent with an initial role in the axial elongation of the body, and only secondarily in differentiation of similar cell types as the hindbrain, as shown here in pre-metamorphic embryos.

The pattern of cell division we describe in amphioxus differs from what is seen in the vertebrate CNS in that the neuroectoderm of vertebrates proliferates extensively throughout its development. Early neural progenitors (neuroepithelial and radial glial cells) are known to undergo symmetrical divisions across the anteroposterior length of the neural plate and early neural tube (330, 332, 342). These divisions are used to expand the repertoire of stem cells that will later give rise to neurons and glia (330, 334). In fact, the rate of proliferation of these cells directly affects the size and regionalisation of adult mammalian brains. For example, disruption of early signalling (e.g., FGF and Wnt/Bcatenin) controlling neural tube proliferation in mammals deeply affects the size, thickness and convolution of the cortex (343, 344). In contrast, in ascidians cells have been observed proliferating in the larval sensory vesicle and, to a lesser extent, in the visceral ganglion, thereby resembling more closely the anterior proliferation we observed in amphioxus. However, proliferation is absent posteriorly in the ascidian neural tube, indicating that neural morphology in these animals is primarily driven by cell re-arrangement and cell shape change (345, 346). This diversity of proliferative strategies in the different chordate subphyla supports the idea that tweaks in the timing and magnitude of cell division have played important roles in the emergence of neural complexity during chordate evolution.

### 5.7.2 Retino-hypothalamic fate of the amphioxus ANE

The second theme of this chapter was the characterization of the cell type repertoire of the amphioxus brain to follow the fate of the ANE identified in Chapter III. Previous analysis of gene expression during amphioxus neurulation was used to describe the different regions of the amphioxus neural plate. In particular, a recent work by Albuixech-Crespo and collaborators studied the expression of 48 genes by chromogenic *in situ* hybridization in the mid-neurula stage and

interpreted the results in the anatomical context of the prosomeric model, which describes the subdivisions of the vertebrate brain during development (87). The authors divide the brain into two sections: an archencephalic protagma, which includes a rostral hypothalamus-prethalamus primordium and a di-mesencephalic region; and a deuteroencephalic protagma that includes rhombencephalon-like and spinal cord-like regions. However, this study has three limitations in establishing homology between the amphioxus and vertebrate brain regions: first, considering a single developmental stage does not take into account the variation that occurs during development; second, the work focuses on the early patterning of the neuroectoderm but does not investigate which cell types differentiate within each domain; third, the use of chromogenic *in situ* hybridization limits the co-expression analysis and the precise definition of boundaries between different brain regions.

My results refine the early subdivisions of the neural tube by looking at the co-expression of multiple genes across development and outline the cell type repertoire of the larval brain. The frontal eye complex had already been described in previous work using antibody staining and *in situ* hybridization (293, 294), showing that the five rows of cells originally identified by electron microscopy (290, 296) correspond to cells resembling those found in the vertebrate retina. I have further characterized the gene expression in each of the cell types and showed that the “row” organization is acquired well into larval life, while in early larva stages these cells are less regularly distributed. The identity of preinfundibular cells has not been considered in detail. My analysis clearly shows that this region has a hypothalamic signature. The vertebrate hypothalamus is specified within the secondary prosencephalon and is composed of several nuclei that can be identified by the combinatorial expression of different markers (69, 232, 321). Each nucleus will produce neurons expressing a different combination of neurotransmitters and neuropeptides (212, 322). *Otp* and *Bsx* are strongly expressed in the hypothalamus. *Otp* is involved in the development of the paraventricular, supraoptic and arcuate nuclei and the lateral and perimammillary areas, while *Bsx* is expressed in the mammillary body and, together with *Otp* and *Hmx*, in the arcuate nucleus (212, 320–322, 347). In amphioxus, these genes are all expressed in different combinations in preinfundibular cells. It is interesting that I found different combinations of *Bsx*-positive (medial) *Otp*-*Bsx* double-positive (lateral), *Hmx*-positive and rare *Hmx*-*Otp* double-positive neurons in the ventral portion of the CV that expresses miR-7, a known marker of neurosecretory brain areas (348, 349). Strikingly, cells in the same region were found to dynamically express calcitonin-type

neuropeptides (CTFPs). Vasotocin, a precursor of the vasopressin/oxytocin-type neuropeptides expressed in the supraoptic and paraventricular nuclei in vertebrates (212), is instead found in the ventral CV only in the adult, in the same area where *Otp* is expressed. This suggests that the hypothalamic-like region might acquire its full cell type repertoire only in the adult stage, like the telencephalic-like region. The amphioxus hypothalamic region is continuous with the eye field, as has been described in fish, axolotl, frogs, and chicken (350), strongly suggesting that the organization of the secondary prosencephalon might be an ancestral feature of chordate development.

Overall, these results indicate that the ANE, in which the aGRN is active, develops into the retino-hypothalamic area of the amphioxus brain. The analysis of proliferation further confirms this hypothesis. The anterior cells that proliferate at the 6-7ss stage are located in the anterior *Six3/6*-positive and intercalated *Six3/6*-negative domain, which were shown in Chapter III to be the areas where aGRN genes are expressed at this stage. Thanks to the pulse-chase approach, I was able to follow the fate of these cells and demonstrate that they form both serotonergic cells and *Otp*-positive hypothalamic cells. Additionally, the hypothalamic markers that are already expressed at 7ss (*Bsx*, *CTFP1* and *CTFP2*) are downregulated following Wnt overactivation (Appendix VII, Figure 7.3). The fate of the ANE is particularly interesting as the AO is considered to have a dual sensory-neurosecretory function. As the retina and hypothalamus are respectively the main sensory and neurosecretory areas of the vertebrate brain, these results point to the conservation of ANE function in deuterostomes.

### 5.7.3 The adult brain

The vast majority of our knowledge on amphioxus biology is limited to embryological and early larval stages. On one hand, this is due to the fact that cephalochordates are mostly used in evodevo studies, which are focused on the comparison of development. Furthermore, amphioxus have a long larval period (up to several months in *B. lanceolatum*) and are difficult to grow and keep in culture, such that only recently they have started to be kept permanently in laboratories (99). During metamorphosis, highly asymmetric structures in the amphioxus larva, such as the mouth, gills and endostyle, shift in position so that the adult body becomes more symmetric. This process is regulated by a thyroid hormone receptor suggesting the homology of chordate metamorphosis (351). The composition of the nervous system at metamorphosis and in the adult remains poorly understood.

However, previous work by Dr Elia Benito-Gutiérrez showed that the nervous system continues to proliferate and grow during late larval development and metamorphosis (337). In the adult, mitotic neurons can be observed at the ventricular surface, and post-mitotic neurons can be seen migrating basally to sub-ventricular areas, suggesting that new neurons are born and mature in a process similar to the vertebrate CNS. Furthermore, the dorsal portion of the anterior vesicle in adults expressed a set of telencephalic genes, including *FoxG1*, *EmxA*, *Lhx2/9*, and *Pax4/6*, which are not present in early larval stages. This suggested that a new telencephalic-like domain, defined as *pars anterodorsalis* (PAD), appears after metamorphosis (106). My characterization of the adult neural tube showed a dorsal accumulation of glutamatergic and GABAergic neurons that is specific to the anterior vesicle, where the telencephalic genes are expressed. Notably, in vertebrates the two portions of the telencephalon, pallium and subpallium, predominantly form glutamatergic and GABAergic neurons respectively (352, 353). The neurotransmitter distribution therefore provides further support to the telencephalic nature of the PAD. Moreover, although in low amount, anterodorsal glutamatergic and GABAergic neurons could be detected already at the pre-metamorphic stage, suggesting that the formation of this structure might begin to form before the adult stage. The protracted development and growth of the brain is not unique of amphioxus, but in vertebrates the telencephalon is specified relatively early in development (though there are some differences in timing between vertebrate taxa (354)). The pronounced difference in developmental timing between the vertebrate telencephalon and the amphioxus PAD suggests that a telencephalon-like region was present in the chordate ancestor, but the timing of its specification changed in different lineages through heterochrony (106, 304).

The analysis of the rest of the CNS also showed the progressive growth and maturation of the amphioxus neural tube. Cholinergic neurons are expressed ventrally in pre-metamorphic stages, similarly to their localization in early larval stages, indicating that the ventral portion of the neural tube contains the majority of motoneurons (221, 297). On the other hand, glutamatergic and GABAergic neurons are found only in few cells in the early larval neural tube, but their number increases drastically in later stages. In pre-metamorphic larvae, *VGlut* and *GAD* are distributed across the entire CNS behind the brain in dorsolateral positions and are also found in similar positions in the adult intercalated region. The developmental origin of these late developing neurons is still unclear. Their position however suggests that they might derive from the dorsal portion of the larval neural tube, which is still undifferentiated at the 1gs stage (299). Interestingly, mediolateral

cells are proliferating at the beginning of larval life, meaning that they could give rise to novel cell populations that differentiate at late stages. A recent study has reported the detailed distribution of neurotransmitters in the zebrafish spinal cord, showing that cholinergic neurons are entirely located on the ventral side, while GABAergic and glutamatergic cells are more broadly distributed and reach the dorsal portion of the neural tube (355). The distribution of neurons in the amphioxus neural tube closely resembles the one observed in the vertebrate spinal cord and likely dates back to the chordate ancestor. The DV distribution of CNS neurons in vertebrates is known to be controlled by Bmp and Shh signalling coming from the roof and floor plates of the neural tube respectively (356). It would be interesting to check whether a similar mechanism is present in amphioxus, as suggested for example by the dorsal expression of *Zic*. The same study in zebrafish also identified several neurons that co-express more than one neurotransmitter. While extensive co-detection was not found in amphioxus in the present analysis, we did observe serotonergic and glutamatergic double-positive neurons, suggesting that the complex use of multiple transmission modalities predates the origin of vertebrates. Similarly, the analysis of neuropeptide expression showed a close association between calcitonin and cholinergic neurons. Future studies could be aimed at investigating the expression and function of these neuropeptides in amphioxus neurophysiology.

#### 5.7.4 Conclusions

In this chapter I have provided a detailed description of nervous system development, composition and morphogenesis throughout its life cycle. The analysis started from the goal of understanding the fate of cells in which the aGRN is active, but during my PhD extended to cover more general aspects of amphioxus neurobiology.

- ◆ I show that the ANE of amphioxus comprises retino-hypothalamic cell populations that differentiate at the beginning of larval life from neurons born during neurulation. This supports a conserved role for the aGRN in the specification of anterior sensory-neurosecretory areas of the CNS.
- ◆ I also describe the unexpected complexity of the amphioxus hindbrain-like region, that develops during late phases of neurulation in the absence of proliferation and is characterized by a high diversity of cell types in low number. Conversely, the posterior spinal cord displays a different pattern of neurogenesis and differentiates only in late larval stages.

- ◆ The amphioxus CNS continues to develop during the extended larval period and at metamorphosis is composed of different cell types distributed across the DV axis similarly to vertebrates. In the adult, the hypothalamic region observed in the larva is still detectable, and dorsally a telencephalic-like region, the *pars anterodorsalis*, accumulates GABAergic and glutamatergic neurons.

Details on the developmental control of the cell type diversity highlighted in this study are still unclear and will hopefully be investigated in future studies. Moreover, the late development of amphioxus is still drastically understudied and could hold unexpected surprises, as for the late appearance of a telencephalon-like region (106) or the presence of pharyngeal calcitonin (Appendix III). Finally, the characterization of cell types in amphioxus will provide an excellent comparative tool to reconstruct the composition of the ancestral vertebrate brain.

# Chapter VI – The aGRN in vertebrates and the evolution of the vertebrate brain

## 6.1 Introduction

The data presented here indicate that the aGRN was conserved during chordate evolution and is still active in cephalochordates to specify the ANE. I have also shown that the amphioxus ANE develops into retino-hypothalamic-like areas of the larval and adult brain that are homologous to the vertebrate secondary prosencephalon. The analysis of the scRNAseq dataset of zebrafish development (see Chapter III) revealed the vertebrate secondary prosencephalon is precisely the area in which most aGRN orthologs are expressed, with the exception of *FoxQ2*. In addition, previous work on *Saccoglossus* development demonstrated that the molecular regionalization of the hemichordate nervous system (which forms a diffuse epidermal plexus) corresponds to the AP divisions of the vertebrate CNS (92, 161). Taken together, these results suggest the homology of the ANE across deuterostomes. However, it remains to be understood how the vertebrate CNS evolved from the chordate ancestor. In ambulacrarians, the aGRN acts from early development on the animal side of the embryo, defining an apical plate within which the ANE is specified (92, 146, 147, 160). Similarly, in amphioxus the network is active before the appearance of the neuroectoderm. As the neural plate is specified, the anterior portion forms under the influence of the aGRN and acquires an ANE signature. Conversely, in vertebrates most aGRN genes start to be expressed within the neuroectoderm once it has been specified, and there is no distinction between early and late phases of the network (see Chapter III). This key difference raises several questions: if the aGRN was active from early development in the chordate ancestor, what happened during vertebrate evolution? Was the early portion of the network lost in vertebrates? And if so, how was the aGRN integrated in the formation of the vertebrate neural plate?

### 6.1.1 Aims of the chapter:

In this chapter I elaborate testable hypotheses to start approaching these questions. I use amphioxus, zebrafish (*Danio rerio*) and the African clawed frog (*Xenopus laevis*) to analyse the evolution of vertebrate CNS specification, focusing on two distinct aspects of this vast subject. I first explore the

evolution of *FoxQ2* genes in chordates to understand how the loss of early *FoxQ2* expression in vertebrates have impacted the specification of the ANE. I then investigate the role of the vertebrate organizer and the localization of Bmp signalling in chordates to test the link between the formation of the body axes and the specification of the nervous system.

## 6.2 What does the FoxQ2 say? Conservation of a highly dynamic and poorly known gene

FoxQ2 is a member of the highly conserved Forkhead-box (FOX) family of transcription factors. FOX proteins are divided into ~26 classes (named with letters from A to S) that share the presence of a forkhead or winged-helix DNA-binding domain and are involved in virtually all developmental processes (357–359). The forkhead motif is highly conserved in metazoans, but each class can be recognized by small differences within and outside of the domain. The FoxQ2 class was actually discovered in amphioxus as belonging to a separate class from *FoxQ1* genes (215). From there, *FoxQ2* orthologs have been found in most Eumetazoan groups studied to date, including cnidarians (203, 360), protostomes (97, 361) and deuterostomes (146). Recent studies have further highlighted a complex evolutionary history of this class, including several independent duplications or losses, and have suggested a possible early split of this class into two families called *FoxQ2* and *FoxQD* (the latter with a C-terminal eh1-like motif) (159, 359). Among invertebrate deuterostomes, the hemichordate *Saccoglossus kowalevskii* has three (one possibly a *FoxQD* member), the echinoderm *Hemicentrotus pulcherrimus* has two and amphioxus has three (one possibly a *FoxQD* member) *FoxQ2* paralogs (159, 362). In spiralian the number of *FoxQ2* genes is even more variable, with the annelid *Owenia fusiformis* holding the record of 11 *FoxQ2* paralogs (359, 361). Despite this dynamic evolution, the analysis of *FoxQ2* expression revealed an astonishing conservation in the localization of this gene in the anterior (aboral for cnidarians) portion of the body and in the ANE during early development (97, 146, 148) (see Chapter III, section 3.1.3).

### 6.2.1 Phylogenetic analysis of *FoxQ2* genes

Compared to the results that have been gathered recently on several invertebrate groups, little is known about *FoxQ2* in vertebrates. It was initially thought that this class was lost in vertebrates, as *FoxQ2* was not found in the human and mouse genome, but more recently convincing orthologs

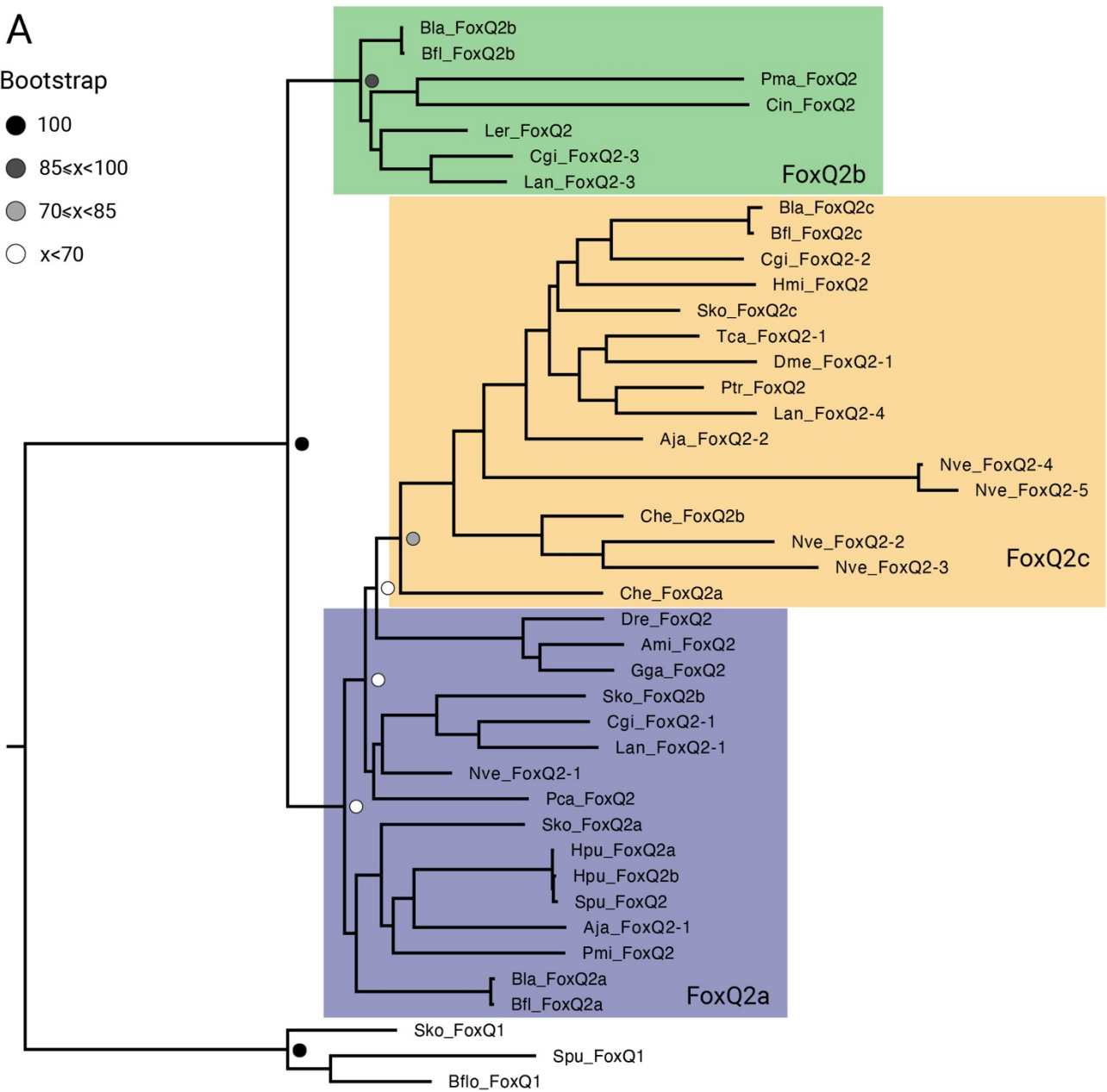
were discovered in teleosts, reptiles and likely in monotremes (213). To expand the panel of chordate *FoxQ2* orthologs, I BLAST-searched the genome of the ascidian *Ciona intestinalis* (Tunicata), the lamprey *Petromizon marinus* (Vertebrata, Cyclostomi), the skate *Leucoraja erinacea* (Vertebrata, Chondrichthyes) and the chicken *Gallus gallus* (Vertebrata, Sauropsida) using zebrafish, amphioxus and hemichordate *FoxQ2* sequences. I detected a single copy of *FoxQ2* in each organism and confirmed that each gene contained the FoxQ2 domain (using NCBI conserved domain search), suggesting that this family is conserved in vertebrates and only lost in the lineage leading to placental mammals and likely in amphibians. Combining the newly discovered sequences with other eumetazoan *FoxQ2* I performed phylogenetic analysis to reconstruct the evolutionary history of this family (Figure 6.1A). I aligned the sequences using muscle and constructed phylogenetic trees using both Maximum Likelihood (IQTree (363)) (Figure 6.1A) and Neighbour Joining (SeaView (364)) (Appendix VIII, Figure A8.1) methods, using *FoxQ1* as outgroup. The analysis revealed the complex relationships among the different *FoxQ2* orthologs and paralogs. A cluster that includes some of the previously hypothesized FoxQD genes is detected with both methods, nested within the tree, supporting an early split of this family. Among deuterostomes, this group included the amphioxus *FoxQ2c*, the hemichordate *FoxQ2c* but curiously no sequences from echinoderms or vertebrates. Surprisingly, the rest of the sequences were additionally split into two groups: one included orthologs that have been found to be involved in the aGRN, including the amphioxus *FoxQ2a*, the hemichordate *FoxQ2a* and *FoxQ2b*, the sea urchin *FoxQ2* and additionally both the teleost and sauropsid *FoxQ2*. The other contained only few sequences coming from both protostomes and deuterostomes, indicating a possible origin at the base of the Bilateria, and included the amphioxus *FoxQ2b* a sequence from one of the mollusc and brachiopod paralogs, and interestingly the tunicate, lamprey and skate orthologs discovered in this study. This organization is further supported by the comparison of the forkhead domain only, which reconstructs a similar topology (Appendix VIII, Figure A8.1).

**Figure 6.1.** *FoxQ2* genes in Metazoa (overleaf). **A.** Phylogenetic analysis (maximum likelihood) of the *FoxQ2* class identify three paralogs: *FoxQ2a* (blue), *FoxQ2b* (green) and *FoxQ2c* (yellow). *FoxQ1* is used as outgroup. Bootstrap values, represented with coloured dots for the main branches, indicate that support for the *FoxQ2* family and for *FoxQ2b* is high while the internal relationships between *FoxQ2a* and *FoxQ2c* have low support. **B.** Expression of *FoxQ2a* paralogs in amphioxus. For species names see Appendix VIII, Table A8.1. Scale bars are 50µm.

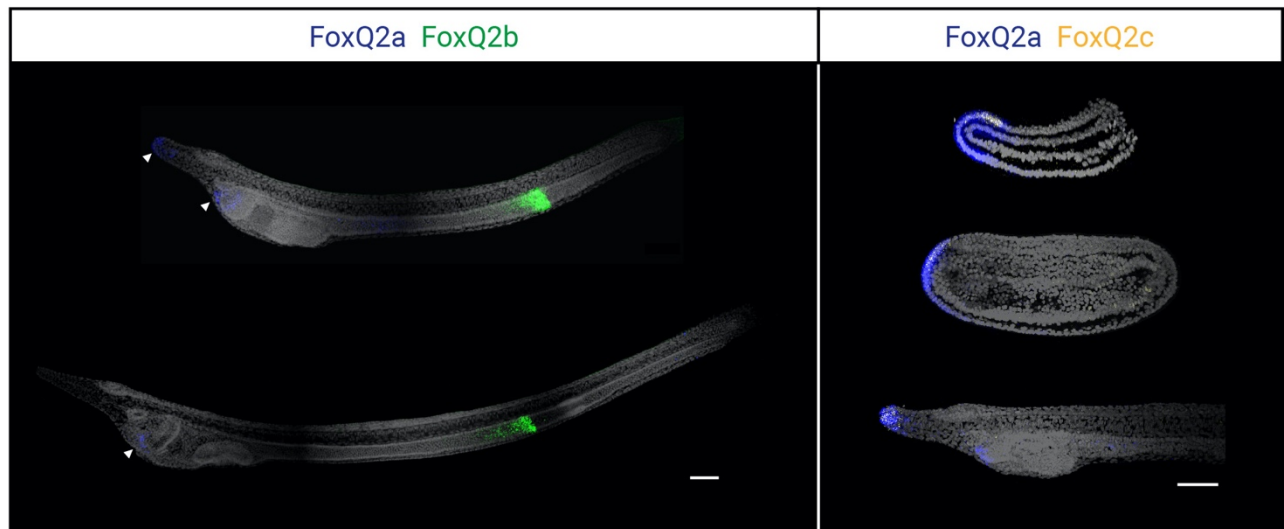
A

Bootstrap

- 100
- 85 ≤ x < 100
- 70 ≤ x < 85
- x < 70



B



To further understand the difference in *FoxQ2* paralogs in amphioxus, I characterized the developmental expression of *FoxQ2b* and *FoxQ2c* (Figure 6.1B). RNAseq indicate that *FoxQ2b* activated later than *FoxQ2a* around the beginning of the larval stage (Appendix VIII, Figure A8.1), and HCR showed that it is expressed in a specific and restricted domain on the posterior side of the gut. The radically different expression pattern from *FoxQ2a* provides further support to the hypothesis that this represents a different family of *FoxQ2* orthologs (Figure 6.1Bi). On the other hand, *FoxQ2c* is expressed at low level from the beginning of neurulation (Appendix VIII, Figure A8.1): while it was not found in G5 embryos (data not shown), at the N0 stage it was found in a small domain nested within the *FoxQ2a* expression. At the 7ss stage, *FoxQ2c* continued to be co-expressed with *FoxQ2a* at low level specifically at the anterior boundary between neural and non-neural ectoderm (Figure 6.1Bii). Finally, at the larval stage it was still found in a few cells at the anterior tip of the rostrum, both together with *FoxQ2a* and by itself (Figure 6.1Bii).

Overall, following the phylogenetic relationships reconstructed here the FoxQ2 class can be divided into three families:

- ◆ *FoxQ2a*, containing *FoxQ2* involved in aGRN patterning and likely evolved in the eumetazoan ancestors;
- ◆ *FoxQ2b*, present only in few protostome and deuterostome groups and not expressed in a similar location to the rest of *FoxQ2* in amphioxus. Possibly evolved in the bilaterian ancestor;
- ◆ *FoxQ2c*, corresponding to the previously described *FoxQD* family. This group is characterized by the presence of a C-terminal eh1-like motif and likely evolved in the eumetazoan ancestor.

### 6.2.2 Expression of vertebrate *FoxQ2*

Given the conservation of *FoxQ2* in chordates highlighted by my phylogenetic analysis, I was interested in understanding its expression pattern in vertebrates. By consulting a published RNAseq dataset of zebrafish development (365), I found that the *FoxQ2* is expressed at low level late in development, after hatching and long after the expression of other aGRN genes (Figure 6.2A). Recently, a scRNAseq dataset on the developing brain of zebrafish from 12hpf to 15dpf has been published, allowing me to probe the expression of *FoxQ2* in later stages (319). The analysis showed that one cell type from 8dpf and two cell types from 15dpf specimens were expressing this gene at

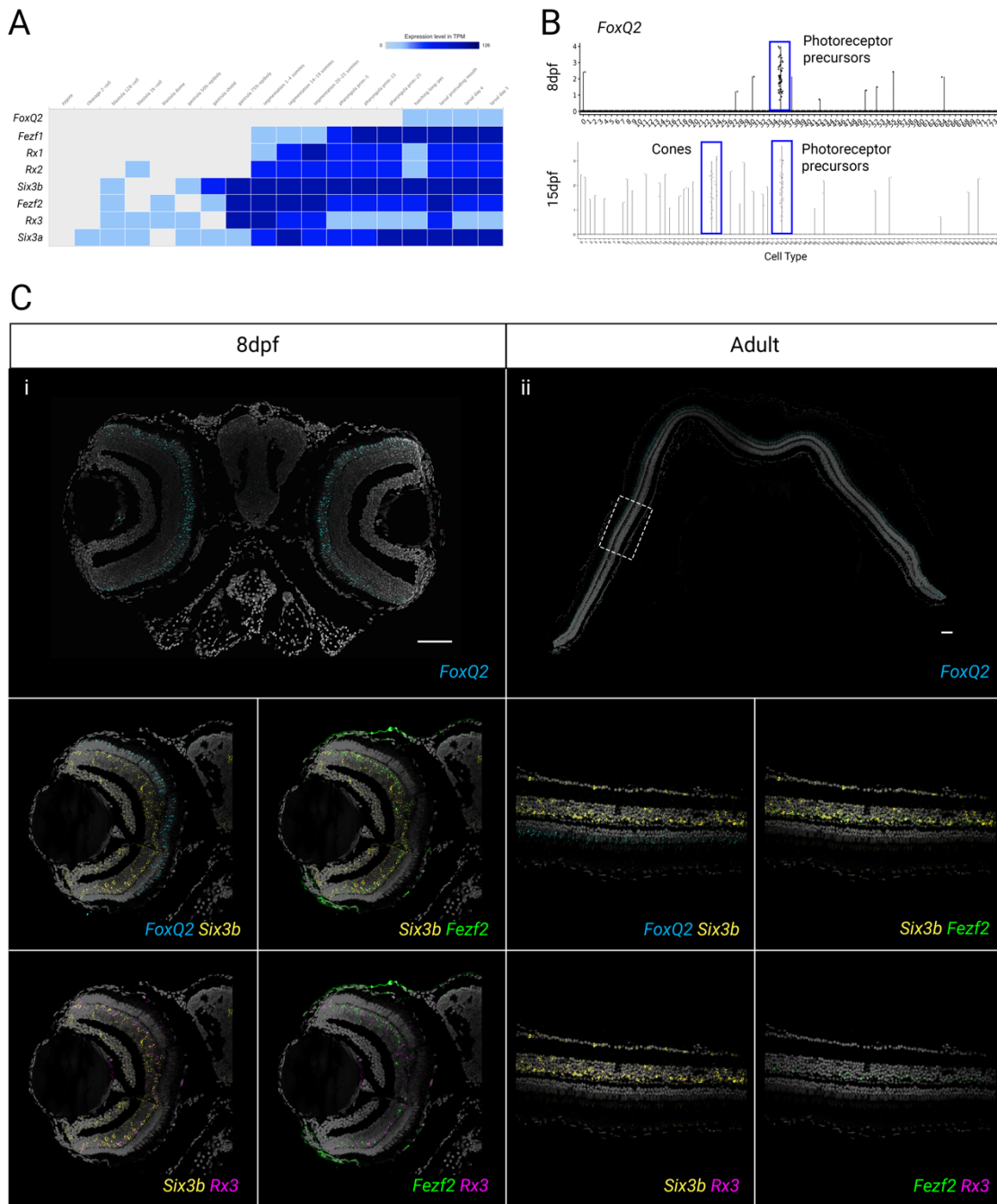


**Figure 6.2.** *FoxQ2* expression in zebrafish. **A.** Developmental expression of selected aGRN genes obtained from published RNAseq dataset (364). *FoxQ2* is expressed only after hatching at low levels. **B.** Violin plots of *FoxQ2* expression across cell types (x-axis) of 8 days post fertilization (dpf) zebrafish larvae, showing *FoxQ2* transcripts in photoreceptor precursors and cone cells. **C.** Expression of *FoxQ2* (cyan), *Six3b* (yellow), *Fezf2* (green) and *Rx3* (magenta) in 8dpf (i) and adult (ii) sections of zebrafish eyes. (i) At 8dpf a transverse section of the head is shown for *FoxQ2* while co-expression is analysed in magnifications of a single eye. (ii) For adults a transverse section of an entire eye is stained for *FoxQ2* while co-expression is visualized in magnifications of a region highlighted by the dashed box. For a reference on the structure of the retina see Appendix VIII, Figure A8.2. Scalebars are 100 $\mu$ m.

low level, identified as photoreceptor precursors and cones (Figure 6.2B). I was particularly intrigued by this pattern as the photoreceptors are part of the retina which in turn forms from the secondary prosencephalon. With candidate stages and cell types, I then set out to characterize the spatial distribution of zebrafish *FoxQ2*. Dr Andrew Gillis (Marine Biological Laboratory, University of Chicago) provided paraffin-embedded cross sections of zebrafish heads at 8dpf, which were used to test the expression of *FoxQ2* together with three aGRN paralogs: *Six3b*, *Fezf2* and *Rx3* (Figure 6.2Ci). *FoxQ2* was clearly visible in a subset of photoreceptor cells in the deeper (apical) retinal photoreceptor layer, while the other three genes were expressed in more superficial (basal) layers. The comparison with the 8dpf and 15dpf scRNAseq dataset allowed me to reconstruct the cell types expressing each gene (Appendix VIII, Figure A8.2). *Fezf2*, which had not been previously considered as a clear marker of the retina, labelled a subset of bipolar cells and possibly some amacrine and horizontal cells, often co-expressing *Six3b*. *Rx3* and *Six3b* were expressed in a separate subset of cone bipolar cells, while *Six3b* was additionally found in the Muller glia and in retinal ganglion cells. While I was preparing experiments to define which subset of photoreceptors expressed *FoxQ2*, Ogawa and collaborators discovered that this gene is specific to blue cones and is required for their development in 5dpf larvae (213). To test whether this was only a developmental function or it persisted throughout the animal's life, I also tested the same combination of genes in sections of adult zebrafish (Figure 6.2Cii). I found that the pattern of the four genes remained very similar to 8dpf, although *Rx3* was expressed at very low levels. In particular, *FoxQ2* was still found in photoreceptor cells, indicating that it is not only involved in the early specification of blue cones but it remains active throughout the animal's life.

**Figure 6.3.** Identification of conserved *FoxQ2* cis-regulatory regions in cephalochordates (overleaf).

**A.** Comparison of sequences upstream of *FoxQ2* in *Branchiostoma lanceolatum* with *Asymmetron*, *B. belcheri*, *B. floridae* and *Epigonichtys* using VISTA revealed conserved non-coding sequences (CNCS) (black arrowheads). **B.** Identification of CNCSs in the *B. lanceolatum* genomic region upstream of *FoxQ2*. These sequences correspond to the open chromatin regions detected by ATACseq (grey boxes) (79). **C.** i) Identification of conserved transcription factor binding sites (TFBS) localized in the CNCS of all five amphioxus species. ii) Barplots showing the expression of the corresponding transcription factors (TFs) from a developmental RNAseq dataset (79). The TFs are maternally expressed and thus might control early *FoxQ2* activation (red bars indicate expression at the 32 cells stage). **D.** Differential expression of selected transcription factors with identified TFBSs in *FoxQ2* cis-regulatory regions between animal and vegetal blastomeres of *B. floridae* (dataset by (369)).

A

5 Amphioxus Genomes

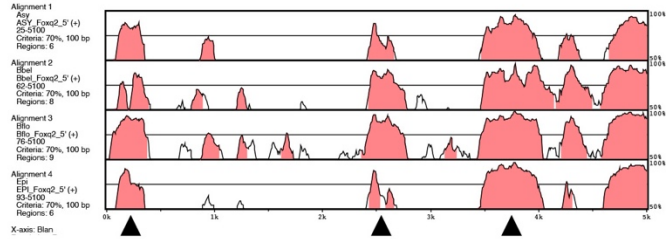


3 *Branchiostoma*  
1 *Asymmetron*  
1 *Epigonichtys*

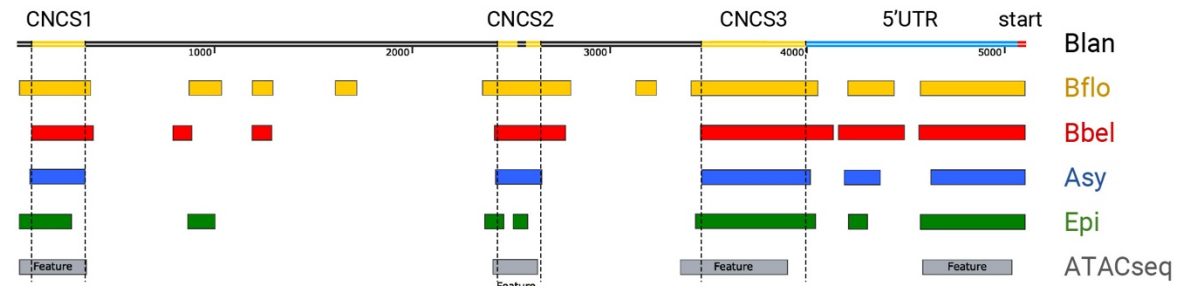
+

*B. lanceolatum* ATAC-seq

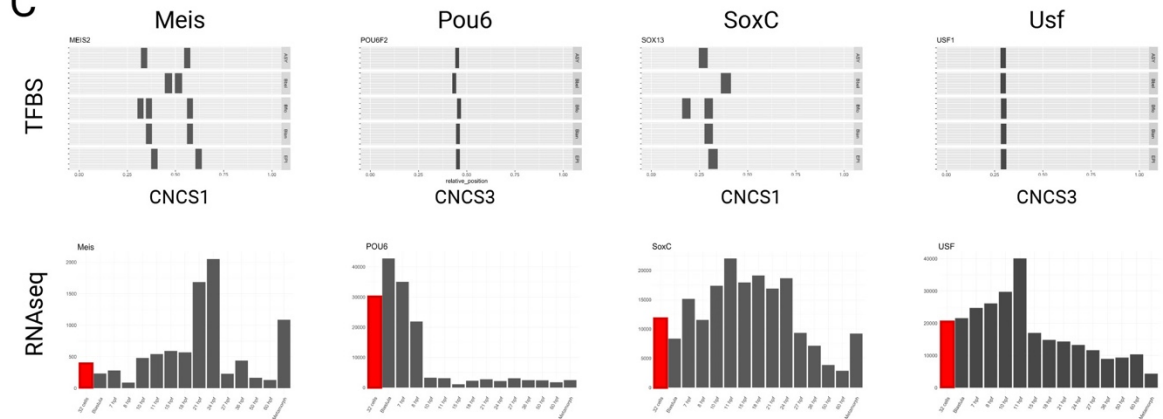
Vista comparison of *B. lanceolatum* with other amphioxus



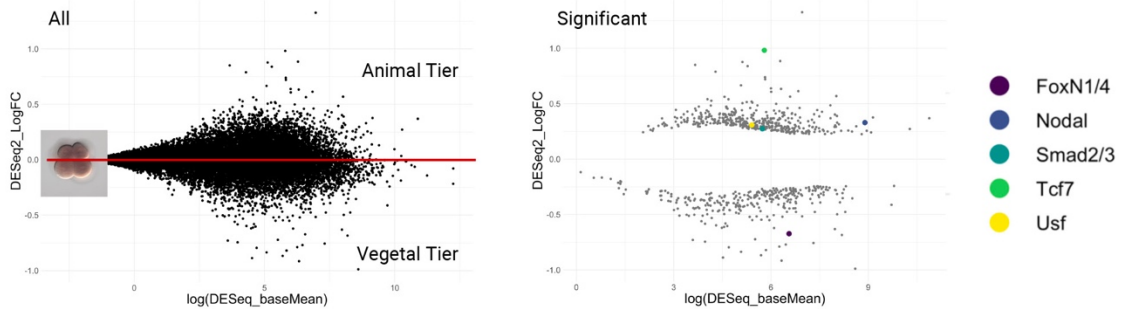
B



C



D



### 6.2.3 Analysis of *FoxQ2* cis-regulatory sequences in amphioxus

In ambulacrarians and amphioxus, *FoxQ2* is one of the first genes to be transcribed after the maternal to zygotic transition (154, 160). From these early stages, *FoxQ2* expression is already limited to the animal side of the embryo, but how this activation is controlled remains a mystery. In sea urchin, *Six3/6* controls the expression of *FoxQ2*, so that in *Six3/6* knock-downs *FoxQ2* disappears from the animal side (152, 154). However, scRNAseq data showed that *FoxQ2* is expressed before *Six3/6*, and therefore cannot act as its primary activator and likely has more control over its maintenance (154). Moreover, in starfish embryos the inhibition of *Six3/6* does not cause the loss of *FoxQ2* (162). *Meis* also influences late *FoxQ2* maintenance in sea urchin: *Meis* knock-down does not affect the early expression of *FoxQ2* but causes its downregulation at later stages (366). Moreover, a recent study investigated cis-regulatory regions upstream of sea urchin *FoxQ2* and found several transcription factor binding sites (TFBS), including one specific to *Meis* (362).

To shed light on the early control of *FoxQ2* expression, during the Covid-19 pandemic I decided to take a similar computational approach and investigate the regulatory sequences around the amphioxus *FoxQ2a* gene. To reconstruct candidate regulatory sequences, I first identified the *FoxQ2a* gene in five amphioxus genomes from the three amphioxus genera (*B. lanceolatum*, *B. floridae*, *B. belcheri*, *Asymmetron*, *Epigonichtys*), selected a region of ~5000bp upstream of the start codon in each species and compared it using mVISTA (367) (Figure 6.2A). With this method, I identified three non-coding regions that are conserved within cephalochordates (named conserved non-coding sequences or CNCS) (Figure 6.2B). Strikingly, by interrogating the *B. lanceolatum* ATAC-seq dataset produced by Marletaz and collaborators (79) I found that these regions precisely correspond to ATAC-seq peaks, indicating that these are open chromatin regions likely containing regulatory sequences (Figure 6.2B). I then used the CiiiDER program (368) to identify for each species the list of possible TFBSs in each one of the three CNCSs. This resulted in an excessively large dataset, but again the use of multiple species meant that I could select only those sites that are conserved among all cephalochordates. With this premise, Daniel Keitley (Department of Zoology, University of Cambridge) devised a computational method to select only those TFBSs that are present in all five species at the same level (with a 10% margin of error) within each CNCS sequence. The number of possible TFBS types recovered was more manageable: 21 for CNCS1, 9 for CNCS2 and 31 for CNCS3. This allowed me to use the *B. lanceolatum* RNAseq dataset (79) to check for members of the

transcription factor families discovered that are expressed at 32 cells, before zygotic transcription has started (Figure 6.2C). Interestingly, candidate transcription factors expressed maternally include *Meis* and *POU6*, which were also identified in sea urchin (362), and *SoxC*. To test whether some of these maternally expressed genes were enriched in the animal side of the embryo, and therefore might control the expression of *FoxQ2*, I analysed the differential expression of animal and vegetal blastomeres obtained in a published RNAseq dataset from 8-cell stages of *B. floridae* (369) (Figure 6.2D). Of the subset of maternally expressed genes investigated, only four were enriched on the animal side at the 8-cell stage: *Nodal*, *Smad2/3*, *Tcf7* and *Usf*.

Overall, the preliminary analysis of conserved *cis*-regulatory sequences for cephalochordate *FoxQ2* did not solve the mystery of *FoxQ2* activation but revealed a high number of candidate regulatory interactions that could be functionally tested in future studies, for example by luciferase assays on cell cultures in which a plasmid containing the regulatory sequence upstream of a luciferase gene is co-injected with mRNAs for candidate regulatory transcription factors.

### 6.3 Apical, animal and anterior: relationship between CNS evolution and body axis formation

In bilaterians, the specification and morphogenesis of the CNS occurs concomitantly with and is influenced by the formation of the body axes, roughly dividing the embryo into anterior, posterior, dorsal, ventral, left and right sides. The process of symmetry breaking that leads to the polarization of the embryo is generally driven by the unequal distribution of maternal determinants or nutrients within the egg (370–372). After the maternal to zygotic transcription these determinants drive differential gene expression in blastomeres, which will have distinct fates during gastrulation depending on their position in the embryo. Many of these cells will also produce different morphogens to influence the differentiation of surrounding tissues (234, 370, 373, 374). In particular, a group of cells that are able to induce fates and guide the morphogenetic pattern of surrounding cells during embryonic development is defined as an *organizer* (375, 376).

In vertebrates, the primary embryonic organizer has been found to control both the induction of specific tissues, including the neural plate, as well as the formation of the body axes. If transplanted

in a different embryo, this organizer can in fact induce the formation of a neural plate and a secondary body axis (223, 376). The function of the primary organizer is best known in amphibians, where it was first discovered by Spemann and Mangold (377). The frog egg has a concentration of VegT and Dsh at the vegetal pole, but due to the cortical rotation of the cytoplasm that follows fertilization Dsh translates on the future dorsal side of the embryo, where it blocks the degradation of  $\beta$ -catenin that therefore accumulates dorsally. Moreover, a dorso-ventral gradient of Nodal is established by  $\beta$ -catenin and VegT. On the dorsal side,  $\beta$ -catenin activates other factors such as Siamois and Twin while Nodal signals through Smad2/3, and together they control the expression of organizer genes, which include Goosecoid (*Gsc*), Bmp inhibitors such as Chordin (*Chd*), Noggin and Follistatin, and Wnt inhibitors of the Dkk and sFRP families (223, 242, 373, 374, 378, 379).

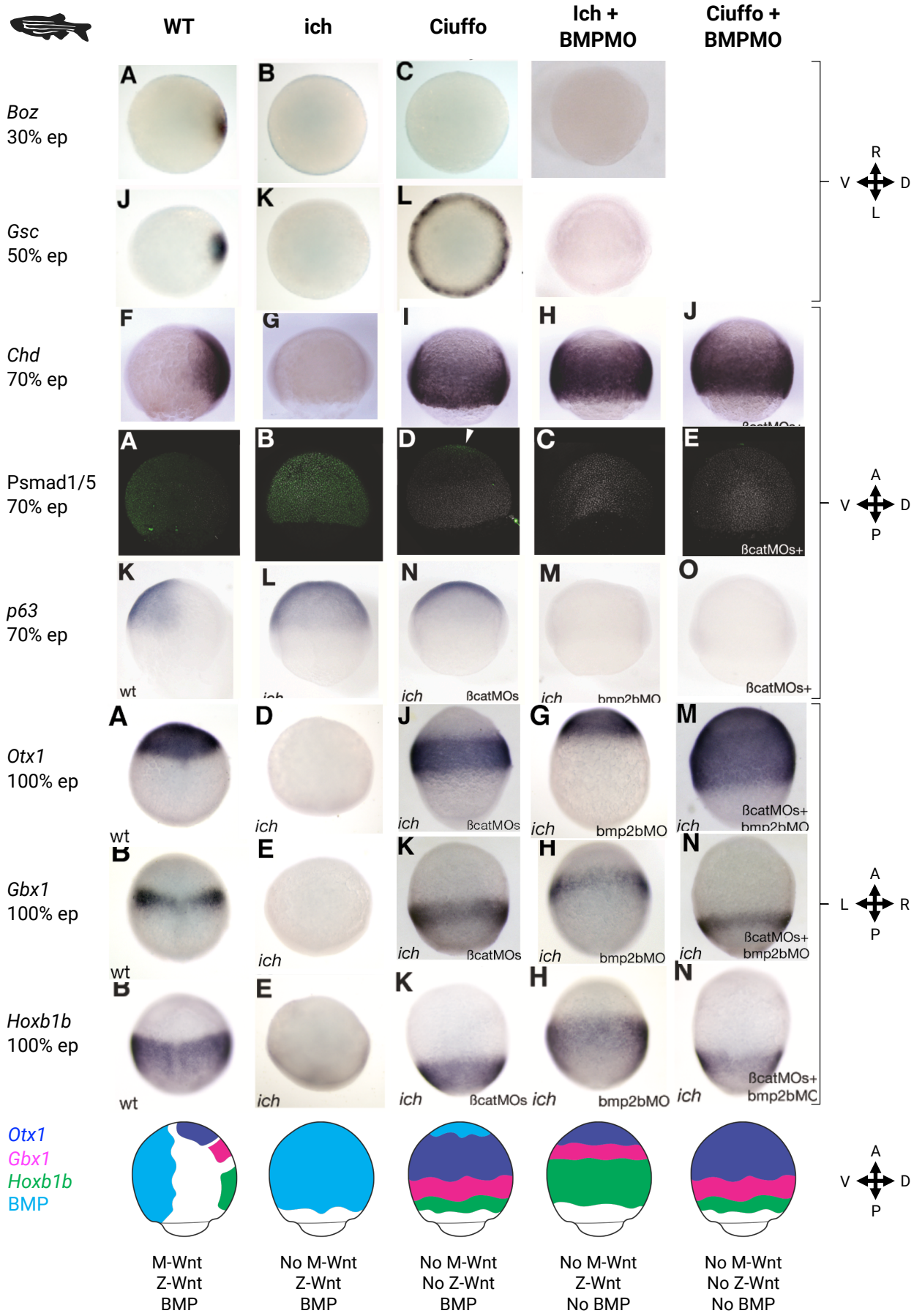
The organizer is positioned at the dorsal lip of the blastopore, which is the first that starts to involute at the beginning of gastrulation. On the other hand, the ventral side of the embryo with low  $\beta$ -catenin and Nodal signalling starts expressing Bmp. The activity of Bmp is maintained ventral by the action of the Bmp inhibitors in the organizer. During gastrulation, the dorsal lip of the blastopore is composed of a dynamic population of cells that enter the embryo and are progressively patterned to form the prechordal plate and the notochord. These cells continue to express organizer genes, so that the prechordal plate releases both Wnt (Dkk and sFRP) and Bmp (Chordin, Noggin) inhibitors while the notochord produces only Bmp inhibitors, continuing to restrict Bmp signalling on the ventral side. In vertebrates Bmp has a strong anti-neural function and is instead required for the specification of the non-neural ectoderm. Therefore, the activity of the organizer is required to allow the development of the neural plate on the dorsal side of the body (223). If the formation of the organizer is blocked by inhibition of early Wnt/ $\beta$ -catenin signalling or if Bmp signalling is ectopically activated, the entire ectoderm acquires an epidermal fate; conversely, if the action of Bmp is inhibited the neuroectoderm expands to cover the whole embryo (380, 381). Although there are differences in the contributions and timing of the organizer in different vertebrate embryos (376), other studies have demonstrated a similar mechanism acting in zebrafish (379, 382–384): the primary organizer is visible in the embryonic shield that forms at the dorsal margin of the embryo by accumulation of  $\beta$ -catenin and Nodal signalling. Overall, these seminal studies demonstrated how the organization of the chordate body plan arise during development and revealed the link between the formation of the body axes and the correct specification and position of the embryonic tissues.

### 6.3.1 The organizer is not required for AP patterning

While maternal  $\beta$ -catenin on the dorsal side is necessary to form the organizer and specify dorsal fate (“early” Wnt function), at the beginning of gastrulation the localization and function of Wnt/ $\beta$ -catenin signalling changes dramatically, controlling the development of posterior and ventral structures (“late” Wnt function) (234, 241, 385). At the same time, the presence of Wnt inhibitors in the anterior prechordal plate ensures the formation of a gradient of Wnt signalling, high posteriorly and low anteriorly, which then influences the regionalization of the CNS (234, 379, 386). The brain forms in the area deprived of Wnt signalling, under the prechordal plate, while the posterior neural plate forms in the area where posterior Wnt signalling is active. It was therefore thought that the activity of the vertebrate organizer was necessary for the DV patterning of the embryo, the induction of the neural plate as well as the AP regionalization of the neural tube. A series of brilliant but little-known studies by the Weinberg Lab however have elucidated that the nervous system can be correctly regionalized antero-posteriorly even in the absence of an organizer, and that the primary organizer function concerning nervous system development is the inhibition of Bmp signalling (387–389) (Figure 6.4).

Their work discovered and exploited the fact that the two  $\beta$ -catenin paralogs in zebrafish have distinct functions: only  $\beta$ -catenin2 is involved in the formation of the organizer, while both  $\beta$ -catenin1 and  $\beta$ -catenin2 are contributing to the ventral/posterior function during gastrulation (388). This meant that by targeting different paralogs the function of each of the two Wnt “phases” could be dissected and studied separately (Figure 6.4). In normal embryos, early  $\beta$ -catenin2 induces the expression of organizer genes such as *Boz*, *Gsc* and *Chd* on the dorsal side. On the other hand, later  $\beta$ -catenin1 and  $\beta$ -catenin2 expressed ventrally redundantly repress *Chd* and activate ventral markers such as *Vox* and *Vent* (387, 388).

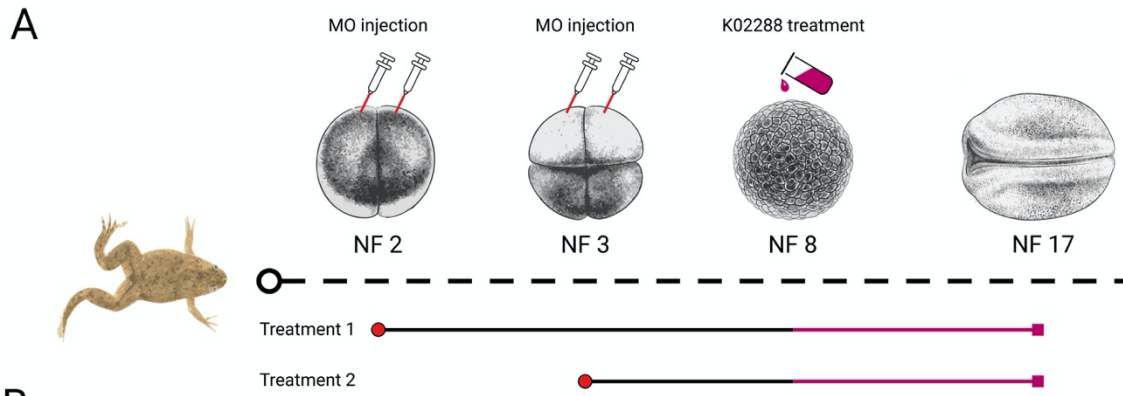
**Figure 6.4.** Summary of the role of Wnt and Bmp signalling in body patterning and nervous system regionalization in zebrafish (overleaf). Organizer genes (*Boz*, *Gsc*, *Chd*), Bmp effector *Psmad1/5*, epidermal marker *p63* and AP neural markers *Otx1*, *Gbx1* and *Hoxb1b* were detected in normal, ichaboid (*ich*), *ciuffo*, *ich* + Bmp morpholino (BMPMO) and *ciuffo* + BMPMO embryos. The effect of each condition and treatment combination is summarized in the schematic at the bottom of the figure. All images are taken from (387–389) and reproduced with permission from Development (The Company of Biologists) and Elsevier.



As a consequence, Bmp signalling is restricted ventrally, where epidermal markers such as *p63* will be expressed, while the nervous system forms dorsally with the correct AP polarity, with anterior expression of *Otx*, more posterior *Gbx* and more posterior *Hox* genes (389). Embryos bred from females homozygous for *ichabod* (here called *ich* embryos), a maternal effect mutation that targets  $\beta$ -catenin2, or embryos treated with  $\beta$ -catenin2 morpholino ( $\beta$ -cat2MO) are completely ventralized and do not form a nervous system (388). In *ich* embryos the absence of maternal  $\beta$ -catenin2 results in the absence of the organizer as shown by downregulation of *Boz*, *Gsc* and *Chd*. However, zygotic  $\beta$ -catenin1 at the vegetal pole is sufficient to inhibit ventral *Chd* expression and consequently, in the absence of repressors, Bmp signalling is active throughout the ectoderm that will be specified as epidermis with no nervous system (387, 389). When both  $\beta$ -catenins are inactivated (either with double morpholinos or by treating *ich* embryos with  $\beta$ -cat1MO) the resulting embryos are dorsalized, possess a nervous system and have been named “*ciuffo*” by the authors (388). Despite the dorsalized phenotype *ciuffo* embryos lacked an organizer, as  $\beta$ -catenin2 is not active and *Boz* and *Gsc* are downregulated. The absence of ventral, zygotic  $\beta$ -catenins however meant that *Chd* is not repressed ventrally and forms a wide posterior band around the germ ring. As a consequence, Bmp signalling is blocked in most of the embryo, and therefore a conspicuous and radial neuroectoderm forms, except at the anterior tip where Bmp is active and epidermal markers are expressed (387, 389). These results showed that the organizer is not necessary to directly induce the nervous system, but to block Bmp signalling and allow the formation of the neuroectoderm. The most surprising result was that in *ciuffo* embryos the nervous system is patterned antero-posteriorly despite the absence of the organizer (and therefore of the axial mesoderm), indicating that the organizer is also not required for the AP patterning and regionalization of the nervous system (389). Because of the absence of zygotic Wnt with a posteriorizing function, the neuroectoderm is actually anteriorized, with expanded *Otx* expression and a posteriorized *Gbx* domain. These results were further confirmed by combining Wnt and Bmp treatments. In *ich* embryos treated with BMP2MO, the organizer does not form but the inhibition of Bmp signalling leads to the development of neuroectoderm throughout the entire ectoderm, while epidermal markers are absent. The presence of zygotic, posteriorizing Wnt signalling also meant that the neuroectoderm is regionalized normally antero-posteriorly, although in a radial pattern. Finally, in *ciuffo* embryos treated with BMP2MO, the absence of both maternal and zygotic Wnt led to an anteriorised neural tube, with *Otx* expressed in more than half the surface of the ectoderm (389).

Older studies performed in frogs suggest that a similar mechanism is conserved in vertebrates: while in frogs it is not possible to target maternal and zygotic Wnt separately, the co-treatment with  $\beta$ -catMO and BMP4/7MO led to the formation of the neuroectoderm with regionalized expression of AP markers (381). During my time at the MBL Embryology course in 2022, I sought to confirm these results by injecting embryos of *X. laevis* with  $\beta$ -catMO and then treating them with a Bmp inhibitor (K02288) (Figure 6.5A). I then detected the localization of the neural marker Sox3 and the expression of two region specific genes: *Six3b* is expressed in the forebrain of stage 17 embryos, while *Gbx2* labels the MHB and is diffusely expressed in the non-neural ectoderm (Figure 6.5B). Both the treatment with BMPi alone and the combination with  $\beta$ -catMO injection at the 2-cell stage resulted in a dramatic expansion of Sox3, which labelled the majority of the embryo in a radial pattern. In the same embryos, the expression of *Six3/6* became radial and covered the anterior portion of the embryo. Interestingly, the epidermal expression of *Gbx* was lost while the stripe of *Gbx* behind the MHB expanded to form a continuous line around the embryo, located ventrally from the *Six3/6* domain and separated from it as in control embryos.

Previous studies also showed that the organizer can be more precisely targeted by injecting  $\beta$ -catMO in the two lighter cells at the 4-cell stage, which have been shown to form the dorsal part of the body by fate map studies (390). Therefore, I tried to combine this later injection with Bmp inhibition (Figure 6.5A) and obtained similar results to the 2-cell injection, with a radial expansion of the neuroectoderm and loss of epidermal expression of *Gbx* (Figure 6.5B). Taken together, these results confirm that in frogs the nervous system can be correctly patterned even in the absence of the organizer if Bmp signalling is inactivated. It is important to specify here that due to the time restriction during the course, I could not carry out all the necessary controls for this experiment: the additional controls would include injection of  $\beta$ -catMO and COMO without K02288 treatment (substituted by DMSO) and treatment of uninjected embryos with K02288. These conditions however have been documented in the literature and are consistent with the results found here (380, 381). It would also be interesting to validate the absence of the organizer by detecting the expression of genes such as *Chd* and *Gsc*.



**B**

	SOX3	<i>Six3b</i> <i>Gbx2</i>
Uninjected Untreated	<p>Head view      Dorsal view</p>	<p>Head view      Lateral view</p>
Control MO + BMPi 2 cells		
Bcat MO + BMPi 2 cells		
Control MO + BMPi 4 cells		
Bcat MO + BMPi 4 cells		<p>A ↑ ↓ P</p>

< **Figure 6.5.** Removing the frog organizer does not affect AP regionalization of the frog nervous system in the absence of Bmp signalling. **A.** Experimental design of  $\beta$ -catenin morpholino injection and treatment with the Bmp inhibitor K02288. **B.** Immunofluorescence for Sox3 (magenta) and *In situ* HCR for *Six3b* (red) and *Gbx2* (cyan) in control and treated frog embryos. Arrows point at the neural expression of *Gbx2* at the midbrain-hindbrain boundary in control embryos.

### 6.3.2 The evolution of Bmp patterning in chordates

The surprising results on the functions of the primary organizer indicate that Bmp has an essential role in the formation of the DV axis as well as the restriction of the embryo neurogenic potential to the dorsal side. But how far back can we trace these functions of Bmp? Early comparative studies between vertebrates and insects suggested that the anti-neural function of Bmp might be a general feature of bilaterians, but recent analyses taking into account a larger number of phyla challenged this view, suggesting that the role of Bmp has been highly dynamic during evolution (28, 29). For example, in hemichordates Bmp is expressed dorsally and might have a role in DV patterning, but the nervous system forms throughout the ectoderm even in the presence of Bmp (391).

In amphioxus,  $\beta$ -catenin accumulates on the vegetal and then dorsal side of the embryo, where organizer genes are expressed in the dorsal lip of the blastopore at the gastrula stage (241, 392). These genes are controlled by maternal Wnt/ $\beta$ -catenin signalling: embryos treated with the Wnt inhibitor C59 from the zygote lack *Gsc*, *Chd* and *Nodal* expression and do not form the neural tube (241). Overall, this indicates that the organizer dates back to the chordate ancestor. Curiously, these changes are similar to the “ich” condition in zebrafish embryos, where only maternal Wnt has been disrupted, while in amphioxus C59 blocks both maternal and zygotic signalling (241, 388). During gastrulation and neurulation, Bmp signalling is active ventrally as in vertebrates, demonstrating that it is a conserved chordate character (393). However, its role in axial patterning and neural specification is somewhat different from vertebrates and difficult to interpret (394). Previous studies have shown that overactivation of Bmp signalling in amphioxus leads to ventralization of the embryo and loss of neural structures, similarly to vertebrates, but the loss of early Bmp function through treatment with dorsomorphin does not dorsalize the embryo as in vertebrates. Early treatment causes a complete loss of neural markers and a maintenance of uncommitted ectoderm, while late treatment caused only a modest expansion of neural fate, which still remains limited to

the dorsal side of the animal (393, 395, 396). This suggested that Bmp already had an anti-neural function in the chordate ancestor, but that at least in cephalochordates its absence is not sufficient to drive neural specification. In fact, in amphioxus Nodal signalling appears to be primarily responsible for neural plate induction (394, 395). Ectopic activation of Nodal signalling leads to embryo dorsalization and the expansion of the neural tissue across the ectoderm, while inhibition of Nodal causes the loss of neural structures (241, 395). When both Bmp and Nodal signalling are experimentally upregulated, the whole ectoderm is initially specified as neural, indicating that Nodal can induce neural differentiation even in the presence of Bmp (395). Overall, these results show that Bmp has a role in DV patterning in cephalochordates, but the mechanisms underlying its involvement in nervous system development appear different than vertebrates and are still unclear (392, 394).

Together with Claudia Pérez Calles, an undergraduate student, we therefore sought to trace the activity of Bmp and Nodal signalling and the competence of different tissues to respond to these morphogens during neurogenesis. Both Bmp and Nodal are members of the TGF $\beta$  family and signal by binding to heterotetrameric TGF $\beta$  receptors that phosphorylate Smad family transcription factors (397). In vertebrates, Nodal binds to a tetramer composed of two pairs of activin receptors, ACVR1 and ACVR2, which activate Smad2/3, while Bmp2 and Bmp4 bind to BMPR1 and BMPR2 and signal through Smad1/5/8 (Appendix VIII, Figure A8.3) (224, 398, 399). We identified orthologs of seven TGF $\beta$  family receptor genes (*ACVR1*, *ACVR2*, *BMPR1*, *BMPR2*, *TGFBR1*, *TGFBR2*, *TGFBR3*) in five amphioxus transcriptomes (*B. lanceolatum*, *B. floridae*, *B. belcheri*, *Asymmetron*, *Epigonichtys*) and performed phylogenetic analysis using FGF receptors as an outgroup (Appendix VIII, Figure A8.4). We show that TGF $\beta$  receptors split early into two ancient groups representing type 1 and type 2 families. We then investigated the expression patterns of BMPRs and ACVRs in N0 and 7ss stages and compared them with the distribution of their ligands – *Bmp2/4* and *Nodal* respectively – their effectors – phosphorylated Smad1/5/8 (PSmad1/5/8) and phosphorylated Smad2/3 (PSmad2/3) respectively – and for Bmp its antagonist *Chd* (Figure 6.6; Figure 6.7). The distribution of receptors and ligands was first explored in our scRNAseq datasets and then the spatial co-expression was analysed using HCR combined with immunohistochemistry for the Smad effectors. As the Smad localization is nuclear, and to make sure to consider the exact location of the receptors and morphogens, only nuclear expression was considered by masking the HCR and immunohistochemistry signal using the DAPI channel.

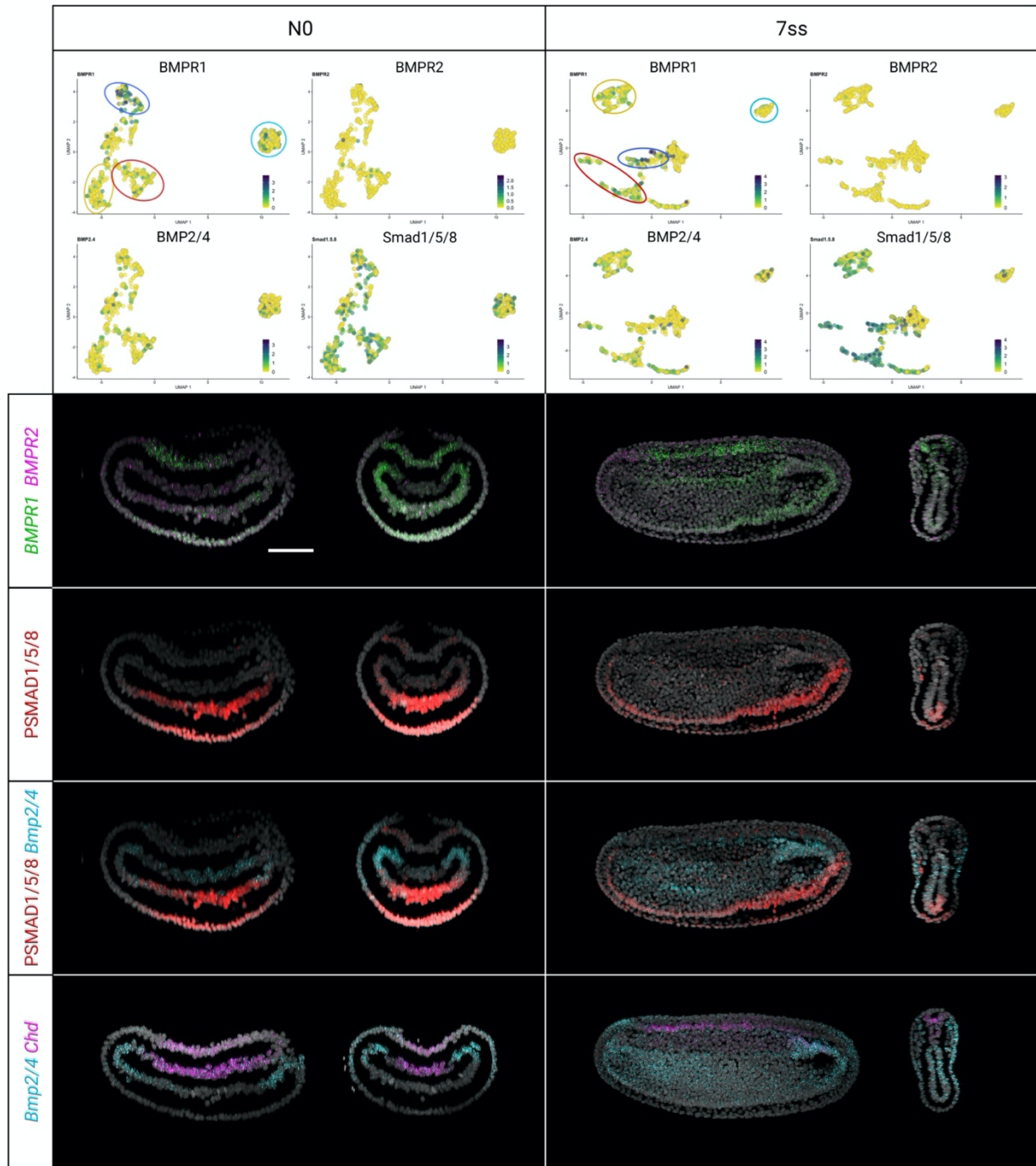


**Figure 6.6.** Bmp signalling during amphioxus neurulation. Analysis of the spatial distribution and co-localization of Bmp receptors *BMPR1* (green) and *BMPR2* (magentas), the ligand *Bmp2/4* (cyan), the effector *Smad1/5/8* (red) and the Bmp inhibitor *Chd* (magenta) on early neurula (N0) and mid neurula (7ss) embryos. The data was obtained from our scRNAseq dataset and combining *in situ* HCR (*BMPR1*, *BMPR2*, *Bmp2/4*, *Chd*) with immunofluorescence for phosphorylated *Smad1/5/8*. Circles in scRNAseq graphs represent neural (blue), epidermal (cyan), mesodermal (red) and endodermal (yellow) cell types. Scale bar is 50 $\mu$ m.

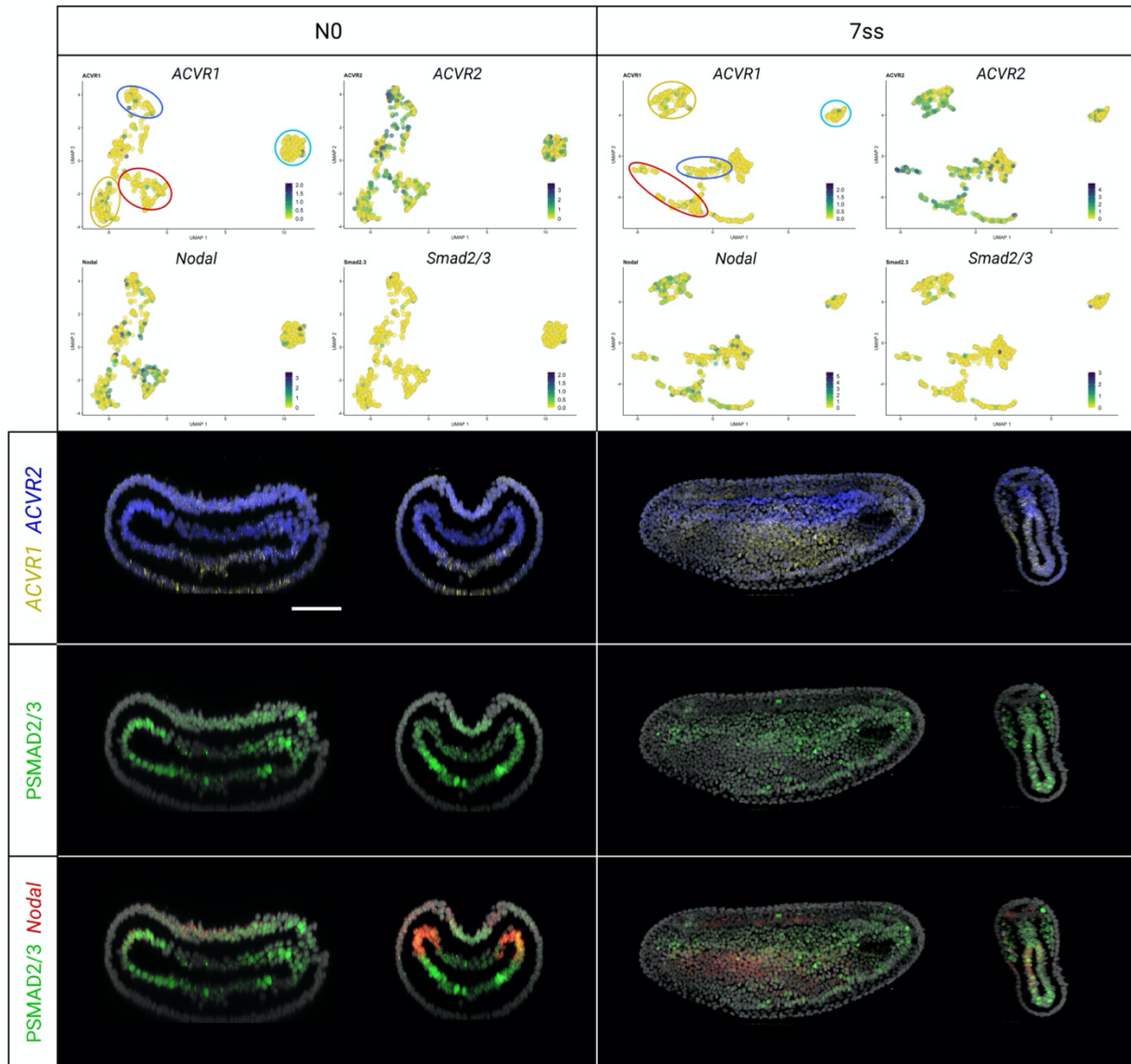


**Figure 6.7.** Nodal signalling during amphioxus neurulation. Analysis of co-localization of nodal/activin receptors *ACVR1* (yellow) and *ACVR2* (blue), *Nodal* (red) and the effector *Smad2/3* (green) in early neurula (N0) and mid neurula (7ss) embryos. . The data was obtained from our scRNAseq dataset and combining *in situ* HCR (*ACVR1*, *ACVR2*, *Nodal*) with immunofluorescence for phosphorylated *Smad2/3*. Circles in scRNAseq graphs represent neural (blue), epidermal (cyan), mesodermal (red) and endodermal (yellow) cell types. Scale bar is 50 $\mu$ m.

*BMPR1* was distributed in several tissues at N0 and 7ss stages, but interestingly in both stages it was most highly expressed in the nervous system, while it was low in the axial mesoderm and the dorsolateral epidermis (Figure 6.6). Conversely, *BMPR2* had a very low level of expression: at N0 it was found in traces in the notochord and the endodermal layer, while at 7ss it appeared in the

nervous system and sparsely in the epidermis. The two receptors therefore colocalize mainly in the endoderm and later in the nervous system. The activity of Bmp was followed using antibodies against the phosphorylated form of Smad1/5/8 and was concentrated on the ventral side of the animal, in particular in the endoderm and the ventralmost portion of the epidermis. These are areas where at least *BMPR1* is expressed, although at 7ss PSmad1/5/8 reached more anteriorly than the area of *BMPR1* (Figure 6.6). At N0 low PSmad1/5/8 immunoreactivity was also detected in the neural plate, as confirmed by the prediction of co-expression with *Elav* detected with the ADAGE pipeline (Appendix VIII, Figure A8.4; the ADAGE pipeline is described in Appendix IV). This is a peculiar result that likely highlights a different mechanism from vertebrates. The cells that express Bmp2/4 are not the same that activate Smad1/5/8 phosphorylation: Bmp2/4 is in fact found in the anteriormost endoderm, the endoderm-mesoderm boundary, the presomitic mesoderm, the ventral blastoporal lip and the dorsolateral epidermis at N0, but is low or absent in the notochord, ventral endoderm, ventral epidermis and neural plate. Similarly, at 7ss it is found in the dorsal endoderm, somites, prechordal plate and lateral epidermis but not in the notochord, neural plate and ventral endoderm. The absence of Bmp activity in the dorsal side of the embryo also seems to be due to the expression of chordin in the notochord and floor plate through neurulation. However, curiously I found that in the posterior mesoderm, at the level of the prechordal plate, *Chd* and *Bmp2/4* are actually co-expressed, meaning that the presence of chordin does not block the transcription of *Bmp2/4* but likely inhibits its action through Smad1/5/8.

ACVR1 was expressed at much lower level than ACVR2: at N0, the first was found in the endoderm, ventral epidermis and at very low level in the neural plate, while the second was widely distributed across the embryo, though it was slightly lower in the epidermis (Figure 6.7). On the other hand, the expression of ACVR1 increased at 7ss, when it was found in the endoderm, notochord and nervous system. ACVR2 continued to be broad, but the highest level of expression was found in the notochord, specifically in the precursors of Muller cells, which form two rows around the central stack-of-coin layer. The two receptors therefore co-localized mostly ventrally and in the nervous system at N0 and more broadly at 7ss. The activity of Nodal signalling was found in the endoderm, the notochord (higher at the two poles) and the neural plate at N0. In the latter, PSmad2/3 was concentrated in medial cells. Conversely, at 7ss no immunoreactivity was detected in the neural tube, but the antibody labelled notochord, somites and endoderm. Similar to Bmp signalling, the ligand *Nodal* was not expressed in the areas where Smad2/3 is phosphorylated: at N0 *Nodal* was

highly expressed in the presomitic mesoderm and was also found in the neural plate, though mostly in lateral cells in which PSmad2/3 activity was not detected. At 7ss, *Nodal* transcripts were still found throughout the nervous system (except the floor plate), while in internal tissues the expression becomes polarized to the left side in the somites and endoderm. It is interesting to consider however that while *Nodal* expression is asymmetric, PSmad2/3 localization remains bilateral.

In summary, this analysis represented the first example of TGF $\beta$  receptors expression in cephalochordates and an attempt to combine receptors, ligands and effectors to obtain a complete view of the way two of the main developmental signalling pathways, Bmp and Nodal, act during amphioxus development. In the future, this data will be combined with experiments that manipulate these two pathways to understand how the changes previously highlighted in the literature are molecularly controlled.

## 6.4 Discussion

### 6.4.1 Patterning and evolution of the vertebrate CNS

Our analysis of zebrafish scRNAseq data showed that most aGRN genes are active in the hypothalamus and partially in the retina. These areas belong to the secondary prosencephalon, which forms the rostral portion of the vertebrate CNS (see Chapter III). This result was particularly fascinating as it not only strengthens the argument for an ancient and conserved system for ANE specification, but it provides a basis for understanding the origin of the complex vertebrate forebrain. In fact, previous work established the partial structure of the vertebrate “forebrain network”, revealing many similarities with the ANE specification in other deuterostomes (208, 209). The anterior neural plate forms in the absence of Wnt signalling, which is concentrated posteriorly (but is distanced from the anterior body due to elongation) and is repressed anteriorly by the presence of Wnt inhibitors (64, 209). *Otx* and *Six3/6* orthologs are initially required to define the anterior neural plate and likely confer competence to form the different forebrain derivatives (telencephalon, retina, hypothalamus) (211, 400). The secondary prosencephalon will then activate downstream genes such as *Fezf*, *Rx*, *Nk2.1*, *Lhx2* and *Pax6* that confer specific identities to the different forebrain regions depending on their combination and expression level (209). Moreover, the effects of Wnt/ $\beta$ -catenin disruption and of knock-down of aGRN genes are similar to those

described for invertebrate deuterostomes: early repression of Wnt signalling causes expansion of the secondary prosencephalon (telencephalon and hypothalamus), while ectopic expression of Wnt or removal of Wnt inhibitors causes loss of anterior structures (234, 401). However, Wnt ligands that regulate the specification and positioning of the ANE are produced not at the vegetal/blastoporal level, but in posterior brain areas. In particular, several studies have highlighted that Wnt8 and possibly Wnt3 produced by the prospective diencephalon function as posteriorizing signals inducing the expression of *Irx* in the diencephalon and repressing *Six3* (236, 401, 402). On the other hand, *Six3* represses Wnt expression in the hypothalamus and telencephalon, thus allowing their specification (210, 211, 403), and there is evidence of a dynamic restriction of *Six3* in the early neural plate from the prospective ZLI to the end of the hypothalamus (404, 405). Strikingly, the posteriorizing action of Wnt8 in the forebrain is mediated by Frz8 paralogs in zebrafish (402). This data strongly supports the homology of the aGRN that patterns the ANE, but also highlights key differences between vertebrate and invertebrate deuterostomes. One is the absence of early *FoxQ2* expression in vertebrate embryos. In fact, despite the extensive conservation of this gene across eumetazoans, until recently nothing was known about its presence, expression and function in vertebrates. The comparison of multiple genomes in recent years however revealed *FoxQ2* sequences in teleosts and sauropsids, and I found orthologs in most vertebrate taxa, with the exception of amphibians and mammals. The phylogenetic analysis of *FoxQ2* revealed three distinct families, all of which are represented in amphioxus, and possibly the presence of two *FoxQ2* paralogs (*FoxQ2a* and *FoxQ2b*) at the base of the vertebrates. However, in each lineage only a single paralog remains, while the other was lost.

By consulting available scRNAseq datasets of zebrafish development and using HCR I found that *FoxQ2a* is expressed after the hatching stage – confirming the absence of this gene in early development – in photoreceptor cells of the retina, and that this pattern persists in the adult. While I was preparing to investigate further which cell types express this gene, a fascinating paper was published detailing the function of zebrafish *FoxQ2* (213). The authors discovered that *FoxQ2* is necessary for the specification of blue cones by activating the expression of the blue opsin gene (*sws2*). Additionally, zebrafish *FoxQ2* is controlled by *Six6b* and *Six7*, which are both *Six3/6* orthologs (406). These results are particularly interesting as the retina is derived from the ANE, suggesting that a link between the ANE, the expression of *Six3/6* genes and *FoxQ2* is still present in vertebrates. The same study provided a synteny analysis of *FoxQ2* genes identified in bony fishes, showing how

the gene is still present in monotreme mammals (which retain blue cones) but was lost during the evolution of placental mammals together with the loss of blue vision (213). The compared genes belong to the *FoxQ2a* family, so it would be interesting to expand the synteny analysis to cartilaginous fishes and cyclostomes that possess *FoxQ2b* genes, and which are therefore expected to reside in different chromosomic locations. The function of *FoxQ2a* has also been investigated in echinoderms: in sea urchins and starfish the downregulation of *FoxQ2* does not lead to a defective AP axis, which forms rather normally, but causes the loss of ANE neurons and a disruption of the aGRN (155). Following *FoxQ2* knock-down, *Nk2.1* and *Fezf* expression is lost specifically from the sea urchin apical plate and serotonergic neurons fail to develop, and in starfish *Rx*, *Lhx2/9* and *Dkk3* are not activated (155, 157, 162). Interestingly, the ANE of sea urchin contains photoreceptor cells expressing a GO-opsin (407). Although the role of *FoxQ2* expression in photoreceptor development has not been tested in this species, the fact that *FoxQ2* is required to activate *Nk2.1* which is then expressed in photoreceptor cells suggests that this gene might have a conserved function in the specification of anterior sensory photoreceptors (408). Another interesting point that emerges from the phylogenetic analysis is that *FoxQ2c*, which contains a C-terminal EH-i-like motif, is an ancient paralog of *FoxQ2a*, and that each of the two genes has been lost in certain lineages and retained in others. Despite this dynamic evolutionary history, the embryonic expression of these genes remains similar to *FoxQ2a*: in amphioxus, hemichordates and annelids *FoxQ2c* is expressed in domains that are partially or totally overlapping with *FoxQ2a* (159, 361). Moreover, even in lineages that have lost *FoxQ2a*, such as in arthropods, *FoxQ2c* is expressed in the anterior portion of the neuroectoderm, supporting the conservation of the aGRN across bilaterians (195). This suggests that the two genes might have a partially redundant function, and consistently *FoxQ2c* was shown to regulate the expression of *Six3/6*, *Rx* and *Chx* and control the development of the central brain primordium in *Tribolium* (148).

Overall, the comparative analysis of *FoxQ2* genes supports an ancestral role of *FoxQ2a* (and likely *FoxQ2c*) in the specification and positioning of the ANE during early embryogenesis. But if *FoxQ2* is important for the correct formation of the ANE in bilaterians, and most other aGRN genes still contribute to the formation of the vertebrate forebrain in vertebrates, how can we explain its loss in the vertebrate aGRN? I thought that one possible explanation could be found in the evolution of the primary organizer. The organizer in fact was thought to have a role in the AP patterning of the nervous system, by specifying the prechordal plate that provided a source of Wnt inhibitors

necessary for forebrain specification (242). If a Wnt gradient was sufficient to give positional information, that could provide a possible scenario for the evolution of aGRN in vertebrates. However, in zebrafish the neural plate can be correctly patterned antero-posteriorly even in the absence of the organizer if Bmp activity is suppressed (389). I have also confirmed previous studies showing that a similar mechanism is present in amphibians, indicating that it might be ancestral to vertebrates.

The primary organizer therefore has mainly a role in DV patterning by inhibiting Bmp signalling to allow the dorsal specification of the neuroectoderm. As will be further explained in Chapter VII, this suggests that the evolution of the chordate CNS was mostly guided by the changes in neuroectoderm specification and positioning, while the patterning and regionalization relied on ancient and conserved networks, including the aGRN. Following this hypothesis, I became interested in how the function of Bmp in neural specification changed during chordate evolution. In amphioxus, Bmp is able to repress neural fate, indicating that it is an ancestral chordate function, but its downregulation is not sufficient to expand the neural plate throughout the ectoderm, as Nodal activity is also necessary (393, 395). I therefore looked at the distribution of Nodal and Bmp signalling in amphioxus. Bmp receptors are highly expressed during the early phases of neural development, showing the competence of the neural plate to respond to Bmp signalling and providing an explanation for the requirement of dorsal Bmp inhibitors. Interestingly, while *BMPR1* and *ACVR2* were highly expressed, their counterparts *BMPR2* and *ACVR1* were very low throughout neurulation. As in vertebrates *ACVR2* is known to interact with both Nodal and Bmps, the expression pattern described here might indicate that a similar mechanism pre-dated the origin of vertebrates (399). In general, the analysis showed a conserved function for Smad1/5/8-mediated Bmp signalling on the ventral side and a Smad2/3-mediated Nodal signalling on the dorsal side (but also in the endoderm). At the same time, the co-localization analysis revealed important differences between amphioxus and vertebrates. First, in the tailbud region *Bmp2/4* and *Chd* are co-expressed, although *Chd* action is sufficient to inhibit Bmp activity. Second, during neurulation *Bmp2/4* is upregulated in the anterior portion of the ectoderm, at the interface between the anterior tip of the CV and the epidermis, corresponding to the expression domain of *Six3/6*. In vertebrates, Bmp activity in the anterior non-neural ectoderm has a role in the regionalization of the forebrain and *Bmp4* was shown to have a mutually antagonistic relationship with *Six3* (409). This is drastically different from the condition in amphioxus, in which *Bmp2/4* and *Six3/6* are co-expressed but Bmp

signalling does not seem to be active in the anterior epidermis. If *Bmps* and *Six3/6* acquired mutually repressive roles during vertebrate evolution, then this together with the loss of *FoxQ2* might explain the restriction of the aGRN in the neuroectoderm, where *Bmp* signalling is blocked by chordin and other organizer-derived inhibitors.

#### 6.4.2 Conclusions

A question that remained unanswered in the previous chapters was how the aGRN evolved in the vertebrate lineage and how this might have impacted the evolution of the chordate brain. Naturally, this vast subject cannot be solved in a few paragraphs, but here I have explored two main aspects that can help to explain the similarities and differences in CNS development between amphioxus and vertebrates:

- ◆ One of the main differences in the aGRN in vertebrates is the absence of early *FoxQ2* expression. However, I found that this gene is still conserved in most vertebrate taxa and had a complex and dynamic evolutionary history. The data suggests that three paralogs were present in the bilaterian ancestor, two of which are still found in vertebrates, though each lineage retains only one. The expression in zebrafish further suggests that *FoxQ2* remained associated with the ANE but lost the early function in providing positional information.
- ◆ This early loss might be due to changes in the specification of the body axes during the chordate lineage. In fact, while an organizer is present in amphioxus and vertebrates, and necessary for the correct formation of the DV axis, there are differences in the action of *Bmp* and Nodal signalling. I have first combined previous data with experiments on *Xenopus laevis* to show that these differences are not due to a direct action of the organizer on the AP regionalization of the nervous system. I have then dissected *Bmp* and Nodal signalling in amphioxus neurulation, showing a general conservation of their roles in chordate DV axis formation but also highlighting the absence of *Bmp* signalling in the anterior ectoderm.

These results leave many exciting questions open for future studies. First, how exactly did *FoxQ2* lose its early function? One way to find out would be to combine analysis of cis-regulatory sequences with misexpression of *FoxQ2* early in zebrafish development, to understand whether it can still control the expression of aGRN genes or if the network structure has changed more profoundly. Second, a more refined view on *Bmp* roles in the development of the amphioxus nervous system is

required to explain some of the differences with vertebrates. For example, while in vertebrates Bmp inhibition is sufficient to turn the whole ectoderm neural, it does not work in the same way in amphioxus. It would be ideal to explore the evolution of Bmp function, examining the changes in the receptors and effector distribution when Bmp signalling is misregulated. Third, if Bmp signalling and the organizer are primarily required for DV axis specification, a fascinating question remains on how the precise AP regionalization of the nervous system is controlled in vertebrate embryos, and in particular how the early forebrain fate, characterized by the aGRN, is initially specified.



# Chapter VII – Discussion

## 7.1 The evolution of the chordate nervous system

### 7.1.1 Tracing the origin of the chordate brain

The evolution of the nervous system has long been a source of fascination for biologists, because of its control of behaviour, which is key to the survival and success of animals, as well as its incredible complexity. This is perhaps particularly true for our own brain, often conceitedly defined as “the most complex object in the known universe”, since it is responsible for many of the traits and abilities that we consider uniquely human, such as imagination and autonoetic consciousness (410, 411). Despite our great interest in the origin of the brain in our phylum, the diversity of neural architectures in metazoans has made it difficult to reconstruct the deep evolutionary history of the nervous system. Consequently, to this day several hypotheses propose different and sometimes conflicting scenarios for the origin of the chordate CNS (reviewed in (63, 136, 227)).

- ◆ The chimeric brain hypothesis considers the similarities between the CNS in annelids, arthropods and chordates, and their relationship to the diffuse nervous system of cnidarians. It proposes that two distinct networks were present in the eumetazoan ancestor controlling the formation of an apical nervous system and a blastoporal nervous system (17, 412). These two systems were then integrated in the bilaterian ancestor that had a chimeric CNS, in which the apical component gave rise to photosensory, circadian and neurosecretory regions while the blastoporal component formed the sensory/locomotory cords controlling muscles, separated based on their dorsoventral position in the neuroectoderm. According to the chimeric brain hypothesis therefore part of the secondary prosencephalon is homologous to the AO of ambulacrarians and the brain of annelids, while the rest of the neural tube is homologous to the nerve cord of annelids and possibly of enteropneust hemichordates. Even though a common origin of the anterior nervous system has been speculated by other authors (146, 148, 413), the analysis of a growing number of phyla has challenged the homology of the blastoporal nervous system, as it was shown that the DV patterning of the CNS and the role of Bmp signalling in CNS development have changed dynamically over the course of evolution (28, 29).

- ◆ Similarly, Burke postulates that the ancestral deuterostome had a “bipartite” nervous system, made of animal and axial portions (138). In echinoderms and hemichordates, the two portions are separated across the life cycle, with the animal portion in the larva and the axial portion in the adult, while in chordates they form at the same time. This hypothesis considers the posterior brain and spinal cord of vertebrates homologous to the dorsal nerve cord of echinoderms and hemichordates, but there is currently no agreement on whether these structures are in fact related, given the diversity of gene expression and developmental origin (92). Moreover, in this scenario it remains unclear which condition was ancestral and how the structure of the chordate CNS evolved.
- ◆ By investigating the molecular regionalization of the hemichordate body, Lowe and collaborators showed that the ectoderm of hemichordates is patterned in the same way as the chordate CNS and possesses homologs of the vertebrate brain organizers (98, 161). Thus, they hypothesized that the diffuse nerve net might be homologous to the chordate CNS (92, 226). With this premise, the anterior portion of the hemichordate ectoderm in which the aGRN is active forms the AO in indirectly-developing species and the proboscis, and is homologous to the vertebrate forebrain. The medial portion that forms the adult collar corresponds to the midbrain, and the posterior region that forms the adult trunk is homologous to the hindbrain and spinal cord. In the scenario proposed by Lowe, the diffuse net was ancestral to deuterostomes and it was “condensed” into the CNS of vertebrates, but the alternative assumption is equally probable based on this data. However, in both cases the origin of the hemichordate and echinoderm nerve cords remain unexplained, and a better understanding of how these structures are molecularly specified is needed for appropriate comparisons (166, 414).
- ◆ Other scenarios consider the larvae of ambulacrarians, protostomes and chordates as secondary independent acquisitions, hence refuting the homology of AOs (29, 30, 140). Some of these hypotheses regard the adult nerve cords of ambulacrarians as homologous to the chordate CNS (136). The majority of them posit a complex bilaterian ancestor already possessing a brain, which was lost in the ambulacrarian lineage, while the AO was co-opted in several lineages independently. However, these hypotheses have several shortcomings. First, the high conservation of the ANE across Eumetazoa makes it less parsimonious to consider it convergent in several larval forms. Second, as for the chimeric brain, molecular studies have also shown a large degree of divergence in the patterning of bilaterian nerve

cords, compared to the high conservation of ANE patterning, which remains unexplained under these premises. Third, there are several problems in the comparison with the ambulacrarian lineage. Little is known about the development of the adult nervous system in echinoderms, but the preliminary data on gene expression suggests that the nerve cords in each arm are patterned differently than the chordate CNS (415). Moreover, the adult nervous system forms only after metamorphosis, but the similarities between hemichordates and chordates start early in development. If the echinoderm and hemichordate adult cords are homologous, the differences in the way they are specified remains unexplained. Finally, adult enteropneust hemichordate have two nerve cords (dorsal and ventral), but their relationship with the chordate CNS remains highly contentious, therefore it is unclear which one would correspond to the vertebrate CNS.

The work presented in this thesis provides new data that contributes to this debate. I showed that the aGRN that contributes to the development of the AO in ambulacrarians (and other eumetazoans) is conserved in chordates. The network can be reconstructed in amphioxus, in which early and late phases corresponding to those found in ambulacrarians can be distinguished. In the early phase, upstream aGRN genes (*FoxQ2*, *Six3/6*, *Frz5/8*) are expressed throughout the animal side of the embryo, before the specification of the neuroectoderm, while on the vegetal side Wnt/ $\beta$ -catenin signalling prevents their expression and specifies vegetal/posterior fate. At gastrulation the aGRN genes restrict towards the anterior/animal pole, where Wnt inhibitors (*sFRP1/2/5a* and *Dkk3*) likely block their downregulation. During neurulation, downstream aGRN genes (*Fezf*, *Rx*, *Otx*, *Nk2.1*, *Lhx2/9*) are activated on the anterior portion of the neural plate that develops within the aGRN domain. The ectodermal expression of aGRN genes in amphioxus is negatively regulated by Wnt signalling as in ambulacrarians, so that Wnt overactivation leads to the downregulation of the entire network. The anterior neural plate shows specific proliferation and neurogenic profiles, giving rise to neurons of the anterior CV at the larval stage. These include serotonergic neurons, one of the hallmarks of AOs, and contain sensory and neurosecretory populations that show extensive similarity to vertebrate retino-hypothalamic cell types. The retina and hypothalamus in vertebrates are part of the secondary prosencephalon, which is the area that shares most molecular similarity with the AO of ambulacrarians and the amphioxus CV. The function of the aGRN within the anterior neural plate is to determine anterior identity in the CV: downregulating aGRN genes after the

specification of the neural plate (by Wnt overactivation) does not affect the number of neurons in the CNS but anterior neurons lose their identity and acquire a more posterior fate.

Taking all the results together, I propose that the aGRN is conserved and homologous in bilaterians. The ancient network is composed of at least 12 genes, including transcription factors (*FoxQ2*, *Six3/6*, *Fezf*, *Rx*, *Otx*, *Nk2.1*, *Lhx2/9* and *Hbn*), a Wnt receptor (*Frz5/8*) and Wnt inhibitors (*sFRP1/2/5*, *Dkk1* and *Dkk3*) (Figure 7.1). It is highly likely that this network evolved from a more ancient one that was present in the Eumetazoa ancestor, but it was modified in the early evolution of bilaterians (see below). This network contributes to define the animal-vegetal axis, possibly by instructing cells with positional information that guide them to animal fate, and is necessary to specify the anterior neuroectoderm (ANE), which is also homologous in all bilaterians. In the larvae of many marine ciliated larvae the ANE will develop into the AO, while in chordates the ANE specify the anterior portion of the CNS. The data on amphioxus also suggests that the aGRN works by instructing neurons that develop under its influence (within the ANE) with an “anterior” sensory-neurosecretory fate. Therefore, the aGRN is an ancient network that functions irrespective of the nervous system organization, the degree of centralization and the pattern of neurogenesis in a particular taxon. However, its anterior position and the integrative sensory/neurosecretory fate of its neurons support the notion that the ANE is a “centralized” component of the nervous system in bilaterians.

I also propose a scenario for the evolution of the nervous system in deuterostomes, summarized in Figure 7.1. The ancestral deuterostome possessed an ANE patterned by an aGRN, which was active early during development and controlled by vegetal Wnt/ $\beta$ -catenin signalling. The appearance, life cycle and ecology of this ancestor are still highly debated: a recent review combining paleontological and molecular data supported a vermiform motile animal with an indirect development characterized by a simple larval phase, but sessile ancestors have also been hypothesized (416). The data presented here does not allow to settle this debate but provide support for an ancestral indirect development, given the similarities between deuterostome larvae, including crinoids. It also indicates that an ANE was present in this ancestor, possibly specifying sensory-neurosecretory cell types. If a larva was indeed present at the base of deuterostomes, I speculate that it had an AO-like structure with serotonergic neurons, although the cell type composition might have been different from modern larvae. From the deuterostome ancestor, in the ambulacrarian lineage a dipleurula-

type larva evolved from the ancestral deuterostome larva. The aGRN was conserved in the chordate lineage, was still active from early development and controlled by vegetal Wnt/ $\beta$ -catenin signalling. In chordates however neurogenesis became restricted to the dorsal side of the animal, probably through a neuroinhibitory function of Bmp opposed by the dorsal organizer. The position of the neuroectoderm meant that only the anterior region of the neural plate was under the influence of the aGRN and acquired a sensory-neurosecretory character. The chordate ANE forms the rostral portion of the forebrain, the secondary prosencephalon. This condition is still visible in amphioxus, in which the aGRN patterns the anterior ectoderm, both neural and non-neural. On the other hand, during vertebrate evolution the network was restricted to the neuroectoderm, started later in development and lost one of its upstream components, *FoxQ2*. The expression of aGRN genes was still controlled by Wnt/ $\beta$ -catenin signalling, but the source of Wnt ligands is the posterior forebrain and midbrain rather than the vegetal side of the embryo. Possible explanations for this modification will be considered in the next sections.

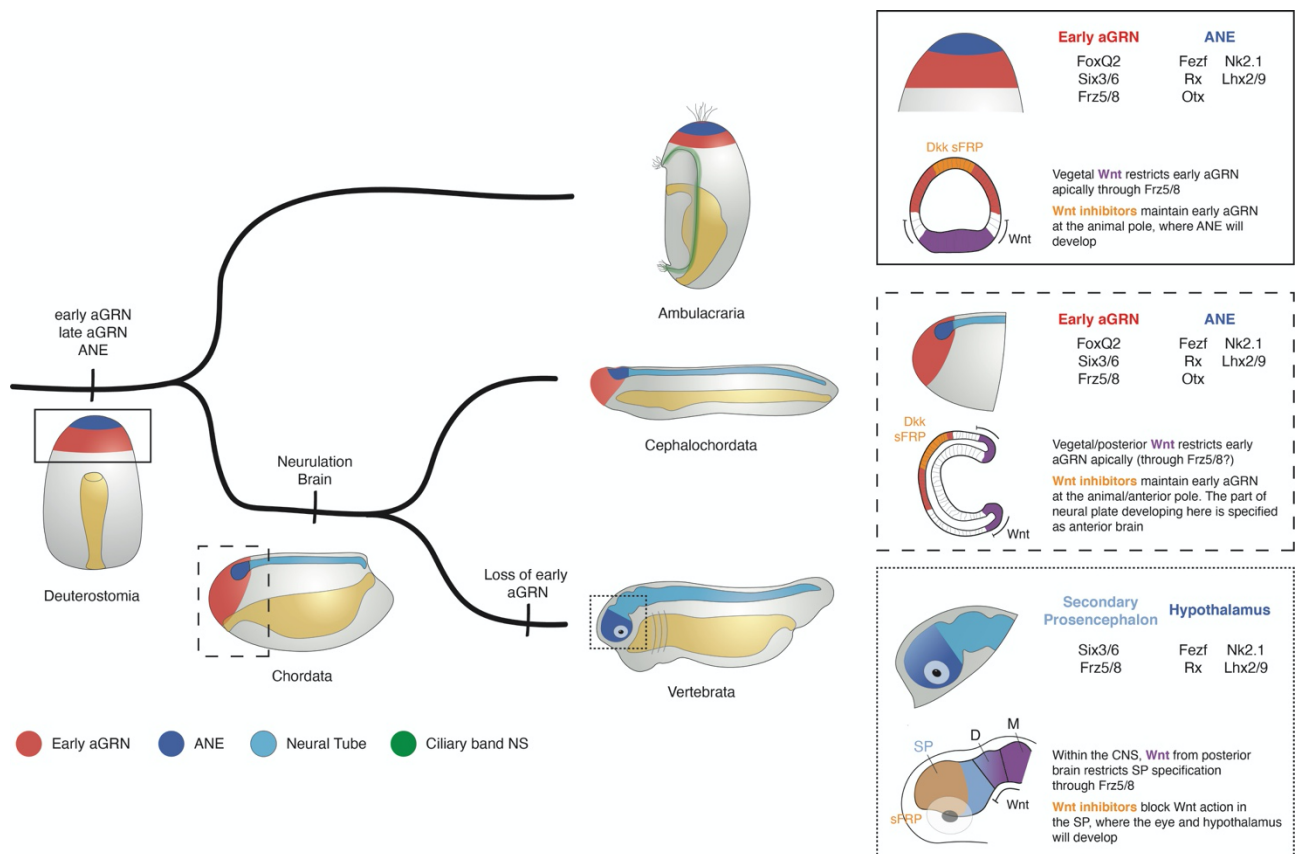


**Figure 7.1.** Proposed scenario for nervous system evolution in deuterostomes.

The scenario described here considers the AO of echinoderms and hemichordates larvae as homologous to the chordate “secondary prosencephalon” region. The similarity in AP gene expression between the hemichordate ectoderm (in both larva and juvenile) and the chordate CNS suggests the correspondence between the nerve net of hemichordates and the CNS of chordates, as previously suggested (161). The radialized pattern of AP markers seen in vertebrates in the absence of the organizer and Bmp signalling further supports this hypothesis (389). As a consequence, the deuterostome ancestor might already have had a regionalized CNS. However, it is important to stress that this study does not allow to resolve which organization was ancestral to deuterostomes: the ancestor could have had a poorly centralized system that was then dorsalized in the chordate lineage, or it could already possess nerve cords/tubes that were secondarily lost in the ambulacrarian lineage. But how do echinoderms fit in this framework? The analysis of crinoid development demonstrated that the AO forms in all echinoderm classes within the apical plate where *Six3/6* and *FoxQ2* are expressed, further supporting the ancestral origin of the ANE. The adult nervous system is more difficult to consider. I show in Appendix II that in the crinoid post-metamorphic stage, the pentacrinoid, *Six3/6* and *Lhx2/9* are expressed in the oral region, where the ectoneural system forms. This result provides strong support for the correspondence of the echinoderm OA axis of adult echinoderms with the AP axis of adult hemichordates (136, 268). However, the AP axis of adult indirect-developing hemichordates derives from the AV axis of the larva, and the expression of anterior genes such as *Six3/6* is continuous through metamorphosis (160, 165). Similarly. In amphioxus the animal portion of the embryo/larva where aGRN genes are expressed corresponds to the head of the adult. The tissue that forms the oral ectoderm of crinoids (and other echinoderms) instead derives from the lateral vestibular ectoderm of the larva, where anterior markers are not expressed in the larva. In fact, ectodermal expression of both *Six3/6* and *Lhx2/9* disappears in the settled doliolaria larva of *A. mediterranea* and only resumes in the vestibular ectoderm in the cystidean stage (Appendix II). Based on these results, it is possible that at least a portion of the aGRN has been co-opted in adult echinoderms to specify the oral/ectoneural nervous system, which however is not homologous to the ANE of hemichordates and chordates.

Finally, the comparison with protostomes and cnidarians supports the conservation of the aGRN across eumetazoans: in all these groups it is possible to identify a *Six3/6*- and *FoxQ2*-positive apical plate, controlled by vegetal Wnt signalling through *Frz5/8*, within which an AO develops (200, 203, 204). However, some of the “late network” genes, such as *Hbn* and *Nk2.1*, as well as genes associated

with the ANE like *Otp* are expressed at the vegetal pole in cnidarians (207). This suggests that the “early aGRN” can be traced back to the eumetazoan ancestor, but it modified extensively during bilaterian evolution to integrate components that were previously separated. This could be partially in support of the chimeric brain hypothesis, although the divergence of the DV patterning in bilaterians remains to be explained. Another hypothesis is that in bilaterians there has been a partial inversion of the AV axis, as previously suggested (417), such that the “early aGRN” present in the ancestor of the bilaterians was located on the same side as these “late” genes, and then started to control them. Alternatively, it could be that the AO of cnidarians and bilaterians share only a portion of the network and are not homologous as a structure.

### 7.1.2 The complex simplicity of the amphioxus nervous system

Due to their key phylogenetic position as the sister group to the other chordates, cephalochordates are compared to vertebrates (and less often tunicates) to reconstruct the evolution of our phylum. By elucidating the ancestral features of the chordate neural tube we can understand how the CNS in modern descendants, and in particular the vertebrate brain, evolved. The analysis of aGRN conservation in deuterostomes showed that the rostral portion of the neural plate of amphioxus, which forms the anterior CV, is homologous to the secondary prosencephalon, and at the larval stage is composed of retina-like and hypothalamic-like components. The frontal eye complex contains at least five cell types that have been previously shown to have transcriptional and functional similarities to the vertebrate retina (88). The ventral portion of the anterior CV, roughly corresponding to the intercalated *Six3/6*-negative domain up to the infundibular organ, comprises cell types with a hypothalamic signature highlighted by the expression of *Otp*, *Bsx*, *FoxD* and *miR-7*. Most of these cells are born during neurulation, demonstrating the presence of intercalated addition of cells that is required to form the full repertoire of the brain. The anterior CV continues to grow in the long larval period, and after metamorphosis shows a new dorsal population of cells, the PAD, that include glutamatergic and GABAergic neurons and a transcriptional pattern similar to the vertebrate telencephalon (106). Moreover, the expression of hypothalamic markers *Otp* and *Vt* is still detected in the ventral portion of the brain. While the reason for the drastic heterochrony in the activation of telencephalic markers remains to be explained, these results suggest that the chordate ancestor already possessed an anterior secondary prosencephalon molecularly regionalized into distinct functional components. Caudal to the infundibular organ, the posterior

CV was previously hypothesized to be a di-mesencephalic (DiMes) domain that in vertebrates was further regionalized into diencephalon and mesencephalon (87). While my results do not dispute this hypothesis, the expression of *Six3/6* in amphioxus in this region remains problematic. In vertebrates, *Six3/6* is expressed primarily in the secondary prosencephalon, although there is some evidence of an early expression in the diencephalon that is quickly downregulated in the early neural plate (232, 405). It is possible that in amphioxus the posterior *Six3/6* is not repressed, or alternatively the persistence of *Six3/6* could be a modification specific to the cephalochordate lineage. Interestingly, *Frz5/8* is not expressed in this posterior brain region in amphioxus, possibly indicating that Wnt signalling is not able to repress *Six3/6* there.

Previous studies have described the pseudo-segmented expression of several markers posterior to the cerebral vesicle. This, together with the presence of ventrolateral GABAergic, glycinergic and cholinergic cell types, justified the homology of this region with the vertebrate hindbrain (86, 87, 221). In this study, I reveal an unexpected complexity of these early neural populations which are divided in several subtypes expressing distinct transcription factors and neuropeptides. The low number of cell types and the absence of proliferation mean that in future studies each of these neurons could be followed to look at their contributions and functions in detail. In late larval stages, the number and location of differentiated neurons increase drastically, and the DV distribution of cell types resembles the one seen in the vertebrate neural tube, with dorsal glutamatergic and GABAergic neurons and a ventral concentration of cholinergic cells that likely include motoneurons. The ANE, DiMes and hindbrain are specified early in amphioxus, while the posterior spinal cord region is very small and undifferentiated during neurulation, shows a remarkably different pattern of neurogenesis and is initially involved in body elongation. In larval stages neurogenesis resumes in this region, and mature neurons start to appear only in late larvae. This pattern is consistent with other bilaterians in which the anterior portion of the ectoderm is the first to form during development (97, 160, 413). However, similar to indirect developing hemichordates and annelids it also shows that the more posterior regions do not form only after metamorphosis in “minimally indirect” developers but grow slowly from the posterior portion of the body.

Overall, the comparison of CNS in chordates suggests that the ancestral neural tube was already complex and regionalized in at least three or four domains. This would indicate that the AP and DV regionalization of the nervous system might pre-date the evolution of chordates, but was then

modified independently in each deuterostome phylum. If the ancestral chordate brain was already relatively complex, the evolution of the vertebrate brain may have built on this complexity by vastly increasing the number of cells and the diversity of cell types.

### 7.1.3 The evolution of the vertebrate forebrain

The conserved aGRN acted from early development on the animal side of the embryo in ancestral chordates, in both neural and non-neural progenitors. In vertebrates instead aGRN genes are expressed only within the secondary prosencephalon after it has formed. While the similarities between the ANE of ambulacrarians and the vertebrate forebrain have been described before (146, 408), these differences remain unexplained. The loss of *FoxQ2* expression in vertebrates might be a major contributor to these differences. *FoxQ2* is one of the upstream factors in the aGRN and the first to be expressed in both ambulacrarians and cephalochordates. Conversely, it is not expressed during embryonic development in any vertebrate studied to date. It is possible that together with the loss of early *FoxQ2* expression there was a shift in the activation of the aGRN, which came under the control of neurogenic transcription factors. In support of this scenario, previous research demonstrated that *Six3* expression in vertebrates is activated by *Sox2*, a member of the SoxB family (418, 419). Interestingly, *FoxQ2* has not been lost from the vertebrate genome, and in zebrafish it is expressed in the retina after hatching. It is possible that *FoxQ2* maintained part of its specification functions in the development of the retinal photoreceptors, leading to a drastic heterochronic shift in its expression. It would be interesting to examine the effect of ectopic activation of *FoxQ2* early in zebrafish development, to understand whether it could still act in an early aGRN phase or whether the regulatory interactions have been completely modified during vertebrate evolution.

The localization of Wnt ligands and receptors and the results of Wnt overactivation in early amphioxus embryos indicate that vegetal Wnt signalling is responsible for the restriction of early aGRN markers to the animal side, as in ambulacrarians. Recent data has also shown that maternal Wnt/ $\beta$ -catenin signalling is required for the correct formation of the primary organizer and the correct DV patterning of the embryo (241). This function is also found in vertebrates, suggesting that it is ancestral to chordates, but maternal Wnt/ $\beta$ -catenin signalling does not have a direct effect on AP patterning and the expression of aGRN genes. By blocking early Wnt/ $\beta$ -catenin signalling as well as *Bmp* the expression of neural markers across the AP axis, including aGRN genes such as *Rx* and

*Otx*, was not impaired (389). Instead, the expression of aGRN markers within the secondary prosencephalon is regulated by a different source of Wnt ligands, the diencephalon (234, 402, 420).

It is not possible with the present data to determine the timing and sequence of these changes, but I hypothesize that during vertebrate evolution the expression of *FoxQ2* was lost and the early aGRN came under the control of *Sox2*, which is expressed throughout the early neural plate and tube. During neurogenesis, zygotic Wnt signalling specifies posterior fates and represses *Six3/6* orthologs in most of the neural tube, and additional Wnt ligands produced in the diencephalon, mesencephalon and MHB restricts the expression of *Six3* and the rest of the aGRN to the secondary prosencephalon, where it specifies the ANE. It should be noted however that the precise control of early *Six3* expression and forebrain specification in vertebrates is not completely understood, and new candidates might be discovered in the future (209).

## 7.2 Conclusions and future directions

The results presented in this thesis elucidate the evolutionary origin of the chordate secondary prosencephalon as part of an ancient and conserved ANE, controlled by a highly conserved regulatory network (aGRN) and involved in the integration of sensory information and in physiological and motor control through both neurotransmitter and neuropeptide release. This scenario is in accordance with similar hypotheses that have been proposed in the last decade (146, 408) but provides direct comparative evidence between chordates and ambulacrarians and a mechanism that accounts for the conservation of the aGRN as well as the drastic modifications in neural organization in each deuterostome phylum.

The quest to reconstruct the evolution of the nervous system in deuterostomes however is far from over. One of the main questions that stems from this and other works is that changes in how and where neurogenesis is started in the ectoderm have had a significant impact on the evolution of the nervous system. One of the functions of the ancient aGRN is to confer anterior identity to neurons regardless of their organization. Whether they are organized in a neural tube as in chordates, in a nerve net like adult hemichordates, in an AO forming from a restricted group of neural cells as in sea urchin or from more scattered progenitors as in starfish, the neurons that develop within the domain in which the aGRN is active will form the ANE. In future studies, a focus on how

neuroectoderm specification is controlled in different phyla will hopefully help us reconstruct the dynamic history of deuterostome nervous systems.

The structure of the chordate aGRN must be further elucidated to understand the evolution of the forebrain in more detail. In vertebrates, it would be interesting to test whether *FoxQ2* can still function in the early stages if ectopically expressed, and to elucidate how the expression of *Six3/6* and *Otx* paralogs is controlled in the anterior neural plate. In amphioxus, which once again demonstrated its potential in retracing the evolution of our phylum, many queries still await an answer. A logical continuation of this project would be to investigate the structure of the aGRN by misregulating the expression of each gene (either by morpholino knock-down or overexpression through mRNA injection) and examine their effect. As injections are tricky in amphioxus, mainly due to the low survival rate, during my PhD I have tried to use vivo-morpholinos, which can supposedly enter cells without need of injection thanks to the addition of a molecular transporter (421), but without success (data not shown). From a developmental point of view, I was also fascinated by the unexpected cell type diversity that forms in such a small and simple nervous system. I have shown that for the amphioxus brain molecular patterning as well as precisely timed cell division are involved in generating the cell type repertoire of the retina- and hypothalamus-like regions. It would be intriguing to extend this analysis to the hindbrain, where ventrolateral cells do not proliferate during neurulation but form several distinct cell types. Moreover, most analyses on chordate nervous system evolution have focused on the molecular specification of cell types, but in the future these studies should be integrated with new work on the function and connectivity of the different brain regions: what is the function of the amphioxus CV, and how is it connected to the rest of the nervous system? These functional questions extend beyond chordates: to this date very little is known about how AOs work in ambulacrarians and what are their precise roles in bilaterian larvae. Similarly, although hemichordates are in a unique position to reconstruct the evolution of deuterostomes, most of the studies up until now have focused on early patterning, but examining the cell type composition of the enteropneust nervous system will be essential for a more complete comparison with chordates and echinoderms. The rapid expansion of connectomics and scRNAseq techniques on a variety of organisms will certainly help answering these questions in the near future.

Finally, although I focused on the extensive similarities between the amphioxus and vertebrate nervous systems, more than 500 million years of evolution since the split from their ancestor led to

several differences in the neural architecture in each lineage. In particular in amphioxus there are numerous specialized cell types, like Joseph cells, Hesse organs (photoreceptors) and the Rhode cells whose origin is completely unknown. Similarly, each vertebrate taxon has specific cell types in the forebrain that are emerging from scRNAseq studies (353, 422). A new and exciting field is now starting to examine how, from a similar and conserved developmental starting point, these different cell types have evolved in each lineage.

The last two decades have seen a true revolution in the way we study and understand animal evolution. We are now closer than ever before to elucidate the relationships between all metazoan taxa and trace the origin of their complexity, but at the same time each discovery introduces new exciting questions. As for many other aspects of the animal body plan, we are discovering that evolution has built on ancient and conserved molecular mechanisms to produce the diversity of neural architectures that we see in modern species. By continuing to expand our knowledge on the development and physiology of a growing number of animals, we will be able to reconstruct the evolution of the nervous system throughout the tree of life that in Darwin's words "*fills with its dead and broken branches the crust of the earth, and covers the surface with its ever-branching and beautiful ramifications*".

# Bibliography

1. R. Dawkins, *The selfish gene* (Oxford University Press, 1976).
2. A. Verkhatsky, Early evolutionary history (from Bacteria to Hemichordata) of the omnipresent purinergic signalling: A tribute to Geoff Burnstock inquisitive mind. *Biochem Pharmacol.* **187**, 114261 (2021).
3. C. P. Ponting, L. Aravind, J. Schultz, P. Bork, E. v Koonin, Eukaryotic signalling domain homologues in Archaea and Bacteria. Ancient ancestry and horizontal gene transfer. *J Mol Biol.* **289**, 729 (1999).
4. H. Plattner, A. Verkhatsky, The ancient roots of calcium signalling evolutionary tree. *Cell Calcium.* **57**, 123–132 (2015).
5. A. M. Castelfranco, D. K. Hartline, Evolution of rapid nerve conduction. *Brain Res.* **1641**, 11–33 (2016).
6. A. Pires-daSilva, R. J. Sommer, The evolution of signalling pathways in animal development. *Nat Rev Genet.* **4**, 39–49 (2003).
7. N. Riebli, H. Reichert, "The first nervous system" in *The Wiley-Blackwell Handbook of Evolutionary Neuroscience* (2016), pp. 125–152.
8. G. Jékely, The chemical brain hypothesis for the origin of nervous systems. *Philosophical Transactions of the Royal Society B: Biological Sciences.* **376**, 20190761 (2021).
9. N. D. Holland, Early central nervous system evolution: an era of skin brains? *Nat Rev Neurosci.* **4**, 1–11 (2003).
10. P. Simion, H. Philippe, D. Baurain, M. Jager, D. J. Richter, A. di Franco, B. Roure, N. Satoh, É. Quéinnec, A. Ereskovsky, P. Lapébie, E. Corre, F. Delsuc, N. King, G. Wörheide, M. Manuel, A large and consistent phylogenomic dataset supports sponges as the sister group to all other animals. *Current Biology.* **27**, 958–967 (2017).
11. M. L. Borowiec, E. K. Lee, J. C. Chiu, D. C. Plachetzki, Extracting phylogenetic signal and accounting for bias in whole-genome data sets supports the Ctenophora as sister to remaining Metazoa. *BMC Genomics.* **16** (2015), doi:10.1186/s12864-015-2146-4.
12. N. King, A. Rokas, Embracing uncertainty in reconstructing early animal evolution. *Current Biology.* **27** (2017), pp. R1081–R1088.
13. C. W. Dunn, G. Giribet, G. D. Edgecombe, A. Hejnol, Animal phylogeny and its evolutionary implications. *Annu Rev Ecol Evol Syst.* **45**, 371–395 (2014).
14. G. Jékely, J. Paps, C. Nielsen, The phylogenetic position of ctenophores and the origin(s) of nervous systems. *Evodevo.* **6** (2015), , doi:10.1186/2041-9139-6-1.
15. J. M. Musser, K. J. Schippers, M. Nickel, G. Mizzon, A. B. Kohn, C. Pape, P. Ronchi, N. Papadopoulos, A. J. Tarashansky, J. U. Hammel, F. Wolf, C. Liang, A. Hernández-Plaza, C. P. Cantalapiedra, K. Achim, N. L. Schieber, L. Pan, F. Ruperti, W. R. Francis, S. Vargas, S. Kling, M. Renkert, M. Polikarpov, G. Bourenkov, R. Feuda, I. Gaspar, P. Burkhardt, B. Wang, P. Bork, M. Beck, T. R. Schneider, A. Kreshuk, G. Wörheide, J. Huerta-Cepas, Y. Schwab, L. L. Moroz, D. Arendt, Profiling cellular diversity in sponges informs animal cell type and nervous system evolution. *Science* (1979). **374**, 717–723 (2021).
16. D. Arendt, E. Benito-Gutierrez, T. Brunet, H. Marlow, Gastric pouches and the mucociliary sole: Setting the stage for nervous system evolution. *Philosophical Transactions of the Royal Society B: Biological Sciences.* **370**, 20150286 (2015).
17. D. Arendt, M. A. Tosches, H. Marlow, From nerve net to nerve ring, nerve cord and brain-evolution of the nervous system. *Nat Rev Neurosci.* **17**, 61–72 (2016).
18. C. Nielsen, Life cycle evolution: Was the eumetazoan ancestor a holopelagic, planktotrophic gastraea? *BMC Evol Biol.* **13** (2013), doi:10.1186/1471-2148-13-171.
19. D. Arendt, A. S. Denes, G. Jékely, K. Tessmar-Raible, The evolution of nervous system centralization. *Philosophical Transactions of the Royal Society B: Biological Sciences.* **363**, 1523–1528 (2008).
20. C. B. Albertin, C. W. Ragsdale, More than one way to a central nervous system. *Nature.* **553**, 34–36 (2017).
21. L. Z. Holland, J. E. Carvalho, H. Escrava, V. Laudet, M. Schubert, S. M. Shimeld, J.-K. Yu, Evolution of bilaterian central nervous systems: a single origin? *Evodevo.* **4**, 1–20 (2013).

22. R. G. Northcutt, Evolution of centralized nervous systems: Two schools of evolutionary thought. *PNAS*. **109**, 10626–10633 (2012).
23. L. W. Swanson, What is the brain? *Trends in Neuroscience*. **23**, 519–527 (2000).
24. E. Perea-Atienza, K. Hoff, B. Gavilán, M. Chiodin, J. F. Abril, K. J. Hoff, A. J. Poustka, P. Martinez, The nervous system of Xenacoelomorpha: A genomic perspective. *Journal of Experimental Biology*. **218**, 618–628 (2015).
25. J. G. Achatz, P. Martinez, The nervous system of *Isodiametra pulchra* (Acoela) with a discussion on the neuroanatomy of the Xenacoelomorpha and its evolutionary implications. *Front Zool*. **9**, 1–21 (2012).
26. A. Hejnlol, K. Pang, Xenacoelomorpha's significance for understanding bilaterian evolution. *Curr Opin Genet Dev*. **39**, 48–54 (2016).
27. H. Philippe, A. J. Poustka, M. Chiodin, K. J. Hoff, C. Dessimoz, B. Tomiczek, P. H. Schiffer, S. Müller, D. Domman, M. Horn, H. Kuhl, B. Timmermann, N. Satoh, T. Hikosaka-Katayama, H. Nakano, M. L. Rowe, M. R. Elphick, M. Thomas-Chollier, T. Hankeln, F. Mertes, A. Wallberg, J. P. Rast, R. R. Copley, P. Martinez, M. J. Telford, Mitigating anticipated effects of systematic errors supports sister-group relationship between Xenacoelomorpha and Ambulacraria. *Current Biology*. **29**, 1818–1826 (2019).
28. J. M. Martín-Durán, K. Pang, A. Børve, H. S. Lê, A. Furu, J. T. Cannon, U. Jondelius, A. Hejnlol, Convergent evolution of bilaterian nerve cords. *Nature*. **553**, 45–50 (2018).
29. M. J. Layden, "Origin and evolution of nervous systems" in *Old questions and young approaches to animal evolution* (2019), pp. 151–171.
30. J. M. Martin-Durán, A. Hejnlol, A developmental perspective on the evolution of the nervous system. *Dev Biol* (2019), doi:10.1016/j.ydbio.2019.10.003.
31. L. Z. Holland, "Invertebrate origins of vertebrate nervous systems" in *Evolution of Nervous Systems* (Elsevier, Second Edi., 2017; <http://linkinghub.elsevier.com/retrieve/pii/B9780128040423000014>), vol. 1, pp. 3–23.
32. K. E. von Baer, *Über Entwicklungsgeschichte der Thiere; Beobachtung und Reflexion*. (Bei den Gebrüdern Bornträger, Königsberg, 1828).
33. J. Huxley, *Evolution, the Modern Synthesis* (George Allen & Unwin, London, 1942).
34. G. B. Muller, Evo-devo: extending the evolutionary synthesis. *Nat Rev Genet*. **8**, 943–949 (2007).
35. S. B. Carroll, Evo-Devo and an expanding evolutionary synthesis: a genetic theory of morphological evolution. *Cell*. **134**, 25–36 (2008).
36. P. J. Wittkopp, G. Kalay, Cis-regulatory elements: Molecular mechanisms and evolutionary processes underlying divergence. *Nat Rev Genet*. **13**, 59–69 (2012).
37. G. A. Wray, The evolutionary significance of cis-regulatory mutations. *Nat Rev Genet*. **8** (2007), pp. 206–216.
38. E. H. Davidson, D. H. Erwin, Gene regulatory networks and the evolution of animal body plans. *Science* (1979). **311**, 796–800 (2006).
39. R. Owen, *Lectures on comparative anatomy and physiology of the invertebrate animals delivered at the Royal College of Surgeons in 1843* (Longman, Brown, Green & Longmans, London, 1843).
40. D. Arendt, J. M. Musser, C. V. H. Baker, A. Bergman, C. Cepko, D. H. Erwin, M. Pavlicev, G. Schlosser, S. Widder, M. D. Laubichler, G. P. Wagner, The origin and evolution of cell types. *Nat Rev Genet*. **17**, 744–757 (2016).
41. M. Sachkova, P. Burkhardt, *Development*, in press, doi:10.1242/dev.178996.
42. J. C. Marioni, D. Arendt, How single-cell genomics is changing evolutionary and developmental biology. *Annu Rev Cell Dev Biol*. **33**, 537–553 (2017).
43. G. P. Wagner, The developmental genetics of homology. *Nat Rev Genet*. **8**, 473–479 (2007).
44. D. Arendt, Genes and homology in nervous system evolution: Comparing gene functions, expression patterns, and cell type molecular fingerprints. *Theory in Biosciences*. **124**, 185–197 (2005).
45. G. K. Davis, N. H. Patel, The origin and evolution of segmentation. *Trends in Genetics*. **15**, M69–M72 (1999).
46. N. Shubin, C. Tabin, S. Carroll, Deep homology and the origins of evolutionary novelty. *Nature*. **457** (2009), pp. 818–823.

47. K. M. Koenig, J. M. Gross, Evolution and development of complex eyes: a celebration of diversity. *Development*. **147**, ddev182923 (2020).
48. G. F. Striedter, R. G. Northcutt, Biological hierarchies and the concept of homology. *Brain Behaviour and Evolution*. **38**, 177–189 (1991).
49. J. Dugas-Ford, C. W. Ragsdale, Levels of homology and the problem of neocortex. *Annu Rev Neurosci*. **38**, 351–368 (2015).
50. S. D. Briscoe, C. W. Ragsdale, Evolution of the chordate telencephalon. *Current Biology*. **29** (2019), pp. R647–R662.
51. W. P. Maddison, Gene trees in species trees. *Syst Biol*. **46**, 523–536 (1997).
52. N. Tomić, V. B. Meyer-Rochow, Atavisms: Medical, genetic, and evolutionary implications. *Perspect Biol Med*. **54**, 332–353 (2011).
53. N. R. Cabej, "Evolution by reverting to ancestral characters" in *Epigenetic Principles of Evolution* (Elsevier, 2019), pp. 535–561.
54. S. Bank, S. Bradler, A second view on the evolution of flight in stick and leaf insects (Phasmatodea). *BMC Ecol Evol*. **22** (2022), doi:10.1186/s12862-022-02018-5.
55. M. F. Whiting, S. Bradler, T. Maxwell, Loss and recovery of wings in stick insects. *Nature*. **421**, 264–267 (2003).
56. J. W. H. Trueman, B. E. Pfeil, S. A. Kelchner, D. K. Yeates, Did stick insects really regain their wings? *Syst Entomol*. **29**, 138–139 (2004).
57. M. Pagel, Limpets break Dollo's Law. *Trends Ecol Evol*. **19**, 278–280 (2004).
58. C. D. Siler, R. M. Brown, Evidence for repeated acquisition and loss of complex body-form characters in an insular clade of southeast Asian semi-fossorial skinks. *Evolution (N Y)*. **65**, 2641–2663 (2011).
59. J. Gerhart, Evolution of the organizer and the chordate body plan. *International Journal of Developmental Biology*. **45**, 133–153 (2001).
60. L. Z. Holland, V. Laudet, M. Schubert, The chordate amphioxus: An emerging model organism for developmental biology. *Cellular and Molecular Life Sciences*. **61**, 2290–2308 (2004).
61. R. Nieuwenhuys, L. Puelles, *Towards a new neuromorphology* (Springer, Berlin, 2016).
62. F. Sugahara, Y. Murakami, J. Pascual-Anaya, S. Kuratani, Reconstructing the ancestral vertebrate brain. *Development, Growth & Differentiation*. **59**, 163–174 (2017).
63. N. D. Holland, *Philosophical Transactions of the Royal Society B: Biological Sciences*, in press, doi:10.1098/rstb.2015.0047.
64. S. W. Wilson, C. Houart, Early steps in the development of the forebrain. *Dev Cell*. **6**, 167–181 (2004).
65. F. Cavodeassi, C. Houart, Brain regionalization: of signaling centers and boundaries. *Dev Neurobiol*. **72**, 218–233 (2012).
66. L. Puelles, J. L. Ferran, Concept of neural genoarchitecture and its genomic fundament. *Front Neuroanat*. **6**, 1–9 (2012).
67. L. Puelles, S. Martínez, M. Martínez-De-La-Torre, J. L. R. Rubenstein, "Gene maps and related histogenetic domains in the forebrain and midbrain" in *The Rat Nervous System: Fourth Edition* (Elsevier Inc., 2015), pp. 3–24.
68. L. Puelles, "Plan of the developing vertebrate nervous system" in *Patterning and Cell Type Specification in the Developing CNS and PNS* (2013), pp. 187–209.
69. L. Puelles, J. L. R. Rubenstein, A new scenario of hypothalamic organization: rationale of new hypotheses introduced in the updated prosomeric model. *Front Neuroanat*. **9**, 27 (2015).
70. C. Kiecker, A. Lumsden, Compartments and their boundaries in vertebrate brain development. *Nat Rev Neurosci*. **6** (2005), pp. 553–564.
71. C. Houart, L. Caneparo, C. P. Heisenberg, K. A. Barth, M. Take-Uchi, S. W. Wilson, Establishment of the telencephalon during gastrulation by local antagonism of Wnt signaling. *Neuron*. **35**, 255–265 (2002).
72. D. Echevarría, C. Vieira, L. Gimeno, S. Martínez, Neuroepithelial secondary organizers and cell fate specification in the developing brain. *Brain Res Rev*. **43** (2003), pp. 179–191.
73. F. Sugahara, J. Pascual-Anaya, Y. Oisi, S. Kuraku, S. Aota, N. Adachi, W. Takagi, T. Hirai, N. Sato, Y. Murakami, S. Kuratani, Evidence from cyclostomes for complex regionalization of the ancestral vertebrate brain. *Nature*. **531**, 97–100 (2016).

74. Y. Sasakura, K. Mita, Y. Ogura, T. Horie, Ascidiens as excellent chordate models for studying the development of the nervous system during embryogenesis and metamorphosis. *Dev Growth Differ.* **54**, 420–437 (2012).
75. J. Garcia-Fernandez, E. Benito-Gutiérrez, It's a long way from amphioxus: descendants of the earliest chordate. *BioEssays.* **31**, 665–675 (2009).
76. È. Benito-Gutiérrez, Amphioxus as a model for mechanisms in vertebrate development. *eLS* (2011), doi:10.1002/9780470015902.a0021773.
77. O. Simakov, F. Marlétaz, J. X. Yue, B. O'Connell, J. Jenkins, A. Brandt, R. Calef, C. H. Tung, T. K. Huang, J. Schmutz, N. Satoh, J. K. Yu, N. H. Putnam, R. E. Green, D. S. Rokhsar, Deeply conserved synteny resolves early events in vertebrate evolution. *Nat Ecol Evol.* **4**, 820–830 (2020).
78. T. Horie, R. Shinki, Y. Ogura, T. G. Kusakabe, N. Satoh, Y. Sasakura, Ependymal cells of chordate larvae are stem-like cells that form the adult nervous system. *Nature.* **469**, 525–529 (2011).
79. F. Marlétaz, P. N. Firbas, I. Maeso, J. J. Tena, O. Bogdanovic, M. Perry, C. D. R. Wyatt, E. de la Calle-Mustienes, S. Bertrand, D. Burguera, R. D. Acemel, S. J. van Heeringen, S. Naranjo, C. Herrera-Ubeda, K. Skvortsova, S. Jimenez-Gancedo, D. Aldea, Y. Marquez, L. Buono, I. Kozmikova, J. Permanyer, A. Louis, B. Albuixech-Crespo, Y. le Petillon, A. Leon, L. Subirana, P. J. Balwierz, P. E. Duckett, E. Farahani, J. M. Aury, S. Mangenot, P. Wincker, R. Albalat, È. Benito-Gutiérrez, C. Cañestro, F. Castro, S. D'Aniello, D. E. K. Ferrier, S. Huang, V. Laudet, G. A. B. Marais, P. Pontarotti, M. Schubert, H. Seitz, I. Somorjai, T. Takahashi, O. Mirabeau, A. Xu, J. K. Yu, P. Carninci, J. R. Martinez-Morales, H. R. Crollius, Z. Kozmik, M. T. Weirauch, J. Garcia-Fernández, R. Lister, B. Lenhard, P. W. H. Holland, H. Escriva, J. L. Gómez-Skarmeta, M. Irimia, Amphioxus functional genomics and the origins of vertebrate gene regulation. *Nature.* **564**, 64–70 (2018).
80. J. X. Yue, J. K. Yu, N. H. Putnam, L. Z. Holland, The transcriptome of an Amphioxus, *Asymmetron lucayanum*, from the Bahamas: a window into chordate evolution. *Genome Biol Evol.* **6**, 2681–2696 (2014).
81. M. Brasó-Vives, F. Marlétaz, A. Echchiki, F. Mantica, R. D. Acemel, J. L. Gómez-Skarmeta, L. L. Targa, P. Pontarotti, J. J. Tena, I. Maeso, H. Escriva, M. Irimia, M. Robinson-Rechavi, Parallel evolution of amphioxus and vertebrate small-scale gene duplications. *BioRxiv* (2022), doi:10.1101/2022.01.18.476203.
82. F. Delsuc, H. Brinkmann, D. Chourrout, H. Philippe, Tunicates and not cephalochordates are the closest living relatives of vertebrates. *Nature.* **439**, 965–968 (2006).
83. È. Benito-Gutiérrez, A gene catalogue of the amphioxus nervous system. *Int J Biol Sci.* **2**, 149–160 (2006).
84. T. Andrews, thesis, University of Cambridge (2020).
85. T. C. Lacalli, Landmarks and subdomains in the larval brain of Branchiostoma: vertebrate homologs and invertebrate antecedents. *Isr J Zool.* **42**, 131–146 (1996).
86. S. Candiani, M. Pestarino, "Cephalochordate nervous system" in *Oxford Research Encyclopedia of Neuroscience* (Oxford University Press, 2018).
87. B. Albuixech-Crespo, L. López-Blanch, D. Burguera, I. Maeso, L. Sánchez-Arrones, J. A. Moreno-Bravo, I. Somorjai, J. Pascual-Anaya, E. Puelles, P. Bovolenta, J. Garcia-Fernández, L. Puelles, M. Irimia, J. L. Ferran, *Molecular regionalization of the developing amphioxus neural tube challenges major partitions of the vertebrate brain* (2017), vol. 15.
88. P. Vopalensky, J. Pergner, M. Liegertova, E. Benito-Gutiérrez, D. Arendt, Z. Kozmik, Molecular analysis of the amphioxus frontal eye unravels the evolutionary origin of the retina and pigment cells of the vertebrate eye. *Proceedings of the National Academy of Sciences.* **109**, 15383–15388 (2012).
89. L. Z. Holland, N. D. Holland, "Cephalochordates: A window into vertebrate origins" in *Current Topics in Developmental Biology* (Elsevier Inc., ed. 1, 2021; <http://dx.doi.org/10.1016/bs.ctdb.2020.07.001>), vol. 141, pp. 119–147.
90. F. Strano, V. Micaroni, E. Beli, S. Mercurio, G. Scari, R. Pennati, S. Piraino, On the larva and the zooid of the pterobranch *Rhabdopleura recondita* Beli, Cameron and Piraino, 2018 (Hemichordata, Graptolithina). *Marine Biodiversity.* **49**, 1657–1666 (2019).
91. T. Stach, A. Gruhl, S. Kaul-Strehlow, The central and peripheral nervous system of *Cephalodiscus gracilis* (Pterobranchia, Deuterostomia). *Zoomorphology.* **131**, 11–24 (2012).

92. C. J. Lowe, "Molecular insights into deuterostome evolution from hemichordate developmental biology" in *Current Topics in Developmental Biology* (Academic Press Inc., 2021), vol. 141, pp. 75–117.
93. V. Mashanov, O. Zueva, T. Rubilar, L. Epherra, J. E. García-Arrarás, "Echinodermata" in *Structure and Evolution of Invertebrate Nervous Systems*, A. Schmidt-Rhaesa, S. Harzsch, G. Purschke, Eds. (Oxford University Press, 2016), pp. 665–688.
94. A. S. Denes, G. Jékely, P. R. H. Steinmetz, F. Raible, H. Snyman, B. Prud'homme, D. E. K. Ferrier, G. Balavoine, D. Arendt, Molecular architecture of annelid nerve cord supports common origin of nervous system centralization in Bilateria. *Cell*. **129**, 277–288 (2007).
95. R. A. Raff, M. Byrne, The active evolutionary lives of echinoderm larvae. *Heredity (Edinb)*. **97**, 244–252 (2006).
96. M. Byrne, Y. Nakajima, F. C. Chee, R. D. Burke, Apical organs in echinoderm larvae: insights into larval evolution in the Ambulacraria. *Evol Dev*. **9**, 432–445 (2007).
97. H. Marlow, M. A. Tosches, R. Tomer, P. R. Steinmetz, A. Lauri, T. Larsson, D. Arendt, Larval body patterning and apical organs are conserved in animal evolution. *BMC Biol*. **12**, 1–17 (2014).
98. A. M. Pani, E. E. Mullarkey, J. Aronowicz, S. Assimacopoulos, E. A. Grove, C. J. Lowe, Ancient deuterostome origins of vertebrate brain signalling centres. *Nature*. **483**, 289–294 (2012).
99. È. Benito-Gutiérrez, H. Weber, D. V. Bryant, D. Arendt, Methods for generating year-round access to *Amphioxus* in the laboratory. *PLoS One*. **8**, e71599 (2013).
100. J. E. Carvalho, F. Lahaye, L. W. Yong, J. C. Croce, H. Escrivá, J. K. Yu, M. Schubert, An updated staging system for cephalochordate development: one table suits them all. *Front Cell Dev Biol*. **9**, 668006 (2021).
101. T. G. Andrews, G. Gattoni, L. Busby, M. A. Schwimmer, È. Benito-Gutiérrez, "Hybridization chain reaction for quantitative and multiplex imaging of gene expression in amphioxus embryos and adult tissues" in *In Situ Hybridization Protocols*, B. S. Nielsen, J. Jones, Eds. (Springer Nature 2020, Methods in., 2020), pp. 179–194.
102. C. B. Kimmel, W. W. Ballard, S. R. Kimmel, B. Ullmann, T. F. Schilling, Stages of embryonic development of the zebrafish. *Developmental Dynamics*. **203**, 253–310 (1995).
103. P. D. Nieuwkoop, J. Faber, *Normal table of Xenopus laevis* (North-Holland Publishing Co, Amsterdam, 1994).
104. E. E. Maxwell, N. B. Fröbisch, A. C. Heppleston, Variability and conservation in late chondrichthyan development: Ontogeny of the winter skate (*Leucoraja ocellata*). *Anatomical Record*. **291**, 1079–1087 (2008).
105. J. Andrew Gillis, M. S. Modrell, R. Glenn Northcutt, K. C. Catania, C. A. Luer, C. V. H. Baker, Electrosensory ampullary organs are derived from lateral line placodes in cartilaginous fishes. *Development*. **139**, 3142–3146 (2012).
106. È. Benito-Gutiérrez, G. Gattoni, M. Stemmer, S. D. Rohr, L. N. Schuhmacher, J. Tang, A. Marconi, G. Jékely, D. Arendt, The dorsoanterior brain of adult amphioxus shares similarities in expression profile and neuronal composition with the vertebrate telencephalon. *BMC Biol*. **19**, 1–19 (2021).
107. W. Cai, C. H. Kim, H. J. Go, M. Egertová, C. G. Zampronio, A. M. Jones, N. G. Park, M. R. Elphick, Biochemical, anatomical, and pharmacological characterization of Calcitonin-type neuropeptides in Starfish: discovery of an ancient role as muscle relaxants. *Front Neurosci*. **12** (2018), doi:10.3389/fnins.2018.00382.
108. S. Mercurio, G. Gattoni, S. Messinetti, M. Sugni, R. Pennati, Nervous system characterization during the development of a basal echinoderm, the feather star *Antedon mediterranea*. *Journal of Comparative Neurology*. **527**, 1127–1139 (2019).
109. H. M. T. Choi, M. Schwarzkopf, M. E. Fornace, A. Acharya, G. Artavanis, J. Stegmaier, A. Cunha, N. A. Pierce, Third-generation in situ hybridization chain reaction: multiplexed, quantitative, sensitive, versatile, robust. *Development*. **145**, dev165753 (2018).
110. F. Marlétaz, P. N. Firbas, I. Maeso, J. J. Tena, O. Bogdanovic, M. Perry, C. D. R. Wyatt, E. de la Calle-Mustienes, S. Bertrand, D. Burguera, R. D. Acemel, S. J. van Heeringen, S. Naranjo, C. Herrera-Ubeda, K. Skvortsova, S. Jimenez-Gancedo, D. Aldea, Y. Marquez, L. Buono, I. Kozmikova, J. Permanyer, A. Louis, B. Albuixech-Crespo, Y. le Petillon, A. Leon, L. Subirana, P. J. Balwierz, P. E. Duckett, E. Farahani, J.-M. Aury, S. Mangenot, P. Wincker, R. Albalat, È. Benito-Gutiérrez, C. Cañestro, F. Castro,

- S. D'Aniello, D. E. K. Ferrier, S. Huang, V. Laudet, G. A. B. Marais, P. Pontarotti, M. Schubert, H. Seitz, I. Somorjai, T. Takahashi, O. Mirabeau, A. Xu, J.-K. Yu, P. Carninci, J. R. Martinez-Morales, H. R. Crollius, Z. Kozmik, M. T. Weirauch, J. Garcia-Fernández, R. Lister, B. Lenhard, P. W. H. Holland, H. Escriva, J. L. Gómez-Skarmeta, M. Irimia, Amphioxus functional genomics and the origins of vertebrate gene regulation. *Nature*. **564**, 64–70 (2018).
111. M. R. Elphick, D. C. Semmens, L. M. Blowes, J. Levine, C. J. Lowe, M. I. Arnone, M. S. Clark, Reconstructing SALMFamide neuropeptide precursor evolution in the phylum Echinodermata: ophiuroid and crinoid sequence data provide new insights. *Front Endocrinol (Lausanne)*. **6**, 1–10 (2015).
  112. M. Gouy, S. Guindon, O. Gascuel, Sea view version 4: A multiplatform graphical user interface for sequence alignment and phylogenetic tree building. *Mol Biol Evol*. **27**, 221–224 (2010).
  113. C. Kunick, K. Lauenroth, M. Leost, T. Lemcke, 1-Azakenpaullone is a selective inhibitor of glycogen synthase kinase-3. *Bioorg Med Chem Lett*. **14**, 413–416 (2004).
  114. B. Bilir, O. Kucuk, C. S. Moreno, Wnt signaling blockage inhibits cell proliferation and migration, and induces apoptosis in triple-negative breast cancer cells. *J Transl Med*. **11**, 280 (2013).
  115. F. Chehrehasa, A. C. B. Meedeniya, P. Dwyer, G. Abrahamsen, A. Mackay-Sim, EdU, a new thymidine analogue for labelling proliferating cells in the nervous system. *J Neurosci Methods*. **177**, 122–130 (2009).
  116. J. Heasman, M. Kofron, C. Wyliet, B-catenin signaling activity dissected in the early xenopus embryo: A novel antisense approach. *Dev Biol*. **222**, 124–134 (2000).
  117. J. Schindelin, I. Arganda-Carreras, E. Frise, V. Kaynig, M. Longair, T. Pietzsch, S. Preibisch, C. Rueden, S. Saalfeld, B. Schmid, J.-Y. Tinevez, D. J. White, V. Hartenstein, K. Eliceiri, P. Tomancak, A. Cardona, Fiji: an open-source platform for biological-image analysis. *Nat Methods*. **9**, 676–682 (2012).
  118. S. Berg, D. Kutra, T. Kroeger, C. N. Straehle, B. X. Kausler, C. Haubold, M. Schiegg, J. Ales, T. Beier, M. Rudy, K. Eren, J. I. Cervantes, B. Xu, F. Beuttenmueller, A. Wolny, C. Zhang, U. Koethe, F. A. Hamprecht, A. Kreshuk, ilastik: interactive machine learning for (bio)image analysis. *Nat Methods*. **16**, 1226–1232 (2019).
  119. R. Patro, G. Duggal, M. I. Love, R. A. Irizarry, C. Kingsford, Salmon provides fast and bias-aware quantification of transcript expression. *Nat Methods*. **14**, 417–419 (2017).
  120. M. I. Love, W. Huber, S. Anders, Moderated estimation of fold change and dispersion for RNA-seq data with DESeq2. *Genome Biol*. **15** (2014), doi:10.1186/s13059-014-0550-8.
  121. A. T. L. Lun, D. J. McCarthy, J. C. Marioni, A step-by-step workflow for low-level analysis of single-cell RNA-seq data with Bioconductor. *F1000Res*. **2122** (2016), doi:10.12688/F1000RESEARCH.9501.1.
  122. C. S. Hickman, "Larvae in invertebrate development and evolution" in *The Origin and Evolution of Larval Forms*, B. K. Hall, M. H. Wake, Eds. (1999), pp. 22–59.
  123. L. A. Levin, T. S. Bridges, "Pattern and diversity in reproduction and development" in *Ecology of Marine Invertebrate Larvae*, L. McEdwards, Ed. (1995).
  124. K. J. Peterson, R. A. Cameron, E. H. Davidson, Set-aside cells in maximal indirect development: evolutionary and developmental significance. *Bioessays*. **19**, 623–631 (1997).
  125. E. Haeckel, *Studien zur Gastraea-Theorie* (Jena, 1877).
  126. R. A. Raff, Origins of the other metazoan body plans: The evolution of larval forms. *Philosophical Transactions of the Royal Society B: Biological Sciences*. **363**, 1473–1479 (2008).
  127. A. Minelli, The origins of larval forms: What the data indicate, and what they don't. *BioEssays*. **32** (2010), pp. 5–8.
  128. S. Richter, T. Stach, A. Wanninger, "Perspective - Nervous system development in bilaterian larvae: testing the concept of "primary larvae"" in *Structure and evolution of invertebrate nervous systems* (Oxford University Press, 2015), pp. 313–324.
  129. G. Jägersten, *Evolution of the Metazoan life cycle - a comprehensive theory* (Academic Press Inc, 1972).
  130. A. Perez-Posada, C.-Y. Lin, C.-Y. Lin, Y.-C. Chen, J. Luis Gómez Skarmeta, J.-K. Yu, Y.-H. Su, J. J. Tena, Insights into deuterostome evolution from the biphasic transcriptional programmes of hemichordates. *bioRxiv* (2022), doi:10.1101/2022.06.10.495707.
  131. S. Richter, G. Brenneis, M. Fritsch, O. S. Møller, M. E. J. Stegner, R. Loesel, S. Faller, C. M. Heuer, G. Purschke, C. Döring, A. Schmidt-Rhaesa, B. H. Rothe, G. Scholtz, T. Stach, S. Kaul, L. Vogt, P. Grobe,

- A. Wanninger, C. H. G. Müller, V. Rieger, S. Harzsch, Invertebrate neurophylogeny: Suggested terms and definitions for a neuroanatomical glossary. *Front Zool.* **7**, 1–49 (2010).
132. A. Hay-Schmidt, The evolution of the serotonergic nervous system. *Proceedings of the Royal Society B: Biological Sciences.* **267**, 1071–1079 (2000).
  133. M. Conzelmann, E. A. Williams, S. Tunaru, N. Randel, R. Shahidi, A. Asadulina, J. Berger, S. Offermanns, G. Jékely, Conserved MIP receptor-ligand pair regulates Platynereis larval settlement. *Proc Natl Acad Sci U S A.* **110**, 8224–8229 (2013).
  134. M. G. Hadfield, E. A. Meleshkevitch, D. Y. . Boudko, The apical sensory organ of a gastropod veliger is a receptor for settlement cues. *Biological Bulletin.* **198**, 67–76 (2000).
  135. V. F. Hinman, R. D. Burke, Embryonic neurogenesis in echinoderms. *Wiley Interdiscip Rev Dev Biol.* **7**, 1–15 (2018).
  136. L. Formery, M. Schubert, J. C. Croce, Ambulacrarians and the ancestry of deuterostome nervous systems. *Results Probl Cell Differ.* **68**, 31–59 (2019).
  137. T. C. Lacalli, Apical organs, epithelial domains, and the origin of the chordate central nervous system. *Integr Comp Biol.* **34**, 533–541 (1994).
  138. R. D. Burke, Deuterostome neuroanatomy and the body plan paradox. *Evol Dev.* **13**, 110–115 (2011).
  139. L. R. McEdward, B. G. Miner, Larval and life-cycle patterns in echinoderms. *Can J Zool.* **79**, 1125–1170 (2001).
  140. L. P. Nezhlin, Tornaria of hemichordates and other dipleurula-type larvae: A comparison. *Journal of Zoological Systematics and Evolutionary Research.* **38**, 149–156 (2000).
  141. D. R. McClay, "Development of a larval nervous system in the sea urchin" in *Current Topics in Developmental Biology* (Academic Press Inc., 2022), vol. 146, pp. 25–48.
  142. P. Paganos, D. Voronov, J. Musser, D. Arendt, M. I. Arnone, Single cell RNA sequencing of the *Strongylocentrotus purpuratus* larva reveals the blueprint of major cell types and nervous system of a non chordate deuterostome. *bioRxiv* (2021), doi:<https://doi.org/10.1101/2021.03.16.435574>.
  143. B. W. Bisgrove, R. D. Burke, Development of the nervous system of the pluteus larva of *Strongylocentrotus droebachiensis*. *Cell Tissue Res.* **248**, 335–343 (1987).
  144. R. D. Burke, D. J. Moller, O. A. Krupke, V. J. Taylor, Sea urchin neural development and the metazoan paradigm of neurogenesis. *Genesis.* **52** (2014), pp. 208–221.
  145. R. Feuda, I. S. Peter, "Homologous gene regulatory networks control development of apical organs and brains in Bilateria" (2022), (available at <https://www.science.org>).
  146. R. Range, Specification and positioning of the anterior neuroectoderm in deuterostome embryos. *Genesis.* **52**, 222–234 (2014).
  147. A. Omori, M. Kikuchi, M. Kondo, "Larval and adult body axes in echinoderms" in *Reproductive and Developmental Strategies* (Springer, Tokyo, 2018), pp. 763–789.
  148. P. Kitzmann, M. Weißkopf, M. I. Schacht, G. Bucher, A key role for foxQ2 in anterior head and central brain patterning in insects. *Development.* **144**, 2969–2981 (2017).
  149. J. Yaguchi, N. Takeda, K. Inaba, S. Yaguchi, Cooperative Wnt-Nodal signals regulate the patterning of anterior neuroectoderm. *PLoS Genet.* **12**, e1006001 (2016).
  150. Z. Wei, J. Yaguchi, S. Yaguchi, R. C. Angerer, L. M. Angerer, The sea urchin animal pole domain is a Six3-dependent neurogenic patterning center. *Development.* **136**, 1583–1583 (2009).
  151. R. Range, R. C. Angerer, L. M. Angerer, Integration of canonical and noncanonical Wnt signaling pathways patterns the neuroectoderm along the anterior-posterior axis of sea urchin embryos. *PLoS Biol.* **11**, e1001467 (2013).
  152. R. Range, Canonical and non-canonical Wnt signaling pathways define the expression domains of Frizzled 5/8 and Frizzled 1/ 2/7 along the early anterior-posterior axis in sea urchin embryos. *Dev Biol.* **444**, 83–92 (2018).
  153. A. Khadka, M. Martínez-Bartolomé, S. D. Burr, R. Range, A novel gene's role in an ancient mechanism: Secreted Frizzled-related protein 1 is a critical component in the anterior-posterior Wnt signaling network that governs the establishment of the anterior neuroectoderm in sea urchin embryos. *Evodevo.* **9**, 1–15 (2018).

154. R. C. Range, Z. Wei, An anterior signaling center patterns and sizes the anterior neuroectoderm of the sea urchin embryo. *Development* . **143**, 1523–1533 (2016).
155. S. Yaguchi, J. Yaguchi, R. C. Angerer, L. M. Angerer, A Wnt-FoxQ2-Nodal pathway links primary and secondary axis specification in sea urchin embryos. *Dev Cell*. **14**, 97–107 (2008).
156. A. J. Poustka, A. Kühn, D. Groth, V. Weise, S. Yaguchi, R. D. Burke, R. Herwig, H. Lehrach, G. Panopoulou, A global view of gene expression in lithium and zinc treated sea urchin embryos: New components of gene regulatory networks. *Genome Biol*. **8** (2007), doi:10.1186/gb-2007-8-5-r85.
157. S. Yaguchi, J. Yaguchi, Z. Wei, Y. Jin, L. M. Angerer, K. Inaba, Fez function is required to maintain the size of the animal plate in the sea urchin embryo. *Development*. **138**, 4233–4243 (2011).
158. S. Yaguchi, J. Yaguchi, Z. Wei, K. Shiba, L. M. Angerer, K. Inaba, AnkAT-1 is a novel gene mediating the apical tuft formation in the sea urchin embryo. *Dev Biol*. **348**, 67–75 (2010).
159. J. H. Fritzenwanker, J. Gerhart, R. M. Freeman, C. J. Lowe, The Fox/Forkhead transcription factor family of the hemichordate *Saccoglossus kowalevskii*. *Evodevo*. **5** (2014), doi:10.1186/2041-9139-5-17.
160. P. Gonzalez, K. R. Uhlinger, C. J. Lowe, The adult body plan of indirect developing hemichordates develops by adding a Hox-patterned trunk to an anterior larval territory. *Current Biology*. **27**, 87–95 (2017).
161. S. Darras, J. H. Fritzenwanker, K. R. Uhlinger, E. Farrelly, A. M. Pani, I. A. Hurley, R. P. Norris, M. Osovitz, M. Terasaki, M. Wu, J. Aronowicz, M. Kirschner, J. C. Gerhart, C. J. Lowe, *Anteroposterior axis patterning by early canonical Wnt signaling during hemichordate development* (2018), vol. 16.
162. A. M. Cheatle Jarvela, K. A. Yankura, V. F. Hinman, A gene regulatory network for apical organ neurogenesis and its spatial control in sea star embryos. *Development*. **143**, 4214–4223 (2016).
163. N. Kawai, R. Kuraishi, H. Kaneko, Wnt, Frizzled, and sFRP gene expression patterns during gastrulation in the starfish *Patiria (Asterina) pectinifera*. *Gene Expression Patterns*. **21**, 19–27 (2016).
164. B. S. McCauley, E. Akyar, L. Filliger, V. F. Hinman, Expression of wnt and frizzled genes during early sea star development. *Gene Expression Patterns*. **13**, 437–444 (2013).
165. P. Gonzalez, J. Z. Jiang, C. J. Lowe, The development and metamorphosis of the indirect developing acorn worm *Schizocardium californicum* (Enteropneusta: Spengelidae). *Front Zool*. **15**, 1–24 (2018).
166. S. Kaul-Strehlow, M. Urata, T. Minokawa, T. Stach, A. Wanninger, Neurogenesis in directly and indirectly developing enteropneusts: of nets and cords. *Org Divers Evol*. **15**, 405–422 (2015).
167. L. P. Nezhlin, E. E. Voronezhskaya, Early peripheral sensory neurons in the development of trochozoan animals. *Russ J Dev Biol*. **48**, 130–143 (2017).
168. T. Lacalli, Structure and development of the apical organ in trochophores of *Spirobranchus polycerus*, *Phyllodoce maculata* and *Phyllodoce mucosa* (Polychaeta). *Proceedings of the Royal Society of London B*. **212**, 381–402 (1981).
169. A. M. Carrillo-Baltodano, O. Seudre, K. Guynes, J. M. Martín-Durán, Early embryogenesis and organogenesis in the annelid *Owenia fusiformis*. *Evodevo*. **12** (2021), doi:10.1186/s13227-021-00176-z.
170. A. H. L. Fischer, T. Henrich, D. Arendt, The normal development of *Platynereis dumerilii* (Nereididae, Annelida). *Front Zool*. **7** (2010), doi:10.1186/1742-9994-7-31.
171. S. Kumar, S. C. Tumu, C. Helm, H. Hausen, The development of early pioneer neurons in the annelid *Malacoceros fuliginosus*. *BMC Evol Biol*. **20** (2020), doi:10.1186/s12862-020-01680-x.
172. A. Pavlicek, T. Schwaha, A. Wanninger, Towards a ground pattern reconstruction of bivalve nervous systems: neurogenesis in the zebra mussel *Dreissena polymorpha*. *Org Divers Evol*. **18**, 101–114 (2018).
173. A. Wanninger, G. Haszprunar, The development of the serotonergic and FMRF-amidergic nervous system in *Antalis entalis* (Mollusca, Scaphopoda). *Zoomorphology*. **122**, 77–85 (2003).
174. S. Friedrich, A. Wanninger, M. Brückner, G. Haszprunar, Neurogenesis in the mossy chiton, *Mopalia muscosa* (Gould) (Polyplacophora): Evidence against molluscan metamerism. *J Morphol*. **253**, 109–117 (2002).
175. S. C. Kempf, L. R. Page, A. Pires, Development of serotonin-like immunoreactivity in the embryos and larvae of nudibranch mollusks with emphasis on the structure and possible function of the apical sensory organ. *Journal of Comparative Neurology*. **386**, 507–528 (1997).

176. O. v. Yurchenko, O. I. Skiteva, E. E. Voronezhskaya, V. A. Dyachuk, Nervous system development in the Pacific oyster, *Crassostrea gigas* (Mollusca: Bivalvia). *Front Zool.* **15** (2018), doi:10.1186/s12983-018-0259-8.
177. A. Altenburger, A. Wanninger, Neuromuscular development in *Novocrania anomala*: evidence for the presence of serotonin and a spiralian-like apical organ in lecithotrophic brachiopod larvae. *Evol Dev.* **12**, 16–24 (2010).
178. S. Santagata, C. Resh, A. Hejzol, M. Q. Martindale, Y. J. Passamanek, Development of the larval anterior neurogenic domains of *Terebratalia transversa* (Brachiopoda) provides insights into the diversification of larval apical organs and the spiralian nervous system. *Evodevo.* **3**, 1–20 (2012).
179. S. A. Maslakova, Development to metamorphosis of the nemertean pilidium larva. *Front Zool.* **7**, 1–18 (2010).
180. S. Hindinger, T. Schwaha, A. Wanninger, Immunocytochemical studies reveal novel neural structures in nemertean pilidium larvae and provide evidence for incorporation of larval components into the juvenile nervous system. *Front Zool.* **10** (2013), doi:10.1186/1742-9994-10-31.
181. C. Andrikou, Y. J. Passamanek, C. J. Lowe, M. Q. Martindale, A. Hejzol, Molecular patterning during the development of *Phoronopsis harmeri* reveals similarities to rhynchonelliform brachiopods. *Evodevo.* **10** (2019), doi:10.1186/s13227-019-0146-1.
182. E. N. Temereva, E. B. Tsitrin, Development and organization of the larval nervous system in *Phoronopsis harmeri*: new insights into phoronid phylogeny. *Front Zool.* **11** (2014) (available at <http://www.frontiersinzoology.com/content/11/1/3>).
183. A. Wanninger, J. Fuchs, G. Haszprunar, Anatomy of the serotonergic nervous system of an entoproct creeping-type larva and its phylogenetic implications. *Invertebrate Biology.* **126**, 268–278 (2007).
184. A. Gruhl, Serotonergic and FMRFamideergic nervous system in gymnolaemate bryozoan larvae. *Zoomorphology.* **128**, 135–156 (2009).
185. K. A. Rawlinson, Embryonic and post-embryonic development of the polyclad flatworm *Maritigrella crozieri*; implications for the evolution of spiralian life history traits. *Front Zool.* **7**, 1–25 (2010).
186. E. Redl, M. Scherholz, T. Wollesen, C. Todt, A. Wanninger, Expression of *six3* and *otx* in Solenogastres (Mollusca) supports an ancestral role in bilaterian anterior-posterior axis patterning. *Evol Dev.* **20**, 17–28 (2018).
187. K. J. Perry, D. C. Lyons, M. Truchado-Garcia, A. H. L. Fischer, L. W. Helfrich, K. B. Johansson, J. C. Diamond, C. Grande, J. Q. Henry, Deployment of Regulatory Genes During Gastrulation and Germ Layer Specification in a Model Spiralian Mollusc *Crepidula*. *Developmental Dynamics.* **244**, 1215–1248 (2015).
188. J. M. Martín-Durán, B. C. Vellutini, A. Hejzol, Evolution and development of the adelphophagic, intracapsular Schmid's larva of the nemertean *Lineus ruber*. *Evodevo.* **6** (2015), doi:10.1186/s13227-015-0023-5.
189. L. S. Hiebert, S. A. Maslakova, Expression of *Hox*, *Cdx*, and *Six3/6* genes in the hoplonemertean *Pantionemertes californiensis* offers insight into the evolution of maximally indirect development in the phylum Nemertea. *Evodevo.* **6**, 1–15 (2015).
190. F. W. Smith, M. Cumming, B. Goldstein, Analyses of nervous system patterning genes in the tardigrade *Hypsibius exemplaris* illuminate the evolution of panarthropod brains. *Evodevo.* **9** (2018), doi:10.1186/s13227-018-0106-1.
191. B. J. Eriksson, L. Samadi, A. Schmid, The expression pattern of the genes *engrailed*, *pax6*, *otd* and *six3* with special respect to head and eye development in *Euperipatoides kanangrensis* Reid 1996 (Onychophora: Peripatopsidae). *Dev Genes Evol.* **223**, 237–246 (2013).
192. N. Posnien, N. D. B. Koniszewski, H. J. Hein, G. Bucher, Candidate gene screen in the red flour beetle *Tribolium* reveals *six3* as ancient regulator of anterior median head and central complex development. *PLoS Genet.* **7** (2011), doi:10.1371/journal.pgen.1002416.
193. M. I. Schacht, C. Schomburg, G. Bucher, *six3* acts upstream of *foxQ2* in labrum and neural development in the spider *Parasteatoda tepidariorum*. *Dev Genes Evol.* **230**, 95–104 (2020).

194. V. S. Hunnekuhl, M. Akam, An anterior medial cell population with an apical-organ-like transcriptional profile that pioneers the central nervous system in the centipede *Strigamia maritima*. *Dev Biol.* **396**, 136–149 (2014).
195. B. He, M. Buescher, M. S. Farnworth, F. Strobl, E. Stelzer, N. D. B. Koniszewski, D. Mühlen, G. Bucher, An ancestral apical brain region contributes to the central complex under the control of foxQ2 in the beetle *Tribolium castaneum*. *Elife*, 1–29 (2019).
196. M. Irimia, C. Piñeiro, I. Maeso, J. L. Gómez-Skarmeta, F. Casares, J. Garcia-Fernández, Conserved developmental expression of *Fezf* in chordates and *Drosophila* and the origin of the Zona Limitans Intrathalamica (ZLI) brain organizer. *Evodevo.* **1**, 7 (2010).
197. H. H. Lee, M. Frasch, Survey of forkhead domain encoding genes in the *Drosophila* genome: classification and embryonic expression patterns. *Developmental Dynamics.* **229**, 357–366 (2004).
198. N. Nakanishi, D. Yuan, D. K. Jacobs, V. Hartenstein, Early development, pattern, and reorganization of the planula nervous system in *Aurelia* (Cnidaria, Scyphozoa). *Dev Genes Evol.* **218**, 511–524 (2008).
199. S. Piraino, G. Zega, C. di Benedetto, A. Leone, A. Dell'Anna, R. Pennati, D. Candia Carnevali, V. Schmid, H. Reichert, Complex neural architecture in the diploblastic larva of *Clava multicornis* (Hydrozoa, Cnidaria). *Journal of Comparative Neurology.* **519**, 1931–1951 (2011).
200. E. Gilbert, C. Teeling, T. Lebedeva, S. Pedersen, N. Christmas, G. Genikhovich, V. Modepalli, Molecular and cellular architecture of the larval sensory organ in the cnidarian *Nematostella vectensis*. *Development.* **149** (2022), doi:10.1242/dev.200833.
201. H. Zang, N. Nakanishi, Expression analysis of cnidarian-specific neuropeptides in a sea anemone unveils an apical-organ-associated nerve net that disintegrates at metamorphosis. *Front Endocrinol (Lausanne).* **11** (2020), doi:10.3389/fendo.2020.00063.
202. C. Sinigaglia, H. Busengdal, A. Lerner, P. Oliveri, F. Rentzsch, Molecular characterization of the apical organ of the anthozoan *Nematostella vectensis*. *Dev Biol.* **398**, 120–133 (2015).
203. C. Sinigaglia, H. Busengdal, L. Leclère, U. Technau, F. Rentzsch, The bilaterian head patterning gene *six3/6* controls aboral domain development in a cnidarian. *PLoS Biol.* **11** (2013), doi:10.1371/journal.pbio.1001488.
204. L. Leclère, M. Bause, C. Sinigaglia, J. Steger, F. Rentzsch, Development of the aboral domain in *Nematostella* requires  $\beta$ -catenin and the opposing activities of *Six3/6* and *Frizzled5/8*. *Development.* **143**, 1766–1777 (2016).
205. H. Marlow, D. Q. Matus, M. Q. Martindale, Ectopic activation of the canonical wnt signaling pathway affects ectodermal patterning along the primary axis during larval development in the anthozoan *Nematostella vectensis*. *Dev Biol.* **380**, 324–334 (2013).
206. T. Lebedeva, A. J. Aman, T. Graf, I. Niedermoser, B. Zimmermann, Y. Kraus, M. Schatka, A. Demilly, U. Technau, G. Genikhovich, Cnidarian-bilaterian comparison reveals the ancestral regulatory logic of the  $\beta$ -catenin dependent axial patterning. *Nat Commun.* **12** (2021), doi:10.1038/s41467-021-24346-8.
207. M. E. Mazza, K. Pang, A. M. Reitzel, M. Q. Martindale, J. R. Finnerty, A conserved cluster of three PRD-class homeobox genes (*homeobrain*, *rx* and *orthopedia*) in the Cnidaria and Protostomia. *Evodevo.* **1** (2010) (available at <http://www.evodevojournal.com/content/1/1/3><http://www.evodevojournal.com/content/1/1/3>).
208. L. Beccari, R. Marco-Ferreres, P. Bovolenta, The logic of gene regulatory networks in early vertebrate forebrain patterning. *Mech Dev.* **130**, 95–111 (2013).
209. F. Cavodeassi, T. Moreno-Mármol, M. Hernandez-Bejarano, P. Bovolenta, "Principles of early vertebrate forebrain formation" in *Organogenetic Gene Networks: Genetic Control of Organ Formation* (Springer International Publishing, 2016), pp. 299–317.
210. A. Lavado, O. v. Lagutin, G. Oliver, *Six3* inactivation causes progressive caudalization and aberrant patterning of the mammalian diencephalon. *Development.* **135**, 441–450 (2008).
211. O. v. Lagutin, C. C. Zhu, D. Kobayashi, J. Topczewski, K. Shimamura, L. Puellas, H. R. C. Russell, P. J. McKinnon, L. Solnica-Krezel, G. Oliver, *Six3* repression of Wnt signaling in the anterior neuroectoderm is essential for vertebrate forebrain development. *Genes Dev.* **17**, 368–379 (2003).
212. Y. Xie, R. I. Dorsky, Development of the hypothalamus: Conservation, modification and innovation. *Development (Cambridge).* **144** (2017), pp. 1588–1599.

213. Y. Ogawa, T. Shiraki, Y. Fukada, D. Kojima, "Foxq2 determines blue cone identity in zebrafish" (2021), (available at <https://www.science.org>).
214. Z. Kozmik, N. D. Holland, J. Kreslova, D. Oliveri, M. Schubert, K. Jonasova, L. Z. Holland, M. Pestarino, V. Benes, S. Candiani, Pax-Six-Eya-Dach network during amphioxus development: Conservation in vitro but context specificity in vivo. *Dev Biol.* **306**, 143–159 (2007).
215. J. K. Yu, N. D. Holland, L. Z. Holland, AmphiFoxQ2, a novel winged helix/forkhead gene, exclusively marks the anterior end of the amphioxus embryo. *Dev Genes Evol.* **213**, 102–105 (2003).
216. S. Foster, N. Oulhen, G. Wessel, A single cell RNA sequencing resource for early sea urchin development. *Development.* **147** (2020), doi:10.1242/dev.191528.
217. D. E. Wagner, C. Weinreb, Z. M. Collins, J. A. Briggs, S. G. Megason, A. M. Klein, Single-cell mapping of gene expression landscapes and lineage in the zebrafish embryo. *Science (1979)*. **360**, 981–987 (2018).
218. P. Ma, X. Liu, Z. Xu, H. Liu, X. Ding, Z. Huang, C. Shi, L. Liang, L. Xu, X. Li, G. Li, Y. He, Z. Ding, C. Chai, H. Wang, J. Qiu, J. Zhu, X. Wang, P. Ding, S. Zhou, Y. Yuan, W. Wu, C. Wan, Y. Yan, Y. Zhou, Q. J. Zhou, G. D. Wang, Q. Zhang, X. Xu, G. Li, S. Zhang, B. Mao, D. Chen, Joint profiling of gene expression and chromatin accessibility during amphioxus development at single-cell resolution. *Cell Rep.* **39** (2022), doi:10.1016/j.celrep.2022.110979.
219. G. Gattoni, T. G. R. Andrews, E. Benito-Gutiérrez, Restricted proliferation during neurogenesis contributes to regionalization of the amphioxus nervous system. *bioRxiv* (2021), doi:10.1101/2021.12.22.473870.
220. T. Onai, A. Takai, D. H. E. Setiamarga, L. Z. Holland, Essential role of Dkk3 for head formation by inhibiting Wnt/ $\beta$ -catenin and Nodal/Vg1 signaling pathways in the basal chordate amphioxus. *Evol Dev.* **350**, 338–350 (2012).
221. S. Candiani, L. Moronti, P. Ramoino, M. Schubert, M. Pestarino, A neurochemical map of the developing amphioxus nervous system. *BMC Neurosci.* **13** (2012), doi:10.1186/1471-2202-13-59.
222. T. Onai, Canonical Wnt/ $\beta$ -catenin and Notch signaling regulate animal/vegetal axial patterning in the cephalochordate amphioxus. *Evol Dev*, 1–13 (2018).
223. E. M. de Robertis, H. Kuroda, Dorsal-ventral patterning and neural induction in *Xenopus* embryos. *Annu Rev Cell Dev Biol.* **20**, 285–308 (2004).
224. B. Schmierer, C. S. Hill, TGF $\beta$ -SMAD signal transduction: molecular specificity and functional flexibility. *Nat Rev Mol Cell Biol.* **8** (2007), pp. 970–982.
225. D. Meulemans, M. Bronner-Fraser, The amphioxus SoxB family: implications for the evolution of vertebrate placodes. *Int. J. Biol. Sci.* **3** (2007).
226. C. J. Lowe, D. N. Clarke, D. M. Medeiros, D. S. Rokhsar, J. Gerhart, The deuterostome context of chordate origins. *Nature.* **520**, 456–465 (2015).
227. N. D. Holland, L. Z. Holland, P. W. H. Holland, Scenarios for the making of vertebrates. *Nature.* **520**, 450–455 (2015).
228. L. Formery, F. Orange, A. Formery, S. Yaguchi, C. J. Lowe, M. Schubert, J. C. Croce, Neural anatomy of echinoid early juveniles and comparison of nervous system organization in echinoderms. *Journal of Comparative Neurology.* **529**, 1135–1156 (2021).
229. T. J. Bailey, H. El-Hodiri, L. Zhang, R. Shah, P. H. Mathers, M. Jamrich, Regulation of development by Rx genes. *International Journal of Developmental Biology.* **48** (2004), pp. 761–770.
230. A. Wolf, S. Ryu, Specification of posterior hypothalamic neurons requires coordinated activities of Fezf2, Otp, Sim1a and Foxb1.2. *Development (Cambridge)*. **140**, 1762–1773 (2013).
231. J. L. Ferran, L. Puelles, J. L. R. Rubenstein, Molecular codes defining rostrocaudal domains in the embryonic mouse hypothalamus. *Front Neuroanat.* **9**, 1–14 (2015).
232. C. Diaz, L. Puelles, Developmental genes and malformations in the hypothalamus. *Front Neuroanat.* **14** (2020), , doi:10.3389/fnana.2020.607111.
233. C. Kiecker, C. Niehrs, A morphogen gradient of Wnt/ $\beta$ -catenin signalling regulates anteroposterior neural patterning in *Xenopus*. *Development.* **128**, 4189–4201 (2001).
234. C. P. Petersen, P. W. Reddien, Wnt Signaling and the Polarity of the Primary Body Axis. *Cell.* **139** (2009), pp. 1056–1068.

235. G. M. Kelly, P. Greenstein, D. F. Erezyilmaz, R. T. Moon, Zebrafish *wnt8* and *wnt8b* share a common activity but are involved in distinct developmental pathways. *Development*. **121**, 1787–1789 (1995).
236. M. M. Braun, A. Etheridge, A. Bernard, C. P. Robertson, H. Roelink, Wnt signaling is required at distinct stages of development for the induction of the posterior forebrain. *Development*. **130**, 5579–5587 (2003).
237. I. M. L. Somorjai, J. Martí-Solans, M. Diaz-Gracia, H. Nishida, K. S. Imai, H. Escrivà, C. Cañestro, R. Albalat, Wnt evolution and function shuffling in liberal and conservative chordate genomes. *Genome Biol.* **19** (2018), doi:10.1186/s13059-018-1468-3.
238. D. R. McClay, E. Miranda, S. L. Feinberg, Neurogenesis in the sea urchin embryo is initiated uniquely in three domains. *Development (Cambridge)*. **145** (2018), doi:10.1242/dev.167742.
239. M. Cui, N. Siriwon, E. Li, E. H. Davidson, I. S. Peter, Specific functions of the Wnt signaling system in gene regulatory networks throughout the early sea urchin embryo. *Proceedings of the National Academy of Sciences*. **111**, E5029–E5038 (2014).
240. T. Onai, H. Lin, M. Schubert, D. Koop, P. W. Osborne, S. Alvarez, R. Alvarez, N. D. Holland, L. Z. Holland, Retinoic acid and Wnt/ $\beta$ -catenin have complementary roles in anterior/posterior patterning embryos of the basal chordate amphioxus. *Dev Biol.* **332**, 223–233 (2009).
241. I. Kozmikova, Z. Kozmik, Wnt/ $\beta$ -catenin signaling is an evolutionarily conserved determinant of chordate dorsal organizer. *Elife*. **9**, 1–29 (2020).
242. E. M. de Robertis, J. Larrain, M. Oelgeschlager, O. Wessley, The establishment of Spemann's organizer and patterning of the vertebrate embryo. *Nat Rev Genet.* **1**, 171–181 (2000).
243. H. Hikasa, S. Y. Sokol, Wnt signaling in vertebrate axis specification. *Cold Spring Harb Perspect Biol.* **5** (2013), , doi:10.1101/cshperspect.a007955.
244. L. H. Hyman, *The Invertebrates: Echinodermata* (McGraw-Hill Publications, 1955).
245. M. I. Arnone, M. Byrne, P. Martinez, "Echinodermata" in *Evolutionary Developmental Biology of Invertebrates 6: Deuterostomia* (Springer-Verlag Vienna, 2015), pp. 1–58.
246. M. J. Telford, C. J. Lowe, C. B. Cameron, O. Ortega-Martinez, J. Aronowicz, P. Oliveri, R. R. Copley, Phylogenomic analysis of echinoderm class relationships supports Asterozoa. *Proceedings of the Royal Society B: Biological Sciences*. **281** (2014), doi:10.1098/rspb.2014.0479.
247. Y. Li, A. Omori, R. L. Flores, S. Satterfield, C. Nguyen, T. Ota, T. Tsurugaya, T. Ikuta, K. Ikeo, M. Kikuchi, J. C. K. Leong, A. Reich, M. Hao, W. Wan, Y. Dong, Y. Ren, S. Zhang, T. Zeng, M. Uesaka, Y. Uchida, X. Li, T. F. Shibata, T. Bino, K. Ogawa, S. Shigenobu, M. Kondo, F. Wang, L. Chen, G. Wessel, H. Saiga, R. A. Cameron, B. Livingston, C. Bradham, W. Wang, N. Irie, Genomic insights of body plan transitions from bilateral to pentameral symmetry in Echinoderms. *Commun Biol.* **3** (2020), doi:10.1038/s42003-020-1091-1.
248. L. M. Angerer, S. Yaguchi, R. C. Angerer, R. D. Burke, The evolution of nervous system patterning: insights from sea urchin development. *Development*. **138**, 3613–3623 (2011).
249. M. I. Arnone, C. Andrikou, R. Annunziata, Echinoderm systems for gene regulatory studies in evolution and development. *Curr Opin Genet Dev.* **39**, 129–137 (2016).
250. S. G. Ernst, A century of sea urchin development. *Am Zool.* **37**, 250–259 (1997).
251. T. D. Mayorova, S. Tian, W. Cai, D. C. Semmens, E. A. Odekunle, M. Zandawala, Y. Badi, M. L. Rowe, M. Egertová, M. R. Elphick, Localization of neuropeptide gene expression in larvae of an echinoderm, the starfish *Asterias rubens*. *Front Neurosci.* **10** (2016), doi:10.3389/fnins.2016.00553.
252. S. Garner, I. Zysk, G. Byrne, M. Kramer, D. Moller, V. Taylor, R. D. Burke, Neurogenesis in sea urchin embryos and the diversity of deuterostome neurogenic mechanisms. *Development (Cambridge)*. **143**, 286–297 (2016).
253. K. A. Yankura, C. S. Koechlein, A. F. Cryan, A. Cheatle, V. F. Hinman, Gene regulatory network for neurogenesis in a sea star embryo connects broad neural specification and localized patterning. *Proc Natl Acad Sci U S A.* **110**, 8591–8596 (2013).
254. J. L. S. Cobb, "The nervous systems of Echinodermata: recent results and new approaches" in *The Nervous Systems of Invertebrates: an Evolutionary and Comparative Approach*, O. Breidbach, W. Kutsh, Eds. (Springer Science & Business Media, 1995), pp. 407–424.

255. V. S. Mashanov, Ā. O. R. Zueva, T. Heinzeller, B. Aschauer, I. Y. Dolmatov, Developmental origin of the adult nervous system in a holothurian: an attempt to unravel the enigma of neurogenesis in echinoderms. *Evol Dev.* **9**, 244–256 (2007).
256. M. R. Elphick, "Neuropeptide signaling in echinoderms: from "physiologic activity of nerve extracts" to neuropeptidomics and beyond" in *Advances in Invertebrate Neuroendocrinology*, S. Saleuddin, A. B. Lange, I. Orchard, Eds. (2020), pp. 125–172.
257. J. R. Thompson, P. Paganos, G. Benvenuto, M. I. Arnone, P. Oliveri, Post-metamorphic skeletal growth in the sea urchin *Paracentrotus lividus* and implications for body plan evolution. *Evodevo.* **12** (2021), doi:10.1186/s13227-021-00174-1.
258. A. H. Clarks, *A monograph of the existing crinoids* (United States National Museum, Bulletin 82, 1921).
259. T. Mortensen, "Studies in the development of crinoids" in *Papers from the Department of Marine Biology of the Carnegie Institution of Washington* (1920), vol. 16.
260. M. D. Candia Carnevali, F. Bonasoro, Microscopic overview of crinoid regeneration. *Microsc Res Tech.* **55**, 403–426 (2001).
261. G. W. Rouse, L. S. Jermiin, N. G. Wilson, I. Eeckhaut, D. Lanterbecq, T. Oji, C. M. Young, T. Browning, P. Cisternas, L. E. Helgen, M. Stuckey, C. G. Messing, Fixed, free, and fixed: The fickle phylogeny of extant Crinoidea (Echinodermata) and their Permian-Triassic origin. *Mol Phylogenet Evol.* **66**, 161–181 (2013).
262. H. Nakano, Y. Nakajima, S. Amemiya, Nervous system development of two crinoid species, the sea lily *Metacrinus rotundus* and the feather star *Oxycomanthus japonicus*. *Dev Genes Evol.* **219**, 565–576 (2009).
263. A. Barbaglio, C. Turchi, G. Melone, C. di Benedetto, T. Martinello, M. Patrino, M. Biggiogero, I. C. Wilkie, M. D. Candia Carnevali, Larval development in the feather star *Antedon mediterranea*. *Invertebr Reprod Dev.* **56**, 124–137 (2012).
264. N. Holland, The fine structure of *Comanthus japonica* (Echinodermata: Crinoidea) from zygote through early gastrula. *Tissue & Cell* **10**, 93–110 (1978).
265. N. D. Holland, The fine structure of the embryo during the gastrula stage of *Comanthus japonica* (Echinodermata, Crinoidea). *Tissue Cell.* **8**, 491–510 (1976).
266. F.-S. Chia, R. D. Burke, R. Koss, P. v. Mladenov, S. S. Rumrill, Fine structure of the *Doliolaria* larva of the feather star *Florometra serratissima* (Echinodermata: Crinoidea), with special emphasis on the nervous system. *J Morphol.* **189**, 99–120 (1986).
267. S. Engle, thesis, Freien Universität Berlin, Berlin (2012).
268. K. J. Peterson, C. Arenas-Mena, E. H. Davidson, The A/P axis in echinoderm ontogeny and evolution: evidence from fossils and molecules. *Evol Dev.* **2**, 93–101 (2000).
269. P. V. Mladenov, F. S. Chia, Development, settling behaviour, metamorphosis and pentacrinoid feeding and growth of the feather star *Florometra serratissima*. *Mar Biol.* **79**, 309–323 (1983).
270. T. Heinzeller, U. Welsh, "Crinoidea" in *Microscopic Anatomy of Invertebrates Volume 14: Echinodermata* (Wiley-Liss, 1994), pp. 9–148.
271. A. Barbaglio, A. Biressi, G. Melone, F. Bonasoro, R. Lavado, C. Porte, M. D. Candia Carnevali, Reproductive cycle of *Antedon mediterranea* (Crinoidea, Echinodermata): correlation between morphology and physiology. *Zoomorphology.* **128**, 119–134 (2009).
272. M. R. Elphick, D. C. Semmens, L. M. Blowes, J. Levine, C. J. Lowe, M. I. Arnone, M. S. Clark, Reconstructing SALMFamide neuropeptide precursor evolution in the phylum Echinodermata: Ophiuroid and crinoid sequence data provide new insights. *Front Endocrinol (Lausanne).* **6** (2015), doi:10.3389/fendo.2015.00002.
273. C. W. Dunn, A. Hejnal, D. Q. Matus, K. Pang, W. E. Browne, S. A. Smith, E. Seaver, G. W. Rouse, M. Obst, G. D. Edgecombe, M. v. Sørensen, S. H. D. Haddock, A. Schmidt-Rhaesa, A. Okusu, R. M. Kristensen, W. C. Wheeler, M. Q. Martindale, G. Giribet, Broad phylogenomic sampling improves resolution of the animal tree of life. *Nature.* **452**, 745–749 (2008).
274. A.-J. Beer, C. Moss, M. Thorndyke, M. Thorndyket, Development of serotonin-like and SALMFamide-like immunoreactivity in the nervous system of the sea urchin *Psammechinus miliaris*. *Biological Bulletin.* **200**, 268–280 (2001).

275. N. Murabe, H. Hatoyama, S. Hase, M. Komatsu, R. D. Burke, H. Kaneko, Y. Nakajima, Neural architecture of the brachiolaria larva of the starfish, *Asterina pectinifera*. *Journal of Comparative Neurology*. **509**, 271–282 (2008).
276. M. Byrne, M. A. Sewell, P. Selvakumaraswamy, T. A. A. Prowse, The larval apical organ in the holothuroid *Chiridota gigas* (Apodida): inferences on evolution of the ambulacrarian larval nervous system. *Biological Bulletin*. **211**, 95–100 (2006).
277. A. Omori, T. F. Shibata, K. Akasaka, Gene expression analysis of three homeobox genes throughout early and late development of a feather star *Anneissia japonica*. *Dev Genes Evol*. **230**, 305–314 (2020).
278. A. Omori, K. Akasaka, D. Kurokawa, S. Amemiya, Gene expression analysis of Six3, Pax6, and Otx in the early development of the stalked crinoid *Metacrinus rotundus*. *Gene Expression Patterns*. **11**, 48–56 (2011).
279. M. A. Rahmani, T. Ueharai, Induction of metamorphosis and substratum preference in four sympatric and closely related species of sea urchins (genus *Echinometra*) in Okinawa. *Zool Stud*. **40**, 29–43 (2001).
280. M. Garcia-Lavandeira, A. Silva, M. Abad, A. Pazos, J. Sanchez, M. L. Pèrez-Parallé, Effects of GABA and epinephrine on the settlement and metamorphosis of the larvae of four species of bivalve molluscs. *J Exp Mar Biol Ecol*. **316**, 149–156 (2005).
281. P. Laimek, S. Clark, M. Stewart, F. Pfeiffer, C. Wanichanon, P. Hanna, P. Sobhon, The presence of GABA in gastropod mucus and its role in inducing larval settlement. *J Exp Mar Biol Ecol*. **354**, 182–191 (2008).
282. M. R. Elphick, SALMFamide salmagundi: The biology of a neuropeptide family in echinoderms. *Gen Comp Endocrinol*. **205** (2014), pp. 23–35.
283. M. R. Elphick, S. Achhala, N. Martynyuk, The evolution and diversity of SALMFamide neuropeptides. *PLoS One*. **8** (2013), doi:10.1371/journal.pone.0059076.
284. A. Aleotti, I. C. Wilkie, L. A. Yañez-Guerra, G. Gattoni, T. A. Rahman, R. F. Wademan, Z. Ahmad, D. A. Ivanova, D. C. Semmens, J. Delroisse, W. Cai, E. Odekunle, M. Egertová, C. Ferrario, M. Sugni, F. Bonasoro, M. R. Elphick, Discovery and functional characterization of neuropeptides in crinoid echinoderms. *Front Neurosci*. **16**, 1006594 (2022).
285. N. J. Wood, T. Mattiello, M. L. Rowe, L. Ward, M. Perillo, M. I. Arnone, M. R. Elphick, P. Oliveri, Neuropeptidergic systems in pluteus larvae of the sea urchin *Strongylocentrotus purpuratus*: Neurochemical complexity in a “Simple” nervous system. *Front Endocrinol (Lausanne)*. **9** (2018), doi:10.3389/fendo.2018.00628.
286. H. F. Carter, J. R. Thompson, M. R. Elphick, P. Oliveri, The development and neuronal complexity of bipinnaria larvae of the sea star *Asterias rubens*. *Integr Comp Biol*. **61**, 337–351 (2021).
287. H. Zeng, What is a cell type and how to define it? *Cell*. **185** (2022), pp. 2739–2755.
288. B. (Hatschek, *The amphioxus and its development* (Swan Sonnenschein & Co, London, 1893).
289. A. Kowalevsky, Entwicklungsgeschichte des Amphioxus lanceolatus. *Mém. Acad. Imp. Sci. St-Pétersb.* **11** (1867).
290. T. C. Lacalli, Frontal eye circuitry, rostral sensory pathways and brain organization in amphioxus larvae: Evidence from 3D reconstructions. *Philosophical Transactions of the Royal Society B: Biological Sciences*. **351**, 243–263 (1996).
291. H. Wicht, T. C. Lacalli, The nervous system of amphioxus: structure, development, and evolutionary significance. *Can J Zool*. **83**, 122–150 (2005).
292. T. C. Lacalli, N. D. Holland, J. E. West, Landmarks in the anterior central nervous system of amphioxus larvae. *Philosophical Transactions of the Royal Society B*. **344**, 165–185 (1994).
293. P. Vopalensky, J. Pergner, M. Liegertova, E. Benito-Gutiérrez, D. Arendt, Z. Kozmik, Molecular analysis of the amphioxus frontal eye unravels the evolutionary origin of the retina and pigment cells of the vertebrate eye. *Proceedings of the National Academy of Sciences*. **109**, 15383–15388 (2012).
294. J. Pergner, A. Vavrova, I. Kozmikova, Z. Kozmik, Molecular fingerprint of amphioxus frontal eye illuminates the evolution of homologous cell types in the chordate retina. *Front Cell Dev Biol*. **8**, 1–16 (2020).
295. J. Pergner, Z. Kozmik, Amphioxus photoreceptors - Insights into the evolution of vertebrate opsins, vision and circadian rhythmicity. *International Journal of Developmental Biology*. **61**, 665–681 (2017).

296. T. C. Lacalli, "Sensory systems in amphioxus: A window on the ancestral chordate condition" in *Brain, Behavior and Evolution* (2004), vol. 64, pp. 148–162.
297. T. Lacalli, S. Candiani, Locomotory control in amphioxus larvae: New insights from neurotransmitter data. *Evodevo*. **8**, 1–8 (2017).
298. L. F. C. Castro, S. L. K. Rasmussen, P. W. H. Holland, N. D. Holland, L. Z. Holland, A Gbx homeobox gene in amphioxus: Insights into ancestry of the ANTP class and evolution of the midbrain/hindbrain boundary. *Dev Biol*. **295**, 40–51 (2006).
299. M. Bozzo, T. C. Lacalli, V. Obino, F. Caicci, E. Marcenaro, T. Bachetti, L. Manni, M. Pestarino, M. Schubert, S. Candiani, Amphioxus neuroglia: molecular characterization and evidence for early compartmentalization of the developing nerve cord. *Glia*. **69**, 1654–1678 (2021).
300. H. Wada, J. Garcia-Fernández, P. W. H. Holland, Colinear and segmental expression of amphioxus Hox genes. *Dev Biol*. **213**, 131–141 (1999).
301. Q. Bone, The central nervous system in amphioxus. *Journal of Comparative Neurology*. **115**, 27–64 (1960).
302. D. Ekhart, H. W. Korf, H. Wicht, Cytoarchitecture, topography, and descending supraspinal projections in the anterior central nervous system of *Branchiostoma lanceolatum*. *Journal of Comparative Neurology*. **466**, 319–330 (2003).
303. A. Castro, M. Becerra, M. J. Manso, R. Anadón, Neuronal organization of the brain in the adult amphioxus (*Branchiostoma lanceolatum*): A study with acetylated tubulin immunohistochemistry. *Journal of Comparative Neurology*. **523**, 2211–2232 (2015).
304. T. Lacalli, Innovation through heterochrony: an amphioxus perspective on telencephalon origin and function. *Front Ecol Evol*. **9** (2021), doi:10.3389/fevo.2021.666722.
305. V. Hartenstein, A. Stollewerk, The evolution of early neurogenesis. *Dev Cell*. **32**, 390–407 (2015).
306. L. Z. Holland, M. Schubert, N. D. Holland, T. Neuman, Evolutionary conservation of the presumptive neural plate markers *AmphiSox1/2/3* and *AmphiNeurogenin* in the invertebrate chordate amphioxus. *Dev Biol*. **226**, 18–33 (2000).
307. E. Benito-Gutiérrez, M. Illas, J. X. Comella, J. Garcia-Fernández, Outlining the nascent nervous system of *Branchiostoma floridae* (amphioxus) by the pan-neural marker *AmphiElav*. *Brain Res Bull*. **66**, 518–521 (2005).
308. K. Yasui, S. Tabata, T. Ueki, M. Uemura, S. C. Zhang, Early development of the peripheral nervous system in a lancelet species. *Journal of Comparative Neurology*. **393**, 415–425 (1998).
309. E. Hedlund, Q. Deng, Single-cell RNA sequencing: technical advancements and biological applications. *Mol Aspects Med*. **59** (2018), pp. 36–46.
310. R. A. Amezcua, A. T. L. Lun, E. Becht, V. J. Carey, L. N. Carpp, L. Geistlinger, F. Marini, K. Rue-Albrecht, D. Risso, C. Soneson, L. Waldron, H. Pagès, M. L. Smith, W. Huber, M. Morgan, R. Gottardo, S. C. Hicks, Orchestrating single-cell analysis with Bioconductor. *Nat Methods*. **17**, 137–145 (2020).
311. C. Ziegenhain, B. Vieth, S. Parekh, B. Reinius, A. Guillaumet-Adkins, M. Smets, H. Leonhardt, H. Heyn, I. Hellmann, W. Enard, Comparative analysis of single-cell RNA sequencing methods. *Mol Cell*. **65**, 631–643.e4 (2017).
312. D. Grün, A. van Oudenaarden, Design and Analysis of Single-Cell Sequencing Experiments. *Cell*. **163** (2015), pp. 799–810.
313. H. García-Castro, N. J. Kenny, M. Iglesias, P. Álvarez-Campos, V. Mason, A. Elek, A. Schönauer, V. A. Sleight, J. Neiro, A. Aboobaker, J. Permanyer, M. Irimia, A. Sebé-Pedrós, J. Solana, ACME dissociation: a versatile cell fixation-dissociation method for single-cell transcriptomics. *Genome Biol*. **22** (2021), doi:10.1186/s13059-021-02302-5.
314. A. Lafzi, C. Moutinho, S. Picelli, H. Heyn, Tutorial: guidelines for the experimental design of single-cell RNA sequencing studies. *Nat Protoc*. **13** (2018), pp. 2742–2757.
315. V. Fernandez Vallone, K. Ludwik, H. Stachelscheid, "cellenONE® as automated single cell seeding platform for hiPSC subcloning" (2022).
316. A. Leon, L. Subirana, K. Magre, I. Cases, J. J. Tena, M. Irimia, J. L. Gomez-Skarmeta, H. Escrava, S. Bertrand, Gene regulatory networks of epidermal and neural fate choice in a chordate. *Mol Biol Evol*. **39** (2022), doi:10.1093/molbev/msac055.

317. M. Zawisza-álvarez, C. Pérez-Calles, G. Gattoni, J. Garcia-Fernández, È. Benito-Gutiérrez, C. Herrera-úbeda, The ADAR family in amphioxus: RNA editing and conserved orthologous site predictions. *Genes (Basel)*. **11**, 1–13 (2020).
318. D. Aldea, L. Subirana, C. Keime, L. Meister, I. Maeso, S. Marcellini, J. L. Gomez-Skarmeta, S. Bertrand, H. Escriva, Genetic regulation of amphioxus somitogenesis informs the evolution of the vertebrate head mesoderm. *Nat Ecol Evol*. **3**, 1233–1240 (2019).
319. B. Raj, J. A. Farrell, J. Liu, J. el Kholtei, A. N. Carte, J. Navajas Acedo, L. Y. Du, A. McKenna, Đ. Relić, J. M. Leslie, A. F. Schier, Emergence of neuronal diversity during vertebrate brain development. *Neuron*. **108**, 1058-1074.e6 (2020).
320. L. del Giacco, A. Pistocchi, F. Cotelli, A. E. Fortunato, P. Sordino, A peek inside the neurosecretory brain through Orthopedia lenses. *Developmental Dynamics*. **237**, 2295–2303 (2008).
321. T. Schredelseker, W. Driever, Conserved genoarchitecture of the basal hypothalamus in zebrafish embryos. *Front Neuroanat*. **14** (2020), doi:10.3389/fnana.2020.00003.
322. T. Schredelseker, F. Veit, R. I. Dorsky, W. Driever, Bsx is essential for differentiation of multiple neuromodulatory cell populations in the secondary prosencephalon. *Front Neurosci*. **14** (2020), doi:10.3389/fnins.2020.00525.
323. W. Wang, J. Fredrik Grimmer, T. R. van de Water, T. Lufkin, Hmx2 and Hmx3 homeobox genes direct development of the murine inner ear and hypothalamus and can be functionally replaced by *Drosophila* Hmx. *Dev Cell*. **7**, 439–453 (2004).
324. K. Tessmar-Raible, The evolution of neurosecretory centers in bilaterian forebrains: Insights from protostomes. *Semin Cell Dev Biol*. **18**, 492–501 (2007).
325. S. Candiani, L. Moronti, D. de Pietri Tonelli, G. Garbarino, M. Pestarino, A study of neural-related microRNAs in the developing amphioxus. *Evodevo*. **2** (2011), doi:10.1186/2041-9139-2-15.
326. T. Sekiguch, K. Kuwasako, M. Ogasawara, H. Takahashi, S. Matsubara, T. Osugi, I. Muramatsu, Y. Sasayama, N. Suzuki, H. Satake, Evidence for conservation of the calcitonin superfamily and activity-regulating mechanisms in the basal chordate: *Branchiostoma floridae* Insights into the molecular and functional evolution in chordates. *Journal of Biological Chemistry*. **291**, 2345–2356 (2016).
327. T. Sekiguchi, The calcitonin/calcitonin gene-related peptide family in invertebrate deuterostomes. *Front Endocrinol (Lausanne)*. **9**, 1–11 (2018).
328. F. A. Russell, R. King, S. J. Smillie, X. Kodji, S. D. Brain, Calcitonin gene-related peptide: physiology and pathophysiology. *Physiol Rev*. **94**, 1099–1142 (2014).
329. S. Temple, Q. Shen, "Cell biology of neuronal progenitor cells" in *Patterning and Cell Type Specification in the Developing CNS and PNS* (Elsevier Inc., 2013; <http://dx.doi.org/10.1016/B978-0-12-397265-1.00008-3>), pp. 261–283.
330. X. Qian, Q. Shen, S. K. Goderie, W. He, A. Capela, A. A. Davis, S. Temple, Timing of CNS cell generation. *Neuron*. **28**, 69–80 (2000).
331. V. S. Caviness, T. Takahashi, R. S. Nowakowski, Numbers, time and neocortical neuronogenesis: a general developmental and evolutionary model. *Trends Neurosci*. **18**, 379–383 (1995).
332. M. Götz, W. B. Huttner, The cell biology of neurogenesis. *Nat Rev Mol Cell Biol*. **6**, 777–788 (2005).
333. W. B. Huttner, Y. Kosodo, Symmetric versus asymmetric cell division during neurogenesis in the developing vertebrate central nervous system. *Curr Opin Cell Biol*. **17**, 648–657 (2005).
334. S. C. Noctor, V. Martínez-Cerdeño, L. Ivic, A. R. Kriegstein, Cortical neurons arise in symmetric and asymmetric division zones and migrate through specific phases. *Nat Neurosci*. **7**, 136–144 (2004).
335. N. D. Holland, L. Z. Holland, Stage- and tissue-specific patterns of cell division in embryonic and larval tissues of amphioxus during normal development. *Evol Dev*. **8**, 142–149 (2006).
336. E. Zieger, T. C. Lacalli, M. Pestarino, M. Schubert, S. Candiani, The origin of dopaminergic systems in chordate brains: insights from amphioxus. *Int J Dev Biol*. **61**, 749–761 (2017).
337. E. Benito-Gutiérrez, M. Stemmer, S. D. Rohr, L. N. Schumacher, J. Tang, A. Marconi, G. Jékely, D. Arendt, Patterning of a telencephalon-like region in the adult brain of amphioxus. *bioRxiv* (2018), doi:10.1101/307629.
338. G. Jékely, Global view of the evolution and diversity of metazoan neuropeptide signaling. *Proc Natl Acad Sci U S A*. **110**, 8702–8707 (2013).

339. Y.-C. Cheng, M. Amoyel, X. Qui, Y.-J. Jiang, Q. Xu, D. Wilkinson, Notch activation regulates the segregation and differentiation of rhombomere boundary cells in the zebrafish hindbrain. *Dev Cell*. **6**, 539–550 (2004).
340. J. Shin, J. Poling, H. C. Park, B. Appel, Notch signaling regulates neural precursor allocation and binary neuronal fate decisions in zebrafish. *Development*. **134**, 1911–1920 (2007).
341. T. C. Lacalli, S. J. Kelly, Floor plate, glia and other support cells in the anterior nerve cord of amphioxus larvae. *Acta Zoologica*. **83**, 87–98 (2002).
342. J. Yingling, Y. H. Youn, D. Darling, K. Toyo-oka, T. Pramparo, S. Hirotsune, A. Wynshaw-Boris, Neuroepithelial stem cell proliferation requires LIS1 for precise spindle orientation and symmetric division. *Cell*. **132**, 474–486 (2008).
343. F. M. Vaccarino, M. L. Schwartz, R. Raballo, J. Nilsen, J. Rhee, M. Zhou, T. Doetschman, J. D. Coffin, J. J. Wyland, Y. T. E. Hung, Changes in cerebral cortex size are governed by fibroblast growth factor during embryogenesis. *Nat Neurosci*. **2**, 246–253 (1999).
344. A. Chenn, C. A. Walsh, Regulation of cerebral cortical size by control of cell cycle exit in neural precursors. *Science* (1979). **297**, 365–369 (2002).
345. R. Tarallo, P. Sordino, Time course of programmed cell death in *Ciona intestinalis* in relation to mitotic activity and MAPK signaling. *Developmental Dynamics*. **230**, 251–262 (2004).
346. A. Nakayama, N. Satoh, Y. Sasakura, Tissue-specific profile of DNA replication in the swimming larvae of *Ciona intestinalis*. *Zoolog Sci*. **22**, 301–309 (2005).
347. M. Cremona, E. Colombo, M. Andreazzoli, G. Cossu, V. Broccoli, Bsx, an evolutionary conserved Brain Specific homeobox gene expressed in the septum, epiphysis, mammillary bodies and arcuate nucleus. *Gene Expression Patterns*. **4**, 47–51 (2004).
348. K. Tessmar-Raible, F. Raible, F. Christodoulou, K. Guy, M. Rembold, H. Hausen, D. Arendt, Conserved sensory-neurosecretory cell types in annelid and fish forebrain: insights into hypothalamus evolution. *Cell*. **129**, 1389–1400 (2007).
349. F. Christodoulou, F. Raible, R. Tomer, O. Simakov, K. Trachana, S. Klaus, H. Snyman, G. J. Hannon, P. Bork, D. Arendt, Ancient animal microRNAs and the evolution of tissue identity. *Nature*. **463**, 1084–1088 (2010).
350. N. Staudt, C. Houart, The prethalamus is established during gastrulation and influences diencephalic regionalization. *PLoS Biol*. **5**, 878–888 (2007).
351. M. Paris, H. Escriva, M. Schubert, F. Brunet, J. Brtko, F. Ciesielski, D. Roeklin, V. Vivat-Hannah, E. L. Jamin, J. P. Cravedi, T. S. Scanlan, J. P. Renaud, N. D. Holland, V. Laudet, Amphioxus postembryonic development reveals the homology of chordate metamorphosis. *Current Biology*. **18**, 825–830 (2008).
352. M. A. Tosches, T. M. Yamawaki, R. K. Naumann, A. A. Jacobi, G. Tushev, G. Laurent, Evolution of pallium, hippocampus, and cortical cell types revealed by single-cell transcriptomics in reptiles. *Science* (1979). **360**, 881–888 (2018).
353. M. A. Tosches, G. Laurent, Evolution of neuronal identity in the cerebral cortex. *Curr Opin Neurobiol*. **56**, 199–208 (2019).
354. G. v. Ermakova, A. v. Kucheryavyy, A. G. Zaraisky, A. v. Bayramov, The expression of FoxG1 in the early development of the European river lamprey *Lampetra fluviatilis* demonstrates significant heterochrony with that in other vertebrates. *Gene Expression Patterns*. **34** (2019), doi:10.1016/j.gep.2019.119073.
355. A. Pedroni, K. Ampatzis, Large-scale analysis of the diversity and complexity of the adult spinal cord neurotransmitter typology. *iScience*. **19**, 1189–1201 (2019).
356. L. Wilson, M. Maden, The mechanisms of dorsoventral patterning in the vertebrate neural tube. *Dev Biol*. **282** (2005), pp. 1–13.
357. S. Hannehalli, K. H. Kaestner, The evolution of Fox genes and their role in development and disease. *Nat Rev Genet*. **10** (2009), pp. 233–240.
358. J. K. Yu, F. Mazet, Y. T. Chen, S. W. Huang, K. C. Jung, S. M. Shimeld, The Fox genes of Branchiostoma floridae. *Dev Genes Evol*. **218**, 629–638 (2008).

359. E. Pascual-Carreras, C. Herrera-Úbeda, M. Rosselló, P. Coronel-Córdoba, J. Garcia-Fernández, E. Saló, T. Adell, Analysis of Fox genes in *Schmidtea mediterranea* reveals new families and a conserved role of Smed-foxO in controlling cell death. *Sci Rep.* **11** (2021), doi:10.1038/s41598-020-80627-0.
360. S. Chevalier, A. Martin, L. Leclère, A. Amiel, E. Houliston, Polarised expression of FoxB and FoxQ2 genes during development of the hydrozoan *Clytia hemisphaerica*. *Dev Genes Evol.* **216**, 709–720 (2006).
361. O. Seudre, F. M. Martín-Zamora, V. Rapisarda, I. Luqman, A. M. Carrillo-Baltodano, J. M. Martín-Durán, The Fox gene repertoire in the annelid *Owenia fusiformis* reveals multiple expansions of the foxQ2 class in Spiralia. *Genome Biol Evol* (2022), doi:10.1093/gbe/evac139.
362. A. Yamazaki, A. Yamamoto, J. Yaguchi, S. Yaguchi, cis-Regulatory analysis for later phase of anterior neuroectoderm-specific foxQ2 expression in sea urchin embryos. *Genesis* (2019), doi:10.1002/dvg.23302.
363. J. Trifinopoulos, L. T. Nguyen, A. von Haeseler, B. Q. Minh, W-IQ-TREE: a fast online phylogenetic tool for maximum likelihood analysis. *Nucleic Acids Res.* **44**, W232–W235 (2016).
364. M. Gouy, S. Guindon, O. Gascuel, Sea view version 4: A multiplatform graphical user interface for sequence alignment and phylogenetic tree building. *Mol Biol Evol.* **27**, 221–224 (2010).
365. R. J. White, J. E. Collins, I. M. Sealy, N. Wali, C. M. Dooley, Z. Digby, D. L. Stemple, D. N. Murphy, K. Billis, T. Hourlier, A. Füllgrabe, M. P. Davis, A. J. Enright, E. M. Busch-Nentwich, A high-resolution mRNA expression time course of embryonic development in zebrafish. *Elife.* **6**, e30860 (2017).
366. J. Yaguchi, A. Yamazaki, S. Yaguchi, Meis transcription factor maintains the neurogenic ectoderm and regulates the anterior-posterior patterning in embryos of a sea urchin, *Hemicentrotus pulcherrimus*. *Dev Biol.* **444**, 1–8 (2018).
367. K. A. Frazer, L. Pachter, A. Poliakov, E. M. Rubin, I. Dubchak, VISTA: Computational tools for comparative genomics. *Nucleic Acids Res.* **32**, 273–279 (2004).
368. L. J. Gearing, H. E. Cumming, R. Chapman, A. M. Finkel, I. B. Woodhouse, K. Luu, J. A. Gould, S. C. Forster, P. J. Hertzog, CiiiDER: a tool for predicting and analysing transcription factor binding sites. *PLoS One.* **14**, e0215495 (2019).
369. C. Y. Lin, M. Y. J. Lu, J. X. Yue, K. L. Li, Y. le Pétilion, L. W. Yong, Y. H. Chen, F. Y. Tsai, Y. F. Lyu, C. Y. Chen, S. P. L. Hwang, Y. H. Su, J. K. Yu, Molecular asymmetry in the cephalochordate embryo revealed by single-blastomere transcriptome profiling. *PLoS Genet.* **16** (2020), doi:10.1371/journal.pgen.1009294.
370. J. Heasman, Maternal determinants of embryonic cell fate. *Semin Cell Dev Biol.* **17** (2006), pp. 93–98.
371. S. Wennekamp, S. Mesecke, F. Nédélec, T. Hiiragi, A self-organization framework for symmetry breaking in the mammalian embryo. *Nat Rev Mol Cell Biol.* **14** (2013), pp. 454–461.
372. A. R. Palmer, Symmetry Breaking and the Evolution of Development. *Science* (1979). **306**, 828–833 (2004).
373. J. Heasman, Patterning the early *Xenopus* embryo. *Development.* **133** (2006), pp. 1205–1217.
374. C. Carron, D. L. Shi, Specification of anteroposterior axis by combinatorial signaling during *Xenopus* development. *Wiley Interdiscip Rev Dev Biol.* **5**, 150–168 (2016).
375. C. Anderson, C. D. Stern, "Organizers in Development" in *Current Topics in Developmental Biology* (Academic Press Inc., 2016), vol. 117, pp. 435–454.
376. A. Martínez Arias, B. Steventon, On the nature and function of organizers. *Development.* **145**, dev159525 (2018).
377. H. Spemann, H. Mangold, Über induktion von embryonalanlagen durch implantation artfremder organisatoren. *Arch Mikrosk Anat Entwicklmech.* **100**, 599–638 (1924).
378. C. Niehrs, Regionally specific induction by the Spemann-Mangold organizer. *Nat Rev Genet.* **5** (2004), pp. 425–434.
379. S. F. Gilbert, M. J. F. Barresi, *Developmental biology* (Sinauer Associates, Inc., Sunderland, 2016; <http://labs.devbio.com>), vol. 11th edition.
380. M. K. Khokha, J. Yeh, T. C. Grammer, R. M. Harland, Depletion of three BMP antagonists from Spemann's organizer leads to a catastrophic loss of dorsal structures. *Dev Cell.* **8**, 401–411 (2005).
381. B. Reversade, H. Kuroda, H. Lee, A. Mays, E. M. de Robertis, Depletion of *Bmp2*, *Bmp4*, *Bmp7* and Spemann organizer signals induces massive brain formation in *Xenopus* embryos. *Development.* **132**, 3381–3392 (2005).

382. Y. G. Langdon, M. C. Mullins, Maternal and zygotic control of zebrafish dorsoventral axial patterning. *Annu Rev Genet.* **45**, 357–377 (2011).
383. A. F. Schier, W. S. Talbot, The zebrafish organizer. *Curr Opin Genet Dev.* **8**, 464–471 (1998).
384. F. L. Marlow, "Setting up for gastrulation in zebrafish" in *Current Topics in Developmental Biology* (Academic Press Inc., 2020), vol. 136, pp. 33–83.
385. H. Hikasa, S. Y. Sokol, Wnt signaling in vertebrate axis specification. *Cold Spring Harb Perspect Biol.* **5** (2013), , doi:10.1101/cshperspect.a007955.
386. D. Kimelman, B. L. Martin, Anterior-posterior patterning in early development: Three strategies. *Wiley Interdiscip Rev Dev Biol.* **1**, 253–266 (2012).
387. M. Varga, S. Maegawa, G. Bellipanni, E. S. Weinberg, Chordin expression, mediated by Nodal and FGF signaling, is restricted by redundant function of two  $\beta$ -catenins in the zebrafish embryo. *Mech Dev.* **124**, 775–791 (2007).
388. G. Bellipanni, M. Varga, S. Maegawa, Y. Imai, C. Kelly, A. P. Myers, F. Chu, W. S. Talbot, E. S. Weinberg, Essential and opposing roles of zebrafish  $\beta$ -catenins in the formation of dorsal axial structures and neuroectoderm. *Development.* **133**, 1299–1309 (2006).
389. M. Varga, S. Maegawa, E. S. Weinberg, Correct anteroposterior patterning of the zebrafish neuroectoderm in the absence of the early dorsal organizer. *BMC Dev Biol.* **11**, 26 (2011).
390. J. Heasman, M. Kofron, C. Wyliet,  $\beta$ -catenin signaling activity dissected in the early *Xenopus* embryo: a novel antisense approach. *Dev Biol.* **222**, 124–134 (2000).
391. C. J. Lowe, M. Terasaki, M. Wu, R. M. Freeman, L. Runft, K. Kwan, S. Haigo, J. Aronowicz, E. Lander, C. Gruber, M. Smith, M. Kirschner, J. Gerhart, Dorsoventral patterning in hemichordates: Insights into early chordate evolution. *PLoS Biol.* **4**, 1603–1619 (2006).
392. J. K. Yu, Y. Satou, N. D. Holland, T. Shin-I, Y. Kohara, N. Satoh, M. Bronner-Fraser, L. Z. Holland, Axial patterning in cephalochordates and the evolution of the organizer. *Nature.* **445**, 613–617 (2007).
393. I. Kozmikova, S. Candiani, P. Fabian, D. Gurska, Z. Kozmik, Essential role of Bmp signaling and its positive feedback loop in the early cell fate evolution of chordates. *Dev Biol.* **382**, 538–554 (2013).
394. I. Kozmikova, J. Yu, Dorsal-ventral patterning in amphioxus: current understanding, unresolved issues, and future directions. *International Journal of Developmental Biology.* **61**, 601–610 (2017).
395. Y. le Petillon, G. Luxardi, P. Scerbo, M. Cibois, A. Leon, L. Subirana, M. Irimia, L. Kodjabachian, H. Escriva, S. Bertrand, Nodal-Activin pathway is a conserved neural induction signal in chordates. *Nat Ecol Evol.* **1**, 1192–1200 (2017).
396. T. Onai, J. Yu, I. L. Blitz, K. W. Y. Cho, L. Z. Holland, Opposing Nodal/Vg1 and BMP signals mediate axial patterning in embryos of the basal chordate amphioxus. *Dev Biol.* **344**, 377–389 (2010).
397. A. Herpin, C. Lelong, P. Favrel, Transforming growth factor- $\beta$ -related proteins: An ancestral and widespread superfamily of cytokines in metazoans. *Dev Comp Immunol.* **28**, 461–485 (2004).
398. A. Moustakas, C. H. Heldin, The regulation of TGF $\beta$  signal transduction. *Development.* **136** (2009), pp. 3699–3714.
399. J. Massagué, TGF $\beta$  signalling in context. *Nat Rev Mol Cell Biol.* **13** (2012), pp. 616–630.
400. D. Acampora, S. Mazan, Y. Lallemand, V. Avantaggiato, M. Maury, A. Simeone, P. Brulet, Forebrain and midbrain regions are deleted in *Otx2*<sup>-/-</sup> mutants due to a defective anterior neuroectoderm specification during gastrulation. *Development.* **121**, 3279–3290 (1995).
401. C. E. Erter, T. P. Wilm, N. Basler, C. V. E. Wright, L. Solnica-Krezel, Wnt8 is required in lateral mesendodermal precursors for neural posteriorization in vivo. *Development.* **128**, 3571–3583 (2001).
402. S. H. Kim, J. Shin, H. C. Park, S. Y. Yeo, S. K. Hong, S. Han, M. Rhee, C. H. Kim, A. B. Chitnis, T. L. Huh, Specification of an anterior neuroectoderm patterning by Frizzled8a-mediated Wnt8b signalling during late gastrulation in zebrafish. *Development.* **129**, 4443–4455 (2002).
403. M. Kobayashi, R. Toyama, H. Takeda, I. B. Dawid, K. Kawakami, Overexpression of the forebrain-specific homeobox gene *six3* induces rostral forebrain enlargement in zebrafish. *Development.* **125**, 2973–2982 (1998).
404. H. C. Seo, Ø. Drivenes, S. Ellingsen, A. Fjose, Expression of two zebrafish homologues of the murine *Six3* gene demarcates the initial eye primordia. *Mech Dev.* **73**, 45–57 (1998).

405. L. Sánchez-Arrones, J. L. Ferrán, L. Rodríguez-Gallardo, L. Puelles, Incipient forebrain boundaries traced by differential gene expression and fate mapping in the chick neural plate. *Dev Biol.* **335**, 43–65 (2009).
406. Y. Ogawa, T. Shiraki, Y. Asano, A. Muto, K. Kawakami, Y. Suzuki, D. Kojima, Y. Fukada, Six6 and Six7 coordinately regulate expression of middle-wavelength opsins in zebrafish. *Proc Natl Acad Sci U S A.* **116**, 4651–4660 (2019).
407. J. E. Valencia, R. Feuda, D. O. Mellott, R. D. Burke, I. S. Peter, Ciliary photoreceptors in sea urchin larvae indicate pan-deuterostome cell type conservation. *BMC Biol.* **19** (2021), doi:10.1186/s12915-021-01194-y.
408. R. Feuda, I. S. Peter, Homologous gene regulatory networks control development of apical organs and brains in Bilateria. *Sci Adv.* **8**, eabo2416 (2022).
409. G. Gestri, M. Carl, I. Appolloni, S. W. Wilson, G. Barsacchi, M. Andreazzoli, Six3 functions in anterior neural plate specification by promoting cell proliferation and inhibiting Bmp4 expression. *Development.* **132**, 2401–2413 (2005).
410. C. Koch, What is consciousness? *Nature.* **557**, S9–S12 (2018).
411. J. E. LeDoux, As soon as there was life, there was danger: the deep history of survival behaviours and the shallower history of consciousness. *Philos Trans R Soc Lond B Biol Sci.* **377**, 20210292 (2022).
412. M. A. Tosches, D. Arendt, The bilaterian forebrain: an evolutionary chimaera. *Curr Opin Neurobiol.* **23**, 1–10 (2013).
413. P. R. H. Steinmetz, R. Urbach, N. Posnien, J. Eriksson, R. P. Kostyuchenko, C. Brena, K. Guy, M. Akam, G. Bucher, D. Arendt, Six3 demarcates the anterior-most developing brain region in bilaterian animals. *Evodevo.* **1**, 1–9 (2010).
414. D. Cunningham, E. S. Casey, Spatiotemporal development of the embryonic nervous system of *saccoglossus kowalevskii*. *Dev Biol.* **386**, 252–263 (2014).
415. R. Mooi, B. David, Radial symmetry, the anterior/posterior axis, and echinoderm hox genes. *Annu Rev Ecol Evol Syst.* **39** (2008), pp. 43–62.
416. K. Nanglu, S. R. Cole, D. F. Wright, C. Souto, Worms and gills, plates and spines: the evolutionary origins and incredible disparity of deuterostomes revealed by fossils, genes, and development. *Biological Reviews* (2022), doi:10.1111/brv.12908.
417. M. Q. Martindale, A. Hejnol, A developmental perspective: changes in the position of the blastopore during bilaterian evolution. *Dev Cell.* **17**, 162–174 (2009).
418. L. Beccari, I. Conte, E. Cisneros, P. Bovolenta, Sox2-mediated differential activation of Six3.2 contributes to forebrain patterning. *Development.* **139**, 151–164 (2012).
419. L. Beccari, R. Marco-Ferreres, N. Tabanera, A. Manfredi, M. Souren, B. Wittbrodt, I. Conte, J. Wittbrodt, P. Bovolenta, A trans-Regulatory code for the forebrain expression of Six3.2 in the Medaka fish. *Journal of Biological Chemistry.* **290**, 26927–26942 (2015).
420. D. Brafman, K. Willert, Wnt/ $\beta$ -catenin signaling during early vertebrate neural development. *Dev Neurobiol.* **77** (2017), pp. 1239–1259.
421. P. A. Morcos, Y. Li, S. Jiang, Vivo-Morpholinos: a non-peptide transporter delivers Morpholinos into a wide array of mouse tissues. *Biotechniques.* **45**, 613–623 (2008).
422. J. Woych, A. O. Gurrola, A. Deryckere, E. C. B. Jaeger, E. Gumnit, G. Merello, J. Gu, A. J. Araus, N. D. Leigh, M. Yun, A. Simon, M. A. Tosches, Cell-type profiling in salamanders identifies innovations in vertebrate forebrain evolution. *Science* (1979). **377** (2022), doi:10.1126/science.abp9186.
423. L. Puelles, M. Harrison, G. Paxinos, C. Watson, A developmental ontology for the mammalian brain based on the prosomeric model. *Trends Neurosci.* **36** (2013), pp. 570–578.

## Appendix I – List of abbreviations

aGRN: anterior gene regulatory network	IO: isthmic organizer
ANC: aboral nerve centre	LR: left-right
ANE: anterior neuroectoderm	MeOH: methanol
ANR: anterior neural ridge	MHB: midbrain-hindbrain boundary
AO: apical organ	nfH <sub>2</sub> O: nuclease free water
AP: antero-posterior	PAD: pars anterodorsalis
ASW: artificial sea water	PBS: phosphate buffer saline
AZA: azakenpaullone	PBT: PBS + 0.1% Triton X-100
β-catMO: β-catenin morpholino	PFA: paraformaldehyde
BMP: bone morphogenetic proteins	PK: proteinase K
CMFSW: Ca <sup>2+</sup> -Mg <sup>2+</sup> -free artificial sea water	RNAseq: RNA sequencing
CNCS: conserved non-coding sequences	scRNAseq: single cell RNA sequencing
CNS: central nervous system	sFRP: secreted frizzled-related protein
COMO: standard control morpholino	Shh: sonic hedgehod
CV: cerebral vesicle	Ss: somites
DMSO: dimethylsulfoxide	SSCT: 5x SSC + 0.1% Triton X-100
Dkk: Dickkopf	TFBS: transcription factor binding site
Dpf: days post fertilization	UMI: unique molecular identifier
DV: dorso-ventral	ZLI: zona limitans intrathalamica
EdU: 5-Ethynyl-2'-deoxyuridine	
EtOH: ethanol	
Fgf: fibroblast growth factor	
FOX: forkhead-box	
Frz: Frizzled	
GRNs: gene regulatory networks	
HCR: <i>in situ</i> hybridization chain reaction	
HpF: hours post fertilization	
HU: hydroxyurea	



## Appendix II – The mysteries of crinoid metamorphosis

### Introduction

Despite the rich fossil record, the evolutionary origin of echinoderms' peculiar body plan remains unclear. Recent paleontological research uncovered fossils with a stereom and bilateral symmetry, possibly indicating the ancestral echinoderm condition (1). However, it is still debated how pentaradial symmetry evolved from this bilaterally symmetric animal. The difficulty in reconstructing the origin of adult features is exacerbated by the variety of life history and reproductive strategies in echinoderms. Most echinoderms develop indirectly, but direct development evolved several times independently, and even asexual reproduction through autotomy is observed (2, 3). In indirectly-developing species, the adult body is formed at metamorphosis. Eleutherozoans have a catastrophic metamorphosis during which the vast majority of larval tissues are discarded and the adult body develops from a rudiment on the left side of the larva, formed by cells of the left coelomic sac and the vestibular ectoderm (4, 5). On the other hand, crinoids have a more gradual metamorphosis in which larval tissues are rearranged to form the adult (6, 7). Therefore, studying crinoid metamorphosis could help to understand the formation of the echinoderm adult body plan. In particular, it would be interesting to understand how and from which cell types the adult nervous system forms. The key event of crinoid metamorphosis is the 90° rotation of the internal organs to reach the oral (posterior in the larva) position (5, 8). The vestibulum, which was located on the larval ventral surface, is internalized and rotates ventrally, to form the future oral surface of the ectoderm; the hydrocoel positions underneath the vestibule and pushes on the vestibular surface, forming the first tube feet of the pentacrinoid. The right somatocoel is thought to position on the aboral surface, forming the chambered organ, projecting within the stalk and surrounding most of the gut, while the left somatocoel positions orally within the calyx and the left axocoel forms the hydropore that connect the water vascular system to the external environment. The enteric sac elongates and form the digestive tube that opens with the mouth and anus. In collaboration with the lab of Prof. Roberta Pennati (University of Milan) and Prof. Maurice Elphick (Queen Mary University of London), I have characterized crinoid metamorphosis and the composition of the nervous system in post-metamorphic stages of *Antedon mediterranea*.

## Results

A standing question in echinoderm neurobiology is the developmental origin of the post-metamorphic adult nervous system. In fact, the evidence gathered until now suggests that larval neurons degenerate at metamorphosis in all echinoderms (9–11). In eleutherozoans it was traditionally thought that the ectoneural and hyponeural systems came from the ectodermal and (surprisingly) mesodermal derivatives of the adult rudiment, but studies on sea cucumbers showed that the whole nervous system derives from the rudiment ectoderm (12). In crinoids however the larval tissues are not discarded, and therefore adult neurons could originate from several candidate cell types. Ideally, to understand the origin of adult neurons the fate of specific larval cell types should be followed across development, but before reaching that stage there are two important milestones to reach: first, to elucidate the molecular and morphogenetic events of metamorphosis and how the larval tissues modify to form the adult; second, to characterize the post-metamorphic nervous system to identify its relationship with other echinoderm taxa.

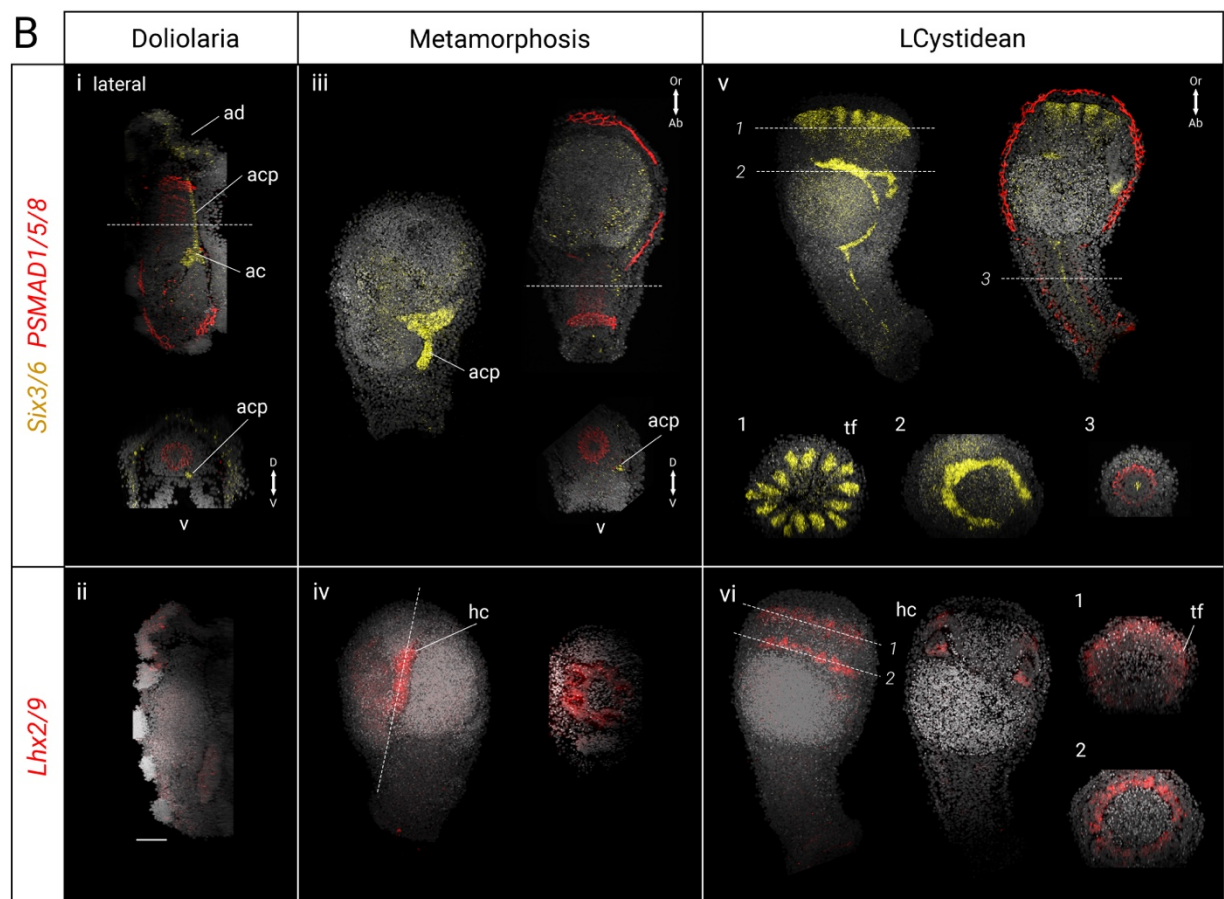
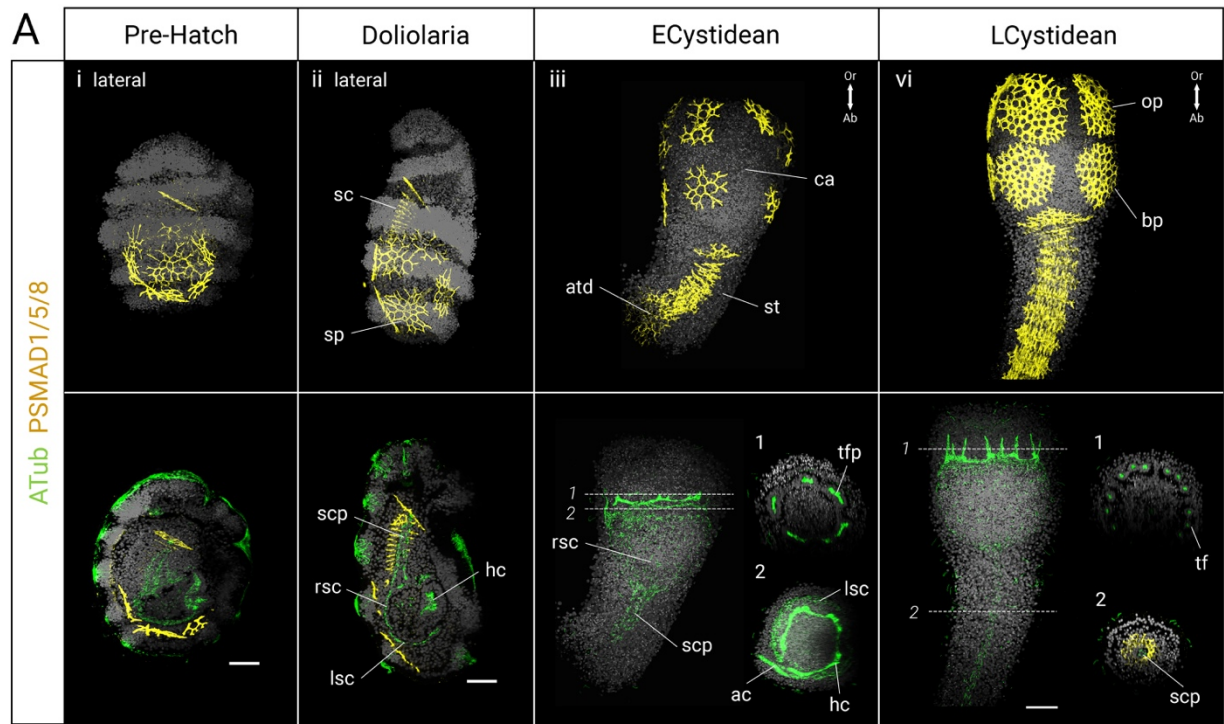
### 1 Following crinoid organs through metamorphosis

To expand previous microscopy descriptions of metamorphosis, I used acetylated tubulin, *Six3/6* and *Lhx2/9* as markers to follow the fate of larval tissues during and after metamorphosis. Moreover, by testing different antibodies on doliolaria larvae I discovered that immunostaining for mammalian phosphorylated Smad1/5/8 (PSMAD1/5/8), an effector of Bmp signalling, strongly labels the ossicles of the skeleton (Figure A2.1A). This is clearly caused by the binding of the antibody to a different epitope, as the skeleton is an inorganic structure, but the high specificity of the antibody means that we can use it to follow the development of the crinoid skeleton. Surprisingly, the ossicles could already be detected in the pre-hatching doliolaria: at this stage, the ten skeletal plates that will form the support structure of the pentacrinoid calyx had already developed, while the columnar ossicles of the stalk were just forming (Figure A2.1Ai). The whole skeleton was fully visible in the doliolaria: the skeletal plates encircled the coelomic cavities while the projection of the right somatocoel already ran within the columnar ossicles, as seen by colocalization with acetylated tubulin (Figure A2.1Aii).

In the settled larva, the ectodermal expression of *FoxQ2*, *Six3/6* and *Lhx2/9* disappeared from the apical surface (which is now attached to the substrate and becomes the aboral side of the animal)

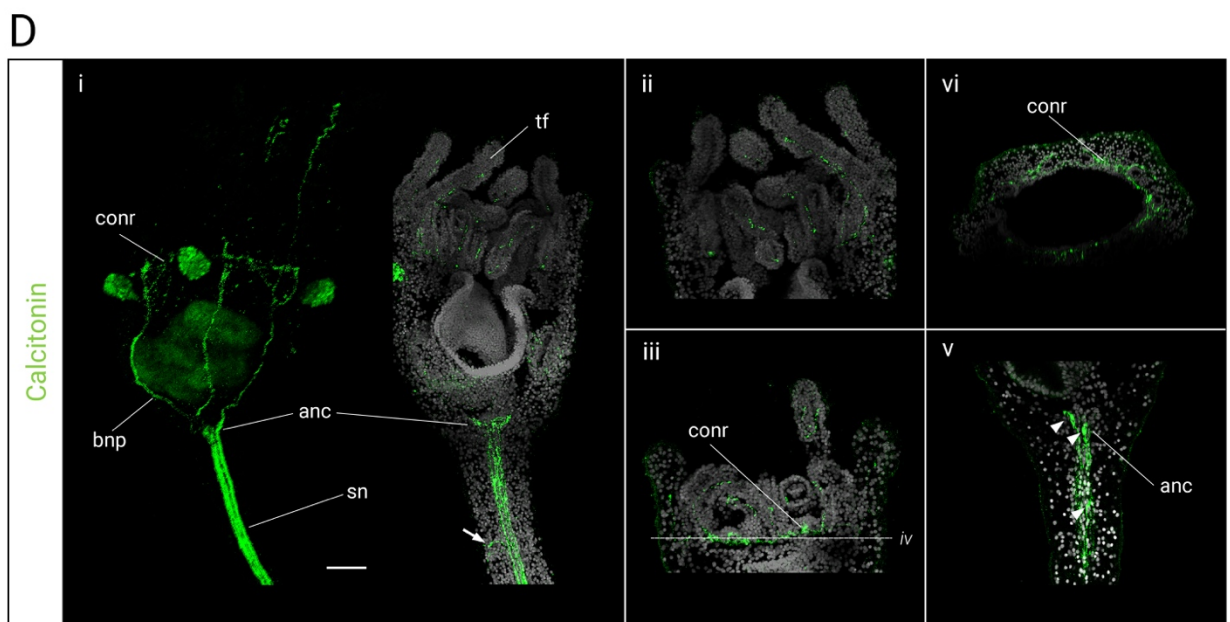
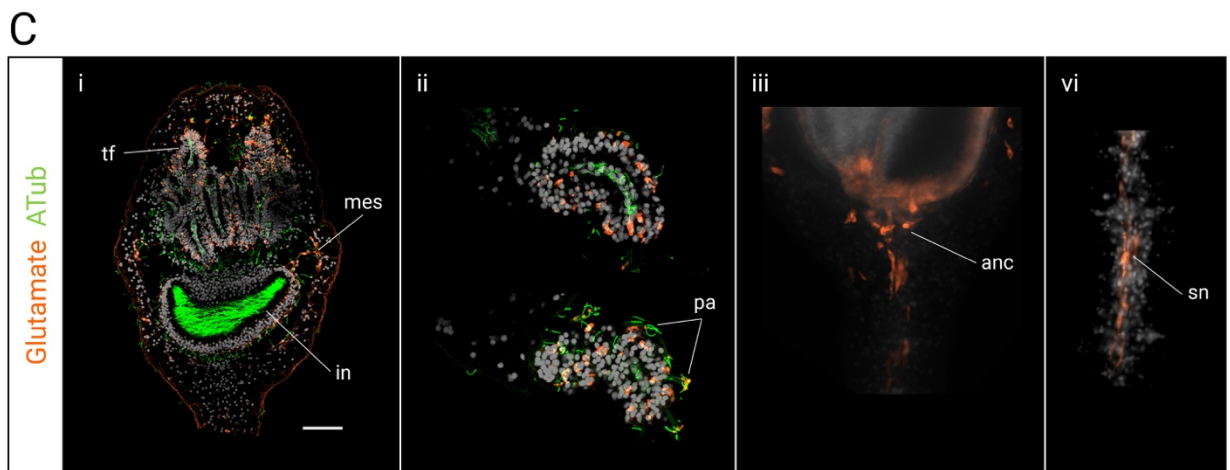
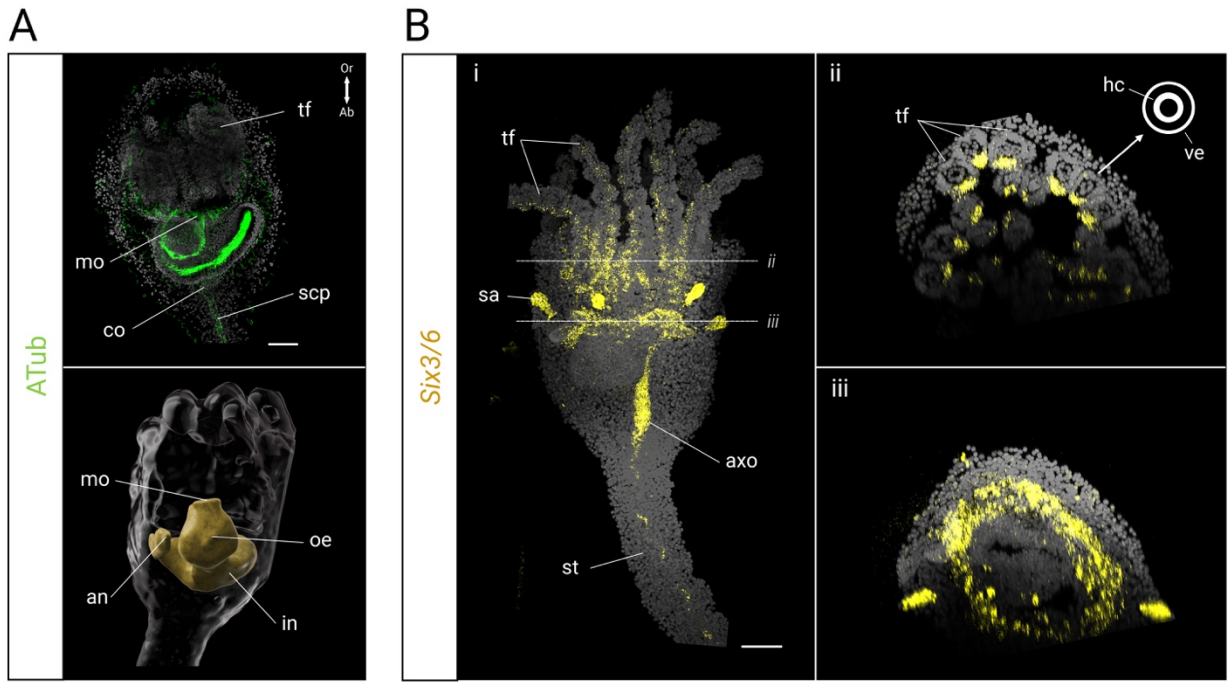
and the thickened epithelium of the ciliary band could not be detected (Figure A2.1Bi-iv). However, *Six3/6* continued to be expressed in the axocoel, which projected on the aboral side (Figure A2.1Biii). Note that this structure derives from the thin *Six3/6* positive projection found in the doliolaria (See Chapter IV) and is not part of the somatocoel, being outside of the columnar ossicles. *Lhx2/9* continued to label the hydrocoel, which is starting to rotate after the ingression of the ectodermal vestibule (Figure A2.1Biv). In cross section, the hydrocoel clearly showed a pentaradial organization in five circles. Behind the hydrocoel, the enteric sac expanded and seemed filled with small DAPI-positive corpuscles.

In the early cystidean, sparse cilia were found in the somatocoels: while the distinction between the left and right somatocoels was not clear, they enveloped the enteric sac (Figure A2.1Aiii). Moreover, the right somatocoel formed a funnel shape at the base of the calyx and then projected into the developing stalk. Numerous highly immunoreactive cilia labelled the internal surface of the hydrocoel, organized as a ring around the future oral surface. From the ring, five very short “bumps” directed orally. The ectoderm was not ciliated, but in later cystidean stages sparse cilia appeared in the epidermis, suggesting a new wave of ciliogenesis after metamorphosis (Figure A2.1Aiv). The organization of internal organs of the juvenile became more defined in the late cystidean stage. The skeletal plates grew larger and closer to each other (Figure A2.1Aiv). The somatocoels were still surrounding the enteric sac, which was filled by small corpuscles. The right somatocoel elongated with the stalk and became thinner. Moreover, at this stage *Six3/6* was expressed in cells at the centre of the stalk, presumably belonging to the right somatocoel (Figure A2.1Bv). This population is separate from the axocoelic one as it is found within the columnar ossicles. From the base of the calyx, stalk *Six3/6* expression looked continuous with a single streak that directs orally and ended with an oral horseshoe-shaped band below the vestibule (Figure A2.1Bv). In the hydrocoel, which still surrounded the oral surface, from each of the five anterior bumps three projections directed orally, pushing the vestibular epithelium and forming the internal rudiment of the first 15 tube feet of the juvenile. On the medial (ie closer to the centre) wall of the hydrocoel, at the base but not the tip of the forming tube feet, strong *Lhx2/9* signal could be detected (Figure A2.1Bvi). Interestingly, both *Six3/6* and *Lhx2/9* started to be highly expressed on the oral surface of the vestibule, at the level of the external surface of the tube feet (Figure A2.1Bv-vi).



< **Figure A2.1.** Morphological and molecular characterization of crinoid metamorphosis. **A.** Changes in the skeletal and ciliary organization analysed with immunofluorescence for phosphorylated Smad1/5/8 (yellow) and acetylated tubulin (green) in pre hatching (i), doliolaria (ii), early cystidean (iii) and late cystidean (iv) stages. **B.** Expression of *Six3/6* and *Lhx2/9* and their relation to skeletal development in doliolaria larvae (i-ii), during settlement and metamorphosis (iii-iv) and in the cystidean phase (v-vi). In both panels numbered insets represent sections at the levels indicated in by the dashed lines in the main images. Scale bars are 50µm. ac: axocoel, acp: axocoel projection, ad: adhesive pit, atd: attachment disk, bp: basal plates, ca: calyz, hc: hydrocoel, lsc: left somatocoel, op: oral plates, rsc: right somatocoel, sc: skeletal columnals, scp: somatocoel projection, sp: skeletal plates, st: stalk, tf: tube feet, tfp: tube feet primordia.

In pentacrinoids the oral wall of the epidermis opened to reveal a mouth connected to an empty gut divided into an oesophagus and intestine region (Figure A2.2A). Curiously, the intestine bent but, at least at this stage, the anus opened laterally and not on the oral surface. Both the oral surface and the gut were highly ciliated, while the epidermis continued to be only sparsely ciliated (Figure A2.2A). On the oral side of the epidermis, five saccules appeared; the function of these structures is still unclear, but they usually show aspecific staining with both antibodies and HCR hairpins. The somatocoels still possessed numerous cilia, and the right somatocoel had a funnel shape (forming the chambered organ) at the base of the calyx and ran through the stalk. However, at this stage *Six3/6* was only sparsely expressed in the stalk somatocoel (Figure A2.2Bi). On the other hand, the thin *Six3/6*-positive line that connected the right somatocoel with the oral side enlarged and could be recognized as a haemal structure called axial organ (Figure A2.2Bi). The axial organ was still connected with a strongly *Six3/6*-positive ring positioned below the mouth (Figure A2.2Biii). At this stage, five pairs of tube feet have formed next to the five triplets, bringing the total number of tube feet to 25. The tube feet bore several projections called papillae, which terminated with a tuft of four or five short cilia. Curiously, only the medial portion of the external ectodermal layer of the tube feet, which faces the mouth, continued to express *Six3/6* (Figure A2.2Bii). Taken together, the combination of labelling techniques allowed me to follow and describe the metamorphic process of the crinoid larva, providing a framework for the description of the post-metamorphic nervous system.



< **Figure A2.2.** Nervous system characterization in the pentacrinoid stage. **A.** Distribution of cilia marked by acetylated tubulin (green) and three-dimensional reconstruction of the digestive system by Imaris segmentation. **B.** Expression of *Six3/6* in the whole pentacrinoid (i) and in cross sections (ii-iii) at the levels marked by the dashed lines in (i). **C.** Distribution of glutamate (orange) and acetylated tubulin (green) immunoreactivity in the calyx (i), tube feet (ii), aboral nerve centre (iii) and stalk (vi). **D.** Calcitonin-like immunofluorescence (green) in the pentacrinoid. Arrow indicates rare neurons that connect the epidermis with the stalk nerve. with magnifications at the level of the tube feet (ii-iii), circumoral nerve ring (longitudinal view in iii and cross view in vi) and aboral nerve centre (v), with arrowheads indicating the position of cell bodies. Scalebars are 50µm. an: anus, anc: aboral nerve centre, axo: axial organ, bnp: brachial nerve primordia, co: chambered organ, conr: circumoral nerve ring, hc: hydrocoel, in: intestine, mes: mesenteries, mo: mouth, oe: oesophagus, pa: papillae, sa: saccules, scp: somatocoel projection, sn: stalk nerve, st: stalk, tf: tube feet, ve: vestibular ectoderm.

## 2 Pentacrinoid nervous system

In my Master's project I have described the localization of  $\beta$ -tubulin, serotonin and GABA in the pentacrinoid of *A. mediterranea*, highlighting the presence of at least ectoneural and entoneural components (13). Here, I expand this analysis by detecting glutamate and calcitonin-like immunoreactivity. Glutamate was distributed broadly, labelling multiple pentacrinoid structures (Figure A2.2Ci). A high number of positive cells were detected in the tube feet (Figure A2.2Cii). Contrary to serotonergic neurons, these cells did not form an obvious axonal net, but positivity was found mainly in the cell bodies. Interestingly, positive puncta were also found at the tip of the papillae. Scattered glutamatergic neurons were also labelled across the calyx epidermis (Figure A2.2Ciii). These cells appeared to be more concentrated on the aboral side and were shown to possess short axonal projections. A variable number of neurons were also labelled in the entoneural system (Figure A2.2Ciii, iv). A few positive cells were sometimes visible just oral to the ANC, while several immunopositive fibers and scattered cell bodies could be seen along the stalk nerve. Finally, the antibody labelled the mesenteries that connect the digestive system to the coelomic tissues.

I have also investigated the distribution of calcitonin-like immunoreactivity in *A. mediterranea* using an antibody raised against starfish (*A. rubens*) calcitonin (ArCT). These experiments were carried out as part of a collaboration between the laboratories of Prof. Michela Sugni at the University of Milan and Prof. Maurice Elphick at Queen Mary University of London. The use of the antibody against

ArCT was justified by the analysis of the C-terminal region of the *A. mediterranea* calcitonin-type neuropeptide AmCT (GGM**FGSSGP-NH2**), which shares similarity (in bold) with the sequence of ArCT (NSP**FGASGP-NH2**) used to generate the antibody (14). The antibody labelled different components of the pentacrinoid nervous system (Figure A2.2D). In the ANC and the proximal portion of the stalk nerve several immunopositive neurons could be detected (Figure A2.2Di, v). Moreover, intense immunolabelling was found in fibers running along the stalk up to the attachment disk. These fibers were organized in five main bundles around the somatocoel located in the centre of the stalk. A few positive cells arranged perpendicularly to these fibers were also seen connecting the entoneural system to the external surface of the stalk. Moreover, from the ANC five groups of labelled fibers extended towards the oral side of the animal (Figure A2.2Di). These fibers contacted other calcitonin-positive cells which formed a superficial and conspicuous circumoral nerve ring (CONR) around the mouth (Figure A2.2Di,iii-iv). The CONR is also connected with single axons that run through the tube feet (Figure A2.2Dii-iii). To ensure that the pattern of calcitonin-like immunoreactivity is due to the specific binding of the antibody, I also performed a control experiment using an antibody pre-absorbed with the ArCT peptide (the pre-absorption was carried out by the Elphick Lab). Samples incubated with pre-absorbed antiserum showed no immunopositivity except for aspecific signal in the saccules (data not shown).

## Discussion

Morphological descriptions compiled during the 20<sup>th</sup> century have accumulated an impressive amount of information on crinoid metamorphosis (7, 8, 15). The complex rearrangement of the internal organs is difficult to follow, but by labelling specific structures we can more easily study their morphogenesis. In particular, *Lhx2/9* and *Six3/6* marked the hydrocoel and axocoel respectively during metamorphosis. *Lhx2/9* expression highlighted that the hydrocoel already has a pentaradial organization in the settled larva. As the first structure to clearly show this symmetry, it would be interesting to understand how it is molecularly specified. *Lhx2/9* was expressed throughout the hydrocoel, suggesting that it has a role in its identity but not in its regionalization. In the cystidean stage however, *Lhx2/9* is expressed only in the medial part of the hydrocoel at the base of the tube feet, indicating a functional differentiation of the coelom after metamorphosis. On the other hand, the expression of *Six3/6* is more dynamic. The axocoel continues to express *Six3/6* after settlement, but a seemingly new population of *Six3/6*-positive cells appear in the stalk and at the base of the

calyx. It is highly unlikely that these cells derive from the axocoel, as previous investigations (and the acetylated tubulin expression data presented here) have clarified that this tissue derives from the anterior projection of the right somatocoel. It is possible however that the thin streak of positive tissue connecting the aboral, somatocoelic side with the oral ring of *Six3/6* expression derives from the axocoel. This line seemingly forms the axial organ of the pentacrinoid, which would therefore be of axocoelic origin. However, other studies have suggested that the axial organ might derive from the somatocoel (6), therefore further studies at higher temporal resolution are needed to understand this question.

During metamorphosis, the enteric sac is filled with small, DAPI-positive corpuscles, which have been identified as small cells with yolk granules and highly heterochromatic nuclei. This organization is significantly different from the one seen in the doliolaria, and the short time that separates the swimming and settled stages means it is unlikely that enteric cells underwent a high number of cell divisions. Accordingly, immunohistochemistry for phosphorylated histone H3 (PHH3) have not detected a significant increase of mitotic cells in the enteric sac (data not shown). An alternative possibility is that these represent cell fragments, possibly used as source of energy. In the pentacrinoid the gut has formed and has a complex turned shape, but the anus opens laterally rather than orally. This suggests that the U-shaped gut typical of pelmatozoans is a secondary acquisition that forms during development, as suggested by recent fossil evidence (16).

While most of the larval tissues are maintained in the pentacrinoid stage, the doliolaria nervous system seems to degenerate at metamorphosis, and the apical expression of aGRN genes is lost shortly after settlement. Previous studies have shown that the new, post-metamorphic nervous system already comprises ectoneural and entoneural components (6, 13). The ectoneural system is concentrated at the level of the tube feet and comprises a dense net of serotonergic and GABAergic neurons, while the entoneural component forms the ANC, stalk nerve and brachial nerve primordia, which direct orally (13). Previous analyses have shown that SALMFamides are expressed in the ANC and in several other tissues, including the mouth and the gut, but not in the tube feet (17). Moreover, serotonergic and GABAergic cells are also interspersed along the epidermis of the calyx, likely forming a peripheral basiepithelial plexus (13). Here, I further explored the diversity of neural populations in the pentacrinoid nervous system by detecting the localization of glutamate and calcitonin. Glutamatergic cells are concentrated in the ectodermal component of the tube feet.

Labelled cells did not have long projections: this could be due to the particular staining of the antibody or could indicate that these cells act locally. Moreover, antibody staining was also detected at the tip of the papillae. We have previously shown that cells from the base of the papillae send short projections to their tips (13). I hypothesise that these cells are glutamatergic, possibly with a sensory function. Thin calcitonin-positive fibers are also found in the tube feet: these axonal projections run alongside the tube feet almost reaching their tips. Overall, the ectoneural system of the tube feet appear to be highly complex and composed of a net of serotonergic, GABAergic, glutamatergic and peptidergic cell populations, likely involved in sensing the external environment and in feeding. The calcitonin-positive fibers of the tube feet were continuous with a conspicuous CONR. The localization of this neuropeptide around the mouth, where SALMFamide-positive cells were also detected, suggests a role of peptidergic neurons in feeding that could be investigated in future studies (17). The expression of calcitonin also revealed that the CONR is in contact with the brachial nerve primordia that project from the ANC, part of the crinoid-specific entoneural system. Here, both calcitonin- and glutamate-immunopositive cells could be detected. The peptidergic cells seem to project into the stalk nerve, which is arranged around the right somatocoel projection. Several glutamatergic and few peptidergic cells were also connecting the stalk nerve with the external environment, likely indicating a sensory component to the stalk.

Taken together, these results demonstrate that the different components of the post-metamorphic nervous system are deeply interconnected. By complementing this analysis on neuronal type with the expression pattern of conserved genes, it is possible to start comparing the crinoid nervous system with other echinoderms and other deuterostomes. Interestingly, both *Six3/6* and *Lhx2/9* started to be expressed in the vestibular ectoderm (from which the tube feet form) in the cystidean stage, and *Six3/6* continued to be strongly expressed in the medial side of the pentacrinoïd tube feet (facing the mouth). The result obtained for *Six3/6* is in accordance with recent data obtained by Omori and collaborators in *Anneissia japonica*, showing that *Six3/6*, *Otx* and *Pax4/6* are expressed in the vestibular ectoderm in the cystidean and then in ectodermal and hyponeural components of the pentacrinoïd, including tube feet and circumoral nerve ring (18). These genes are involved in the specification of the anterior portion of the nervous system in many bilaterians (19, 20). Their expression in the oral portion of the crinoid juvenile indicates that the ectoneural and possibly hyponeural systems have an “anterior” neural fate. Therefore, the investigation of gene expression in the post-metamorphic nervous system is useful in trying to solve one of the standing mysteries

of echinoderm biology: the relation between the body axes in echinoderms and deuterostomes (5, 21, 22). One hypothesis states that each arm corresponds to the AP axis of a bilaterally symmetric animal. This would mean that gene expression along each arm should be similar to the one found along the AP axis in other deuterostomes, but recent results seem to contradict this (23–25). Another scenario that received recent support sees the oral-aboral axis as a shrunken and modified AP axis (5, 22, 23, 26). The “anterior” identity of the oral nervous system supports this second hypothesis, but it remains to be investigated how the arms evolved from this condition. More studies at the molecular and transcriptome level are therefore needed to understand the evolution of the “one genome, two body plans” system active during the enigmatic life cycle of echinoderms.

## References

1. S. Zamora, I. A. Rahman, Deciphering the early evolution of echinoderms with Cambrian fossils. *Palaeontology*. **57**, 1105–1119 (2014).
2. L. R. McEdward, B. G. Miner, Larval and life-cycle patterns in echinoderms. *Can J Zool*. **79**, 1125–1170 (2001).
3. R. A. Raff, M. Byrne, The active evolutionary lives of echinoderm larvae. *Heredity (Edinb)*. **97**, 244–252 (2006).
4. T. C. Lacalli, Larval budding, metamorphosis, and the evolution of life-history patterns in echinoderms. *Invertebrate Biology*. **119**, 234–241 (2000).
5. K. J. Peterson, C. Arenas-Mena, E. H. Davidson, The A/P axis in echinoderm ontogeny and evolution: evidence from fossils and molecules. *Evol Dev*. **2**, 93–101 (2000).
6. S. Engle, thesis, Freie Universität Berlin, Berlin (2012).
7. P. V. Mladenov, F. S. Chia, Development, settling behaviour, metamorphosis and pentacrinoid feeding and growth of the feather star *Florometra serratissima*. *Mar Biol*. **79**, 309–323 (1983).
8. L. H. Hyman, *The Invertebrates: Echinodermata* (McGraw-Hill Publications, 1955).
9. V. Mashanov, O. Zueva, T. Rubilar, L. Epherra, J. E. García-Arrarás, "Echinodermata" in *Structure and Evolution of Invertebrate Nervous Systems*, A. Schmidt-Rhaesa, S. Harzsch, G. Purschke, Eds. (Oxford University Press, 2016), pp. 665–688.
10. V. F. Hinman, R. D. Burke, Embryonic neurogenesis in echinoderms. *Wiley Interdiscip Rev Dev Biol*. **7**, 1–15 (2018).
11. H. Nakano, Y. Nakajima, S. Amemiya, Nervous system development of two crinoid species, the sea lily *Metacrinus rotundus* and the feather star *Oxycomanthus japonicus*. *Dev Genes Evol*. **219**, 565–576 (2009).
12. V. S. Mashanov, Ñ. O. R. Zueva, T. Heinzeller, B. Aschauer, I. Y. Dolmatov, Developmental origin of the adult nervous system in a holothurian : an attempt to unravel the enigma of neurogenesis in echinoderms. *Evol Dev*. **9**, 244–256 (2007).
13. S. Mercurio, G. Gattoni, S. Messinetti, M. Sugni, R. Pennati, Nervous system characterization during the development of a basal echinoderm, the feather star *Antedon mediterranea*. *Journal of Comparative Neurology*. **527**, 1127–1139 (2019).

14. W. Cai, C. H. Kim, H. J. Go, M. Egertová, C. G. Zampronio, A. M. Jones, N. G. Park, M. R. Elphick, Biochemical, anatomical, and pharmacological characterization of Calcitonin-type neuropeptides in Starfish: discovery of an ancient role as muscle relaxants. *Front Neurosci.* **12** (2018), doi:10.3389/fnins.2018.00382.
15. T. Mortensen, "Studies in the development of crinoids" in *Papers from the Department of Marine Biology of the Carnegie Institution of Washington* (1920), vol. 16.
16. I. A. Rahman, J. A. Waters, C. D. Sumrall, A. Astolfo, Early post-metamorphic, Carboniferous blastoid reveals the evolution and development of the digestive system in echinoderms. *Biol Lett.* **11** (2015), doi:10.1098/rsbl.2015.0776.
17. A. Aleotti, I. Wilkie, L. Yañez-Guerra, G. Gattoni, T. Rahman, R. Wademan, Z. Ahmad, D. Ivanova, D. Semmens, J. Delroisse, W. Cai, E. Odekunle, M. Egertova, C. Ferrario, M. Sugni, F. Bonasoro, M. Elphick, Discovery and functional characterization of neuropeptides in crinoid echinoderms. *Front Neurosci* (2022).
18. A. Omori, T. F. Shibata, K. Akasaka, Gene expression analysis of three homeobox genes throughout early and late development of a feather star *Anneissia japonica*. *Dev Genes Evol.* **230**, 305–314 (2020).
19. H. Marlow, M. A. Tosches, R. Tomer, P. R. Steinmetz, A. Lauri, T. Larsson, D. Arendt, Larval body patterning and apical organs are conserved in animal evolution. *BMC Biol.* **12**, 1–17 (2014).
20. P. R. H. Steinmetz, R. Urbach, N. Posnien, J. Eriksson, R. P. Kostyuchenko, C. Brena, K. Guy, M. Akam, G. Bucher, D. Arendt, Six3 demarcates the anterior-most developing brain region in bilaterian animals. *Evodevo.* **1**, 1–9 (2010).
21. R. D. Burke, Deuterostome neuroanatomy and the body plan paradox. *Evol Dev.* **13**, 110–115 (2011).
22. A. B. Smith, Deuterostomes in a twist: the origins of a radical new body plan. *Evol Dev.* **10**, 493–503 (2008).
23. M. Byrne, P. Martinez, V. Morris, Evolution of a pentamerous body plan was not linked to translocation of anterior Hox genes: The echinoderm HOX cluster revisited. *Evol Dev.* **18**, 137–143 (2016).
24. Y. Hara, M. Yamaguchi, K. Akasaka, H. Nakano, M. Nonaka, S. Amemiya, Expression patterns of Hox genes in larvae of the sea lily *Metacrinus rotundus*. *Dev Genes Evol.* **216**, 797–809 (2006).
25. C. Arenas-Mena, A. Cameron, E. Davidson, Spatial expression of Hox cluster genes in the ontogeny of a sea urchin. *Development.* **127**, 4631–4643 (2000).
26. R. Mooi, B. David, Radial symmetry, the anterior/posterior axis, and echinoderm hox genes. *Annu Rev Ecol Evol Syst.* **39** (2008), pp. 43–62.

# Appendix III – Evolution of endodermal expression of calcitonin

## Introduction

In vertebrates, a large number of neuropeptides are found not only in neurons, where they are used for neurotransmission and neuromodulation, but are also released in the blood to work as hormones. Hormones then travel to organs that are very distant from their source and control a variety of functions including homeostasis, growth, metabolism, reproduction and behaviour. While the specialized endocrine glands that release hormones are generally distributed along the body, a considerable number of them develops from the pharyngeal endoderm during development. In mammals, the floor of the pharynx forms the thyroid, the endoderm of third pharyngeal pouch is specified into the thymus and inferior parathyroid and the fourth pouch forms the superior parathyroid and the ultimobranchial bodies (UBs) (1).

The evolutionary history of the UBs is particularly interesting: in mammals, UB cells migrate into the thyroid during development, but in other vertebrates the UB remain throughout their life (2). In both cases, the main cell type of the UB, the C cells, are involved in the regulation of  $Ca^{2+}$  homeostasis through the production of calcitonin (CT). This protein is transcribed from the *CALCA* gene, which also has an alternatively spliced form, the calcitonin gene related peptide (CGRP), that has a role as a neuropeptide in the nervous system (3). Moreover, while in mammals the endodermal origin of the UB is clear, previous studies have suggested that the UB in birds receive ectodermal contributions from the nervous system (2). Unpublished tracing experiments by Dr. Andrew Gillis showed that in teleosts the UBs have an endodermal origin, demonstrating that this is the ancestral origin of vertebrate C cells.

Given the conservation of C cells in vertebrates, we were interested to understand how far back we could trace the endodermal UBs and the expression of CT. CT orthologs are found in both cephalochordates and tunicates. *Amphioxus* has three calcitonin family peptide (*CTFP*) genes, which are arranged in series suggesting a tandem duplication specific to the cephalochordates (4, 5).

As shown in Chapter V, *CTPFs* are expressed in the larval nervous system. In tunicates there is a single *CT* gene that was shown to be expressed in the larval brain by qRT-PCR(6, 7). In larval stages of invertebrate chordates the expression of *CT* orthologs is thus limited to the nervous system and is not found in the endoderm. Together with the reported expression of *CT* in the starfish nervous system (8), this indicates an ancient neuropeptidergic function of *CT* in bilaterians. On the other hand, the localization of *CT* family molecules in the adults of invertebrate chordates is not well understood. Therefore, together with Dr Andrew Gillis I investigated the expression of *CTFP* orthologs in adult paraffin sections of *B. lanceolatum* and *C. intestinalis* to explore the evolution of *CT* signalling.

## Results

### 1 Pharyngeal expression of *CTFPs* in the amphioxus adult

I analysed the expression of all three *CTFP* paralogs together using HCR on longitudinal sections of the amphioxus pharynx. I found widespread co-localization of the three markers at the level of the gills, specifically in cells at the base of gill bars (Figure A3.1A-B). In the adult amphioxus the gill bars consist of a thick surface epithelium divided into three portions: atrial cells are found at the base of the gill bars, facing the epithelium, ciliated cells are located laterally on each side of the bar, and pharyngeal cells are distal and face the pharynx cavity (9). While all gill bars are supported by a skeletal rod, they can be distinguished in two types: primary gill bars possess a coelom while secondary gill bars split from the primary, remaining connected through a collagenous link, and do not possess a coelom (9). From the samples analysed, *CTFPs* expression is found in atrial cells of both primary and secondary gill bars, but the pattern is slightly different: in primary gill bars the expression is weaker and more widespread (Figure A3.1B), while in secondary gill bars it seems to be stronger and more concentrated in specific atrial cells (Figure A3.1C-G). No expression was found at the level of the endostyle, but we found strongly autofluorescent cells located below the endostyle epithelium. These cells were not positive to *CTFP3* as the same pattern could be seen in unstained sections (data not shown). On the other hand, the endostyle expressed a combination of factors, such as *Pax2/5/8* and *Nk2.1* that divide it in different regions as previously described (10). Interestingly, detection of *Pax2/5/8* in longitudinal sections also showed expression of these markers in atrial cells, suggesting that it is also found in *CTFP*-expressing cells.

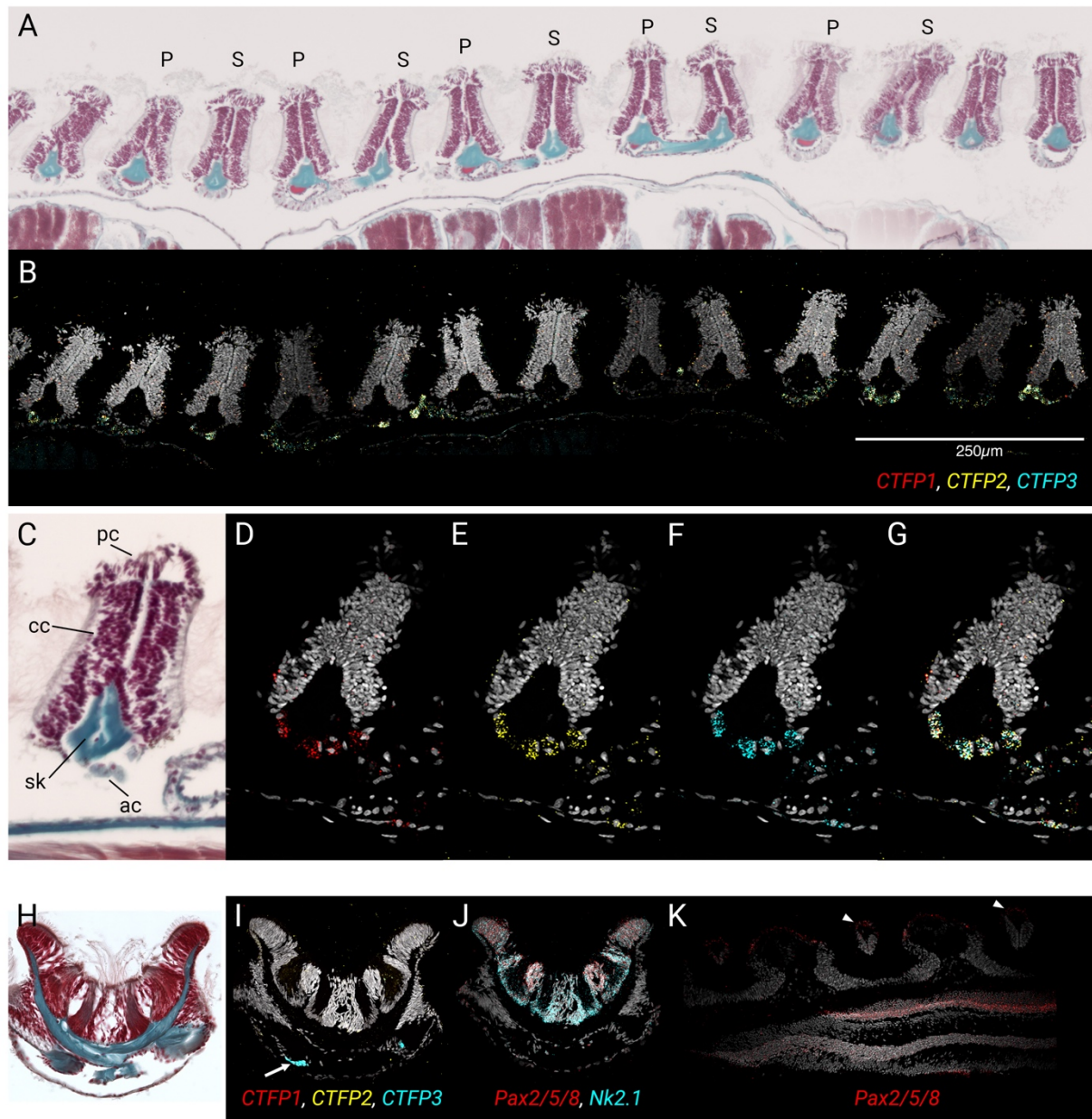


**Figure A3.1** Expression of the amphioxus calcitonin family peptides (CTFPs) in sections of the adult pharynx. **A-G** Masson's trichrome staining and HCR localization of CTFPs transcripts in longitudinal sections. The gills are formed by primary (P) and secondary (S) gill bars. CTFPs are expressed in lateral cells in each gill bar, but expression is higher in secondary bars (A-B). Magnification of a single gill bar, composed of pharyngeal cells (pc), ciliated cells (cc), atrial cells (ac) and a skeletal support (sk) (C). HCR staining shows that CTFPs are expressed in atrial cells (D-G). **H-K** Characterization of the amphioxus endostyle. The three CTFP genes are not expressed in the endostyle, but cells located below it are strongly autofluorescent when hit by light at 488nm (arrow) (I). *Nk2.1* is expressed throughout the endostyle while *Pax2/5/8* is found only in lateral populations (J). A longitudinal section stained for *Pax2/5/8* shows expression in the endostyle but also in atrial cells of the gill bars (arrowhead) (K).

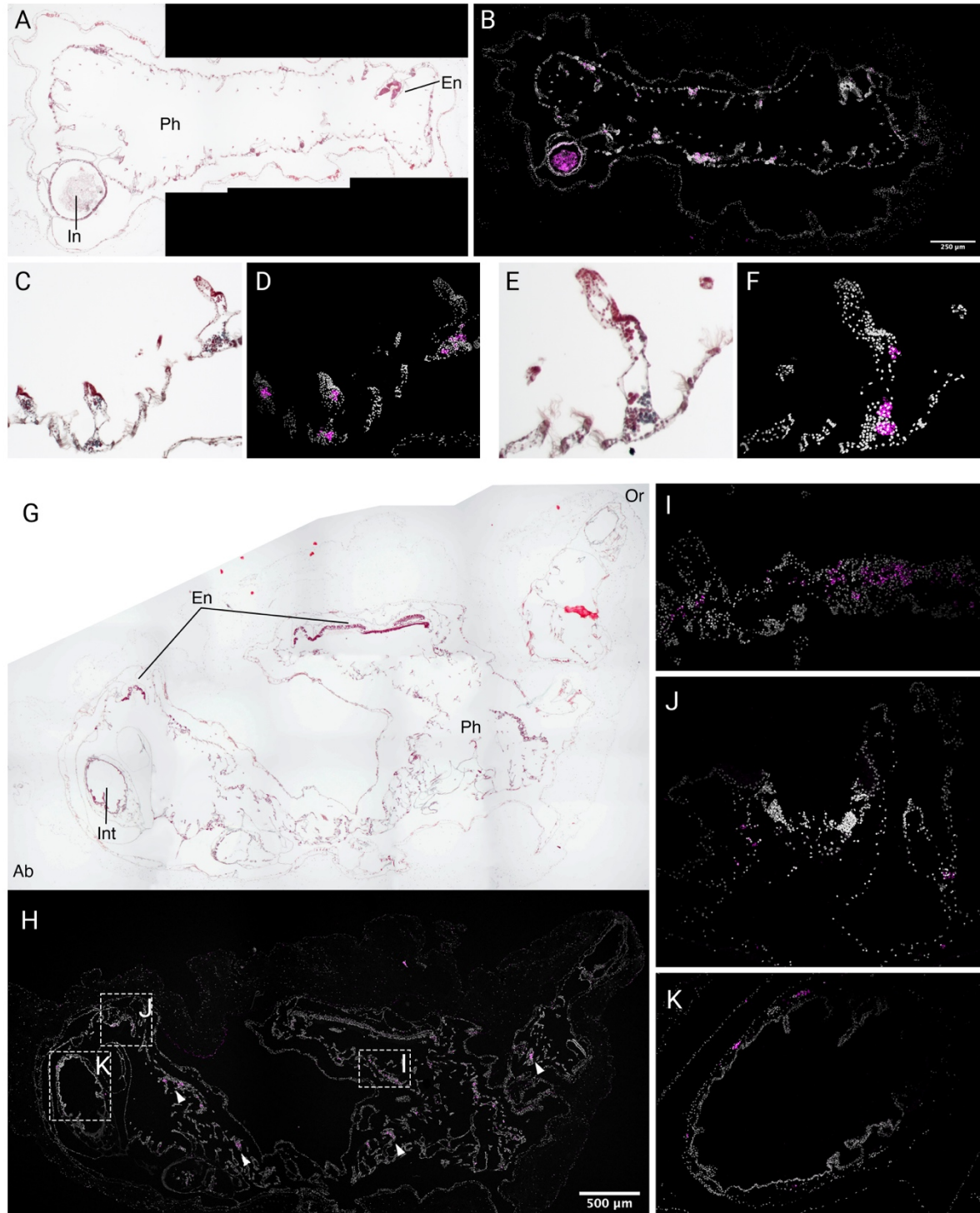


**Figure A3.2** Characterization of calcitonin (CT) expression in sections of adult *Ciona intestinalis*. **A-F** Trichromic and HCR staining in pharyngeal cross sections, highlighting the pharyngeal cavity (Ph), the endostyle (En) and the intestine (In) (A). CT transcripts are localized in the pharynx (B), specifically in cells located within or at the base of the papillae (C-F). These cells are stained differently than the other cells of the papillae by Masson's trichromic staining. **G-K** CT localization along the ascidian body in sagittal sections shows that CT is expressed throughout the pharyngeal endoderm (H-I) and in cells at the base of the intestinal epithelium (K), but not in the endostyle (J).

## 2 Expression of CT in adults of *Ciona intestinalis*

Cross sections of entire adult *Ciona* labelled with probes against *CT* showed widespread expression in the pharynx (Figure A3.2A-B). The ascidian pharynx contains an elaborate ciliated branchial basket that bears outgrowths directing towards the centre of the pharynx called papillae (11). *CT*-positive cells were concentrated at the level of the papillae, mainly at the base of each papilla but also in scattered cells within the papillae (Figure A3.2C-F). The comparison between HCR and trichromic staining shows that *CT*-positive cells are different from the surrounding cells as they are stained in green in trichromic staining. To better understand the pattern of *CT* expression across the oral-aboral axis, I also analysed parasagittal sections (Figure A3.2G-H). This confirmed that *CT* transcripts could be found throughout the pharynx (Figure A3.2H, I), while no signal was detected in the endostyle (Figure A3.2J). Interestingly, I also found *CT*-positive cells associated with the intestine, located below the digestive epithelium, possibly demarcating neurons associated with the digestive system.

## Discussion

The pharyngeal endoderm of invertebrate chordates has long been known to have an ancient and conserved secretory role. Previous work in fact established the homology between the endostyle of cephalochordates and tunicates with the vertebrate thyroid (12, 13). However, the vertebrate pharynx possesses a large number of glands that develop from the embryonic endoderm and whose evolutionary origin remains unclear. Here I have investigated the conservation of calcitonin-type secretory activity, which is carried out by cells of the UBs in vertebrates, in amphioxus and ascidians. Surprisingly, in both taxa calcitonin-type genes are highly expressed in the pharynx. In amphioxus I found co-localization of all three paralogs in atrial cells of the gill bars. These cells have been shown to be secretory, with extended Golgi apparatus and secretory vacuoles, suggesting a possible role in mucus production (9). Electron microscopy studies have shown neural projections running at the base of atrial cells, possibly controlling their secretory activity (9). In *Ciona*, *CT* transcripts were concentrated at the level of the papillae in the branchial basket. Using a *Kaede* reporter gene driven by the promoter of prohormone convertase 2, which is involved in the maturation of neuropeptides and peptide hormones, a previous study showed that *Kaede*-positive cells could be detected at the level of the papillae, supporting our result and indicating that those are likely *CT*-producing cells

(11). It is interesting that in both species the trichromic staining showed that the CT-positive cells were distinctly coloured in green, possibly indicating that they are similar cell types.

Taken together, my investigation of *CT* expression in amphioxus and ascidians revealed a high level of conservation in endodermal calcitonin function in chordates (Figure A3.3). The widespread distribution of CT-type peptides in the pharynx of both cephalochordates and ascidians suggests that the ancestral chordate pharynx possessed a similarly broadly distributed cell type. Although the function of CT-expressing cells was not tested, previous microscopic analysis suggests that these are secretory cells, likely with a role in digestion or mucous secretion, while a role in the regulation of  $Ca^{2+}$  homeostasis remains to be tested. In this scenario, during vertebrate evolution the *CT* expression was restricted to the UBs in the last pharyngeal pouch, together with the evolution of other endodermally-derived glands.

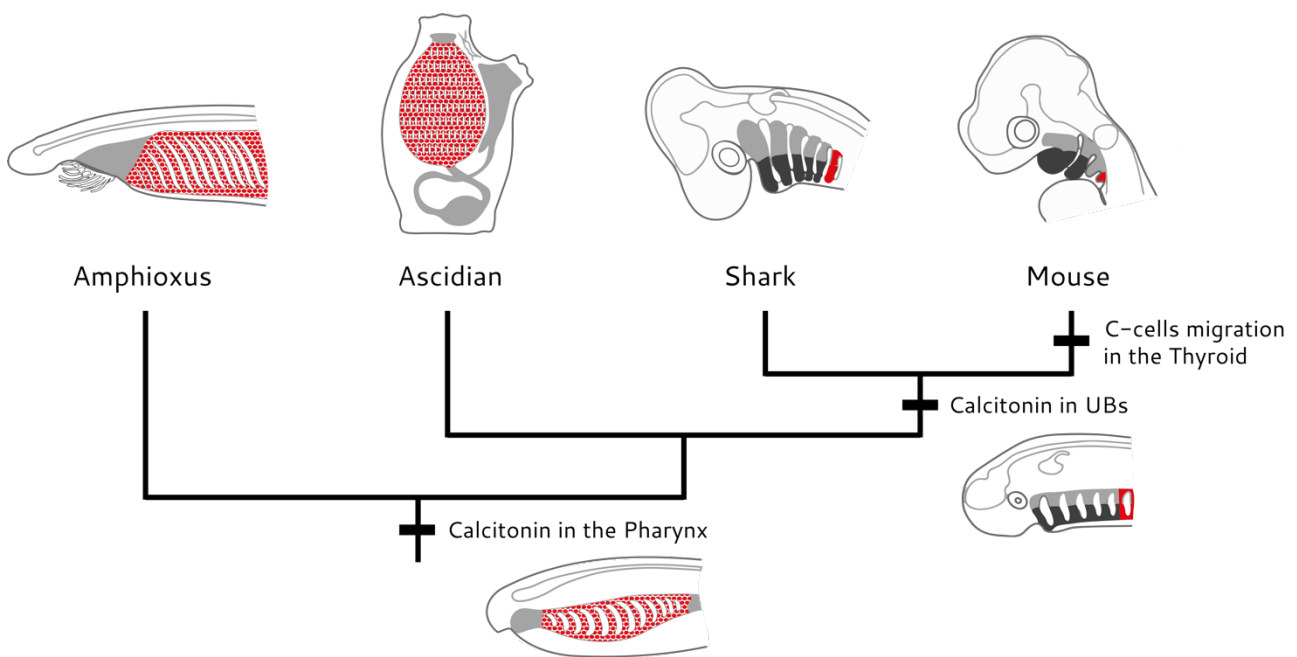


**Figure A3.3** Scenario for the evolution of the endodermal expression of calcitonin in the chordate lineage.

## References

1. A. Grevellec, A. S. Tucker, The pharyngeal pouches and clefts: Development, evolution, structure and derivatives. *Semin Cell Dev Biol.* **21** (2010), pp. 325–332.
2. Y. Kameda, Morphological and molecular evolution of the ultimobranchial gland of nonmammalian vertebrates, with special reference to the chicken C cells. *Developmental Dynamics.* **246**, 719–739 (2017).
3. F. A. Russell, R. King, S. J. Smillie, X. Kodji, S. D. Brain, Calcitonin gene-related peptide: physiology and pathophysiology. *Physiol Rev.* **94**, 1099–1142 (2014).
4. T. Sekiguchi, The calcitonin/calcitonin gene-related peptide family in invertebrate deuterostomes. *Front Endocrinol (Lausanne).* **9**, 1–11 (2018).
5. T. Sekiguchi, K. Kuwasako, M. Ogasawara, H. Takahashi, S. Matsubara, T. Osugi, I. Muramatsu, Y. Sasayama, N. Suzuki, H. Satake, Evidence for conservation of the calcitonin superfamily and activity-regulating mechanisms in the basal chordate: *Branchiostoma floridae* Insights into the molecular and functional evolution in chordates. *Journal of Biological Chemistry.* **291**, 2345–2356 (2016).
6. T. Sekiguchi, N. Suzuki, N. Fujiwara, M. Aoyama, T. Kawada, K. Sugase, Y. Murata, Y. Sasayama, M. Ogasawara, H. Satake, Calcitonin in a protochordate, *Ciona intestinalis* - The prototype of the vertebrate calcitonin/calcitonin gene-related peptide superfamily. *FEBS Journal.* **276**, 4437–4447 (2009).
7. M. Hamada, N. Shimosono, N. Ohta, Y. Satou, T. Horie, T. Kawada, H. Satake, Y. Sasakura, N. Satoh, Expression of neuropeptide- and hormone-encoding genes in the *Ciona intestinalis* larval brain. *Dev Biol.* **352**, 202–214 (2011).
8. W. Cai, C. H. Kim, H. J. Go, M. Egertová, C. G. Zampronio, A. M. Jones, N. G. Park, M. R. Elphick, Biochemical, anatomical, and pharmacological characterization of Calcitonin-type neuropeptides in Starfish: discovery of an ancient role as muscle relaxants. *Front Neurosci.* **12** (2018), doi:10.3389/fnins.2018.00382.
9. D. G. Baskin, P. A. Detmers, Electron microscopic study on the gill bars of *Amphioxus* (*Branchiostoma californiense*) with special reference to neurociliary control. *Cell Tiss. Res.* **166**, 167–178 (1976).
10. J. Hiruta, F. Mazet, K. Yasui, P. Zhang, M. Ogasawara, Comparative expression analysis of transcription factor genes in the endostyle of invertebrate chordates. *Developmental Dynamics.* **233**, 1031–1037 (2005).
11. T. Osugi, Y. Sasakura, H. Satake, The ventral peptidergic system of the adult ascidian *Ciona robusta* (*Ciona intestinalis* Type A) insights from a transgenic animal model. *Sci Rep.* **10** (2020), doi:10.1038/s41598-020-58884-w.
12. M. Ogasawara, Overlapping expression of amphioxus homologs of the thyroid transcription factor-1 gene and thyroid peroxidase gene in the endostyle: insight into evolution of the thyroid gland. *Dev Genes Evol.* **210**, 231–242 (2000).
13. C. Cañestro, S. Bassham, J. H. Postlethwait, Evolution of the thyroid: Anterior-posterior regionalization of the *Oikopleura* endostyle revealed by *Otx*, *Pax2/5/8*, and *Hox1* expression. *Developmental Dynamics.* **237**, 1490–1499 (2008).



## Appendix IV – Amphioxus digitalized atlas of gene expression

During my project I have characterized the expression of 47 genes through amphioxus development, using HCR to co-profile expression of up to four genes at a time (Appendix V). As the HCR signal is non-diffusible and it is possible to distinguish nuclear and cytoplasmic signal, the DAPI staining can be used to mask nuclear HCR signal. Previously in our group, Dr. Toby Andrews (Francis Crick Institute, UK) exploited this feature of HCR developing a pipeline for integrating nuclear signal from multiple embryos, called ASCRIBE (Amphioxus Single-Cell state Resolution with Integration Between Embryos). In each embryo, nuclei were segmented using the machine learning platform Ilastik (1), and the segmentation maps were integrated with the HCR signal in ImageJ, calculating the mean intensity of HCR signal in each nucleus. By normalizing and scaling the length of XYZ axes different specimens can be combined to create “average embryos”.

In a previous analysis in the lab, ASCRIBE was used to combine multiple embryos imaged with the same four HCR probes, to quantify signal intensity and visualize even scattered cells as a coherent domain (2). However, when analysing a large number of genes, it would be ideal to predict co-expression to avoid the test of all possible gene combinations and only choose specific candidates for HCR. The high reproducibility of HCR signal and the simple and invariable shape of amphioxus embryos at early stages mean that qualitative information of gene co-expression can be obtained by combining even embryos that have been labelled with different gene combinations. To this aim, I collaborated with Toby Andrews to develop a new pipeline as an extension of ASCRIBE, called ADAGE (Amphioxus Digitalized Atlas of Gene Expression) (Figure A4.1). I applied ASCRIBE to HCR images of embryos at two developmental stages, N0 and 7ss. After generating a training sample for each stage using Ilastik, I segmented cell nuclei and obtained the mean intensity of HCR signal for 20 genes at N0 stage and 36 genes at 7ss stage. The dataset was imported in R and the length of the axes was normalized in each embryo. The signal intensity for each channel was also normalized to avoid wide differences in intensity when qualitatively comparing the expression of different genes. The axes were then scaled to use the mean for all the embryos considered, allowing us to combine the datasets together into a single “virtual embryo”. The expression of each gene could be plotted on this virtual embryo (Figure A4.2; Figure A4.3).

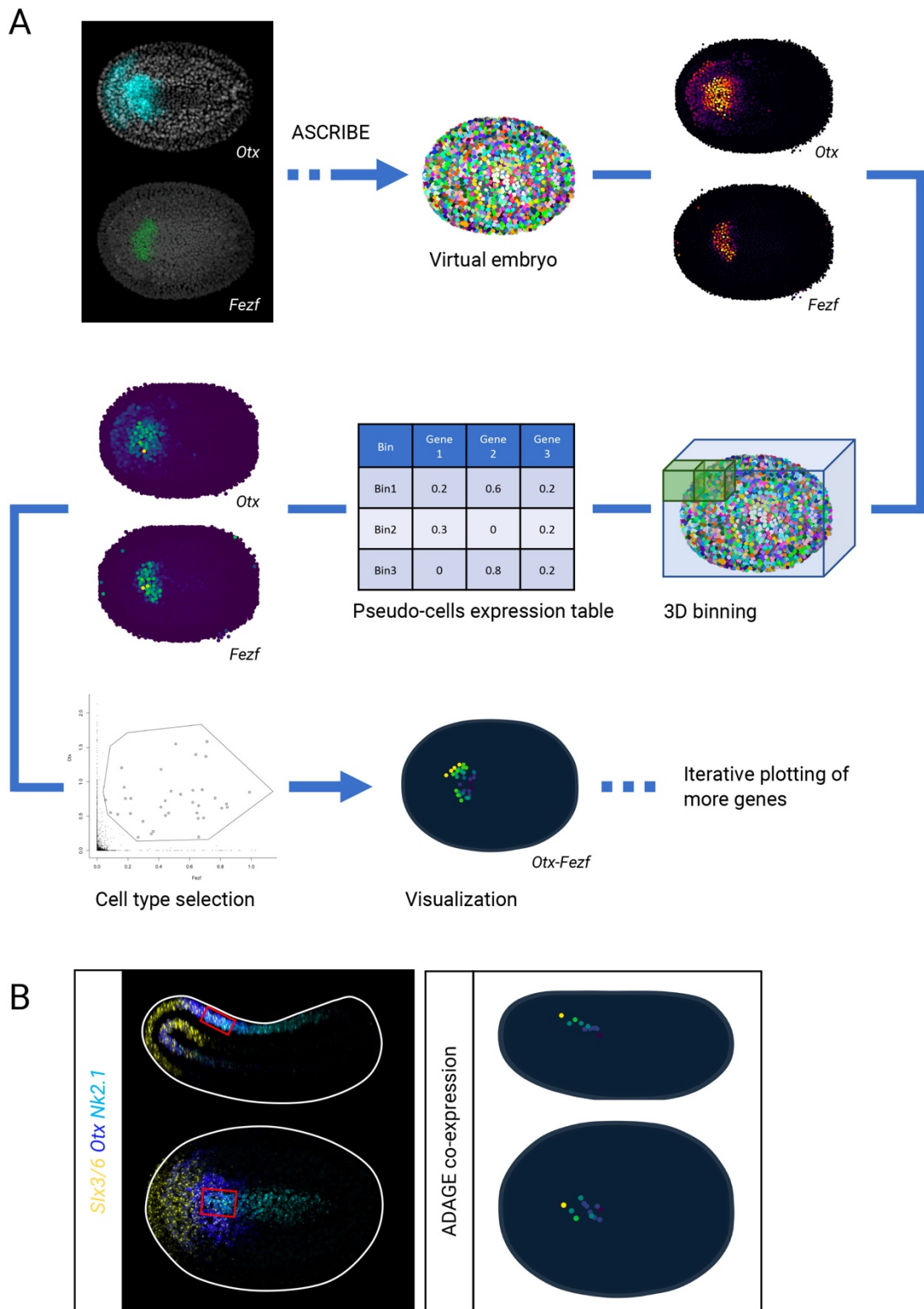


**Figure A4.1.** Amphioxus Digitalized Atlas of Gene Expression (ADAGE). **A.** ADAGE pipeline for the prediction of gene co-expression in virtual embryos. *Otx* and *Fezf* at N0 are used as examples to demonstrate the process, which was repeated for 20 genes at N0 and 36 genes at 7ss. **B.** Test of co-expression prediction of rare *Six3/6- Otx- Nk2.1-* triple positive cells in the anterior floor plate.

Segmented nuclei coming from the same region in different embryos occupy a similar position in the virtual embryo, due to the invariant shape of these early developmental stages. Therefore, we used 3D binning to segment the virtual space of the composite embryo into cubic intervals (bins), with the rationale that each bin would contain the same region across multiple embryos (Figure A4.1A). To take into account the distance between nuclei in real embryos and accommodate for microscopic differences in embryo position, we selected a bin size equal to  $\sim 1.5$  nuclear size. Then, we calculated the average intensity of each HCR signal in the bins and used it as a proxy for the HCR signal within a cell located in the corresponding positions in the embryo. Each bin represents a “pseudocell” containing information on multiple genes, forming a composite embryo with a high-resolution atlas of gene expression during amphioxus neurulation. By iteratively visualizing pairs of genes in scatterplots, pseudocells co-expressing candidate genes could be isolated and plotted within the 3D context of the composite embryo. To test the efficiency and resolution of the pipeline, I investigated the co-localization of three aGRN genes that has been highlighted in chapter III: at the N0 stage, *Six3/6*, *Nk2.1* and *Otx* co-localize in a small medial domain in the anterior portion of the neural plate, corresponding to the rostral tip of the floor plate. Even if this domain comprises only few triple-positive cells, it was clearly visible in ADAGE, demonstrating that this method can correctly identify even rare cell types (Figure 4A4.1B).

It is important to highlight that the ADAGE pipeline is used to visualise qualitative co-expression, but at present does not provide quantitative information on the expression level of each gene. For a quantitative analysis, images should be obtained with the same acquisition settings, and ideally HCR experiments should be performed at the same time. However, if these two conditions are met, then ADAGE could be readily adapted for quantitative investigation as well, providing insights on cell states in addition to the prediction of cell types.

ASCRIBE N0 stage

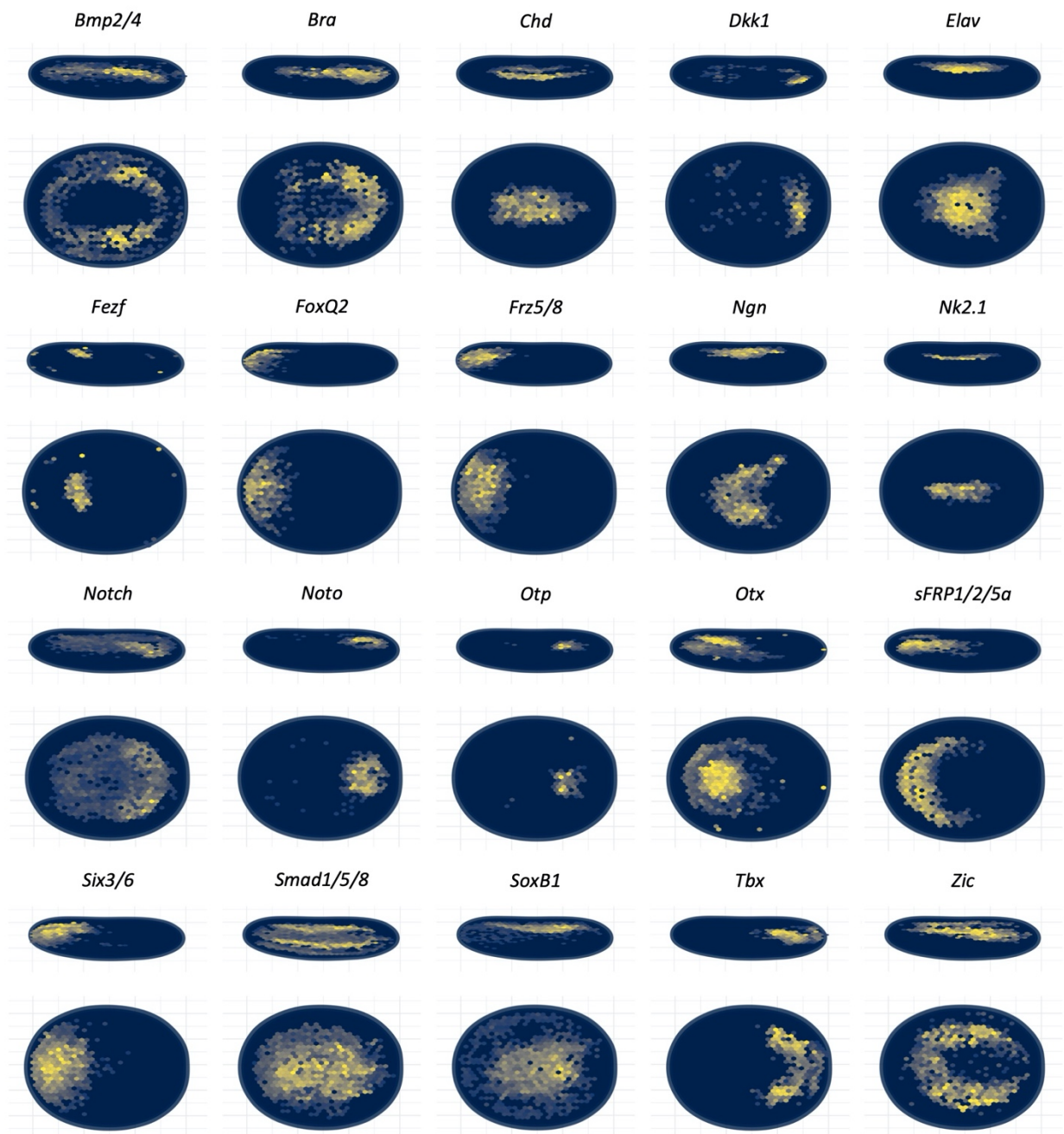


**Figure A4.2.** Lateral and dorsal views of gene expression produced with the ASCRIBE pipeline in virtual embryos at the N0 stage.

ASCRIBE 7ss stage



**Figure A4.3.** Lateral and dorsal views of gene expression produced with the ASCRIBE pipeline in virtual embryos at the 7ss stage.

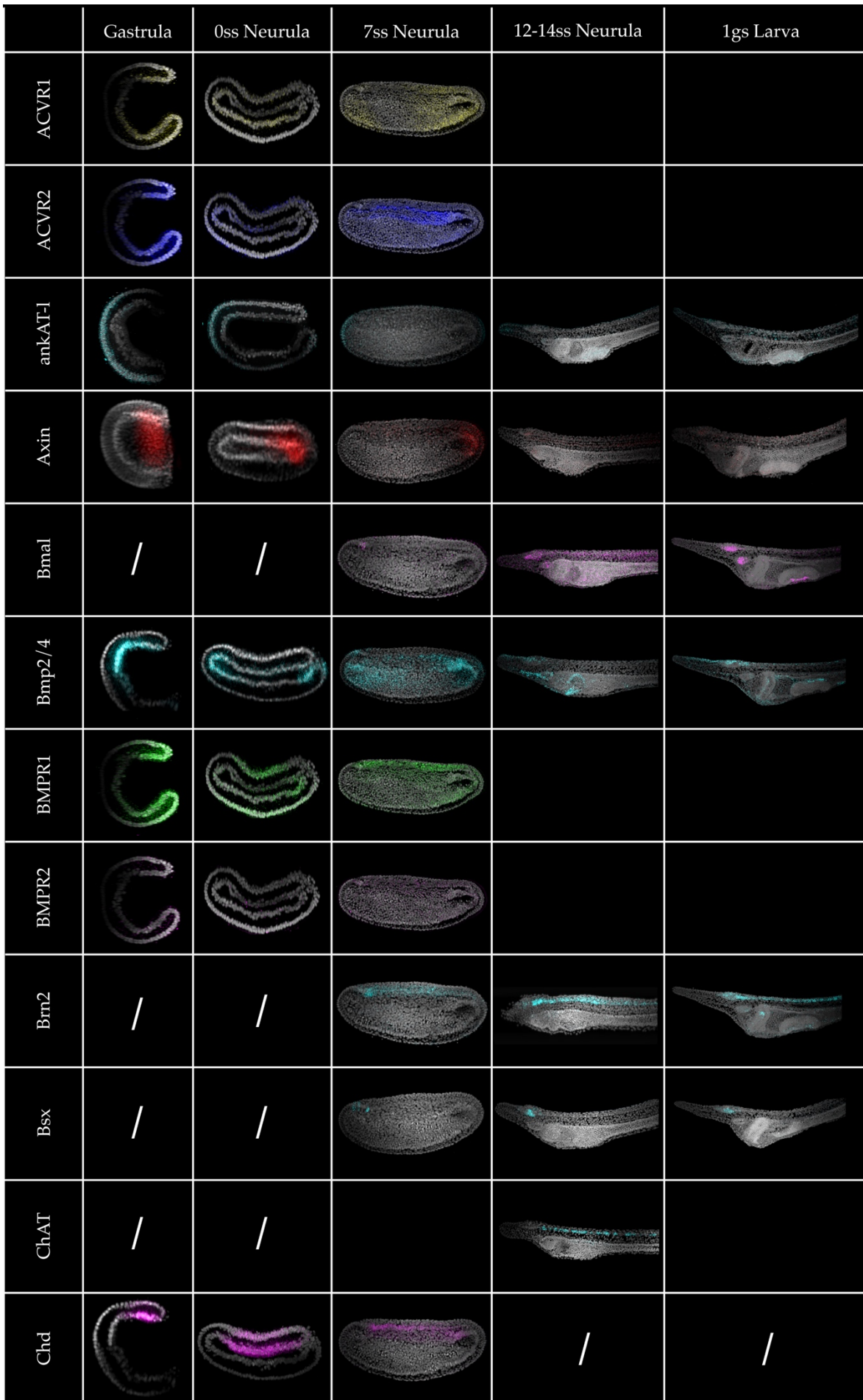
## References

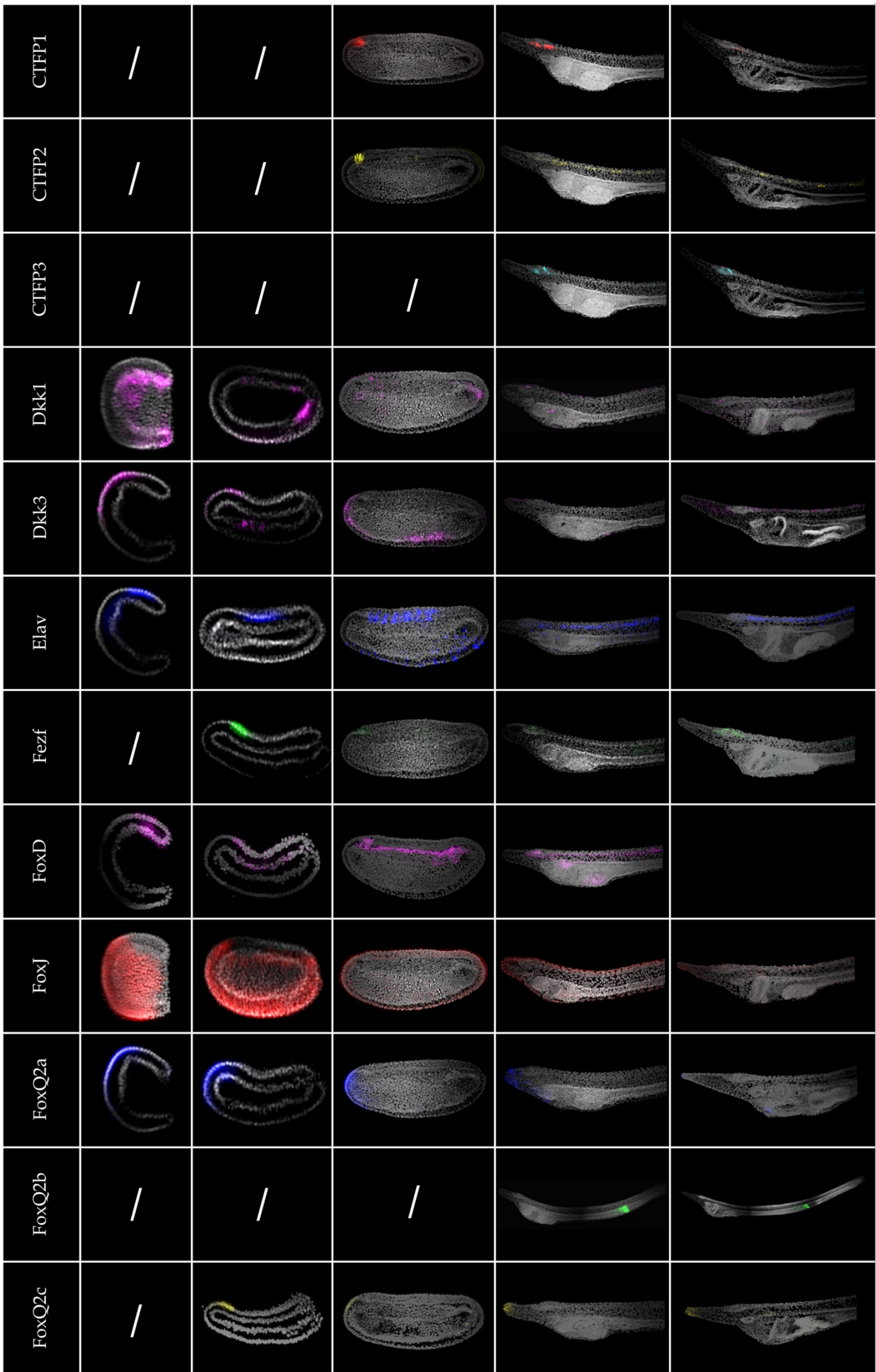
1. S. Berg, D. Kutra, T. Kroeger, C. N. Straehle, B. X. Kausler, C. Haubold, M. Schiegg, J. Ales, T. Beier, M. Rudy, K. Eren, J. I. Cervantes, B. Xu, F. Beuttenmueller, A. Wolny, C. Zhang, U. Koethe, F. A. Hamprecht, A. Kreshuk, ilastik: interactive machine learning for (bio)image analysis. *Nat Methods*. **16**, 1226–1232 (2019).
2. T. Andrews, thesis, University of Cambridge (2020).

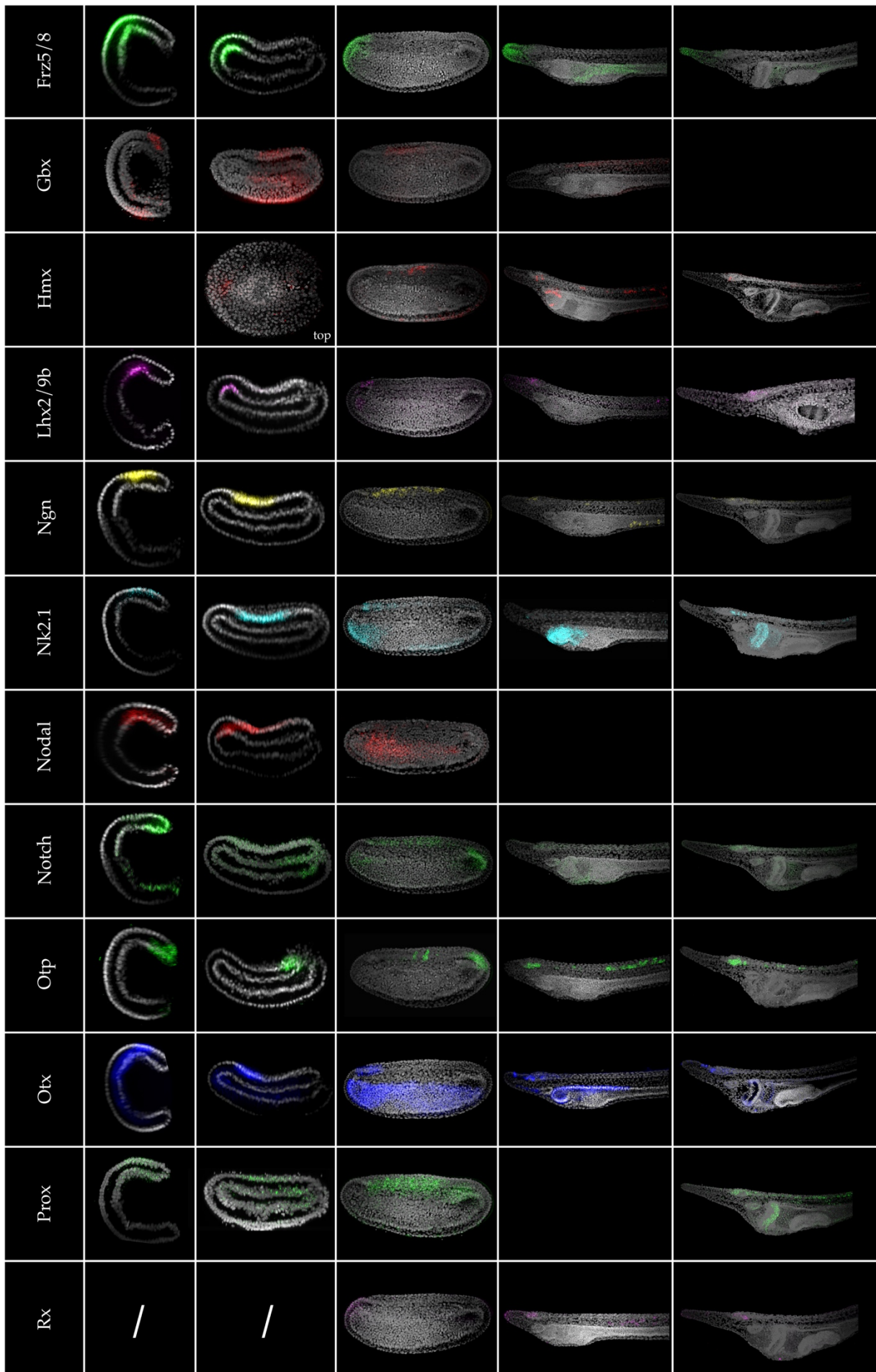
## Appendix V – Dataset of gene expression with *in situ*

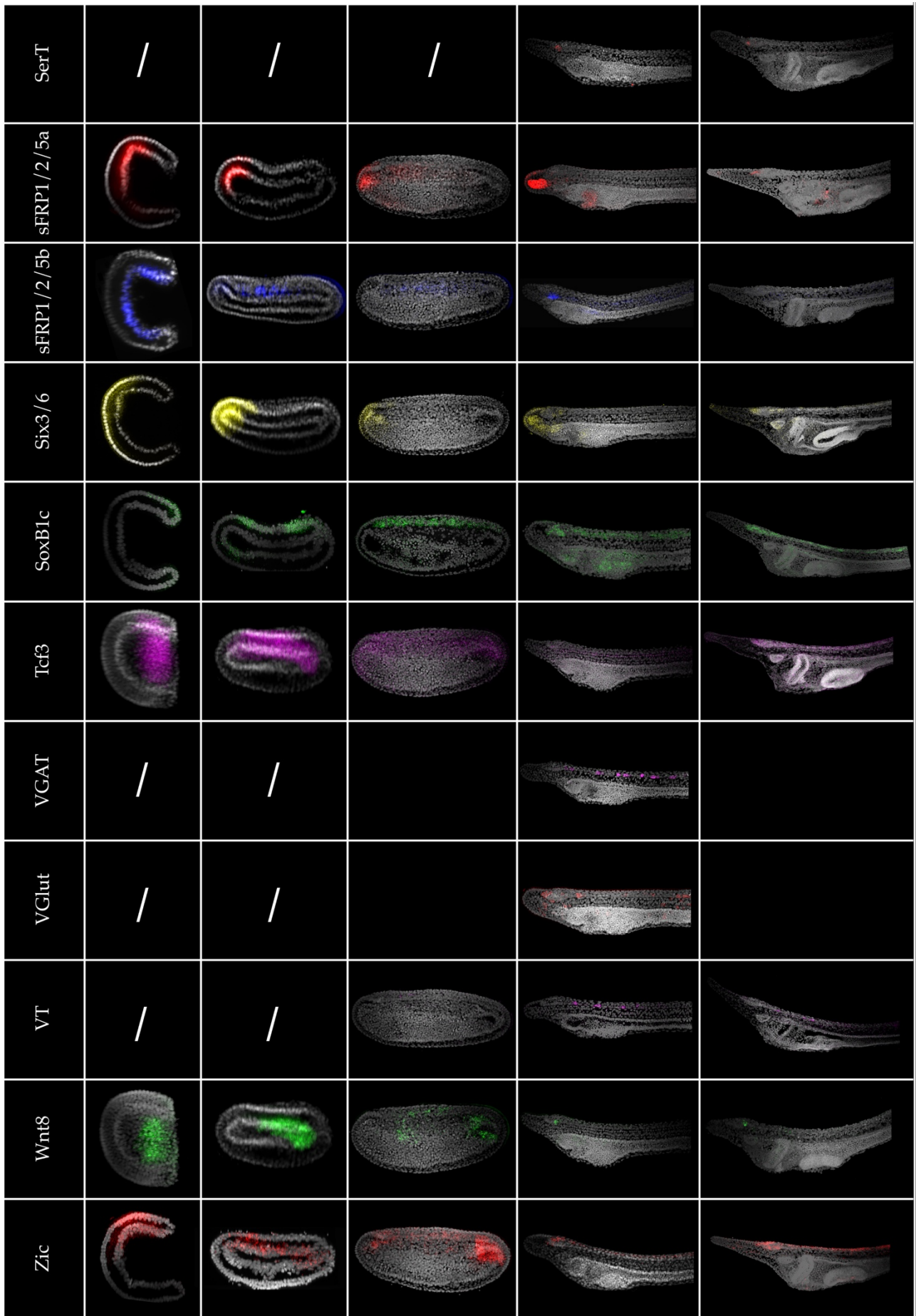
### HCR

Developmental expression of 47 genes used in this thesis listed in alphabetical order. Five stages of development were considered: late gastrula (G5), early neurula (N0), mid neurula (7ss), early larva (12-14ss, L0) and 1 gill slit larva (1gs). All stages are presented in lateral view (unless otherwise indicated), with anterior to the left. Slash lines indicate that the gene is not expressed at the corresponding stage, while empty cells indicate that the expression was not investigated in the corresponding stage.



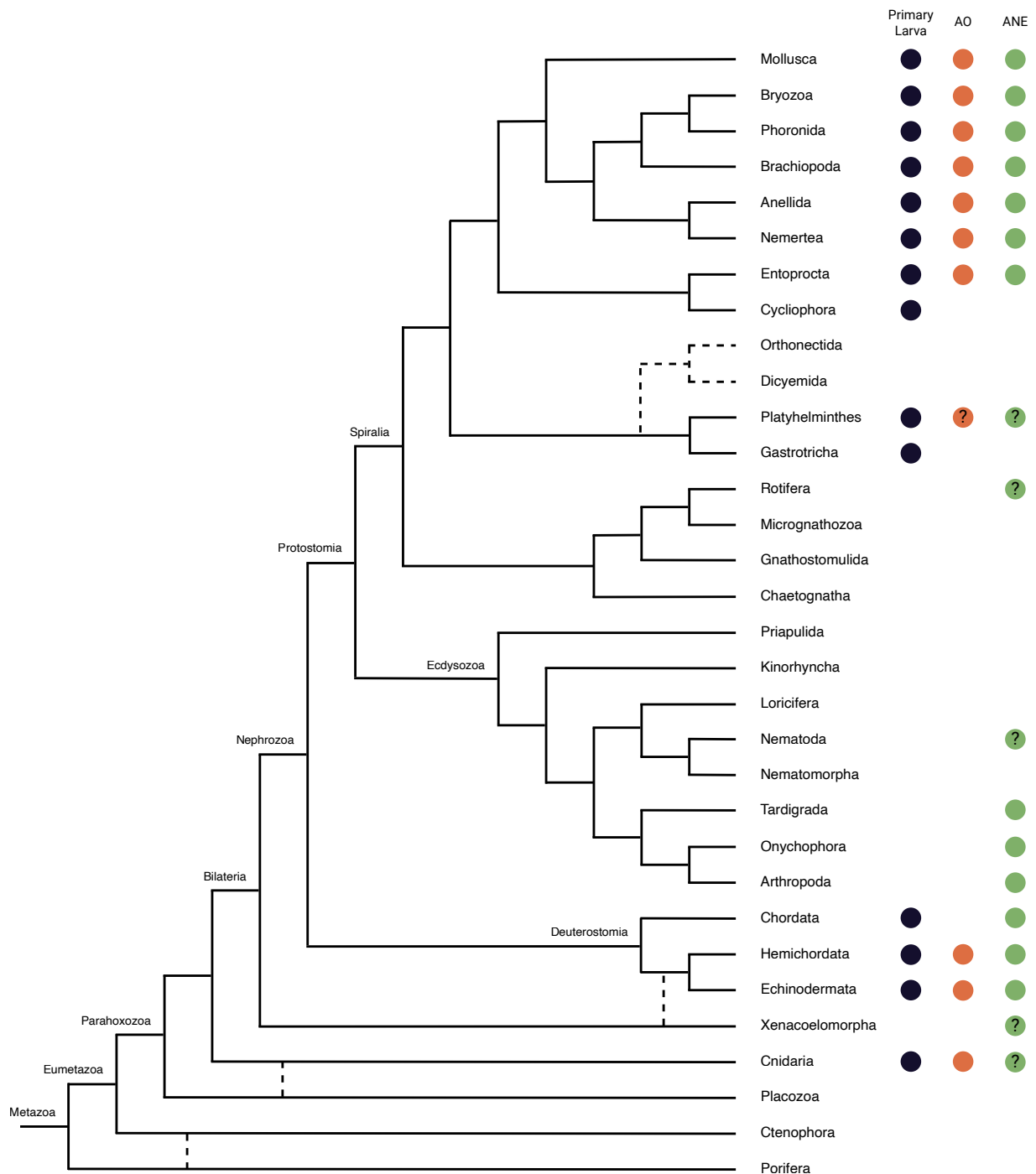




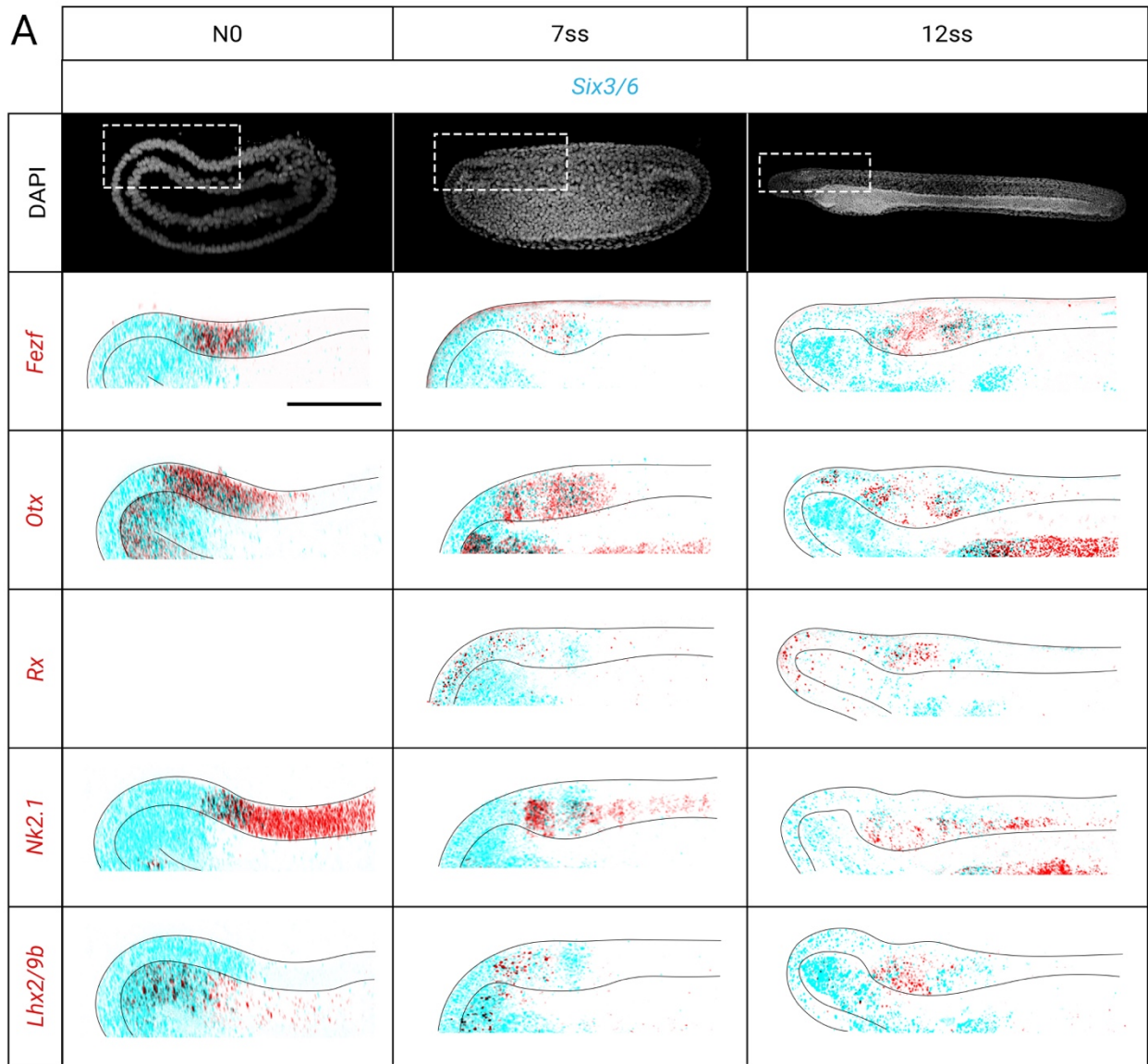




# Appendix VI – Additional material related to Chapter III

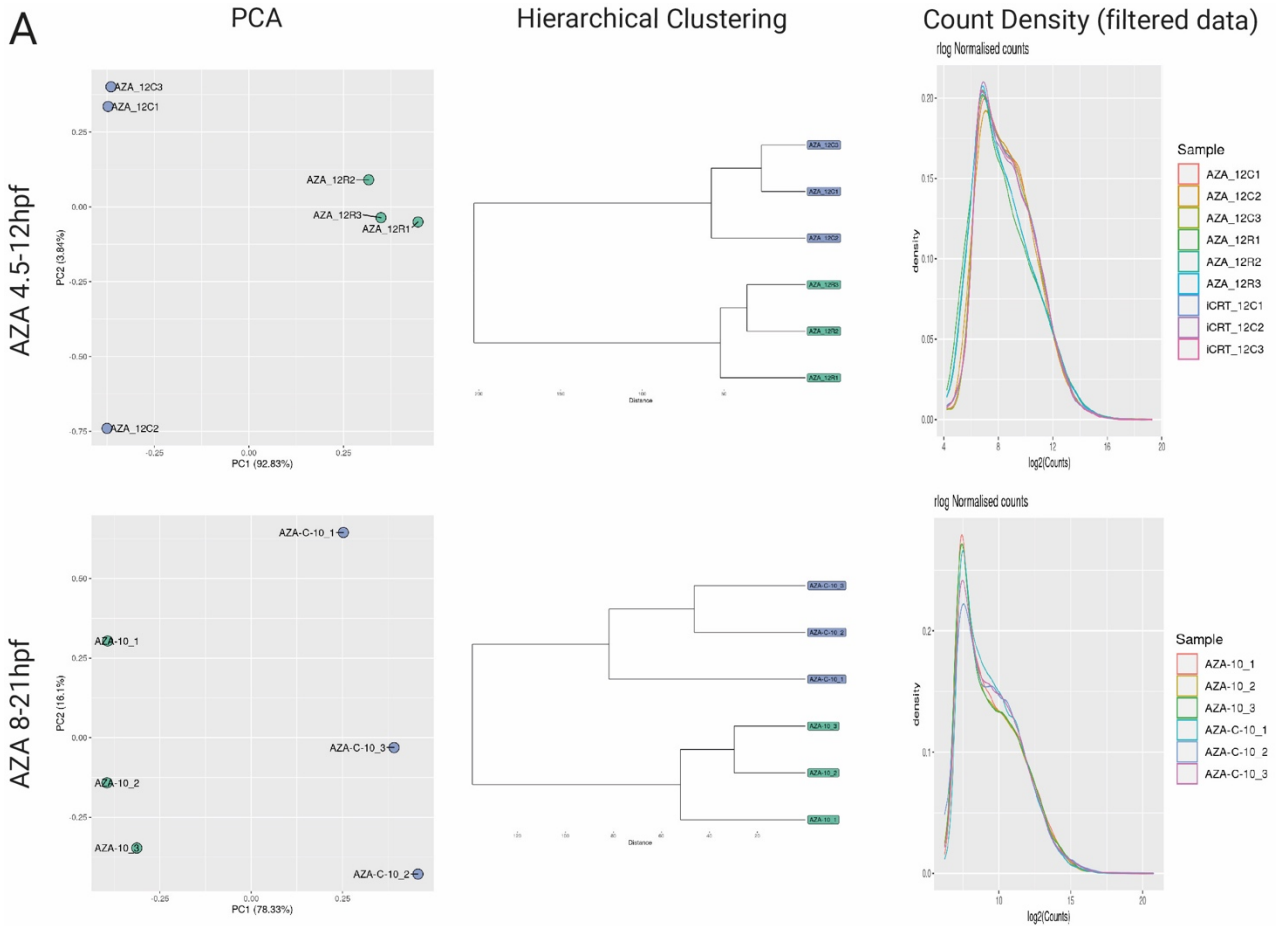


**A6.1** Phylogenetic relationships among animal phyla with distribution of primary larvae, apical organs (AO) and anterior neuroectoderm (ANE). Dashed lines indicate alternative or uncertain phylogenetic relationships.



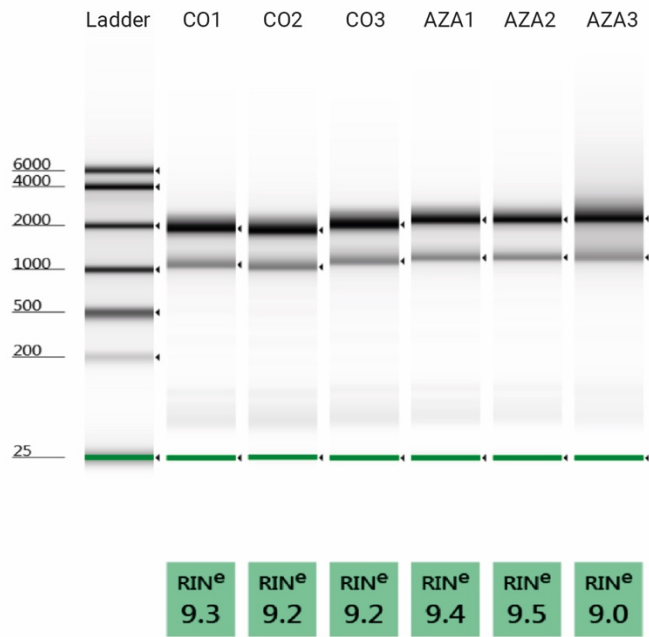
**A6.2** Co-expression of *Six3/6* (cyan) and late anterior gene regulatory network (aGRN) markers (red) during amphioxus neurulation. Co-expression is colored in red.

**A**



**B**

AZA 4.5-12hpf BioAnalyzer



< **Figure A6.3.** Quality controls for RNAseq analysis of differential expression between control and azakenpaullone (AZA) treated embryos. **A.** Principal component analysis (PCA), hierarchical clustering and cound density for the two treatments considered in this study: early treatment (4.5-12 hours post fertilization) and late treatment (8-21 hours post fertilization). The PCA and clustering shows that the two conditions (control and AZA) cluster together and their difference explains the majority of the variability in both treatments. **B.** Bioanalyser analysis of RNA quality performed for early AZA treatment.

## Appendix VII – Additional material related to Chapter V

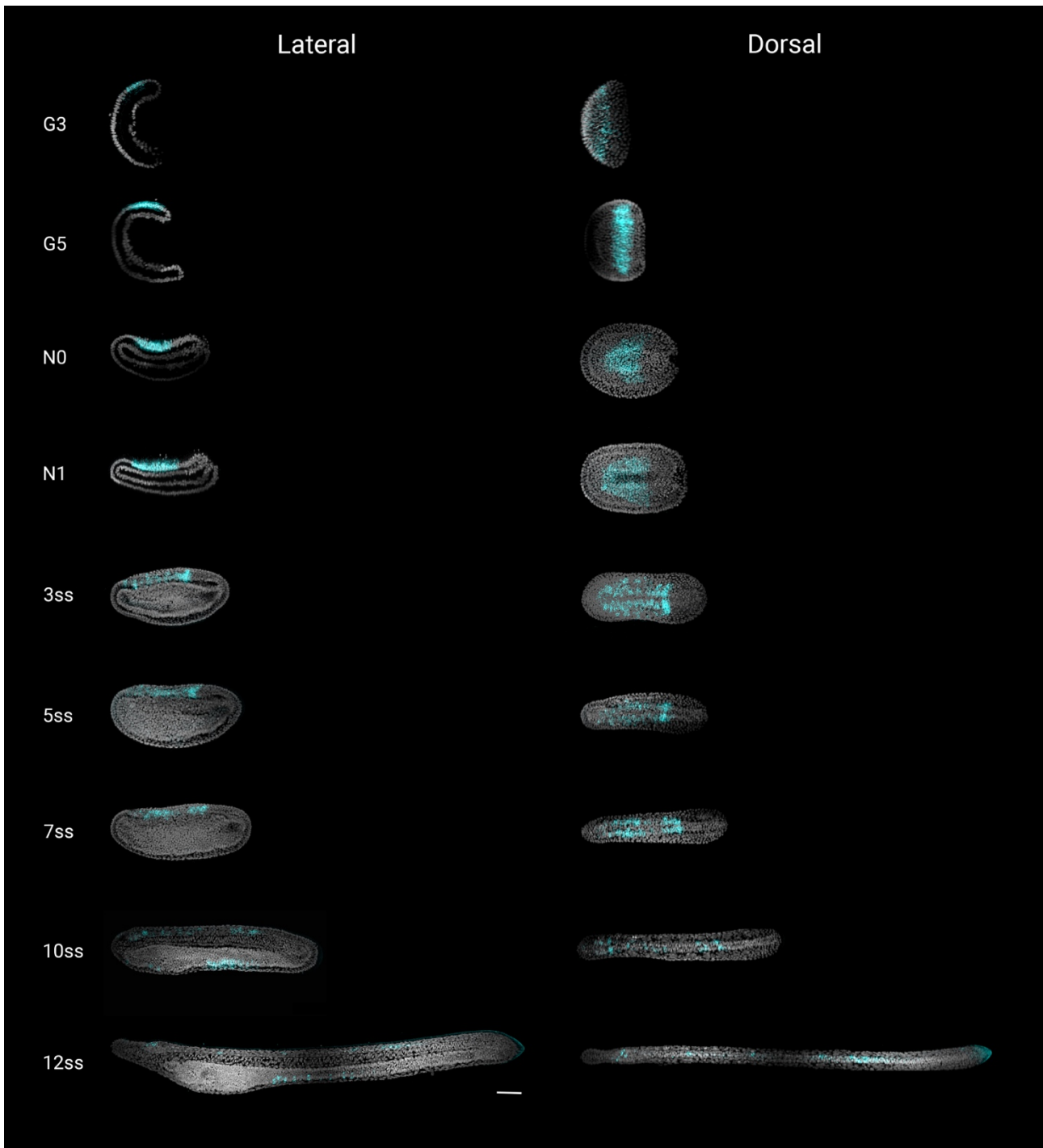
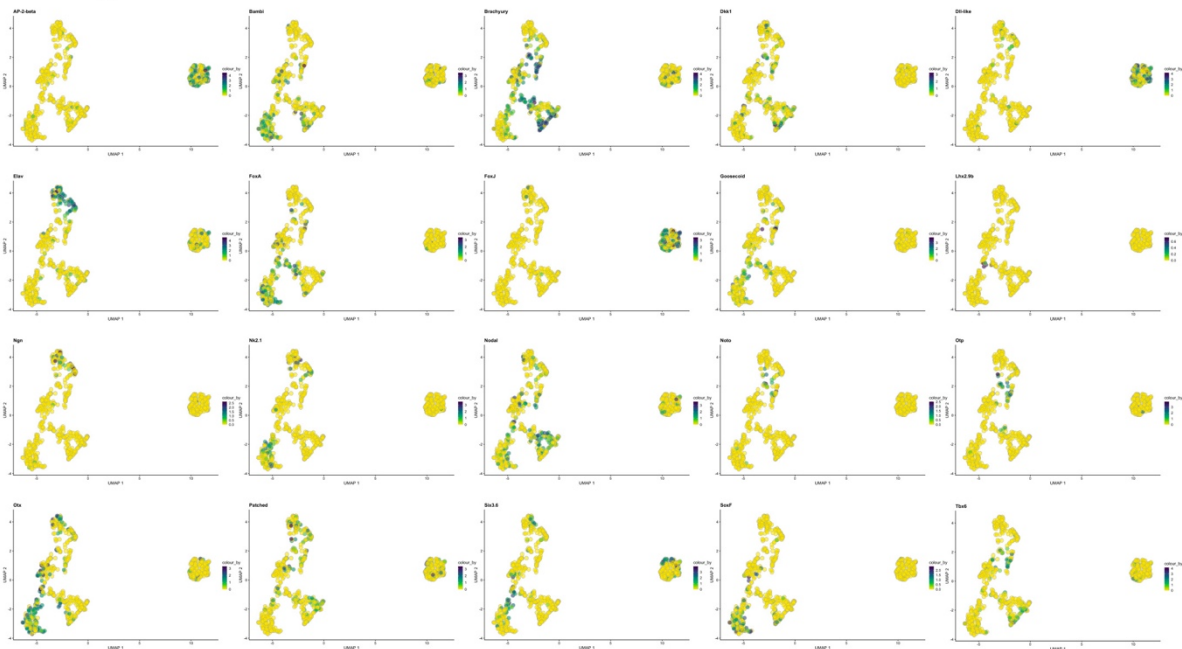
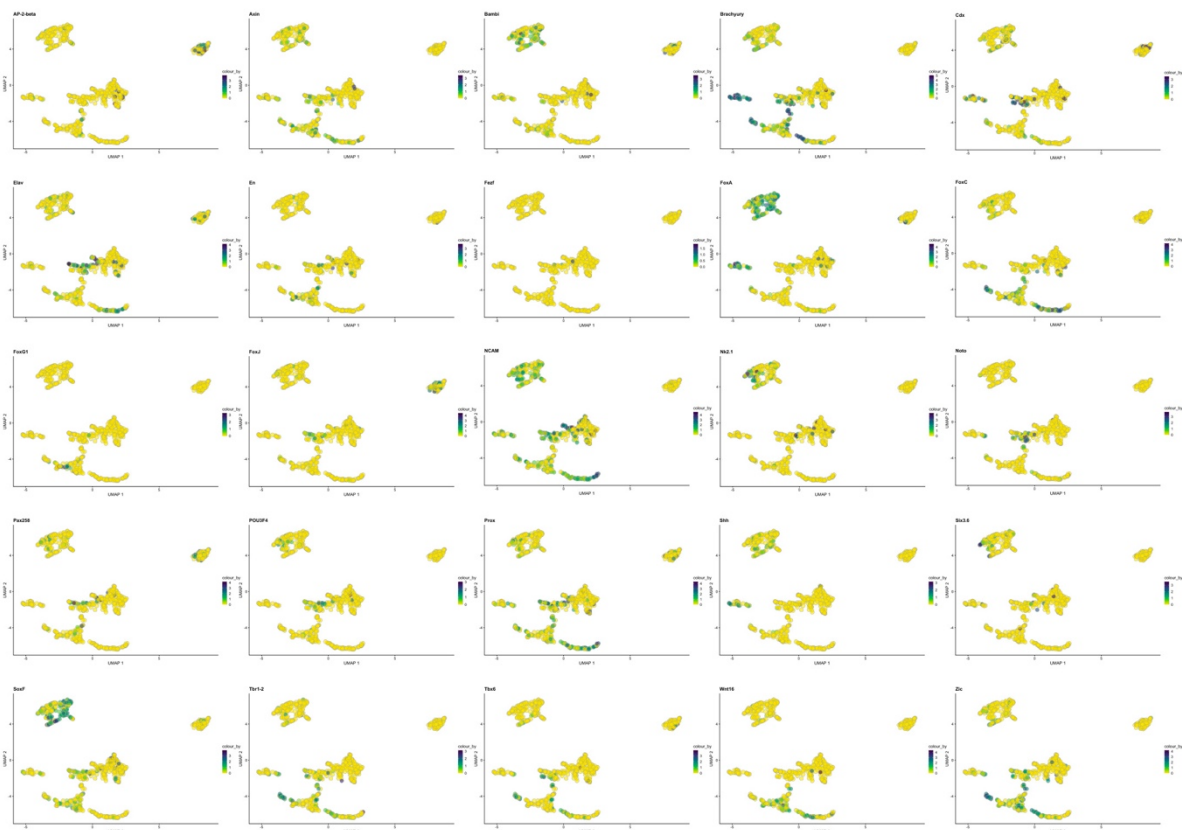


Figure A7.1. Expression of neural marker *Ngn* across amphioxus development.

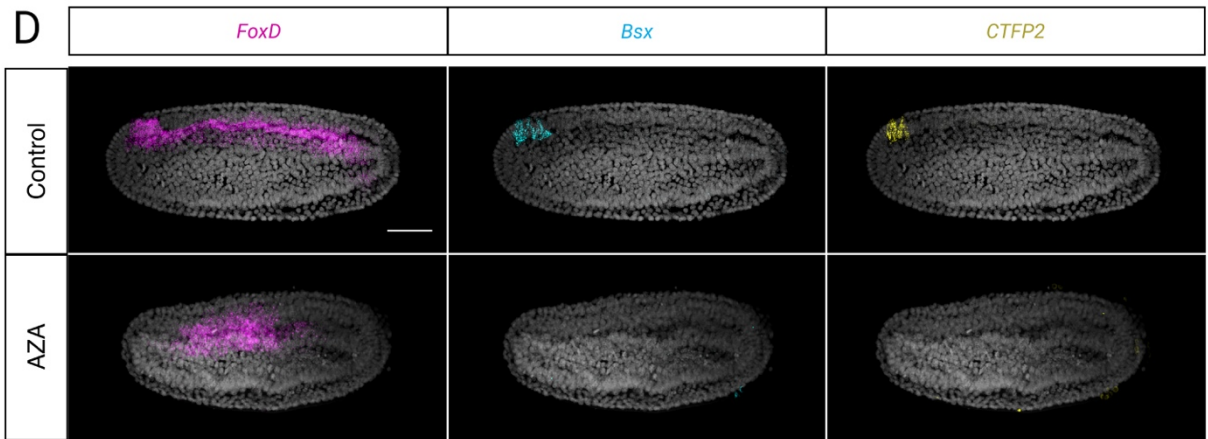
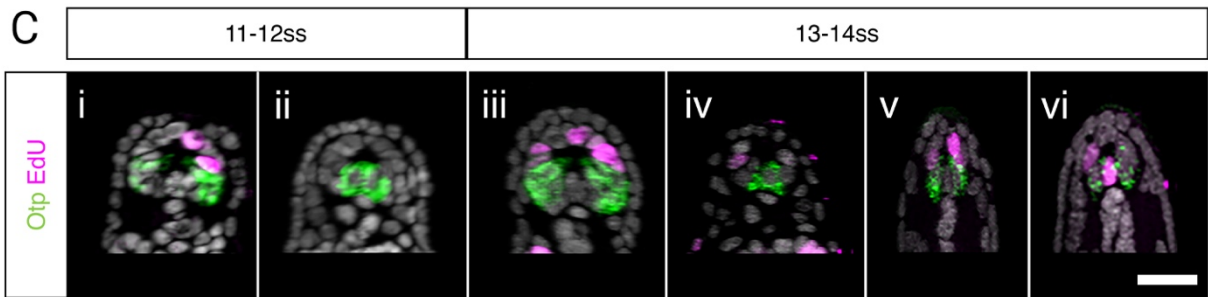
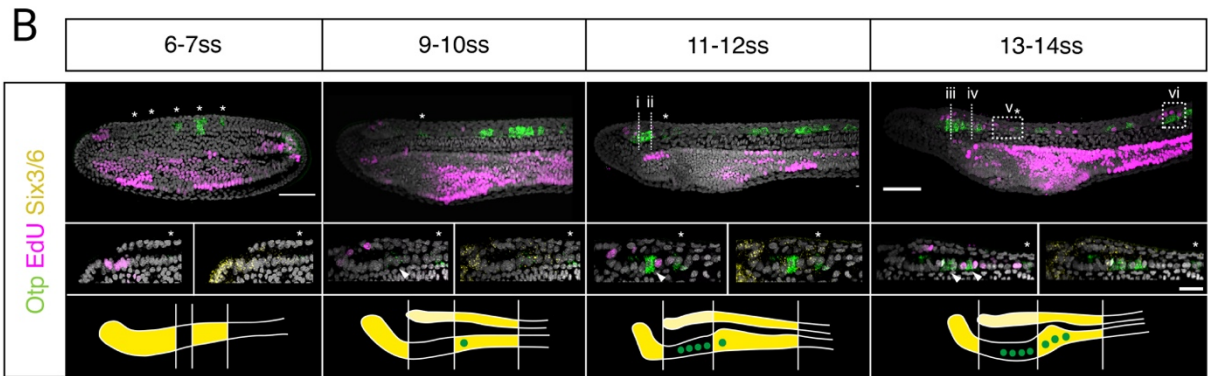
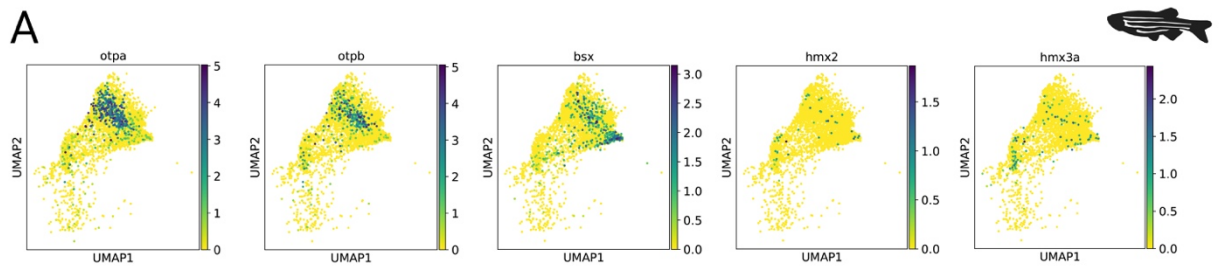
## N0 stage



## 7ss stage



**Figure A7.2.** UMAP plot of the expression of genes used to define cell types in the scRNAseq datasets generated in our lab for N0 and 7ss stages.



< **Figure A7.3.** Expression of hypothalamic markers. **A.** UMAP of hypothalamic cluster in 24 hours post fertilization zebrafish embryos obtained from a published scRNAseq dataset (XXX) showing expression of orthologs of hypothalamic genes considered in this work. **B.** Detailed expression of amphioxus *Otp* related to cell division in the anterior nervous system. At 7 ss *Otp* is expressed in five clusters of cells in the trunk region (asterisks). Expression is strong in the posterior three clusters but very low in the anterior two clusters (asterisk in insets). At 10 ss, a pair of *Otp* positive neurons appear in the posterior *Six3/6* domain of cerebral vesicle (arrowhead in insets), but proliferation is still restricted to the anterior cerebral vesicle. At 12 ss two ventro-lateral clusters of *Otp*-positive cells are visible in the anterior cerebral vesicle. At this stage, cell division starts in the posterior cerebral vesicle; the posterior *Otp*-positive pair is not proliferating but cells adjacent to them are labelled by EdU (insets). At 14 ss, the number of posterior *Otp*-positive neurons increases (arrowhead). Asterisks in all insets show the first *Otp* cluster in the trunk. Patterns of *Six3/6* and *Otp* co-expression are schematically represented at the bottom of each panel for every developmental stage. Scale bar is 50  $\mu\text{m}$ ; 20  $\mu\text{m}$  for insets. **C.** Cross section of 12 and 14 ss embryos showing the anterior ventro-lateral (i, iii), posterior medial (ii, iv), and trunk (v, vi) *Otp* cells. Scale bar is 20  $\mu\text{m}$ . **D.** Differential expression of hypothalamic markers in amphioxus embryos treated with DMSO or azakenpaullone between late gastrula (G5) and mid-neurula stages (7ss). The neural expression of these markers is lost following Wnt overactivation together with anterior cell fate.

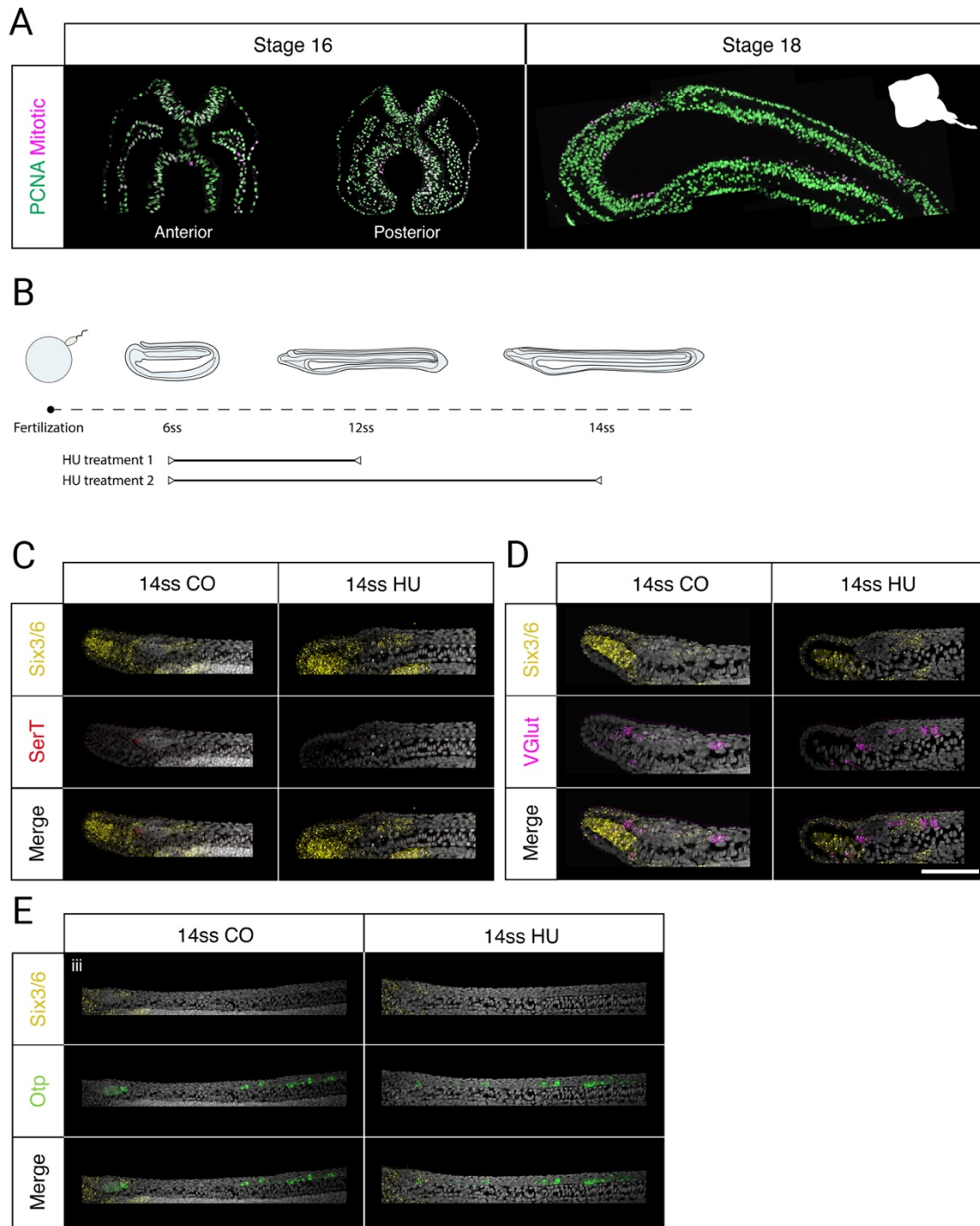


**Figure A7.4.** Proliferation in vertebrate and amphioxus embryos. **A.** Mitotic neurons (magenta) in transverse and sagittal sections of skate embryos at stage 16 and stage 18. The neurons are identified by the absence of PCNA immunoreactivity (green) and are localized throughout the neural plate and neural tube. **B.** Experimental setup for proliferation inhibition by hydroxyurea (HU) treatments. **C-E.** Expression of *Six3/6* (yellow) with *SerT* (red, C), *VGlut* (magenta, D) and *Otp* (green, E) in HU treatments to the early larva (14ss) stage. Scale bars are 50 $\mu$ m in D and 100 $\mu$ m in E.



## Appendix VII – Additional material related to Chapter V

FoxQ2 genes			
Name	Reference code	Species	Taxon
Bla_FoxQ2a	BL22763	<i>Branchiostoma lanceolatum</i>	Chordata, Cephalochordata
Bla_FoxQ2b	BL05937	<i>Branchiostoma lanceolatum</i>	Chordata, Cephalochordata
Bla_FoxQ2c	BL02175	<i>Branchiostoma lanceolatum</i>	Chordata, Cephalochordata
Bfl_FoxQ2a		<i>Branchiostoma floridae</i>	Chordata, Cephalochordata
Bfl_FoxQ2b		<i>Branchiostoma floridae</i>	Chordata, Cephalochordata
Bfl_FoxQ2c		<i>Branchiostoma floridae</i>	Chordata, Cephalochordata
Dre_FoxQ2	AAI51983.1	<i>Danio rerio</i>	Chordata, Vertebrata
Ami_FoxQ2	KYO41182.1	<i>Alligator mississippiensis</i>	Chordata, Vertebrata
Ler_FoxQ2	LSb2-ctg136197	<i>Leucoraja erinacea</i>	Chordata, Vertebrata
Pma_FoxQ2	PMZ_0043577-RA	<i>Petromyzon marinus</i>	Chordata, Vertebrata
Cin_FoxQ2	KH.C12.508	<i>Ciona intestinalis</i>	Chordata, Tunicata
Sko_FoxQ2a	ADB22676	<i>Saccoglossus kowalevskii</i>	Hemichordata, Enteropneusta
Sko_FoxQ2b	ACY92525	<i>Saccoglossus kowalevskii</i>	Hemichordata, Enteropneusta
Sko_FoxQ2c	ACY92524	<i>Saccoglossus kowalevskii</i>	Hemichordata, Enteropneusta
Hpu_FoxQ2a	HPU_15609	<i>Hemicentrotus pulcherrimus</i>	Echinodermata, Echinoidea
Hpu_FoxQ2b	HPU_15608	<i>Hemicentrotus pulcherrimus</i>	Echinodermata, Echinoidea
Spu_FoxQ2	NP_001073018.1	<i>Strongylocentrotus purpuratus</i>	Echinodermata, Echinoidea
Aja_FoxQ2-1	XP_033112874.1	<i>Anneissia japonica</i>	Echinodermata, Crinoidea
Aja_FoxQ2-2	XP_033107528.1	<i>Anneissia japonica</i>	Echinodermata, Crinoidea
Tca_FoxQ2-1	TC004761	<i>Tribolium castaneum</i>	Arthropoda, Hexapoda
Tca_FoxQ2-2	TC001232	<i>Tribolium castaneum</i>	Arthropoda, Hexapoda
Dme_FoxQ2-1	fd102C	<i>Drosophila melanogaster</i>	Arthropoda, Hexapoda
Dme_FoxQ2-2	fd3F	<i>Drosophila melanogaster</i>	Arthropoda, Hexapoda
Pca_FoxQ2	AKU77013.1	<i>Priapulid caudatus</i>	Priapulida
Cgi_FoxQ2-1	EKC20378.1	<i>Crassostea gigas</i>	Mollusca, Bivalvia
Cgi_FoxQ2-2	EKC21576.1	<i>Crassostea gigas</i>	Mollusca, Bivalvia
Cgi_FoxQ2-3	EKC22265.1	<i>Crassostea gigas</i>	Mollusca, Bivalvia

Lan_FoxQ2-1	lana_g26906.t1	<i>Lingula anatina</i>	Brachiopoda
Lan_FoxQ2-2	lana_g10171.t1	<i>Lingula anatina</i>	Brachiopoda
Lan_FoxQ2-3	lana_g9558.t1	<i>Lingula anatina</i>	Brachiopoda
Lan_FoxQ2-4	lana_g60.t1	<i>Lingula anatina</i>	Brachiopoda
Che_FoxQ2a	CLYHEMT023993.1	<i>Clythia hemisferica</i>	Cnidaria
Che_FoxQ2b	CLYHEMT017061.1	<i>Clythia hemisferica</i>	Cnidaria

**Table A8.1.** FoxQ2 sequences used for phylogenetic analysis.

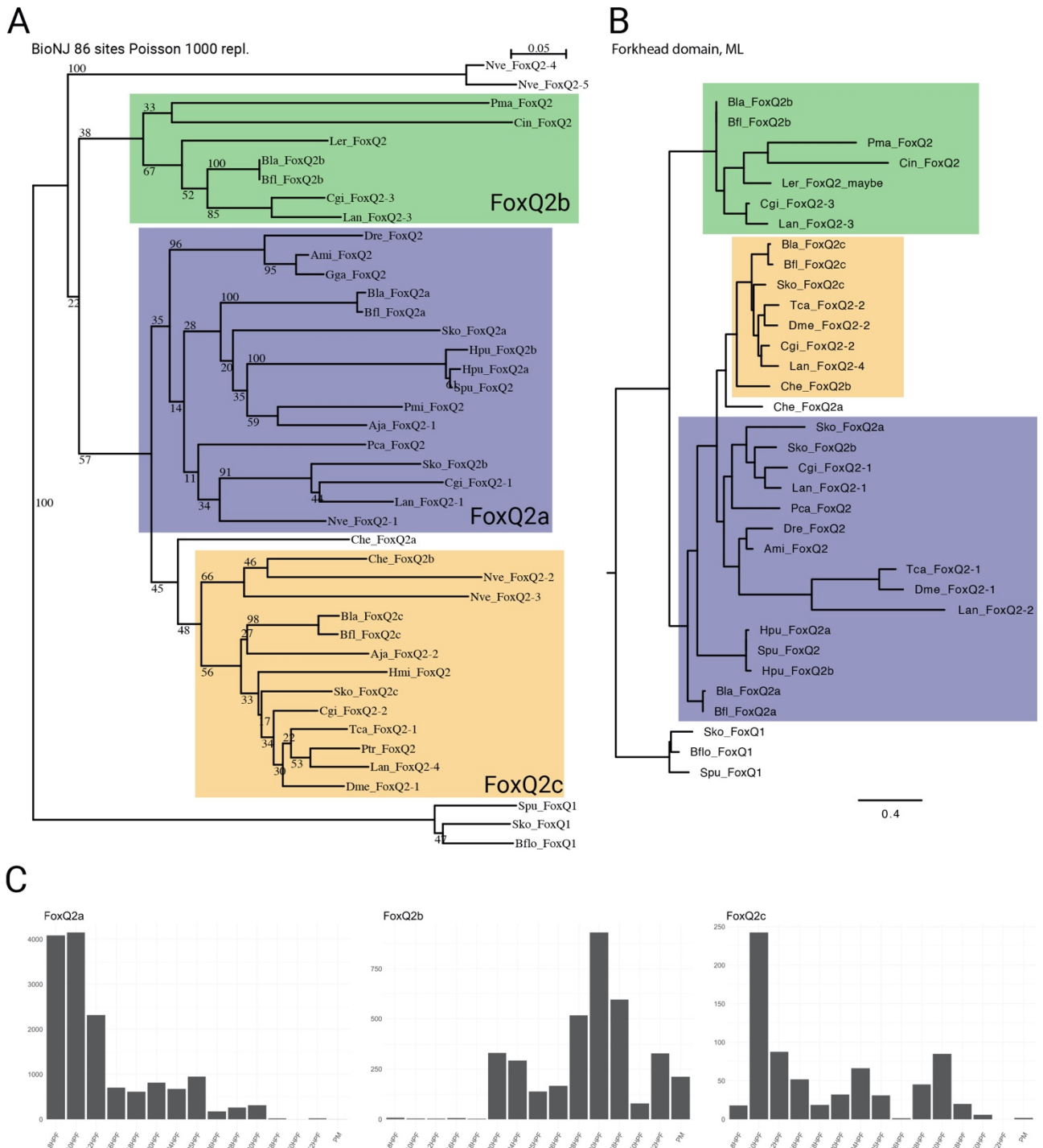


**Figure A8.1.** Additional testing of *FoxQ2* phylogeny. **A.** Neighbour-joining (BioNJ) phylogenetic tree still reconstructs three *FoxQ2* families in eumetazoans. **B.** Similar results are obtained by maximum likelihood (ML) analysis of only the forkhead domain. **C.** Expression of three *FoxQ2* paralogs in amphioxus recapitulates the *in situ* HCR data (RNaseq data from XXX). FoxQ1 is used as outgroup.

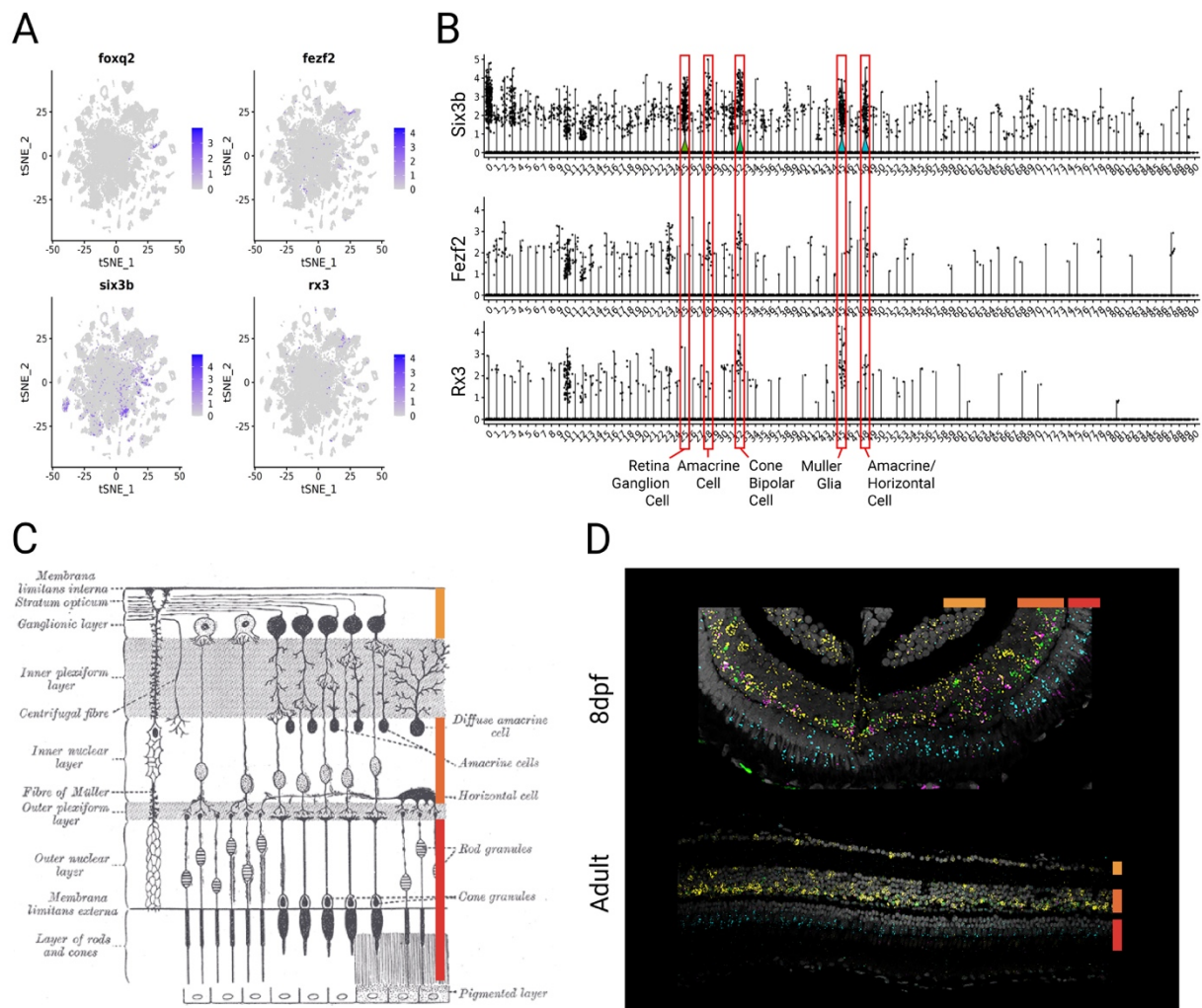
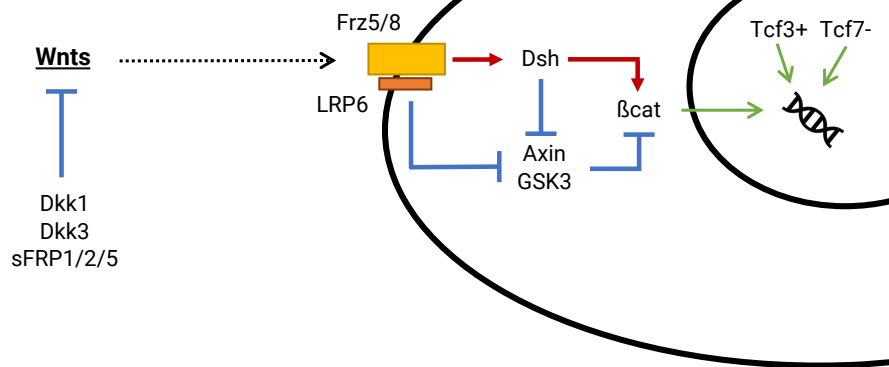
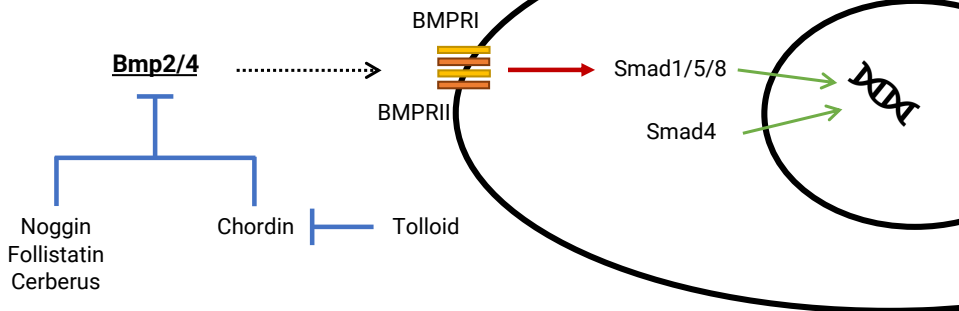


**Figure A8.2.** aGRN markers in zebrafish eye development. **A-B.** scRNAseq analysis of 8dpf zebrafish brains show expression of *FoxQ2* in photoreceptor precursors and of *Six3b*, *Fezf2* and *Rx3* in different retinal populations. **C.** Structure of the vertebrate retina. **D.** Expression of *FoxQ2* (cyan), *Six3b* (yellow), *Fezf2* (green) and *Rx3* (magenta) compared to the retinal structure (compare orange and red lines in C and D).

### Wnt/b-catenin signalling



### BMP signalling



### Nodal signalling

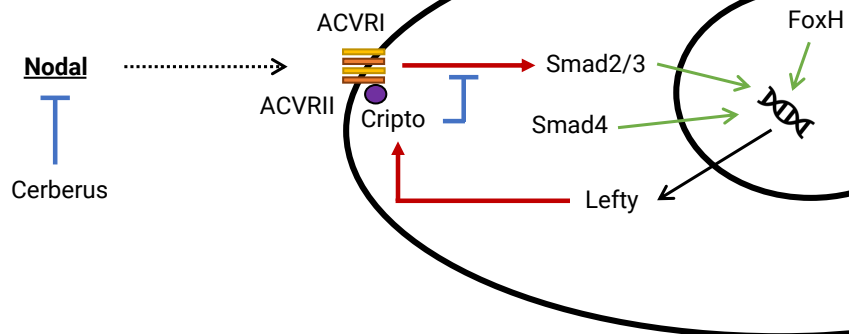
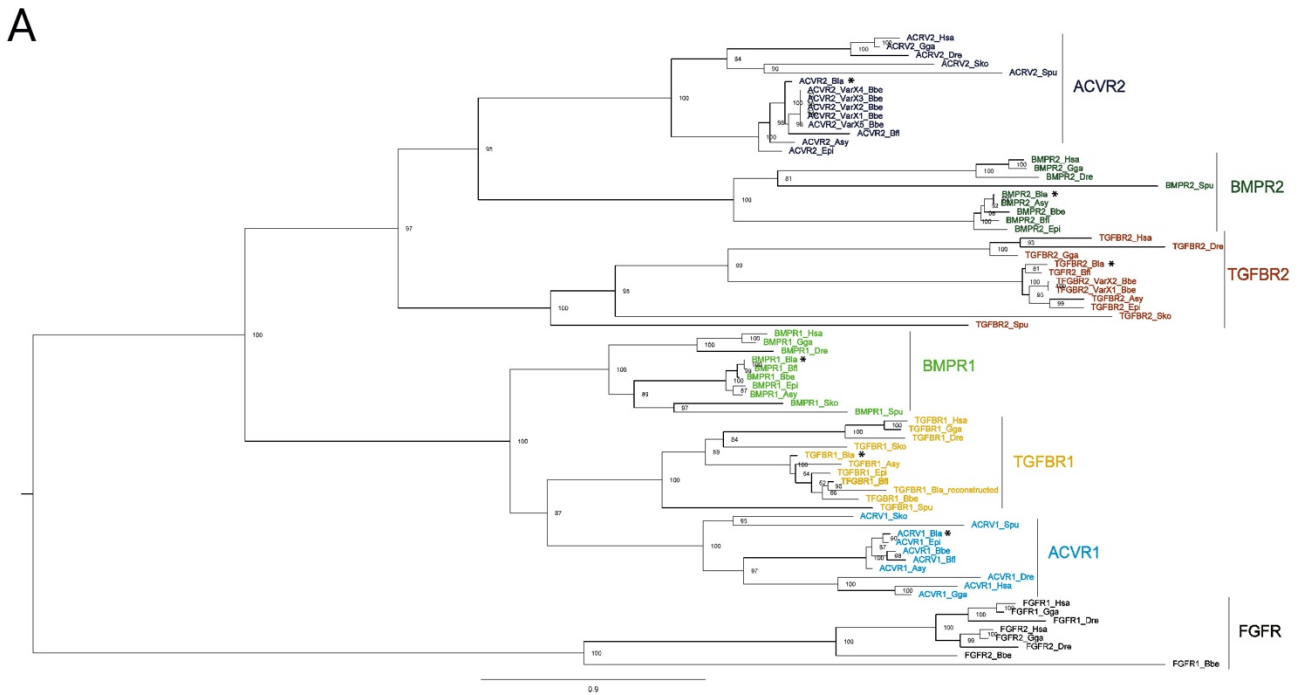


**Figure A8.3.** Schematic summary of Wnt/ $\beta$ -catenin, Bmp and Nodal signalling.



**B** *Elav* + P $\text{Smad}$  1/5/8 - dorsal view

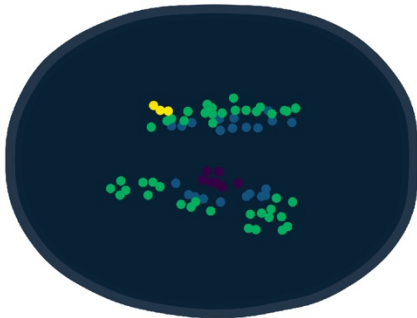


**Figure A8.4.** Tgf $\beta$ -family signalling in amphioxus. **A.** Maximum likelihood phylogenetic analysis of Tgf $\beta$ -family receptors in metazoans. Fgf receptors are used as outgroup. **B.** ADAGE prediction of Bmp activity (visualized through P $\text{Smad}$ 1/5/8) in neural cells (labelled by *Elav*) at the N0 stage (dorsal view).





# Acknowledgments

First, I want to thank my supervisor, Elia Benito-Gutiérrez, for accepting me in her lab and for her endless availability to listen to and discuss my ideas. I am grateful for her trust, for the freedom she has given me throughout the PhD, and for always having her office door open. The long chats during our meetings have been essential to organize my ideas and carry out the project. Thanks also to all the other lab members: Toby Andrews, Michael Schwimmer, Daniel Keitley, Sodai Lotharukpong, Kate Smith and Christo Christov. I have a million reasons to thank Toby, but here I'll just say that without his advice, our drunken chats on evolution and our "rivalry" between team head and team tail this thesis would be very different. I thank Michael for putting up with me through the whole PhD, for our work breaks and for working together on many occasions in these years, and Dan for his bioinformatic wisdom and for all his help. Thanks to the students that have worked with me, contributing to this thesis: Simon Kershenbaum, Claudia Pérez Calles, Maria Izmirlieva, Madeline Foster-Smith, Mark Comer and Jemima Williams. Thanks to my advisors Emília Santos and Marta Zlatic for their guidance, and to the examiners Michael Akam and Maria Ina Arnone for reading and discussing this thesis during a really enjoyable viva. I also want to thank Claire Barnes and the Whitten Studentship for funding my PhD and therefore allowing me to have this wonderful experience in Cambridge.

I strongly believe that science should be based on cooperation, and I am therefore particularly grateful to all the people that collaborated with me and shared their experience. From my Master's lab, I thank Roberta Pennati for her trust and Silvia Mercurio for the long chats and for giving me the chance to continue working with our beloved crinoids. Thanks also to Beatrice De Felice and Marco Parolini for introducing me to ecotoxicology. From the evodevo community in Cambridge, thanks to Dillan Saunders for patiently sharing his zebrafish mastery with me, Lara Busby for going on the American adventure with me, Ben Steventon for allowing me to collaborate with his lab and Andrew Gillis for his precious help through all my PhD and for making me passionate about the endoderm. From the LMB, thanks to Marc Corrales for showing me the world of connectomics and for our nice chats about evolution. From CRUK, thanks to John Marioni and Ashley Sawle for their help in the bioinformatic analysis. I would also like to thank Prof Graziella Bernocchi for her continuous support that means a lot to me.

If I can look at these years with joy is mainly thanks to the incredible friends I have in my life. First of all, thanks to my wonderful, irreplaceable group: Alessandro, Alessio, Chiara, Edoardo, Elisa, Francesco, Ginevra, Giovanni, Ilaria, Lucia, Lucia, Roberto and Simone. I want to express again just how important you are to me, and how every moment we spend together fills me with happiness. Thanks to all the friends I met at university, in particular Laura, who showed me the beauty of London and taught me how to be a rebel, and Beatrice, who is always ready for an aperitivo when I go back to Italy. Cambridge was the first place in which I arrived without knowing anyone, but I was lucky enough to find fantastic friends that made me feel like at home: Aaron, Andrea, Gabby, Joa, Kishen and Michael. Knowing that One Man's Tree will remain strong well beyond our time in Cambridge has made it easier for me to plan my next steps. Thanks to the evodevo group: Toby, Michael, Dan, Margherita and her amazing parties, Lara, Dillan, Aleksandra, Bethan and Jana, and to my oversea friends from the embryology course, Panos and Abby.

And finally, I am extremely grateful to my family for the love and enthusiasm with which they have always supported me. It is often easy to take it for granted, but having a strong and loving family means having a stable foundation on which to build your life, and I am so lucky to have that.

When I look back at these four years I spent as a PhD student, I cannot help feeling extremely happy. There have certainly been hard and stressful times, but I have had the opportunity to work on a project I am really passionate about, and to feel the joy of research and discovery. I have been immersed in a unique and intellectually stimulating environment that helped me grow as a scientist and as a person. But most of all, I have met incredible people, friends, colleagues and often both, who made the time I spent in Cambridge wonderful. Thank you all!